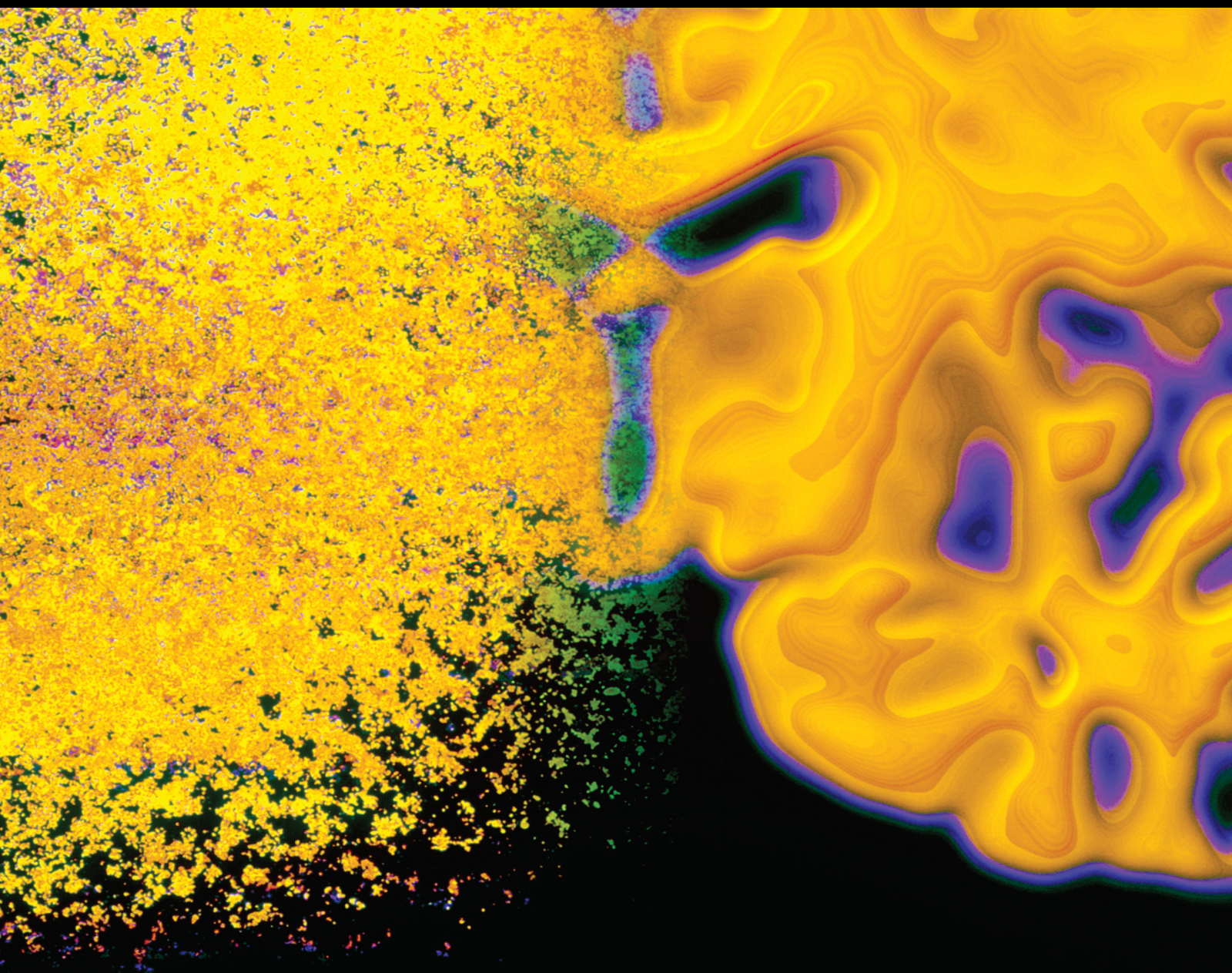


Applications of Theranostics for Detecting and Targeting CNS Injuries and Diseases 2021

Guest Editors: Muh-Shi Lin, Horacio Soto, Hua Lin, and Yu-Yo Sun





Applications of Theranostics for Detecting and Targeting CNS Injuries and Diseases 2021

**Applications of Theranostics for
Detecting and Targeting CNS Injuries
and Diseases 2021**


Guest Editors: Muh-Shi Lin, Horacio Soto, Hua Lin,
and Yu-Yo Sun



Copyright © 2022 Hindawi Limited. All rights reserved.



This is a special issue published in “Behavioural Neurology.” All articles are open access articles distributed under the Creative Commons Attribution License, which permits unrestricted use, distribution, and reproduction in any medium, provided the original work is properly cited.

Chief Editor

Luigi Trojano , Italy

Academic Editors

Ahmad Beydoun, Lebanon
Giuseppe Biagini, Italy
Frederic Blanc , France
Marco Carotenuto, Italy
Danielle C. Cath, The Netherlands
Ming-Jang Chiu , Taiwan
Leungwing Chu , Hong Kong
Dirk Dressler, Germany
Enzo Emanuele, Italy
Luigi Ferini-Strambi, Italy
Pierre O. Fernagut, France
Massimo Filippi , Italy
Yuen Gao , USA
Othman Ghribi , USA
Cheng-Xin Gong , USA
Nikolaos Grigoriadis , Greece
Tauheed Ishrat , USA
Marjan Jahanshahi , United Kingdom
József Janszky , Hungary
Kázmér Karádi , Hungary
Péter Klivényi , Hungary
Norbert Kovács , Hungary
Beata Labuz-Roszak, Poland
Peng Lei, China
Muh-Shi Lin , Taiwan
Simone Lista, Italy
Fabio M. Macciardi , USA
Antonio Orlacchio , Italy
Jesus Pastor , Spain
Olivier Piguet , Australia
Yolande Pijnenburg, The Netherlands
Antonio Pisani , Italy
Francesco Pisani, Italy
Nikolaos K. Robakis, USA
José J. Rodríguez, Spain
Guido Rubboli , Denmark
Elisa Rubino, Italy
Hoon Ryu, USA
Shyam S. Sharma, India
Gianfranco Spalletta , Italy
Nicola Tambasco , Italy
Andrea Truini , Italy
Alberto Verrotti, Italy

Karsten Witt , Germany
Masahito Yamada, Japan
Mario Zappia, Italy
John H. Zhang , USA











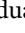



Contents

The Association between Physical Activity and Cognitive Function: Data from the China Health and Nutrition Survey

Qiankun Huang , Jing Zhao , Weiqing Jiang , and Wenfeng Wang 







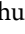






Research Article (12 pages), Article ID 3438078, Volume 2022 (2022)

Prophylactic Zinc Administration Combined with Swimming Exercise Prevents Cognitive-Emotional Disturbances and Tissue Injury following a Transient Hypoxic-Ischemic Insult in the Rat

Ana-Karina Aguilar-Peralta , Alejandro Gonzalez-Vazquez , Constantino Tomas-Sanchez , Victor-Manuel Blanco-Alvarez , Daniel Martinez-Fong , Juan-Antonio Gonzalez-Barrios , Ilhuicamina Daniel Limon , Lourdes Millán-Perez Peña , Gonzalo Flores , Guadalupe Soto-Rodriguez , Eduardo Brambila , Jorge Cebada , Viridiana Vargas-Castro , and Bertha Alicia Leon-Chavez 

Research Article (20 pages), Article ID 5388944, Volume 2022 (2022)

The Improvement of Sepsis-Associated Encephalopathy by P2X7R Inhibitor through Inhibiting the Omi/HtrA2 Apoptotic Signaling Pathway

Kaifang Wang , Meiyan Sun , Zhaodong Juan , Jianxin Zhang , Yingui Sun , Guizhi Wang , Chunling Wang , Yanjing Li , Wenwen Kong , Lulu Fan , Yue Zhang , Hongxiang Zhao , and Xiaoyong Zhao 


Research Article (12 pages), Article ID 3777351, Volume 2022 (2022)

Initial Clinical Experience of Repeat Thrombectomy with a Retrieval Stent (RTRS) with Continuous Proximal Flow Arrest by Balloon Guide Catheter for Acute Intracranial Carotid Occlusion

Wen-huo Chen , Tingyu Yi , Yan-Min Wu , Zhi-nan Pan , Xiu-fen Zheng , Xiao-hui Lin , Ding-lai Lin , and Rong-cheng Chen 

Research Article (7 pages), Article ID 7607324, Volume 2021 (2021)

The Parkinson's Disease Progression Neuroimaging Initiative

Shiyi Zhu , Zizhao Ju , Ping Wu , Fengtao Liu , Jingjie Ge , Huiwei Zhang , Jiaying Lu , Ling Li , Min Wang , Jiehui Jiang , Jian Wang , and Chuantao Zuo 

Research Article (8 pages), Article ID 2230196, Volume 2021 (2021)

Advances regarding Neuroinflammation Biomarkers with Noninvasive Techniques in Epilepsy

Hongrui Ma  and Hua Lin 



Review Article (9 pages), Article ID 7946252, Volume 2021 (2021)

Choline Intake Correlates with Cognitive Performance among Elder Adults in the United States

Lu Liu, Song Qiao, Liying Zhuang, Shanhu Xu, Linhui Chen, Qilun Lai , and Wenfeng Wang 



Research Article (11 pages), Article ID 2962245, Volume 2021 (2021)

Association between Serum 25-Hydroxyvitamin D Level and Stroke Risk: An Analysis Based on the National Health and Nutrition Examination Survey

Lan Wang, Shu Li, G. H. Anuja Sanika, Jinsheng Zhao, Hui Zhang, Lin Zhao , and Wenfeng Wang 


Research Article (9 pages), Article ID 5457881, Volume 2021 (2021)

Effect of the Interaction between Depression and Sleep Disorders on the Stroke Occurrence: An Analysis Based on National Health and Nutritional Examination Survey

Jia Li, Leijun Li, Yan Lv, Yanhai Kang, Mingjin Zhu , and Wenfeng Wang 

Research Article (8 pages), Article ID 6333618, Volume 2021 (2021)

Association between Congenital Cytomegalovirus Infection and Brain Injury in Neonates: A Meta-analysis of Cohort Studies

Li Zhang , Zhankui Li, Xiang Han, Hongyan Du, Yingli Cao, Yingmei Liu, and Wenfeng Wang 




Research Article (9 pages), Article ID 9603660, Volume 2021 (2021)

The First 24 h Hemodynamic Management in NICU after Revascularization Surgery in Moyamoya Disease

Jie Song , Yu Lei , Long Chen , Chao Gao , Wei Ni , Xing Wu , Gang Wu , Ying Mao , Jin Hu , and Yuxiang Gu 


Research Article (7 pages), Article ID 5061173, Volume 2021 (2021)

Effect of Acupuncture on Cognitive Function of Insomnia Patients Compared with Drugs: A Protocol for Meta-analysis and Systematic Review

Shan Qin, Jing Jiang , Wen-Zhong Wu, Xiao-Qiu Wang, Han-Qing Xi, Qin-Qin Fang , Bin Xu, and Cheng-Yong Liu 



Review Article (6 pages), Article ID 6158275, Volume 2021 (2021)

Use of Deep-Learning Genomics to Discriminate Healthy Individuals from Those with Alzheimer's Disease or Mild Cognitive Impairment

Lanlan Li, Yeying Yang, Qi Zhang, Jiao Wang, Jiehui Jiang , and Alzheimer's Disease Neuroimaging Initiative








Research Article (15 pages), Article ID 3359103, Volume 2021 (2021)

Dextromethorphan Dampens Neonatal Astrocyte Activation and Endoplasmic Reticulum Stress Induced by Prenatal Exposure to Buprenorphine

Chun-Hua Lin , Pao-Luh Tao, Huey-Jen Tsay, Yao-Chang Chiang, Wei-Tang Chang, Ing-Kang Ho, and Feng-Shiun Shie 

Research Article (10 pages), Article ID 6301458, Volume 2021 (2021)

Association between Anemia and Risk of Parkinson Disease

Yao-Chin Wang , Abel Po-Hao Huang , Sheng-Po Yuan , Chu-Ya Huang, Chieh-Chen Wu , Tahmina Nasrin Poly , Suleman Atique , and Woon-Man Kung 

Research Article (8 pages), Article ID 8360627, Volume 2021 (2021)

Research Article

The Association between Physical Activity and Cognitive Function: Data from the China Health and Nutrition Survey

Qiankun Huang ¹, Jing Zhao ², Weiqing Jiang ¹ and Wenfeng Wang ³

¹Minhang District Mental Health Center of Shanghai, Shanghai 201112, China

²Shanghai Mental Health Center, Shanghai Jiao Tong University School of Medicine, Shanghai 201108, China

³School of Science, Shanghai Institute of Technology, Shanghai 201418, China

Correspondence should be addressed to Weiqing Jiang; weiqingj2021@outlook.com

Received 5 August 2021; Revised 17 February 2022; Accepted 5 May 2022; Published 20 June 2022

Academic Editor: Yu Yo Sun

Copyright © 2022 Qiankun Huang et al. This is an open access article distributed under the Creative Commons Attribution License, which permits unrestricted use, distribution, and reproduction in any medium, provided the original work is properly cited.

Background. Decreased cognitive function is a common problem in the old adults, which has high risk of progression to Alzheimer's diseases (AD) and other dementias. This study was aimed at finding out the association between physical activity and cognitive function. **Methods.** In total, 1514 participants with the age ≥ 55 years old registered in the China Health and Nutrition Survey (CHNS) database were selected in this study. The association between physical activity and cognitive function was analyzed via the generalized additive model. The association between the variables and the cognitive function score was expressed as β coefficient with 95% confidence intervals (CIs). **Results.** After adjusting age, ethnicity, stratum, marital status, education, memory status, and memory changes, the cognitive function score was increased by 0.011 points for every 1-point increase in domestic score ($\beta = 0.011$, $P = 0.043$). Subgroup analysis indicated that in the female group, for every 1-point increase in the domestic score, the cognitive function score increased by 0.019 points ($\beta = 0.019$, $P = 0.017$). In people with good memory status, each 1-point increase in domestic score increased the cognitive function score of 0.020 points ($\beta = 0.020$, $P = 0.017$). **Conclusions.** The decreased cognitive function was correlated with decreased domestic physical activity. The increased domestic physical activity was associated with an increased cognitive function in females and people with good memory status. The findings might offer a reference for deep understanding of the association between physical activity and cognitive function.

1. Introduction

Cognitive function includes memory, language, judgment, and attention, which may be impaired by neurodegeneration and vascular or dysthymia/dysphoria problems [1, 2]. Cognitive impairment is a common problem in the old adults, ranging from mild cognitive impairment (MCI) to dementia [3]. Cognitive impairment has attracted particular attention on account of its prevalence and clinical impact on patients [4]. Previous studies have reported that individuals with MCI have high risk of progression to Alzheimer's diseases (AD) and other dementias [5]. A study showed that the MCI conversion rate to dementia is about 10% per year, which is increased to 80%-90% after approximately 6 years [6]. This demonstrated that it is valuable to identify methods

to prevent the deterioration of MCI to dementia. Currently, the effect of pharmacological treatment for mild cognitive impairment is modest or some even have no effect, and new therapeutic methods are urgently required for mild cognitive impairment [7]. Recently, nonpharmacological treatments attract more attention concerning the prevention of cognitive function decline.

Physical activity is a widely proposed nonpharmacological method for MCI therapy, and it is mainly composed of occupational, domestic, transportation, and leisure time activities [8]. Growing studies have demonstrated that physical activity can prevent the decline of cognitive function, and the global cognitive function has association with the amount of physical activity [9, 10]. Barnes et al. have demonstrated that physical activity increasing by 10% could

significantly decrease the risk of MCI to dementia [11]. Another study also reported that low physical activity increased risk of MCI to dementia [12]. Currently, the investigation on the association of cognitive function and physical activity among Chinese population remains largely unclear. In this study, the association between physical activity and cognitive function was analyzed according to the data from the China Health and Nutrition Survey (CHNS) based on the generalized additive model. The results of this study might provide a reference for identifying the association between different physical activities and cognitive function and encourage the older adults to take part in more physical activities.

2. Methods

2.1. Study Population. The CHNS is a freely available database established in 1989. It is a large-scale and household-based cohort study with over 30,000 individuals in 9 provinces in China on the health conditions, nutritional statuses, and diseases of subjects by the Chinese Center for Disease Control and Prevention [13]. In the survey, the samples were selected via the random-cluster sampling process in a large higher-income city, a lower-income city, and four counties (1 high-, 2 middle-, and 1 low-income according to per-capita income provided by the National Bureau of Statistics) within each province. Urban and suburban neighborhoods within the cities and villages and townships within the counties were selected randomly as the primary sampling unit, in which twenty households were randomly selected and all household members were interviewed [14]. The survey got the approval from the institutional review committees of the University of North Carolina, the Chinese Institute of Nutrition and Food Safety, and the China Center for Disease Control and Prevention. All participants provided the informed consents. Due to public availability of CHNS database, with private information of all patients being anonymized, the local ethics committee's approval was not required in our study. This cross-sectional study collected the data of 180,713 participants from the CHNS database. Among them, 15,923 were from 1989, 16,033 were from 1991, 15,058 were from 1993, 15,822 were from 1997, 17,054 were from 2000, 16,126 were from 2004, 18,785 were from 2006, 18,913 were from 2009, 23,060 were from 2011, and 23,939 were from 2015. The data of the participants in previous years were excluded ($n = 139,781$) including 15,602 from 1989, 15,070 from 1991, 13,354 from 1993, 14,365 from 1997, 15,359 from 2000, 14,946 from 2004, 16,358 from 2006, 17,112 from 2009, and 17,615 from 2011, and we only analyzed the data collected from the latest year. Participants who did not survey the data of cognitive function or did not complete the items of questionnaire concerning cognitive function were also excluded ($n = 37,238$). After exclusion of participants without the data on age, gender, height, weight, nationality, systolic blood pressure (SBP), diastolic blood pressure (DBP), sleep time, and memory changes ($n = 2180$), finally, 1514 subjects were included in the study. Among them, 23 people were from 2004, 41 people were from 2006, and 1450 were

from 2015. Sensitive analysis depicted that no statistical difference was found concerning the demographic data and physical activity scores including cognitive function, domestic score, occupational score, transportation score, and leisure time score between participants completing the survey on cognitive function and participants finally included (Supplementary Table 1).

2.2. Data Extraction. Clinical data of 1514 subjects were collected including age, gender, nationality (Han or others), stratum (city, suburban, town or county capital city, or rural village), SBP (mmHg), DBP (mmHg), hypertension, diabetes, body mass index (BMI) (kg/m^2), household income (yuan), marital status (never married, married, divorced, widowed, or separated), education, sleep time, history of smoking, drinking, drinking frequency, memory status (bad, good, or OK), memory changes (deteriorated, improved, or stayed the same), domestic score, occupational score, transportation score, and leisure time score.

2.3. Definition and Assessment of the Variables. The cognitive function score is divided into four parts including the immediate memory (10 scores), the delayed recall of a 10-word list (10 scores), counting backward from 20 (2 scores), and serial 7 subtraction (5 scores) [15]. The sum of the four scores makes the final score. The total global cognitive score ranged from 0 to 27. Higher scores indicate better cognitive function. The cognitive function test started with the immediate recall of a 10-word list. The interviewer (trained health worker) read ten words at a speed of two seconds per word. The participants were given two minutes to memorize the ten words. For each correct recalled word, a score of 1 was given. The participants were then asked to count back from 20 to 1. If the participants made a mistake in the first try, a second chance was given. A score of 2 was given to those answered correctly in the first try or 1 in the second try. After the count test, the participants were asked to do five consecutive subtractions of 7 from 100. Each correct subtraction was given a score of 1. Finally, the participants were asked to recall the 10-word list tested before. Each recalled word was given a score of 1.

The physical activity-related variables were calculated into four dimensions: domestic, occupational, transportation, and leisure time [8]. In our study, the data on these four dimensions were collected by staff-administered questionnaires [16]. The assessment of these four dimensions was based on metabolic equivalent- (MET-) hours-per-week to account for both intensity and time spent on activities [17]. Physical activities were reported in average hours-per-week spent in the past year. The level of physical activity was the product of time spent in each activity multiplied by specific MET values based on the "Compendium of Physical Activities" [18]. Domestic activity was measured based on four activities. The MET values assigned were as follows: 2.3 for buying food, 2.25 for preparing food or cooking, 2.15 for laundry, and 3.0 for sweeping rooms. Occupational activity was measured according to the intensity of specific jobs (light, moderate, and heavy), with assigned values of 2.0, 4.0, and 6.0, respectively. Evaluation of transportation

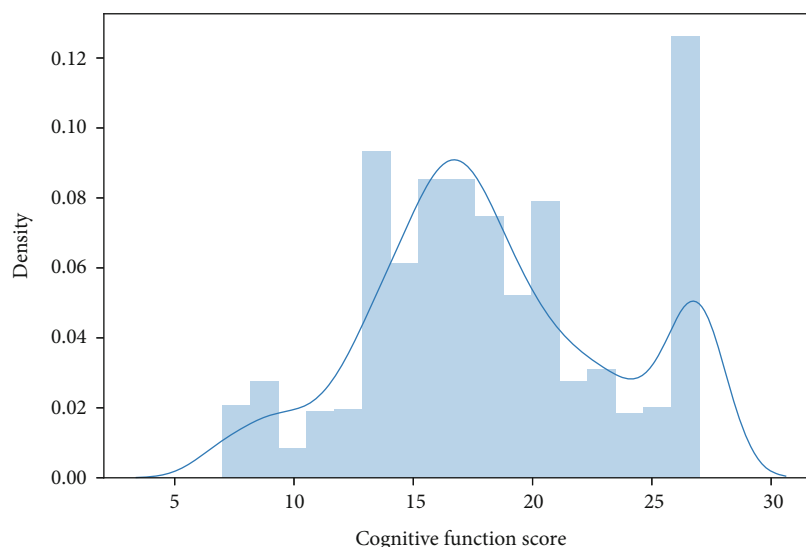


FIGURE 1: The histogram of cognitive function scores.

activity was based on four commuting types to and from work or school. The MET values assigned were as follows: 3.0 for walking, 4.0 for bicycling, and 1.5 for motorized vehicle. The MET values used for leisure time activities were 4.5 for martial arts, 5.0 for gymnastics, dancing, or acrobatics, 7.5 for jogging or swimming, 6.0 for playing soccer, basketball, or tennis, and 5.0 for playing badminton, volleyball, or ping-pong.

Memory status of participants were defined based on the question “how is your memory: (1) very good; (2) good; (3) OK; (4) bad; (5) very bad.” Those who reported “bad” or “very bad” were defined as having a bad memory. Those who reported “very good” and “good” were combined into the “good” group. Memory change was assessed by the question “in the past twelve months, how has your memory changed: (1) improved; (2) stayed the same; (3) deteriorated.”

2.4. The Generalized Additive Model. In the present study, the cognitive function score data were seriously skewed (Figure 1). Then, the restricted cubic spline (RCS) was plotted and revealed that the association between physical activity and cognitive function was nonlinear (Figures 2(a)–2(d)). Additionally, the linear fitting was poor according to the linear fitting residual graph of cognitive function score and exercise-related score (Figures 3(a)–3(d)), so we chose the generalized additive model for analyzing the association between physical activity and cognitive function. The generalized additive model is an extension of generalized linear models that allows nonlinear functional forms between independent variables and the response [19]. The generalized additive model helps in improving the predictive accuracy of Y .

2.5. Statistical Analysis. Statistical analyses were performed by the use of SAS (9.4 Edition, SAS Institute, Cary, NC, USA). The measurement data were displayed as mean \pm standard deviation (mean \pm SD), and the enumeration data

were presented as cases and frequency [N (%)]. The association between physical activity and cognitive function was analyzed via the generalized additive model. The association between the variables and the cognitive function score was expressed as β coefficient with 95% confidence intervals (CIs). All statistical analyses were bilateral, and $P < 0.05$ was considered statistically significant.

3. Results

3.1. The Characteristics of Subjects. A total of 1514 participants were included and analyzed with the screening process shown in Figure 4. Among them, 943 were male, accounting for 62.29%, and 571 were female, accounting for 37.71%. Among the ethnic groups, 1427 were Han, accounting for 94.25%, and 87 were other ethnic groups, accounting for 5.75%. The average SBP was $135.03 \text{ mmHg} \pm 17.37 \text{ mmHg}$. The average DBP was $83.24 \text{ mmHg} \pm 10.44 \text{ mmHg}$. The mean BMI was $24.49 \text{ kg/m}^2 \pm 3.42 \text{ kg/m}^2$. In terms of education level, 861 people received junior middle school education or below, accounting for 56.87%, 490 people received high school education, accounting for 32.36%, and 163 people received university education or above, accounting for 10.77%. The average length of sleep was $7.61 \text{ h} \pm 1.22 \text{ h}$. Other baseline data are displayed in Table 1.

3.2. The Association between Physical Activity and Cognitive Functioning. According to the results in the univariate analysis, age, ethnics, marital status, education memory status, and memory changes were confounders of the association between physical activity and cognitive functioning. In the multivariate analysis, these confounders were adjusted to evaluate the association of physical activity including domestic, occupational, transportation, and leisure time scores with the cognitive function score. The data showed that for every 1-point increase in domestic score, the cognitive function score was increased by 0.011 points ($\beta = 0.011$, 95% CI: 0.001–0.022, $P = 0.043$) (Table 2).

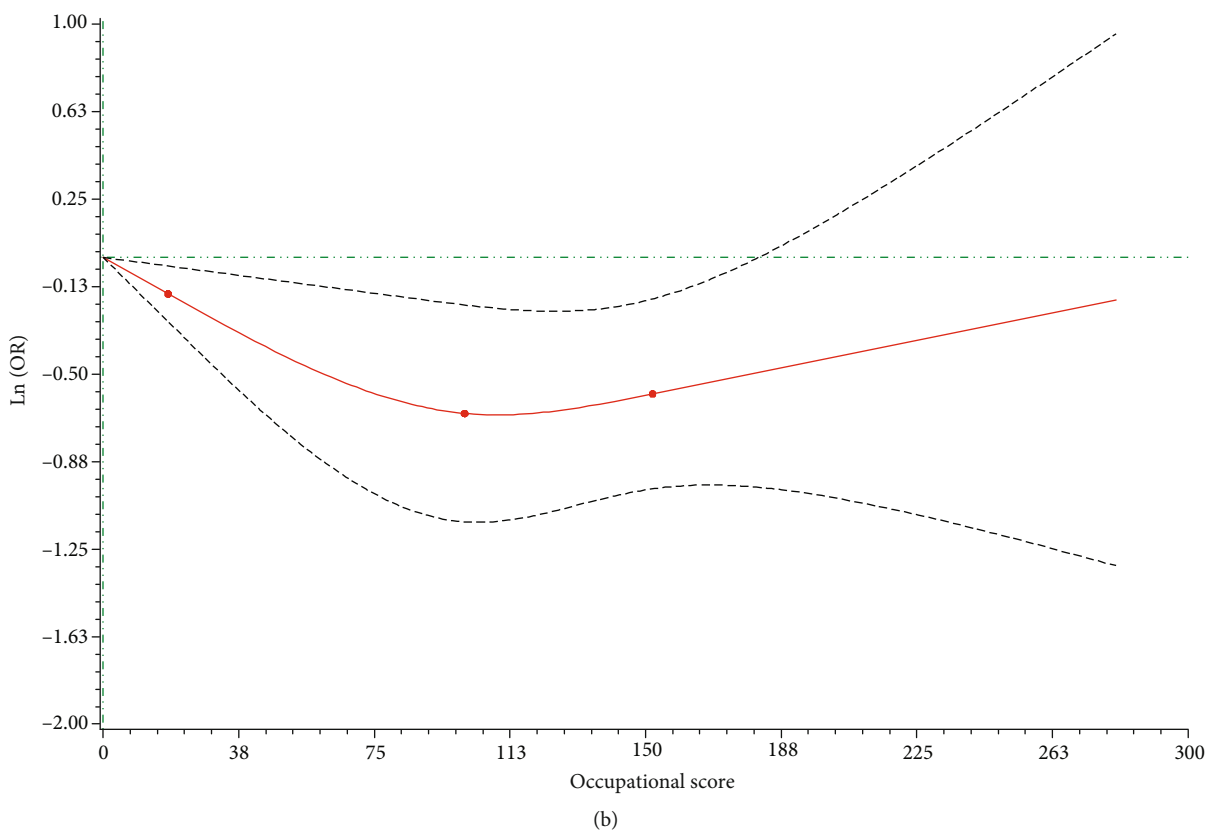
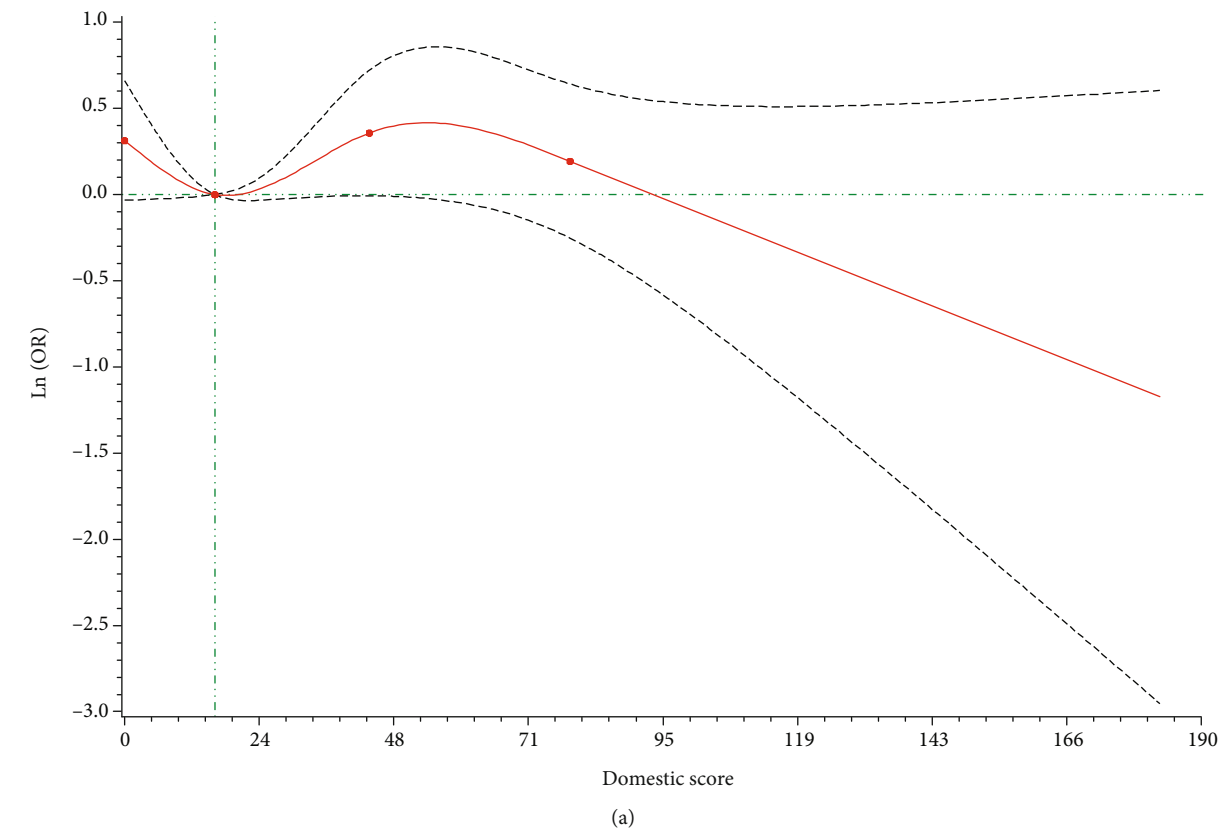


FIGURE 2: Continued.

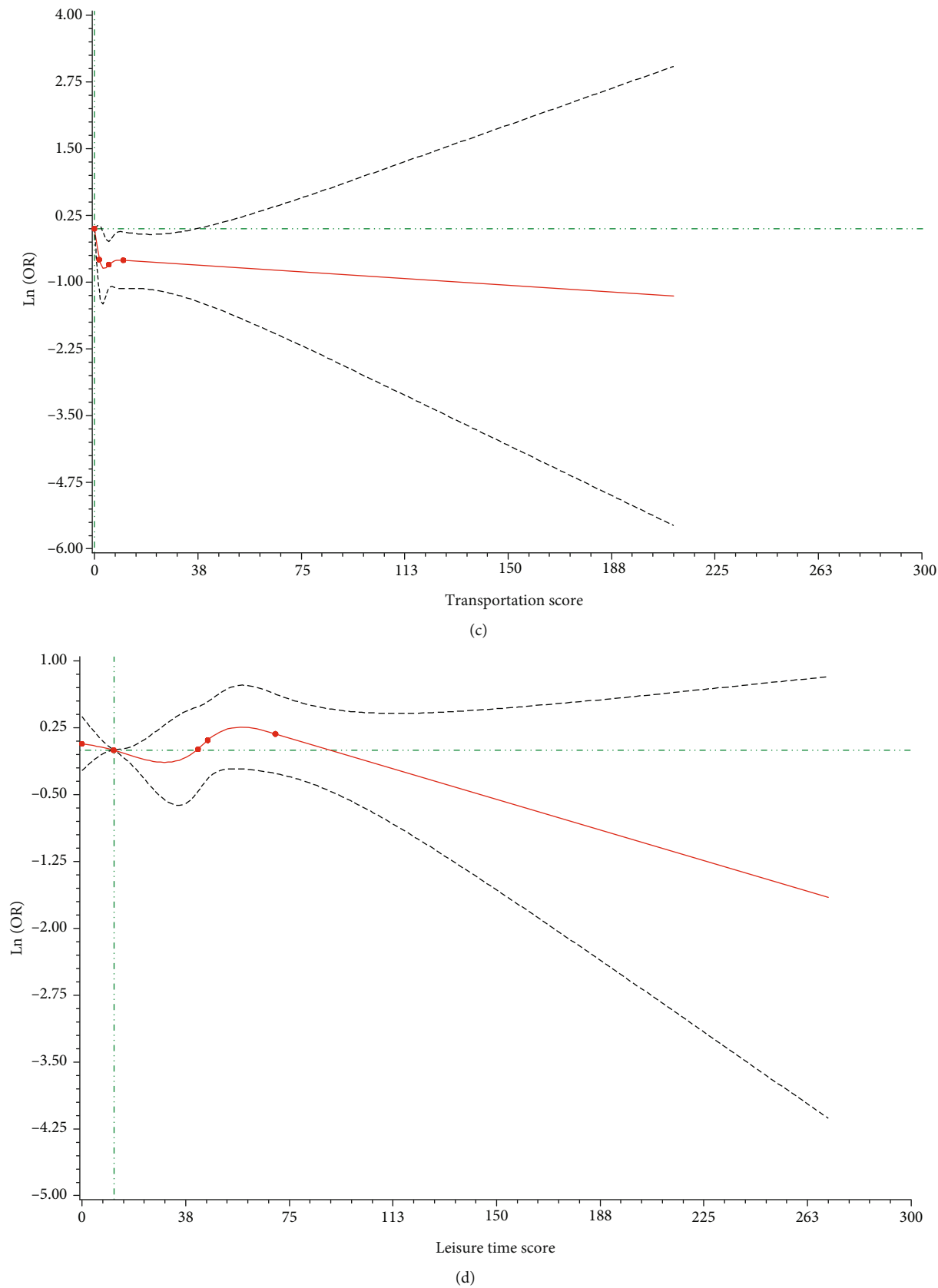
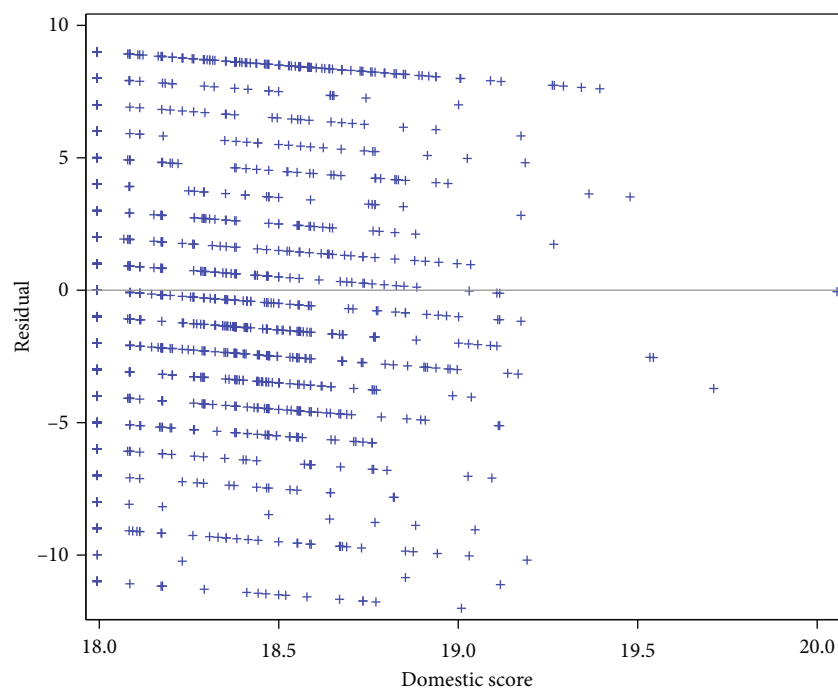
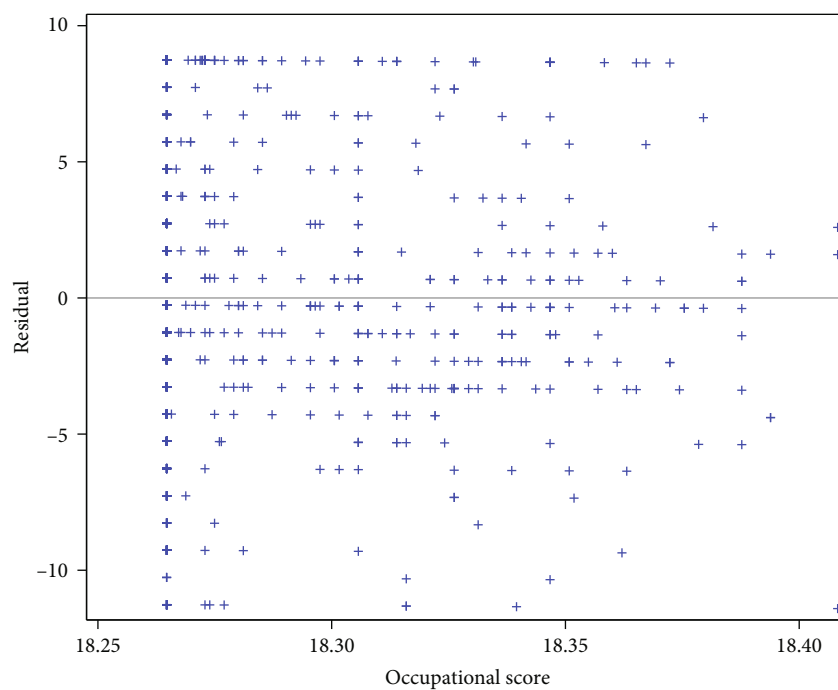


FIGURE 2: The RCS results between scores of (a) domestic, (b) occupational, (c) transportation, and (d) leisure time activities and cognitive function score.



(a)



(b)

FIGURE 3: Continued.

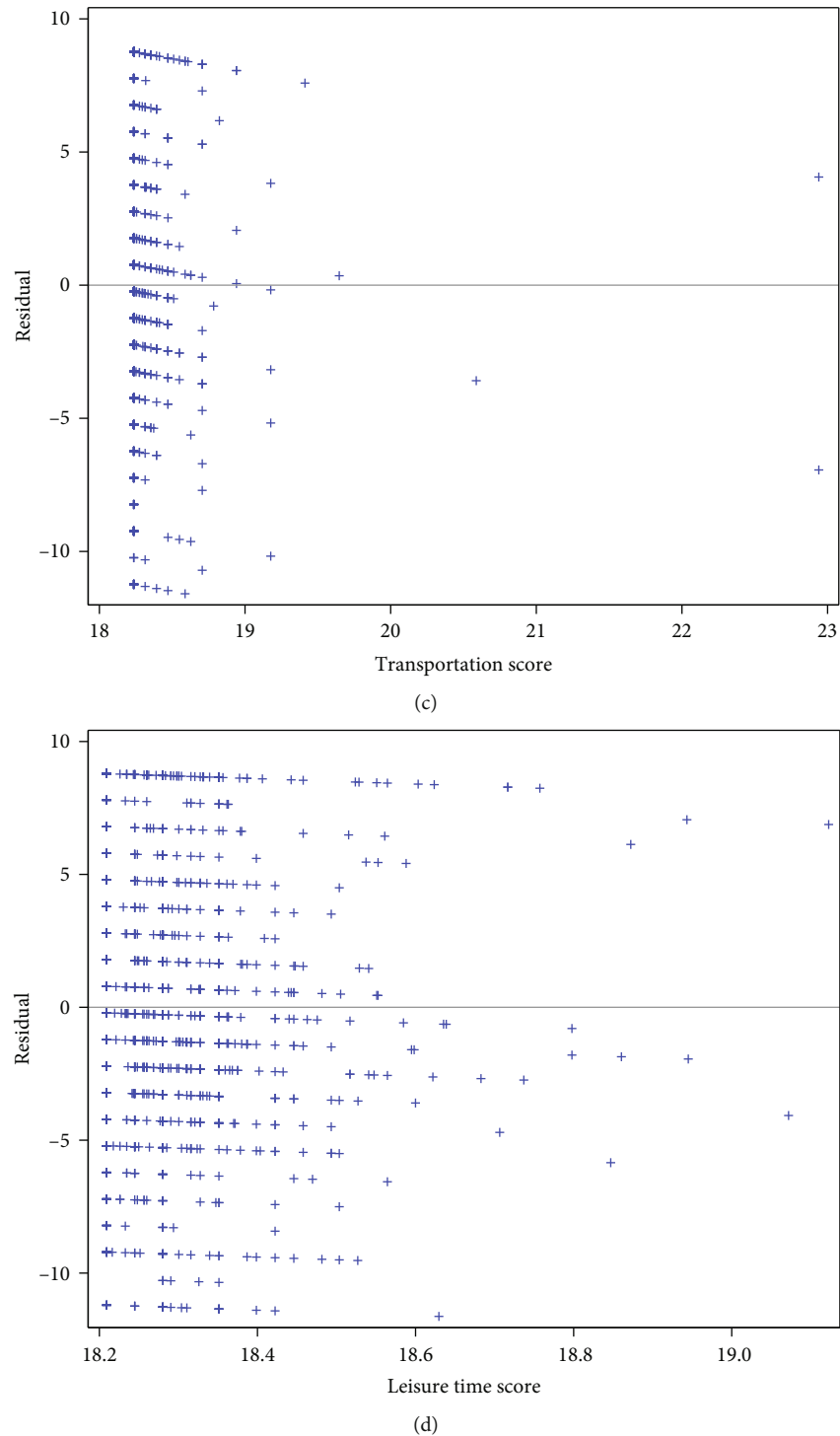


FIGURE 3: The residual graph of linear fitting between scores of (a) domestic, (b) occupational, (c) transportation, and (d) leisure time activities and cognitive function score.

3.3. Subgroup Analysis of Factors Influencing Cognitive Functioning. The detailed information of the domestic score, occupational score, transportation score, and leisure time score in females and males is shown in Supplementary Table 2. The mean domestic score was 12.45 in males and 45.69 in females. The mean occupational score was 31.06 in males and 7.63 in females. The mean transportation

score was 2.27 in males and 1.03 in females. The mean leisure time was 17.44 in males and 23.63 in females. As for the domestic score, occupational score, transportation score, and leisure time score in people with different memory status, the mean domestic score was 25.89 in people with bad memory status, 25.31 in people with good memory status, and 24.33 in people with OK memory

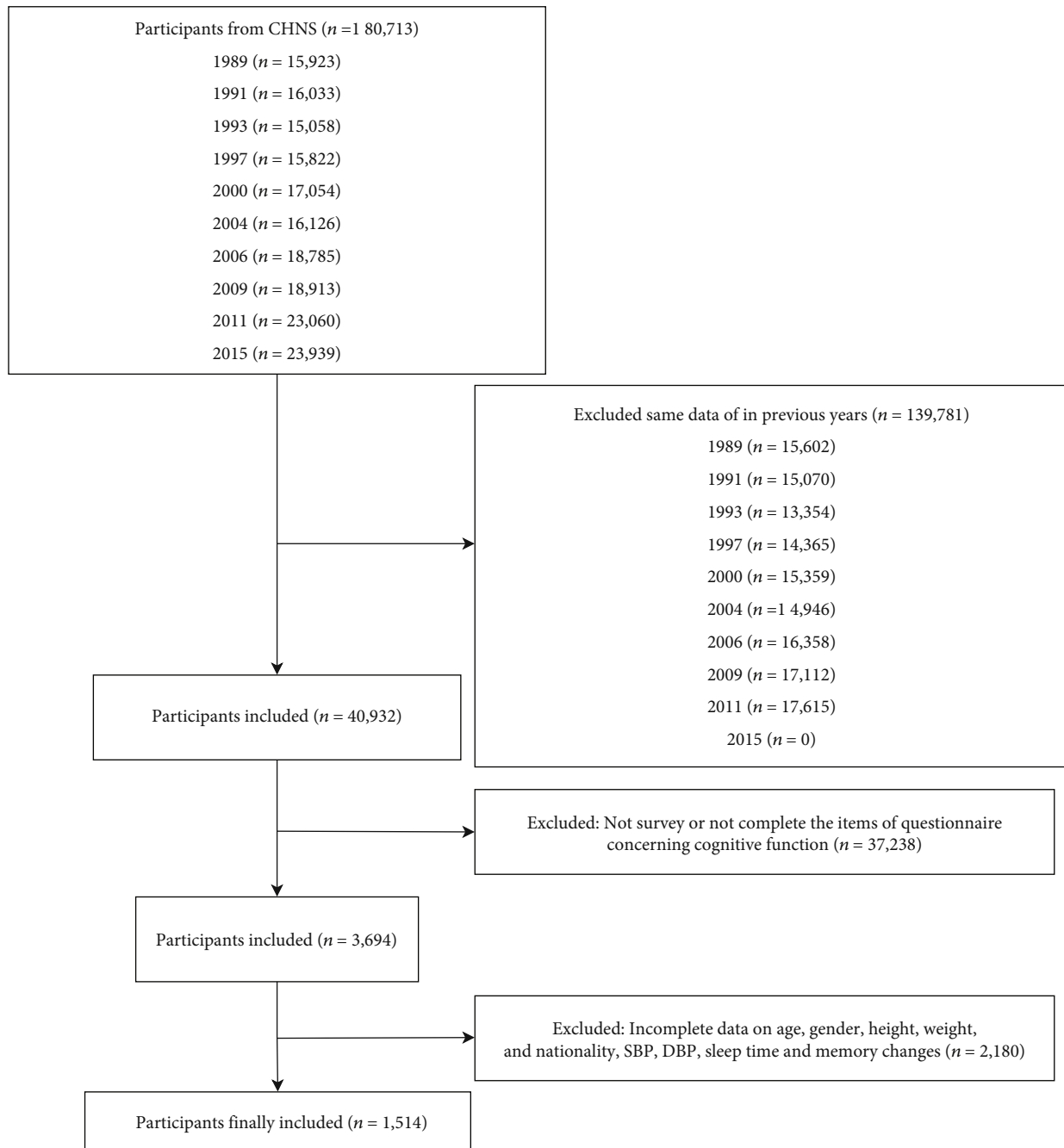


FIGURE 4: The screening process of the participants.

status. The mean occupational score was 8.22 in people with bad memory, 26.36 in people with good memory status, and 21.79 in people with OK memory status. The mean transportation score was 0.52 in people with bad memory status, 2.34 in people with good memory status, and 1.59 in people with OK memory status. The mean leisure time score was 18.20 in people with bad memory status, 20.50 in people with good memory status, and 19.43 in people with OK memory status.

As for subgroup analysis of different genders, there was no statistical significance in the four dimensions in males (all $P > 0.05$). In females, a 1-point increase in domestic

score was associated with an increase of cognitive function score of 0.019 points ($\beta = 0.019$, 95% CI: 0.003-0.035, $P = 0.017$) (Table 3). An increased domestic score was associated with an elevated cognitive function in people with good memory status ($\beta = 0.020$, 95% CI: 0.004-0.036, $P = 0.017$) (Table 4).

4. Discussion

This study collected the clinical data of 1514 participants from the CHNS database and analyzed the association between physical activity-related four dimensions

TABLE 1: The characteristics of the participates.

Variable	Description
Age	64.20 ± 6.94
Gender	
Male	943 (62.29)
Female	571 (37.71)
Ethnicity	
Han	1427 (94.25)
Others	87 (5.75)
Stratum, <i>n</i> (%)	
City	608 (40.16)
Suburban	223 (14.73)
Town or county capital city	256 (16.91)
Rural village	427 (28.20)
Hypertension, <i>n</i> (%)	
No	16 (8.56)
Yes	171 (91.44)
Diabetes	
No	671 (90.55)
Yes	70 (9.45)
Household income (yuan)	20000 (5000, 60000)
SBP	135.03 ± 17.37
DBP	83.24 ± 10.44
BMI	24.49 ± 3.42
Marital status	
Married	1387 (91.61)
Widowed	109 (7.20)
Separated	1 (0.07)
Never married	3 (0.20)
Divorced	14 (0.92)
Education	
Middle school or below	861 (56.87)
High school	490 (32.36)
University and above	163 (10.77)
Sleep time	7.61 ± 1.22
Smoke	
No	1145 (75.63)
Yes	369 (24.37)
Drink	
No	1079 (71.27)
Yes	435 (28.73)
Drink frequency	
No drink	1079 (71.27)
Less than once a week	121 (7.99)
1-2 times a week	87 (5.75)
3-4 times a week	48 (3.17)
Every day	179 (11.82)

TABLE 1: Continued.

Variable	Description
Memory status	
Good	708 (46.76)
OK	616 (40.69)
Bad	190 (12.55)
Memory changes	
Improved	30 (1.98)
Stayed the same	924 (61.03)
Deteriorated	560 (36.99)
Physical activities	
Domestic score	24.99 ± 28.31
Occupational score	22.22 ± 51.32
Transportation score	1.80 ± 9.44
Leisure time score	19.78 ± 28.36

SBP: systolic blood pressure; DBP: diastolic blood pressure; BMI: body mass index. The minimum domestic score was 0 and the maximum domestic score was 182.70. The minimum occupational score was 0 and the maximum occupational score was 280.00. The minimum transportation score was 0 and the maximum occupational score was 210.00. The minimum leisure time score was 0 and the maximum occupational score was 270.00.

(occupational, domestic, transportation, and leisure time activities) and cognitive function based on the generalized additive model. The results indicated that the cognitive function score was increased by 0.011 points for every 1-point increase in domestic score after adjusting the significant variables in univariate analysis including age, ethnicity, stratum, marital status, education, memory status, and memory changes. In addition, subgroup analysis revealed that domestic score was a protective score for the cognitive function in females and people with good memory status. The findings might offer a reference for deep understanding of the association between cognitive function and physical activity.

Physical activity refers to the bodily movement which resulted from skeletal muscles that increases the consumption of energy [20]. The Australian Physical Activity and Sedentary Behavior Guidelines recommend adults ≥ 65 years to perform moderate-intensity physical activity for more than 30 min on most days of the week in addition to usual activities of daily living [21]. Physical activity was reported to have the ability to delay the decline of cognitive function and reduce the risk of dementia through improving blood supply to the brain and reinforcing the nervous system [22, 23]. Physical activity can also strengthen the cardiovascular, immune, and metabolic system functions and regulate the internal environment of the brain [24]. According to the Copenhagen Consensus statement 2019, physical activity was confirmed to be effective in improving the cognitive and brain health in older adults [25]. Physical activity has different domains including occupational, domestic, transportation, and leisure time activities. Previously, studies have revealed that some domestic physical activities including sweeping, vacuuming, window cleaning, and lawn mowing are moderate intensity for middle-aged or older people [26]. In the present study, domestic activity was identified

TABLE 2: Univariate and multivariate analysis of factors influencing cognitive functioning.

Physical activity score	Univariate analysis		Multivariate analysis*	
	β (95% CI)	<i>P</i>	β (95% CI)	<i>P</i>
Domestic score	0.011 (0.002-0.021)	0.017	0.011 (0.001-0.022)	0.043
Occupational score	0.001 (-0.005-0.006)	0.844	-0.002 (-0.008-0.003)	0.403
Transportation score	0.022 (-0.005-0.050)	0.114	0.012 (-0.014-0.039)	0.369
Leisure time score	0.003 (-0.006-0.013)	0.473	-0.003 (0.012-0.006)	0.510

*Multivariable analysis adjusting age, ethnicity, stratum, marital status, education, memory status, and memory changes.

TABLE 3: The analysis of subgroup considering different genders.

Physical activity score	Males		Females	
	β (95% CI)	<i>P</i>	β (95% CI)	<i>P</i>
Domestic score	0.001 (-0.015-0.017)	0.885	0.019 (0.003-0.035)	0.017
Occupational score	-0.002 (-0.008-0.003)	0.439	-0.004 (-0.020-0.011)	0.595
Transportation score	-0.002 (-0.035-0.032)	0.925	0.035 (-0.009-0.079)	0.122
Leisure time score	-0.007 (-0.019-0.005)	0.269	0.002 (-0.012-0.016)	0.824

Multivariable analysis adjusting age, ethnicity, stratum, marital status, education, memory status, and memory changes.

TABLE 4: The association between physical activities and cognitive function in people with different memory status.

Physical activity	Good		Bad		OK	
	β (95% CI)	<i>P</i>	β (95% CI)	<i>P</i>	β (95% CI)	<i>P</i>
Domestic score	0.020 (0.004-0.036)	0.017	0.025 (-0.001-0.050)	0.059	-0.007 (-0.024-0.011)	0.456
Occupational score	-0.002 (-0.010-0.005)	0.498	0.011 (-0.013-0.035)	0.360	-0.004 (-0.011-0.004)	0.366
Transportation score	0.020 (-0.012-0.052)	0.215	0.062 (-0.178-0.301)	0.616	-0.017 (-0.076-0.041)	0.558
Leisure time score	-0.002 (-0.015-0.011)	0.753	0.011 (-0.016-0.038)	0.426	-0.009 (-0.024-0.007)	0.283

Multivariable analysis adjusting age, ethnicity, stratum, marital status, education, and memory changes.

to be associated with the cognitive function in females, and females tended to do more domestic activities than males. The increased domestic score was positively correlated with the cognitive function score. Previously, a study has shown that domestic activity was beneficial for human health [27]. According to the data of a cross-sectional study with 1070 participants in Bahia, domestic physical activities have a positive impact on the control of high blood pressure [28]. This evidence supported the conclusion of our study. Domestic physical activity was also observed to have gender-specific effects on health indicators in Europe [27]; this may be due to the fact that females tend to have more domestic physical activity than males.

Herein, we found elevated domestic score was associated with increased cognitive function in people with good memory status. Memory is fundamental in our day-to-day lives, and memory status may influence the everyday function of people [29]. For those with good memory status, domestic activities such as buying food, preparing food or cooking, laundry, or sweeping rooms were encouraged. The reason may be that people with good memory status may finish the domestic activities such as buying food, preparing food or cooking, laundry, or sweeping rooms more precisely and completely than people with OK or bad memory status. Although the mean and median domestic score were similar in people with bad, OK, or good memory, the domestic

activity intensity in those with good memory status might be higher than that in people with OK or bad memory status. In this study, the maximum domestic score in people with good memory was higher than in those with bad or OK memory, which indicated that people with good memory may be engaged in more and longer time of domestic activities than people with OK or bad memory status. Older adults who have moderate or poor memory may be more sensitive to any negative function changes in daily activities and they may feel that they have less control over their cognitive performance, which lead them to avoid doing activities including domestic activities [30]. Additionally, people with good memory can do domestic activities such as buying food, which help them involve more social networks through communicating with others and then help preserve the cognitive function [31].

In the present study, occupational activity was not statistically associated with the cognitive function in older people; this may be because the CNHS database collected the data of individuals aged 45 and above [32]. In our study, we included the participants with the age ≥ 55 years old and most of them may be retired and those people were not engaged in the occupational activities. Thus, the occupational activities might have little association with the cognitive function in those people. In this study, no statistical association was found between transportation activity and

cognitive function. For many older people, walking was the major transportation activity for them, and other transportation activities such as bicycling and motorized vehicle were not suitable for them. Additionally, for older people, they like to stay at home or just walk at the place close to home. They just want to stay in the place they are familiar with and do not like to go far away. The walking intensity was small in these people. For people that need to go far away, the free older persons' bus pass encourages them to choose public transports rather than cycling or motorized vehicle [33]. Leisure time activity was found not associated with cognitive function in older adults in the present study. As our data was collected from 1989 to 2015, leisure time activity was not popular in older people during that time.

The strength of this study was that we deeply analyzed the association between physical activity and cognitive function from four domains of physical activity including occupational, domestic, transportation, and leisure time activities especially in the Chinese population. In addition, subgroup analysis was performed in terms of different genders and people with different memory status, which might more clearly stratified the association between physical activity and cognitive function in different kinds of people. There were some limitations of this study. Firstly, there was no uniform tools for measuring the intensity of physical activity till now, which may have an impact on the results of this study. Secondly, some data were collected via questionnaire and self-reported, which may result in an uncontrollable source of bias. Thirdly, the CHNS database covers 228 communities in Heilongjiang, Liaoning, Shandong, Henan, Jiangsu, Hunan, Hubei, Guangxi, and Guizhou provinces, which cannot represent the whole country of China, indicating that the results of our study should be interpreted with caution. Fourthly, this was a cross-sectional study; we only found the association between physical activity and cognitive function, but could not identify the cause-effect between them. In the future, prospective randomized controlled trials (RCTs) or longitudinal cohort studies were required to verify the findings in this study.

5. Conclusions

In the study, the clinical data of 1514 subjects from the CHNS database were analyzed to explore the association between physical activity and cognitive function. The results indicated that decreased cognitive function was correlated with the reduction of domestic score after adjusting age, ethnicity, stratum, marital status, education, memory status, and memory changes especially in females and people with good memory status. The results of our study might offer a reference for deep understanding of the association between special physical activity and cognitive function in older people.

Data Availability

The data utilized to support the findings are available from the corresponding authors upon request.

Conflicts of Interest

The authors declare that they have no competing interests.

Acknowledgments

We thank the participants included in our study for their contributions. This research was supported by the special project of integrated Chinese and western medicine in Shanghai General Hospital (ZHYY-ZXYJHZX-202004).

Supplementary Materials

Sensitivity analysis of the missing data and the detailed information of physical activity scores in people from subgroups. (*Supplementary Materials*)















References

- [1] H. J. Woodford and J. George, "Cognitive assessment in the elderly: a review of clinical methods," *QJM: Monthly Journal of the Association of Physicians*, vol. 100, no. 8, pp. 469–484, 2007.
- [2] C. Pinto and A. A. Subramanyam, "Mild cognitive impairment: the dilemma," *Indian Journal of Psychiatry*, vol. 51, Suppl1, pp. S44–S51, 2009.
- [3] W. Liao, X. Zhang, H. Shu, Z. Wang, D. Liu, and Z. Zhang, "The characteristic of cognitive dysfunction in remitted late life depression and amnesic mild cognitive impairment," *Psychiatry Research*, vol. 251, pp. 168–175, 2017.
- [4] A. Di Carlo, M. Baldereschi, L. Amaducci et al., "Cognitive impairment without dementia in older people: prevalence, vascular risk factors, impact on disability. The Italian Longitudinal Study on Aging," *Journal of the American Geriatrics Society*, vol. 48, no. 7, pp. 775–782, 2000.
- [5] J. G. van Uffelen, A. P. M. J. Chin, M. Hopman-Rock, and W. van Mechelen, "The effects of exercise on cognition in older adults with and without cognitive decline: a systematic review," *Clinical Journal of Sport Medicine*, vol. 18, no. 6, pp. 486–500, 2008.
- [6] S. A. Eshkoor, T. A. Hamid, C. Y. Mun, and C. K. Ng, "Mild cognitive impairment and its management in older people," *Clinical Interventions in Aging*, vol. 10, pp. 687–693, 2015.
- [7] T. Tanigawa, H. Takechi, H. Arai, M. Yamada, S. Nishiguchi, and T. Aoyama, "Effect of physical activity on memory function in older adults with mild Alzheimer's disease and mild cognitive impairment," *Geriatrics & Gerontology International*, vol. 14, no. 4, pp. 758–762, 2014.
- [8] H. Zuo, Z. Shi, B. Yuan et al., "Interaction between physical activity and sleep duration in relation to insulin resistance among non-diabetic Chinese adults," *BMC Public Health*, vol. 12, no. 1, article 247, 2012.
- [9] R. A. Fielding, J. M. Guralnik, A. C. King et al., "Dose of physical activity, physical functioning and disability risk in mobility-limited older adults: results from the LIFE study randomized trial," *PLoS One*, vol. 12, no. 8, article e0182155, 2017.
- [10] I. Abraha, J. M. Rimland, F. M. Trotta et al., "Systematic review of systematic reviews of non-pharmacological interventions to treat behavioural disturbances in older patients with dementia. The SENATOR-OnTop series," *BMJ Open*, vol. 7, no. 3, article e012759, 2017.

- [11] D. E. Barnes and K. Yaffe, "The projected effect of risk factor reduction on Alzheimer's disease prevalence," *The Lancet Neurology*, vol. 10, no. 9, pp. 819–828, 2011.
- [12] D. R. Taaffe, F. Irie, K. H. Masaki et al., "Physical activity, physical function, and incident dementia in elderly men: the Honolulu-Asia Aging Study," *The Journals of Gerontology Series A, Biological Sciences and Medical Sciences*, vol. 63, no. 5, pp. 529–535, 2008.
- [13] B. M. Popkin, S. Du, F. Zhai, and B. Zhang, "Cohort profile: the China Health and Nutrition Survey—monitoring and understanding socio-economic and health change in China, 1989–2011," *International Journal of Epidemiology*, vol. 39, no. 6, pp. 1435–1440, 2010.
- [14] B. Zhang, F. Y. Zhai, S. F. Du, and B. M. Popkin, "The China Health and Nutrition Survey, 1989–2011," *Obesity Reviews*, vol. 15, pp. 2–7, 2014.
- [15] Z. Shi, T. El-Obeid, M. Riley, M. Li, A. Page, and J. Liu, "High chili intake and cognitive function among 4582 adults: an open cohort study over 15 years," *Nutrients*, vol. 11, no. 5, p. 1183, 2019.
- [16] C. Tudor-Locke, B. E. Ainsworth, L. S. Adair, and B. M. Popkin, "Physical activity in Filipino youth: the Cebu Longitudinal Health and Nutrition Survey," *International Journal of Obesity*, vol. 27, no. 2, pp. 181–190, 2003.
- [17] S. W. Ng, E. C. Norton, and B. M. Popkin, "Why have physical activity levels declined among Chinese adults? Findings from the 1991–2006 China Health and Nutrition Surveys," *Social Science & Medicine*, vol. 68, no. 7, pp. 1305–1314, 2009.
- [18] B. E. Ainsworth, W. L. Haskell, M. C. Whitt et al., "Compendium of physical activities: an update of activity codes and MET intensities," *Medicine and Science in Sports and Exercise*, vol. 32, pp. S498–S516, 2000.
- [19] M. A. S. Mullah, J. A. Hanley, and A. Benedetti, "Modeling perinatal mortality in twins via generalized additive mixed models: a comparison of estimation approaches," *BMC Medical Research Methodology*, vol. 19, no. 1, p. 209, 2019.
- [20] C. J. Caspersen, K. E. Powell, and G. M. Christenson, "Physical activity, exercise, and physical fitness: definitions and distinctions for health-related research," *Public Health Reports*, vol. 100, no. 2, pp. 126–131, 1985.
- [21] J. Langford, M. P. Dillon, C. L. Granger, and C. Barr, "Physical activity participation amongst individuals with lower limb amputation," *Disability and Rehabilitation*, vol. 41, no. 9, pp. 1063–1070, 2019.
- [22] K. I. Erickson, M. W. Voss, R. S. Prakash et al., "Exercise training increases size of hippocampus and improves memory," *Proceedings of the National Academy of Sciences of the United States of America*, vol. 108, no. 7, pp. 3017–3022, 2011.
- [23] A. G. Thomas, A. Dennis, P. A. Bandettini, and H. Johansen-Berg, "The effects of aerobic activity on brain structure," *Frontiers in Psychology*, vol. 3, p. 86, 2012.
- [24] M. W. Voss, C. Soto, S. Yoo, M. Sodoma, C. Vivar, and H. van Praag, "Exercise and hippocampal memory systems," *Trends in Cognitive Sciences*, vol. 23, no. 4, pp. 318–333, 2019.
- [25] J. Bangsbo, J. Blackwell, C. J. Boraxbekk et al., "Copenhagen Consensus statement 2019: physical activity and ageing," *British Journal of Sports Medicine*, vol. 53, no. 14, pp. 856–858, 2019.
- [26] R. T. Withers, A. G. Brooks, S. M. Gunn, J. L. Plummer, C. J. Gore, and J. Cormack, "Self-selected exercise intensity during household/garden activities and walking in 55 to 65-year-old females," *European Journal of Applied Physiology*, vol. 97, no. 4, pp. 494–504, 2006.
- [27] K. Abu-Omar and A. Rütten, "Relation of leisure time, occupational, domestic, and commuting physical activity to health indicators in Europe," *Preventive Medicine*, vol. 47, no. 3, pp. 319–323, 2008.
- [28] U. E. S. Ribeiro Junior and R. C. P. Fernandes, "Hypertension in workers: the role of physical activity and its different dimensions," *Arquivos Brasileiros de Cardiologia*, vol. 114, no. 5, pp. 755–761, 2020.
- [29] C. L. Fan, K. Romero, and B. Levine, "Older adults with lower autobiographical memory abilities report less age-related decline in everyday cognitive function," *BMC Geriatrics*, vol. 20, no. 1, p. 308, 2020.
- [30] K. J. Chang, C. H. Hong, Y. H. Lee et al., "Memory age identity as a predictor of cognitive function in the elderly: a 2-year follow-up study," *Archives of Gerontology and Geriatrics*, vol. 74, pp. 68–71, 2018.
- [31] Y. Nie, M. Richards, R. Kubinova et al., "Social networks and cognitive function in older adults: findings from the HAPIEE study," *BMC Geriatrics*, vol. 21, no. 1, p. 570, 2021.
- [32] Q. Yao, J. Zhang, K. Yan et al., "Development and validation of a 2-year new-onset stroke risk prediction model for people over age 45 in China," *Medicine*, vol. 99, no. 41, article e22680, 2020.
- [33] S. Coronini-Cronberg, C. Millett, A. A. Laverty, and E. Webb, "The impact of a free older persons' bus pass on active travel and regular walking in England," *American Journal of Public Health*, vol. 102, no. 11, pp. 2141–2148, 2012.

Research Article

Prophylactic Zinc Administration Combined with Swimming Exercise Prevents Cognitive-Emotional Disturbances and Tissue Injury following a Transient Hypoxic-Ischemic Insult in the Rat

Ana-Karina Aguilar-Peralta ¹, Alejandro Gonzalez-Vazquez ¹,
Constantino Tomas-Sanchez ¹, Victor-Manuel Blanco-Alvarez ²,
Daniel Martinez-Fong ^{3,4}, Juan-Antonio Gonzalez-Barrios ⁵,
Ilhuicamina Daniel Limon ¹, Lourdes Millán-Perez Peña ⁶, Gonzalo Flores ⁷,
Guadalupe Soto-Rodriguez ⁸, Eduardo Brambila ¹, Jorge Cebada ⁸,
Viridiana Vargas-Castro ¹ and Bertha Alicia Leon-Chavez ¹

¹Facultad de Ciencias Químicas, Benemérita, Universidad Autónoma de Puebla, 14 Sur y Av. San Claudio, 72570 Puebla Pue, Mexico

²Facultad de Enfermería, Benemérita, Universidad Autónoma de Puebla, 27 Sur 1304, Col. Volcanes, 72410 Puebla Pue, Mexico

³Departamento de Fisiología, Biofísica y Neurociencias, Centro de Investigación y de Estudios Avanzados del Instituto Politécnico Nacional, Apartado Postal 14-740, 07000 México D.F., Mexico

⁴Nanoparticle Therapy Institute, 404 Avenida Monte Blanco, Aguascalientes 20120, Mexico

⁵Laboratorio de Medicina Genómica, Hospital Regional 1° de Octubre, ISSSTE Avenida, Instituto Politécnico Nacional #1669, 07760 México D.F., Mexico

⁶Centro de Química, ICUAP, Benemérita Universidad Autónoma de Puebla, 14 Sur y Av. San Claudio, 72570 Puebla, Mexico

⁷Instituto de Fisiología, Benemérita Universidad Autónoma de Puebla, 14 Sur y Av. San Claudio, 72570 Puebla, Mexico

⁸Facultad de Medicina, Benemérita Universidad Autónoma de Puebla, 13 Sur 2702, Col. Volcanes, 72410 Puebla Pue, Mexico

Correspondence should be addressed to Bertha Alicia Leon-Chavez; alileonch@gmail.com

Received 29 July 2021; Revised 4 March 2022; Accepted 1 April 2022; Published 20 May 2022

Academic Editor: Muh-Shi Lin

Copyright © 2022 Ana-Karina Aguilar-Peralta et al. This is an open access article distributed under the Creative Commons Attribution License, which permits unrestricted use, distribution, and reproduction in any medium, provided the original work is properly cited.

Exercise performance and zinc administration individually yield a protective effect on various neurodegenerative models, including ischemic brain injury. Therefore, this work was aimed at evaluating the combined effect of subacute prophylactic zinc administration and swimming exercise in a transient cerebral ischemia model. The prophylactic zinc administration (2.5 mg/kg of body weight) was provided every 24 h for four days before a 30 min common carotid artery occlusion (CCAO), and 24 h after reperfusion, the rats were subjected to swimming exercise in the Morris Water Maze (MWM). Learning was evaluated daily for five days, and memory on day 12 postreperfusion; anxiety or depression-like behavior was measured by the elevated plus maze and the motor activity by open-field test. Nitrites, lipid peroxidation, and the activity of superoxide dismutase (SOD) and catalase (CAT) were assessed in the temporoparietal cortex and hippocampus. The three nitric oxide (NO) synthase isoforms, chemokines, and their receptor levels were measured by ELISA. Nissl staining evaluated hippocampus cytoarchitecture and Iba-1 immunohistochemistry activated the microglia. Swimming exercise alone could not prevent ischemic damage but, combined with prophylactic zinc administration, reversed the cognitive deficit, decreased NOS and chemokine levels, prevented tissue damage, and increased Iba-1 (+) cell number. These results suggest that the subacute prophylactic zinc administration combined with swimming exercise, but not the individual treatment, prevents the ischemic damage on day 12 postreperfusion in the transient ischemia model.

1. Introduction

Cerebrovascular disease (CVD) is caused by a temporary or sustained deprivation of oxygen and nutrients in one or more brain areas, leading to cerebral parenchyma injury [1]. This disease affects 15 million people worldwide every year and is one of the leading causes of permanent disability and mortality [2]. In addition, ischemia is a more frequent cause than the hemorrhagic process in CVD [3]. The ischemic process disrupts the blood flow, alters cell homeostasis, and induces immediate cell death by necrosis in the infarct core [4]. Furthermore, in the penumbra zone, the ischemic process triggers deleterious events such as excitotoxicity (release of glutamate and calcium), nitrosative and oxidative stress [5], lytic enzyme activation (proteases, lipases, and nucleases), dynamic cytoskeleton alteration [6], and neuroinflammation [7].

Severe cerebral ischemic damage has been reproduced in rodents with cerebral artery occlusion (MCAO) or with common carotid artery occlusion (CCAO) for more than one hour (up to 120 min) [8, 9], which promotes the formation of extensive infarct zones in the brain [10, 11]. Models with shorter occlusion times, such as CCAO for 10 min, do not promote an infarct core [12, 13] but cause learning and memory loss at 12 days postreperfusion [12, 14, 15]. In the 30 min CCAO model, although some authors have reported that it does not cause infarct volume at 24 h postreperfusion [7, 16], others have proven that it mimics the physiopathology of human ischemic-type CVD [17]. The CCAO for 30 min can cause an infarct core and the penumbra zone, affecting several brain regions such as the lateral neocortex, striatum, and ipsilateral hippocampus [18, 19]. In the early phase of 30 min CCAO, it has been reported that the alteration of energy metabolism [20, 21] detonates oxidative/nitrosative stress [16] and neuroinflammation [22, 23]. The humoral response is characterized by the expression of proinflammatory cytokines (IL-1 β , TNF- α , and IFN- γ) [22], adhesion molecules (ICAM-1 and VCAM-1) [21], and chemokines (CCL2, CCL3, CXCL1, CXCL13, and CX3CL1) whose levels maintain up to 5 days postreperfusion [24]. The cellular response includes an increase in microglia number [25, 26] and the presence of infiltrated macrophages, neutrophils, and B lymphocytes [22] in the infarct core [27–29]. Those cellular events correlate with neuronal cell death, and the maximum increase occurs on day 7 postreperfusion [30]. Posteriorly, regeneration processes originated in the subgranular zone (SGZ) [26], and removal of the infarct by astrocytes and microglia occurs until day 14 postreperfusion [27]. However, the neuropsychological alterations prevail [27–29] from 21 days [30] to 90 days postreperfusion [31].

Nevertheless, the constant release of proinflammatory cytokines, chemokines, and adhesion molecules can elicit apoptosis and affect neuroplasticity, which causes cognitive deficits such as learning and memory loss and emotional disturbances such as anxiety or depression-like behavior [32]. Interestingly, some reports have shown that cognitive activity or motor performance protects against neurodegenerative diseases, improving cerebral functionality [33, 34]. Swimming exercise, for example, has shown neuroprotection in animal models of Alzheimer [35], spinal muscular atrophy [36], depression [37], and amyotrophic lateral sclerosis,

thorough increasing the production and release of growth factors [38]. However, the beneficial effect of exercise performance depends on factors like intensity and frequency to trigger efficient cellular adaptation mechanisms to oxidative stress and increase the antioxidative response stimulated by mitochondrial biogenesis [39, 40].

An increasing number of reports support the neuroprotector effect of zinc administration prophylactically [11, 41, 42] or postreperfusion [43]. However, zinc administration can also exacerbate ischemia-induced cerebral injury depending on the dose and time of administration. The neuroprotective effect was found in subacute prophylactic ZnCl₂ administration (2.5 mg/kg/24 h for 4 days, i.p., before 10 min CCAO) [11, 41] and hyperacute ZnCl₂ administration at a dose of 20 mg/kg, i.p., 30 min before 3 min CCAO [44]; 10.9 mg/kg equivalent of zinc, i.p. 30 min before 2 h ischemia [45]; and 6 mg/kg, i.v., after 60 min of 2 h medial carotid artery occlusion (MCAO) [46]. On the contrary, chronic prophylactic ZnCl₂ administration at a dose of 0.5 mg/kg/15 days, i.p. [47], or zinc protoporphyrin IX treatment can exacerbate ischemia-induced cerebral injury [48–50]. Other factors that influence zinc neuroprotection are the time (3 min to 2 h) postreperfusion and the modality of obliteration (unilateral or bilateral) [44, 45] or injury size in the case of traumatic brain injury (TBI) models [51, 52].

The main beneficial effect of zinc is to promote antioxidant and anti-inflammatory actions against ischemic damage. It modulates the formation of ROS by inhibiting NMDAR through its binding to the GluN2A subunit [53, 54]; decreases the reactivity of O₂⁻ due to a structural part of the cytosolic superoxide dismutase (SOD1) [55]; regulates the transcription of reduced glutathione (GSH), SOD, reduced glutathione transferase (GST), and heme oxygenase- (HO-) 1 through Nrf2 [56]; induces BDNF expression [57]; converts pro-BDNF to mature BDNF by activation of zinc-dependent MMPs [58]; prevents the formation of the complex IKK through the interaction of Zn²⁺ via influx by Zip8 [59], or the A20 protein [60], inhibiting the NF- κ B signaling pathway [61] and decreasing neuroinflammation; and increases the density of neuronal precursor cells after a TBI [62], promoting neurogenesis [63, 64]. Furthermore, zinc through microglia-expressed ZEB1 can regulate neuroinflammation after stroke, decreasing neutrophil chemoattraction by CXCL1 [65].

It has been reported that subacute prophylactic zinc administration in the 10 min CCAO model has a neuroprotective effect, reducing nitrosative stress and cell death [11], increasing chemokine and growth factor levels, and improving learning and memory in the Morris Water Maze (MWM) test [41]. On the contrary, zinc deficiency caused anxiety-like behavior in rats submitted to MWM [66]. Besides, chronic prophylactic zinc (0.2 mg/kg by 14 days) combined with therapeutic selenium administration has a neuroprotective and antioxidant effect on hypoxic-ischemic brain events postreperfusion [42].

Based on the neuroprotection of exercise performance and subacute prophylactic zinc administration, this work was aimed at evaluating whether the combined neuroprotection of prophylactic zinc administration (2.5 mg/kg/24 h for four days) and swimming exercise through MWM can be effective

in brain injury caused by 30 min CCAO. The biochemical parameters studied were NO and malondialdehyde and 4-hydroxy-alkenal (MDA+4-HDA) levels and chemokine (CCL2, CXCL1, CXCL13, and CX3CL1) and nitric oxide synthase (NOS-1, NOS-2, and NOS-3) protein levels, measured by ELISA. In addition, Nissl staining and Iba-1 immunohistochemistry were performed on day 12 postreperfusion. At this time, cognition was also evaluated, whereas emotional disturbances were evaluated on day 30 postreperfusion.

2. Methodology

2.1. Experimental Animals. Male Wistar rats (bodyweight 180–240 g) were obtained from the Animal Production Unit of CINVESTAV and maintained in suitable rooms with controlled conditions of temperature ($22 \pm 3^\circ\text{C}$) and light-dark cycles (12 h–12 h; light onset at 07:00). The animals received food (Laboratory Autoclavable Rodent Diet 5010, 130 ppm of zinc) and drinking water *ad libitum*. All procedures were carried out according to the current Mexican legislation, NOM-062-ZOO-1999 (SAGARPA), based on the Guide for the Care and Use of Laboratory Animals, NRC. The experimental procedures were approved by the Institutional Animal Care and Use Committee with protocol number 09-102. All experimental processes were made to minimize animal suffering.

2.2. Experimental Groups. The animals were randomly divided into the following groups: (1) healthy, without swimming exercise treatment, or surgery to normalize the effect of all treatments; (2) MWM, control of swimming exercise trained in MWM; (3) Zn, control with chloride zinc (2.5 mg/kg of body weight, equivalent to 1.2 mg atomic zinc) administration [41]; (4) CCAO, rats with 30 min left CCAO; and (5) Zn + CCAO, prophylactic zinc administration and CCAO.

2.3. Experimental Design. Experimental diagram of the procedures performed, zinc administration, common carotid artery obliteration (CCAO), biochemical determinations, and tests is shown to evaluate cognitive and motor abilities (Figure 1).

2.4. Common Carotid Artery Obliteration (CCAO). The animals were maintained in a sterile room, and surgical instruments were sterilized. Posteriorly, animals were anesthetized with a mixture of ketamine (70 mg/kg) and xylazine (6 mg/kg) at a dose of $200 \mu\text{L}/100 \text{ g}$ of body weight, i.p. After an incision of 0.5 cm long midline skin in the neck area, the left common carotid artery was carefully dissected and occluded for 30 min with a clamp (Bulldog Clamps, INS6000119; Kent Scientific Corporation; Torrington, CT, USA). Upon completion of the occlusion time, the artery reperfusion was visually verified, and the incision was sutured with a 3-0 silk thread (Atramat; Ciudad de Mexico, Mexico). The animals were kept in an individual cage until their complete recovery in the surgery room and then transferred to a temporary vivarium. The animals after experimental processes were euthanized on day 12 postreperfusion using sodium pentobarbital at a dose of 60 mg/kg of body weight [41, 42].

2.5. Morris Water Maze (MWM). MWM pool was used to submit the rats to physical exercise as reported previously [67, 68]. Additionally, this test was utilized to evaluate learning and memory. All experimental groups were trained at 24 h after CCAO with MWM to evaluate the learning and memory. The swimming pool was divided into four quadrants, North (N), West (W), South (S), and East (E), and two clues were placed on the inner walls of the tank, which serve as the orientation and location inside the platform. The MWM consisted of a circular tank (swimming pool) of 150 cm diameter and 80 cm height; the escape platform measuring 10 cm in diameter was placed in the quadrant southeast. The tank will be filled with water ($19\text{--}22^\circ\text{C}$) one centimeter above the platform height to ensure that rats cannot see the escape platform.

The learning test consisted of four probes per day, one for each quadrant, giving 60 seconds (s) to find the platform (escape latency). Once the rats completed the trial, they remained on the platform for 30 s. Then, they were removed from the platform and waited 30 min to start the subsequent trial. The order of performance of the quadrants was N, W, S, and E, for five consecutive days.

The memory test was evaluated seven days after the last day of the learning test. The memory test was carried out for 60 s in the N quadrant, counting the number of times that the rat passed by the escape platform and the time in which it was localized [42].

2.6. Elevated Plus Maze. The elevated plus maze was used to assess the depressive-like behavior and anxiety of the rats. The maze was placed 90 cm from the ground and consisted of two open arms ($25 \times 5 \times 1 \text{ cm}$; white color) and two closed arms ($25 \times 5 \times 16 \text{ cm}$; black color) connected to a central platform ($5 \times 5 \text{ cm}$). The open arms had a wall of 1 cm to reduce the risk of falls, whereas the closed arms had a wall of 16 cm to cover the entire arm.

The test was carried out for 5 min, and the number of times that the animal entered the open and closed arms and the time to remain on them were recorded. In addition, the urination and defecation numbers were also quantified.

2.7. Open Field. The open-field test was also used to assess the unrestricted mobility of rats. The evaluations were carried out in a square wood box of 60 cm divided into nine quadrants per side and 70 cm high. The number of times the subject passed through the central quadrant (quadrant 5) and the distance traveled (total number of quadrants visited multiplied by 20 cm) during 5 min were registered.

2.8. Nitric Oxide Quantification. The NO production was assessed by the accumulation of nitrites (NO_2^-) by the modified technique of Griess as described previously [69]. The cerebral cortex and hippocampus were obtained 1 h after the memory test ($n = 5$ rats in each group), mechanically homogenized in phosphate-buffered saline solution pH 7.4 (PBS), and centrifuged at 12,500 rpm for 30 min at 4°C by using a Z216MK microcentrifuge (HERMLE Labortechnik; Wehingen, Germany). Briefly, the NO concentration was measured in $10 \mu\text{L}$ of supernatant after the addition of

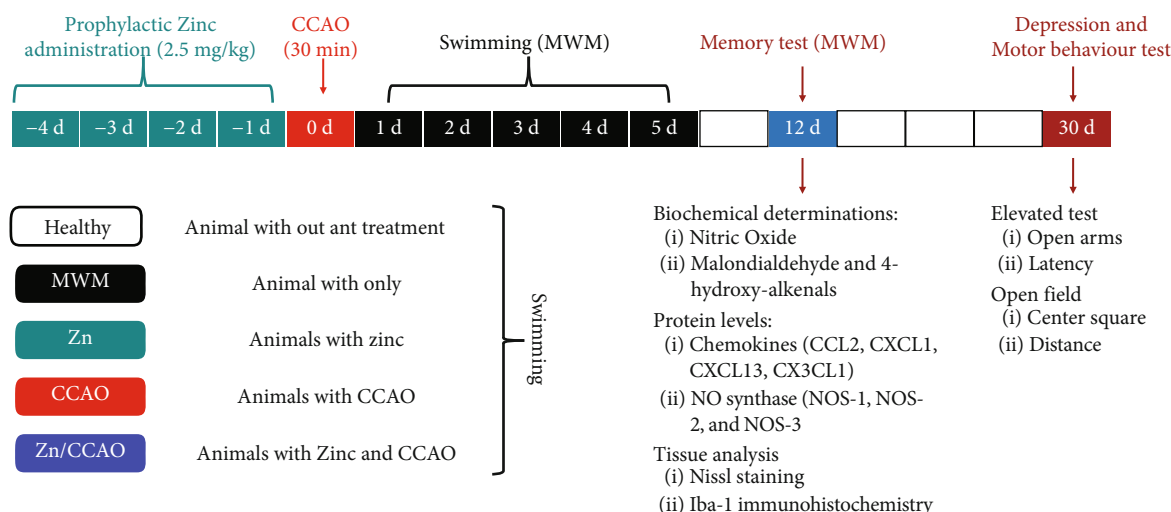


FIGURE 1

10 μL of Griess reagent (composed of equal volumes of 0.1% N-(1-naphthyl) ethylenediamine dihydrochloride and 1.32% sulfanilamide in 60% acetic acid). In addition, the optical density in a 2 μL sample was measured with a NanoDrop 1000 Spectrophotometer (Thermo Fisher Scientific, Bancroft Building, Wilmington, USA) at 540 nm, and the optical density values were interpolated from the standard curve of NaNO_2 (1 to 10 μM) to obtain NO concentration.

2.9. Lipid Peroxidation Quantification. Malondialdehyde (MDA) and 4-hydroxyalkenals (4-HDA) as an index of lipid peroxidation were measured in each group ($n = 5$), following the procedure described previously [69]. The colorimetric reaction was performed in 200 μL of the supernatant supplemented with 650 μL of 10.3 mM N-methyl-2phenyl-indole (Sigma-Aldrich; Saint Louis, MO, USA), which was previously diluted in a mixture of acetonitrile: methanol (3:1) and 150 μL of methanesulfonic acid (Sigma-Aldrich; Saint Louis, MO, USA). This reaction mixture was vortexed and incubated at 45°C for 1 h and then centrifuged at 3000 rpm for 10 min. The absorbance of the reaction in supernatant was read at 586 nm with a SmartSpec 3000 spectrophotometer (Bio-Rad; Hercules, CA, USA). The absorbance values were interpolated from a standard curve of 1,1,3,3-tetramethoxypropane (10 mM stock) in the concentration range of 0.25 to 5 μM to calculate the MDA+4-HDA level in the samples.

2.10. Superoxide Dismutase (SOD) Activity. Total SOD activity was quantified directly in the spectrophotometer quartz cuvette containing 8 μL pyrogallol (initial substrate), 800 μL of Tris-HCl buffer solution (pH 8.2), and 15 μL of EDTA. After 30 s, 60 μL of the supernatant was added, and the absorbance was measured immediately every minute for 3 minutes at 420 nm using a spectrophotometer (Lambda EZ-150; PerkinElmer Company; Waltham, MA, USA). The results were reported as the $\text{U min}^{-1}/\text{mg}$ protein. The equations are detailed in [69].

2.11. Catalase (CAT) Activity. CAT activity was quantified directly in the spectrophotometer quartz cuvette containing 50 μL of the supernatant and 655 μL of PBS 1X. The reaction was initiated by adding 330 μL of H_2O_2 (30 mM), and the absorbance was measured at 240 nm every 30 s for 2 minutes with a spectrophotometer (Lambda EZ-150; PerkinElmer Company; Waltham, MA, USA). The results were reported as the $\text{U min}^{-1}/\text{mg}$ protein [69].

2.12. 2, 3, 5-Triphenyltetrazolium Chloride (TTC) Staining. The tetrazolium salt assays measure mitochondrial activity associated with the electron transport chain, given the rapidity with which most dehydrogenase systems reduce it. Upon reduction, tetrazolium precipitates in the form of a deep red water-insoluble complex. The experimental animals were anesthetized and perfused intracardially with 0.9% isotonic saline solution (SSI); the brains were extracted and coronally sectioned at intervals of 2 mm; then, the sections were incubated for 15 minutes at 37°C in 1% of TTC solution; posteriorly, the tissues were placed overnight in 4% paraformaldehyde solution. After staining, photographs of the brain sections were taken.

2.13. Nissl Staining. Brain slices of 40 μm thick were placed on gelatinized slides, washed with distilled water, and stained with a 0.1% cresyl violet solution (Merck KGaA; San Luis, Missouri, USA) in a 0.25% acetic acid solution for 30 min. Subsequently, the sections were dehydrated in increasing concentrations of ethanol and rinsed with xylene (Hycel; CDMX, Mexico), and Entellan resin (Merck KGaA; Darmstadt, Germany) was used as a mounting medium [11].

2.14. Immunohistochemical Staining. The brains were cryoprotected with 30% sucrose and then cut into 40 μm thick sagittal sections equidistant 1:6. Then, the slices were washed with TBS-1X (Trizma base buffer, pH 7.4) and preincubated with 3% H_2O_2 solution for 30 min to block endogenous peroxidase. After removing excess H_2O_2 with triplicated TBS-1X washes, unspecific binding sites were

blocked with TBS ++ (TBS-1X, Triton X-100, and goat serum) for 30 min at room temperature (RT), and then, the slices were incubated with a primary anti-Iba-1 rabbit antibody (FUJIFILM Wako Chemicals USA Corporation 019-19741) overnight at 4°C. Later, the staining was accomplished using the ABC peroxidase system (the secondary antibody conjugated with biotin and 3,3'-diaminobenzidine (DAB) as a developer). Finally, micrographs of Iba-1 (+) cells were taken with a 20x objective of a microscope (DMLS 2000, Leica Microscope) for further analysis with ImageJ software (RRID: SCR_003070, National Institute of Health).

2.15. ELISA Immunoassay. The ELISA plate of 96 wells (Corning, Camelback, Rd, Glendale, USA) was sensitized with five μg of total protein from the homogenate of the samples and completed to a final volume of 100 μL with carbonate buffer for 24 h at 4°C. Then, the ELISA plates were washed with PBS 1X containing 0.1% Tween 20, and the unspecific binding sites were blocked with 0.5% fetal bovine serum for 30 min. Subsequently, the wells were washed with PBS-0.1% Tween 20, and the primary antibody (dilution 1:500) was added and incubated for 24 h at 4°C. The primary antibodies were mouse anti-nNOS (Sigma Aldrich, SAB4502010), rabbit anti-iNOS (Sigma Aldrich, SAB4502012), rabbit anti-eNOS Rabbit (Sigma Aldrich SAB4502013), rabbit anti-CCL2 (Abcam ab9779), rabbit anti-CXCL1 (Abcam ab9772), rabbit anti-CXCL13 (Abcam ab112521), rabbit anti-CX3CL1 (ThermoFisher SCIEN-TIFIC PA1-29224), rabbit anti-CCR2 (Abcam ab21667), and rabbit anti-CXCR2 (Abcam ab14935). Subsequently, the wells were washed with PBS-0.1% Tween 20, and the secondary polyclonal antibody goat anti-rabbit and goat anti-mouse (dilution 1: 1000; Pierce Technology Co.; Holmdel, NJ, USA) was added. Then, the secondary antibodies conjugated with horseradish peroxidase were incubated for 3 h at RT (1:5000, Pierce Technology Co. Holmdel, NJ, USA), and finally, they were washed with 1X PBS-1% Tween 20, and the ABTS (2,2'-azino-bis- (3-ethyl benzyl-thiazoline-6-sulfonic acid) substrate was incubated for 15 min. The reaction on the plate was read in an ELISA reader (Bio-Rad Benchmark) at 415 nm.

2.16. Hierarchization Score of the Protective Effect of Pharmacological Strategies (HSPEPS). The values of cognitive tests, histopathology, and biochemical probes were expressed according to the modified HSPEPS [69], indicating the efficacy of one or more pharmacological strategies (Register # MX2020010357) treatments. A value lower than healthy was zero, equal to healthy was 1, and higher than healthy was 1.5 or 2, depending on the increasing grade (Table 1). HSPEPS was constructed with the sum of all performance scores of each treatment and study (Table 2).

2.17. Statistical Analysis. The values are mean \pm standard error of the mean (SEM). The difference of escape latency was analyzed with two-way ANOVA and Bonferroni's post hoc multiple comparisons tests, whereas the escape latency on the memory test was analyzed with Kruskal-Wallis and Dunn's post hoc. The elevated plus maze and open-field

TABLE 1: Performance score for each treatment per animal.

Score	Performance
0	Lower than healthy
1	Equal to healthy
1.5-2	Higher than healthy

TABLE 2: Hierarchization score of the protective effect of pharmacological strategies (HSPEPS).

Performance score	Recovering ratio
<Control	Inefficient
=Control	Efficient
>Control	Enhanced

results were analyzed with Student's *t*-test and Welch's post hoc. One-way ANOVA and Dunnett's post hoc were used to analyze the biochemical results, the optical density of Nissl stain, and the number of Iba-1-positive cells in hippocampal areas. All statistical analyses were performed with the Prism software (GraphPad Prism; San Diego, CA, USA; RRID: SCR_0158070). The experimental values were compared with their respective healthy (*), MWM group (Φ), and CCAO group (\dagger). $P < 0.05$ was significant.

3. Results

CCAO caused a loss of acquisition of spatial learning revealed by the increased escape latency ($55.4 \pm 27.09\%$; $\Phi P = 0.0407$) on day 5 of training compared with the MWM group (Figure 2 (a)). In contrast, subacute prophylactic zinc administration significantly decreased the escape latency on days 3 ($32.38 \pm 9.46\%$, $^{\dagger}P = 0.0261$) and 5 ($52.38 \pm 10.21\%$, $^{++}P = 0.0099$) compared with the CCAO group. The Zn group did not show a difference in spatial learning acquisition compared with the MWM group (Figure 2(a)).

Long-term memory test on day 12 postreperfusion showed that CCAO increased the escape latency by $103.44 \pm 17.81\%$ ($\Phi P = 0.0001$), compared with the MWM group (Figure 2(b)). On the contrary, the subacute prophylactic zinc treatment reverted ($44.16 \pm 8.84\%$, $^{+++}P = 0.0249$) the CCAO-induced increase in escape latency (Figure 2 (b)). Furthermore, the CCAO group showed decreased number of platform crossings ($44.16 \pm 8.84\%$; $\Phi P = 0.0249$) compared with the MWM group, which was prevented ($114.88 \pm 17.8\%$; $^{+++}P = 0.0001$) by the subacute prophylactic zinc treatment (Figure 2(c)). These results show that prophylactic zinc administration prevents the cognitive deficit induced by 30 min CCAO.

The elevated plus maze (EPM) test on day 30 postreperfusion showed that CCAO decreased the number of entries to the open arms (OA) ($23.07 \pm 3.84\%$; $\Phi P = 0.0132$) compared with the MWM group (Figure 3(a)). This effect was prevented by the subacute prophylactic zinc administration ($55 \pm 13.22\%$; $^{\dagger}P = 0.0399$) compared with the CCAO group (Figure 3(a)). However, no statistically significant difference

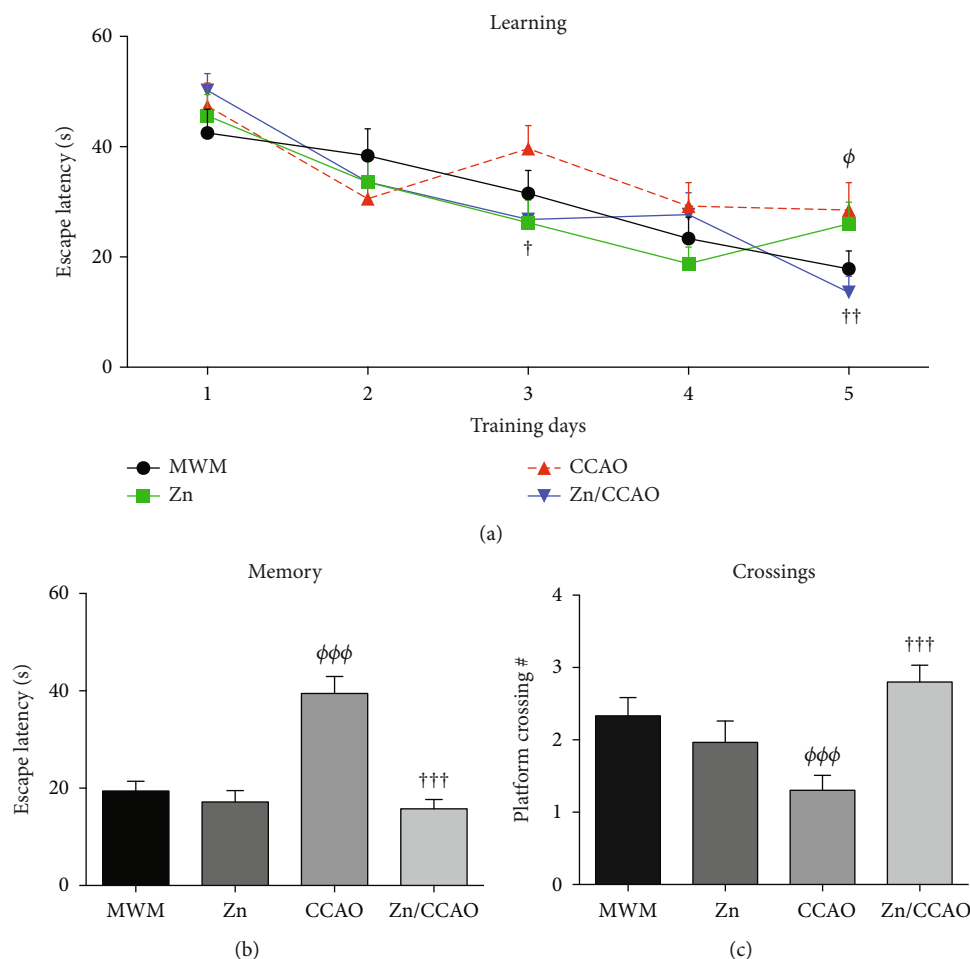


FIGURE 2: The subacute prophylactic zinc administration prevents the cognitive deficit caused by a 30 min CCAO. The values are the mean \pm SEM ($n = 21$ to 30) and analyzed with two-way ANOVA and Bonferroni's post hoc multiple comparisons. In addition, Kruskal-Wallis with Dunn's post hoc test was used to analyze the escape latency in the memory test. $P < 0.05$, ϕ compared with the MWM group and \dagger compared with the CCAO group.

was found in the time of permanency in the OA of EPM (Figure 3(b)). In addition, neither group showed statistically significant differences in the number of urinations and defecations (data not shown).

The open-field test showed that CCAO also affected rat mobility. Both the distance traveled ($32.83 \pm 4.38\%$; $\phi\phi$ $P = 0.0097$) and entries to the central quadrant ($37.16 \pm 7.67\%$; ϕ $P = 0.0379$) were less than those of the MWM group (Figures 3(c) and 3(d)). Those alterations were not modified by subacute prophylactic zinc administration (Figures 3(c) and 3(d)).

The HSPEPS analysis on the cognitive tests showed that the CCAO+MWM group had a lesser value (0.5) than the MWM group (4), and the Zn+CCAO+MWM group yielded values closer to basal values (3.5) of the MWM group (Table 3).

In the temporoparietal cortex, nitrite levels were not different among all experimental groups on day 12 postreperfusion (Figure 4(a)). Meanwhile, in the hippocampus, only the zinc group increased the nitrite levels, while the others groups decreased compared with the healthy group (Figure 4(b)).

However, the MDA+4-HDA levels were significantly elevated in the temporoparietal cortex of all groups compared with the healthy group. The maximum increase was found in the MWM group ($1118.15 \pm 67.31\%$, $***P = 0.0001$), whereas the increase was $591.32 \pm 120.67\%$ ($**P = 0.0025$) in the zinc group, 643.21 ± 40.94 ($**P = 0.0022$) in the CCAO group and 560.34 ± 108.89 ($**P = 0.0038$) in the Zn+CCAO group (Figure 4(c)). In the hippocampus, MDA+4-HDA levels were not different among all groups (Figure 4(d)).

The SOD activity in the temporoparietal cortex (Figure 4(e)) and hippocampus (Figure 4(f)) did not show a statistical difference among all groups on day 12 postreperfusion. However, in this region, CCAO injury increased CAT activity ($242.02 \pm 15.77\%$, $\phi\phi$ $P = 0.0064$) compared with the healthy and MWM groups, and the subacute prophylactic zinc administration reverted this increase ($77.28 \pm 6.58\%$, $\dagger\dagger$ $P = 0.0036$) (Figure 4(g)). In the hippocampus, the CAT activity was not statistically different among all experimental groups (Figure 4(h)).

ELISA measurements in the temporoparietal cortex showed significantly increased NOS levels compared with

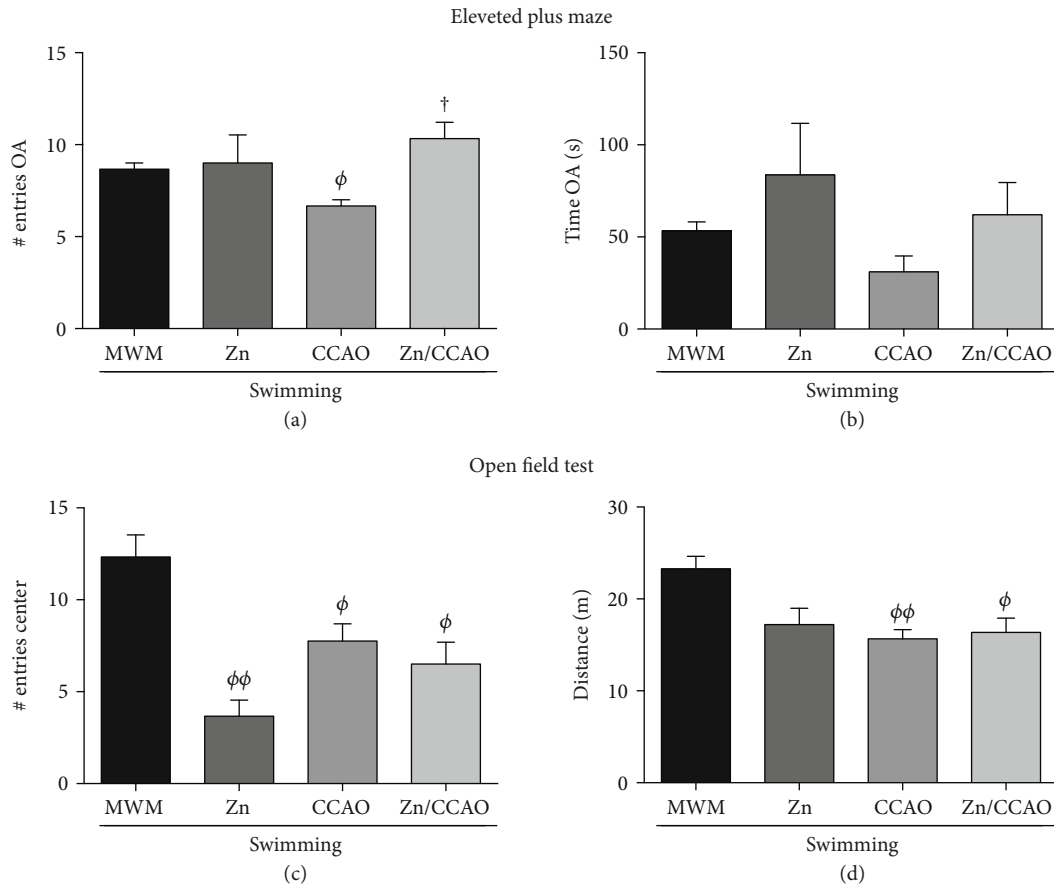


FIGURE 3: The subacute prophylactic zinc administration prevented emotional disturbance but not mobility alterations in rats with a 30 min CCAO on day 30 postreperfusion. The values are mean \pm SEM ($n = 4$) and analyzed with t -test and Welch's post hoc. $P < 0.05$, ϕ compared with the MWM group and \dagger compared with the CCAO group. OA: open arms.

the healthy group on day 12 postreperfusion as follows, nNOS in the CCAO group (Figure 5(a)), iNOS (Figure 5(c)), and eNOS in all groups (Figure 5(e)). The subacute prophylactic zinc administration decreased the levels of nNOS ($13.84 \pm 3.06\%$, $^{\dagger}P = 0.0455$) (Figure 5(a)) and eNOS ($6.12 \pm 0.92\%$, $^{\dagger}P = 0.0161$) compared with the CCAO group (Figure 5(e)). In the hippocampus, no changes related to CCAO and zinc treatment were found in NOS levels on day 12 postreperfusion (Figures 5(b), 5(d), and 5(f)). However, iNOS levels were low ($13.52 \pm 3.61\%$, $\phi P = 0.0316$) in the Zn+CCAO group compared with the rest of the groups (Figure 5(d)), whereas increased eNOS levels ($21.77 \pm 2.96\%$, $\phi P = 0.0305$) were found in the Zn group (Figure 5(f)).

Preliminary results showed that the prophylactic zinc administration in the absence of MWM (Zn+CCAO group) caused greater damage revealed by TTC staining at 24 h and 7 days postreperfusion (data not shown). In contrast, the TTC staining in fresh brains on day 12 postreperfusion showed that the evident infarct core in the CCAO hippocampus was prevented by the prophylactic zinc administration combined with swimming (Zn+CCAO+MWM group) (Figure 6).

Confirming the tissue injury shown by TTC staining (Figure 6), Nissl staining brought about decreased optical density in the three hippocampal layers on day 12 after

TABLE 3: Hierarchization score of the protective effect of pharmacological strategies (HSPEPS) in cognitive test.

Cognitive test	Healthy	MWM	Zn +MWM	CCAO +MWM	Zn/CCAO +MWM
Learning	NA	1	1	0	1
Memory	NA	1	1	0	1
EPM	NA	1	1	0	1
Open field	NA	1	0	0.5	0.5
Total		4	3	0.5	3.5

NA: does not apply.

30 min CCAO compared with the healthy and MWM groups (Figure 7). Meanwhile, the optical density in the three layers was normalized in the Zn+CCAO+MWM group (Figure 7). In addition, healthy rats submitted to the MWM showed a significant increase in optical density in the hippocampus CA3 layer (Figure 7).

Iba-1 immunohistochemistry was used to explore the response of activated microglia cells in the hippocampus. An increased number of Iba-1-positive cells was consistently found in the three hippocampal layers of the CCAO group compared with the healthy group (Figure 8). Surprisingly,

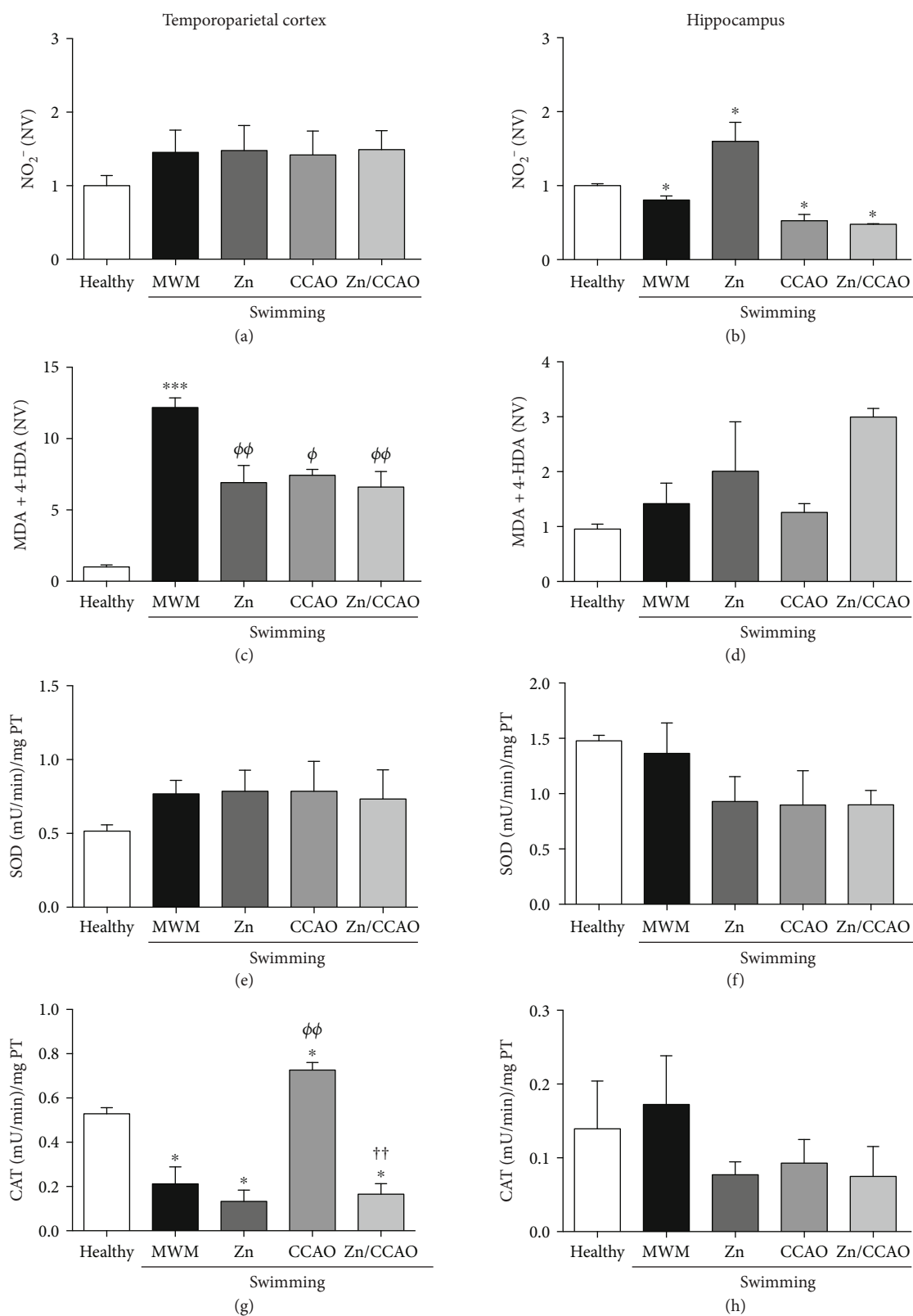


FIGURE 4: The subacute prophylactic zinc administration and swimming prevented nitrosative stress and increased catalase activity on day 12 postreperfusion only in the temporoparietal cortex of rats with 30 min CCAO. The values are mean \pm SEM ($n = 5$) and analyzed with one-way ANOVA and Dunnett's post hoc multiple comparison test. $P < 0.05$, *compared with the Healthy group, ϕ compared with the MWM group, and \dagger compared with the CCAO group; NV: normalized values.

a more considerable increase in Iba-1-positive number was found in the three hippocampal layers than in the CCAO

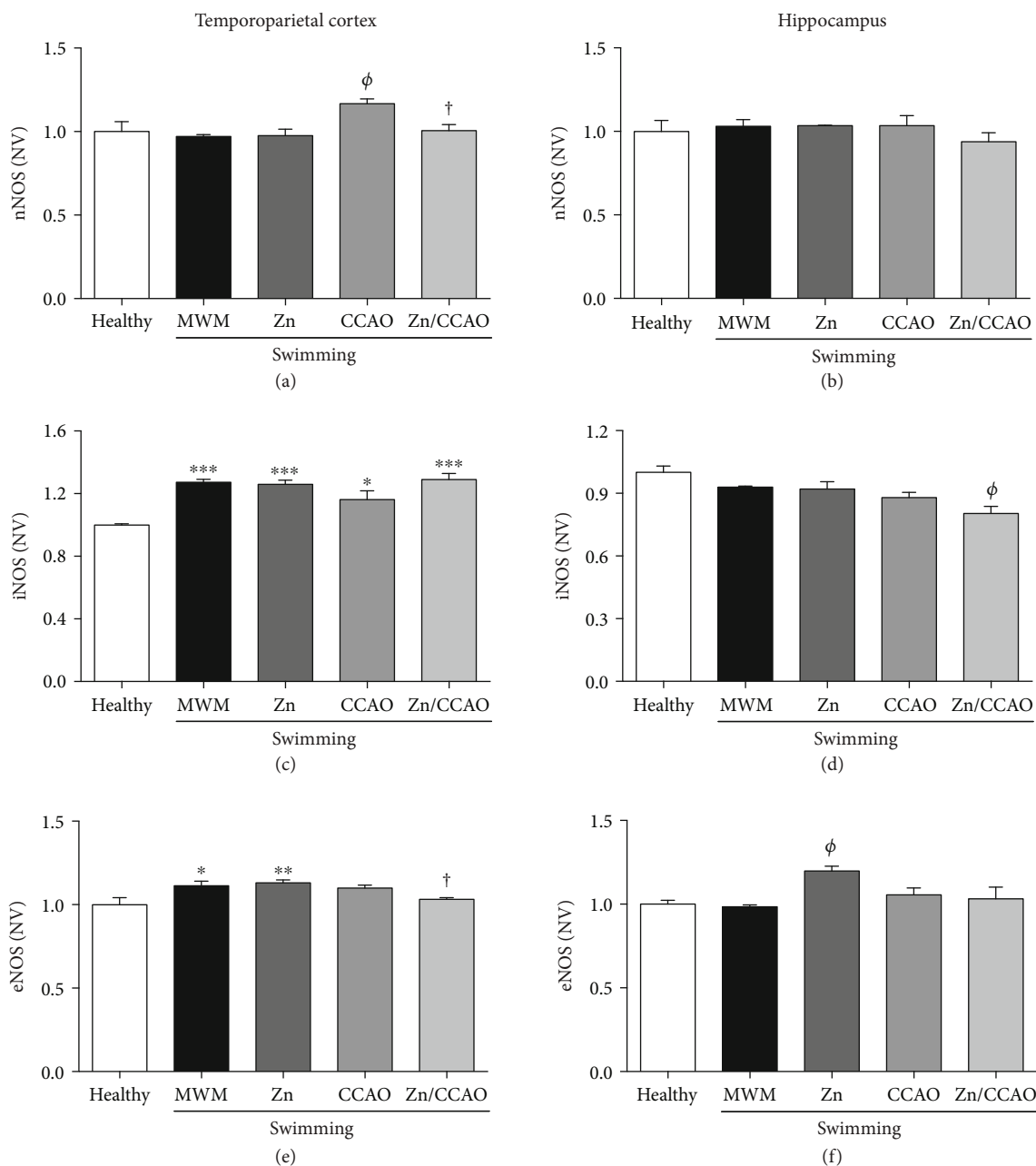


FIGURE 5: The subacute prophylactic zinc and swimming administration prevented increased nNOS and iNOS levels only in the temporoparietal cortex of rats with 30 min CCAO on day 12 postreperfusion. The values are mean \pm SEM ($n = 4$) and analyzed with one-way ANOVA and Dunnett's post hoc multiple comparisons. $P < 0.05$, *compared with the healthy group, ^ϕcompared with the MWM group and [†]compared with the CCAO group. NV: normalized values; nNOS: neuronal nitric oxide synthase; iNOS: inducible nitric oxide synthase; eNOS: endothelial nitric oxide synthase.



FIGURE 6: The subacute prophylactic zinc administration and swimming prevented tissue damage induced by 30 min CCAO in the hippocampus, as revealed by TTC staining. Slices of 2 mm thickness from fresh brains were stained with 2,3,5-triphenyltetrazolium chloride (TTC). Images representative of 3 brains per group. The white arrows indicate the infarct zones in the hippocampus. The arrow indicates the infarct core.

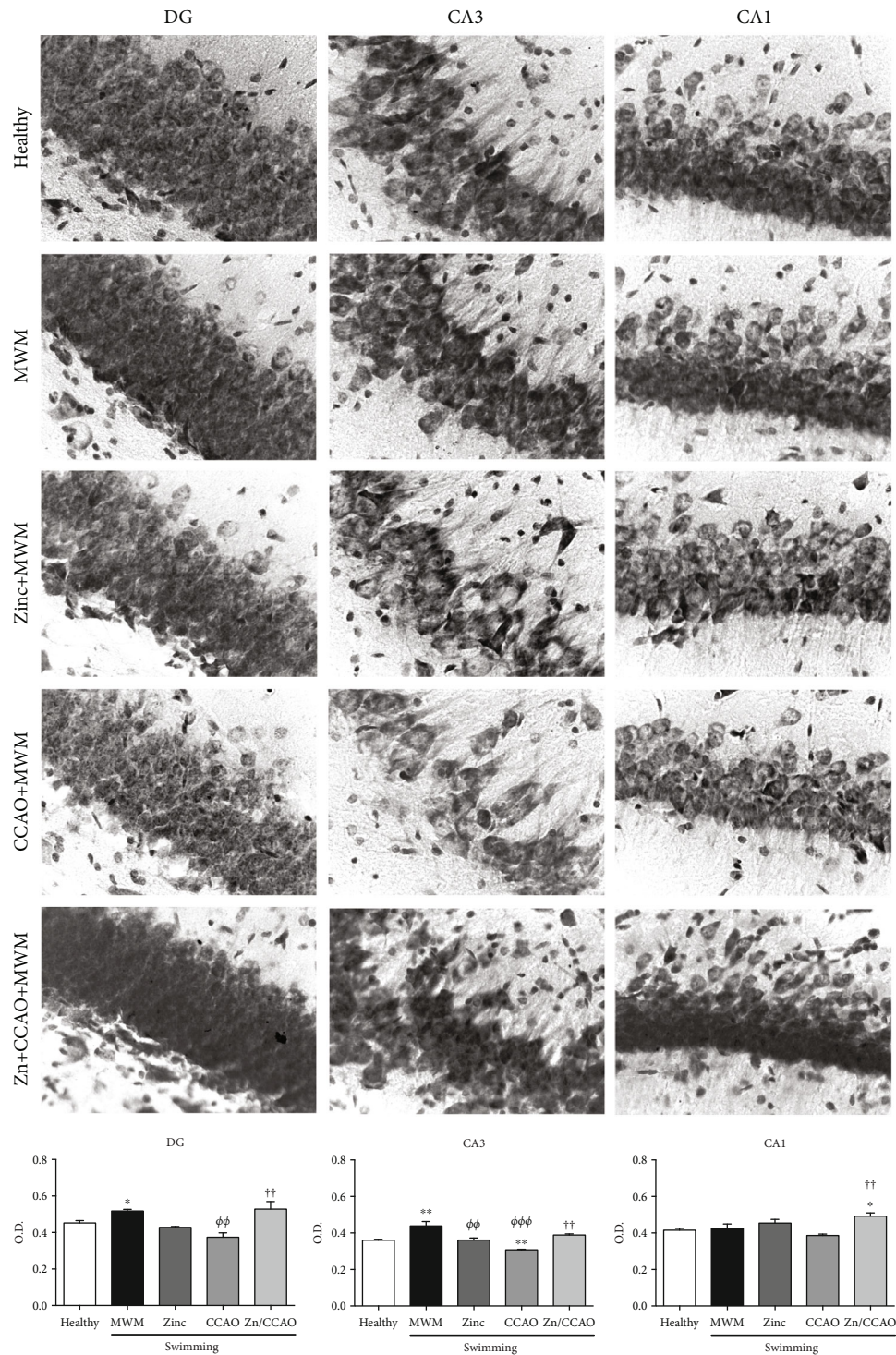


FIGURE 7: The subacute prophylactic zinc administration and swimming (Morris Water Maze, MWM) prevented tissue damage induced by 30 min CCAO in the hippocampus, as revealed by Nissl staining. O.D.: optical density. The values are mean \pm SEM ($n = 4$) and analyzed with one-way ANOVA and Dunnett's post hoc multiple comparisons. $P < 0.05$, *compared with the healthy group, ϕ compared with the MWM group, and \dagger compared with the CCAO group.

group (Figure 8), possibly corresponding to the M2 phenotype microglia response (Figure 8). The number of Iba-1-positive cells was variable in the other groups; whereas it increased in the MWM group, it remained unchanged in the Zn group (Figure 8).

The HSPEPS analysis of the histopathological study showed a high score (7.5) in the MWM group compared to the healthy group (5), and this score was reduced to 5 by the subacute prophylactic zinc administration (Zn+MWM group). On the other hand, the lesser score (4) was seen in

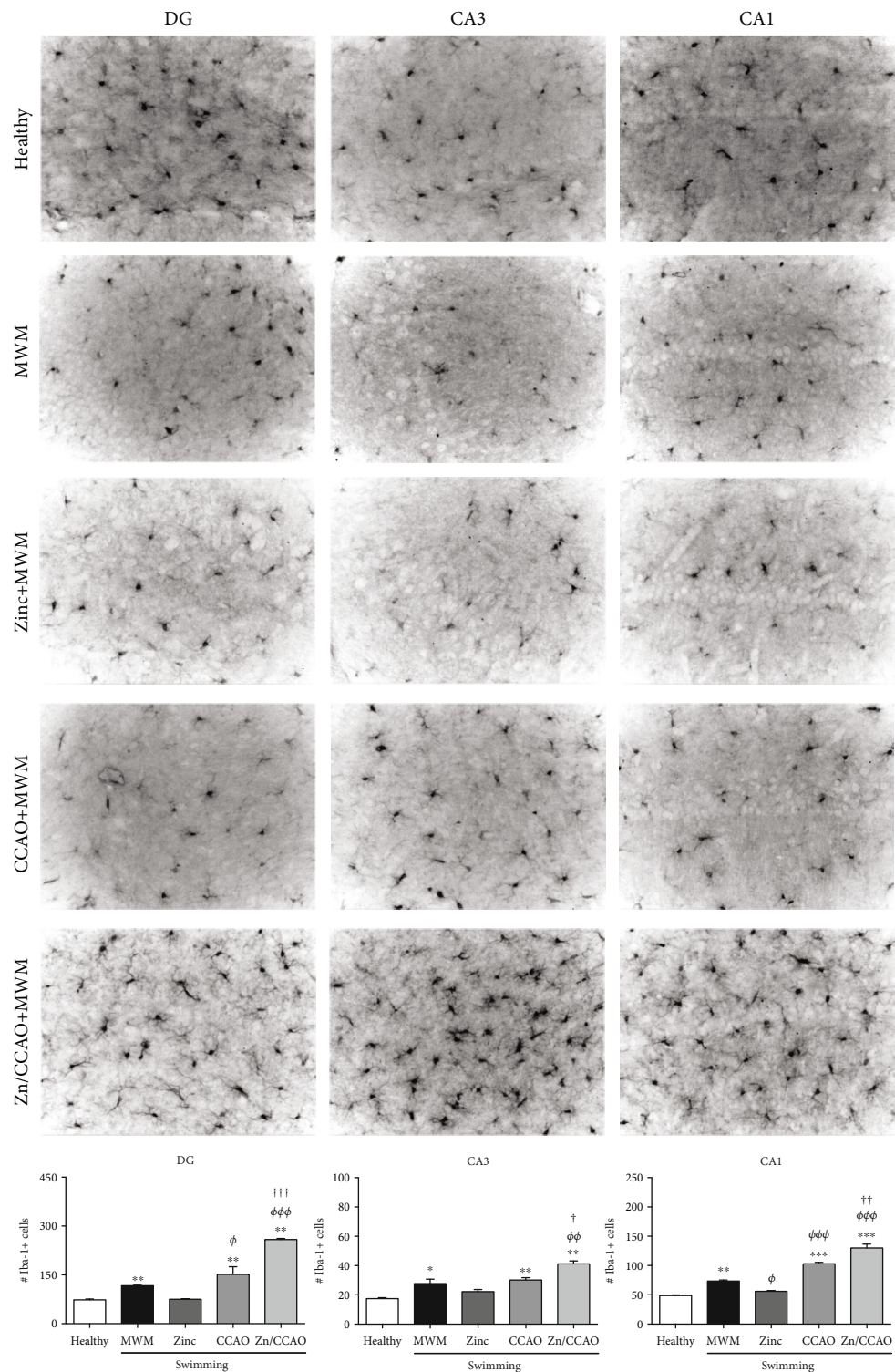


FIGURE 8: The subacute prophylactic zinc administration and swimming (Morris Water Maze, MWM) increased Iba-1 in the hippocampus of rats with 30 min CCAO on day 12 postreperfusion. The values are mean \pm SEM ($n = 4$) and analyzed with one-way ANOVA and Dunnett's post hoc multiple comparisons. $P < 0.05$, *compared with the control group, ϕ compared with the MWM group, and \dagger compared with the CCAO group.

the CCAO+MWM group, revealing the ischemic damage in the hippocampal CA3 layer. Compared with the former group, the score in the Zn+CCAO+MWM group was higher (7), reaching the score in the MWM group (Table 4).

ELISA assays showed variable chemokine levels in all experimental groups of the temporoparietal cortex (Figure 9) and hippocampus (Figure 10). Of relevance to the effect of the combined treatment on ischemia-induced

TABLE 4: Hierarchization score of the protective effect of pharmacological strategies (HSPEPS) in histopathology study.

Histopathology study	Healthy	MWM	Zn+MWM	CCAO+MWM	Zn/CCAO+MWM
TTC	1	1	1	0 hip	1
Nissl hippocampus					
DG	1	2	1	1	1
CA1	1	1	1	1	2
CA3	1	2	1	0	1
Iba-1	1	1.5	1	2	2
Total	5	7.5	5	4	7

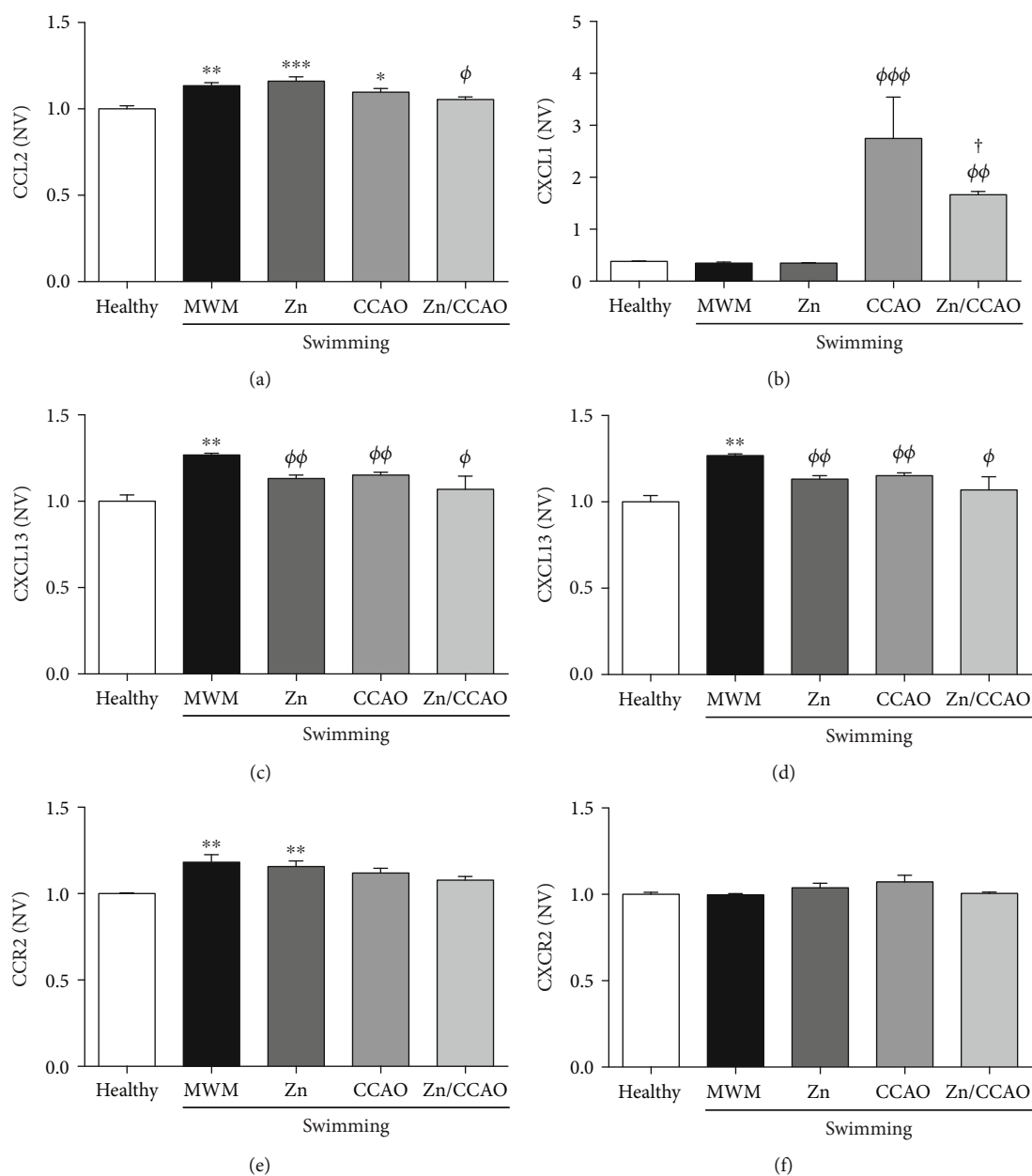


FIGURE 9: The subacute prophylactic zinc administration and swimming partially prevented the CXCL1 increase induced by 30 min CCAO in the temporoparietal cortex on day 12 postreperfusion. The values are mean \pm SEM ($n = 4$) and analyzed with one-way ANOVA and Dunnett's post hoc multiple comparisons. * $P < 0.05$, compared with the control group, ϕ compared with the MWM group, and \dagger compared with the CCAO group. NV: normalized values.

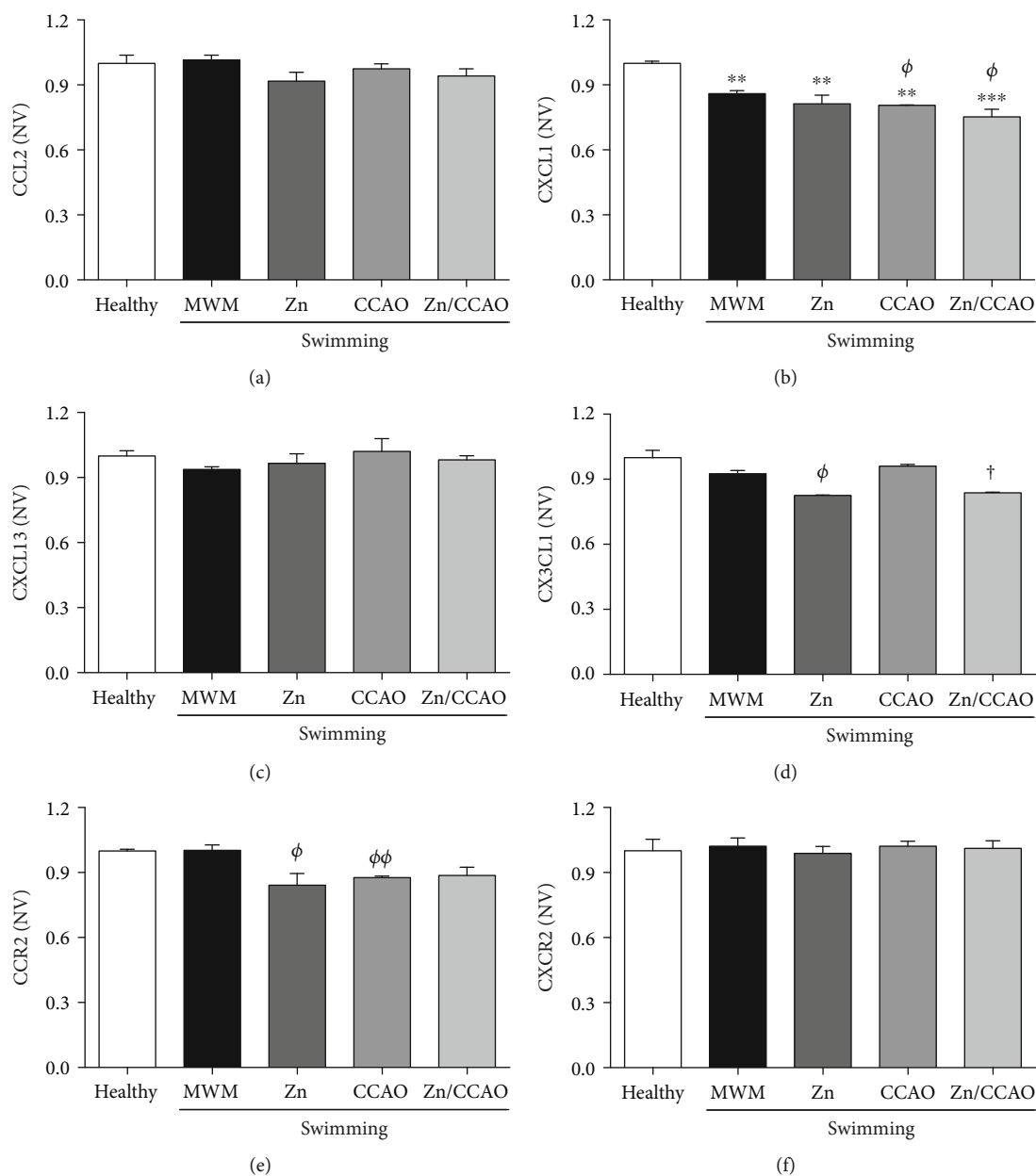


FIGURE 10: CXCL1, CX3CL1, and CCR2 levels were decreased by treatments compared with the MWM group in the hippocampus on day 12 postreperfusion. The values are mean \pm SEM ($n = 4$) and analyzed with one-way ANOVA and Dunnett's post hoc multiple comparisons. $P < 0.05$, *compared with the healthy group, ϕ compared with the MWM group, and \dagger compared with the CCAO group. NV: normalized values.

changes, only CXCL1 was found significantly increased ($688.14 \pm 228.01\%$, $\phi\phi\phi P = 0.0001$) in the temporoparietal cortex of the CCAO group compared with the healthy group (Figure 9(b)). Such an increase was prevented by the subacute prophylactic zinc treatment combined with swimming exercise but could not normalize CXCL1 levels to healthy values (Figure 9(b)).

ELISA assays showed that 30 min CCAO reduced CXCL1 by $14.08 \pm 1.45\%$ ($**P = 0.0095$) (Figure 10(b)) and CCR2 by $14.08 \pm 1.45\%$ ($**P = 0.0095$) (Figure 10(e)) in the hippocampus compared with the healthy group on day 12 postreperfusion. However, this decrease was unchanged

by subacute prophylactic zinc administration combined with swimming (Figures 10(b) and 10(e)).

HSPEPS in biochemical studies included nitrosative stress, NOS isoforms, antioxidant activity, and chemokines. This analysis showed that swimming (MWM group) yielded a higher score (17) than the healthy group (13) that was unmodified by the subacute prophylactic zinc administration (Zn+MWM) and the cerebral ischemia (CCAO+MWM) groups. However, the subacute prophylactic zinc administration combined with a 5-day swimming exercise produced a score (13) similar to the healthy value (Table 5).

TABLE 5: Hierarchization score of the protective effect of pharmacological strategies (HSPEPS) in biochemical studies.

Biochemical studies	Healthy	MWM	Zn +MWM	CCAO +MWM	Zn+CCAO +MWM
LPO	1	2	1.5	1.5	1.5
Nitrites	1	0	2 hip	0	0
SOD	1	1	1	1	1
CAT	1	0	0	2	0
nNOS	1	1	1	2	1
iNOS	1	2	2	2	2
eNOS	1	2	2	1	1
CCL2	1	2	2	2	1
CXCL1	1	1	1	2	1.5
CXCL13	1	2	1	1	1
CX3CL1	1	1	1	1	1
CCR2	1	2	2	1	1
CXCR2	1	1	1	1	1
Total	13	17	17.5	17.5	13

4. Discussion

This work focused on a transient moderate cerebral ischemia whose functional deficiency could still be at least partially reversed by treatments. In particular, the work explored the effect of subacute prophylactic zinc administration combined with swimming exercise on biochemical and cellular alterations in the late stage of ischemia. In this stage, the neurological deficit persists regardless of neuroinflammation which was naturally resolved by the end of the early stage (before two weeks postreperfusion). Our results prove that subacute prophylactic zinc administration combined with a 5-day swimming exercise in MWM avoided the cognitive and emotional deficits commonly presented in the clinic [70, 71], but not motor activity. Furthermore, preventing those deficits is consistent with reducing tissue injury and promoting neuroregeneration in the hippocampus, as TTC and Nissl staining showed. On this basis, it is thought that the increased Iba-1 cell (+) density in the hippocampus would reflect the participation of M2 phenotype microglia trying to remove cell detritus rather than the neuroinflammatory process endurance. Similarly, the increase in nitrosative stress, nNOS, iNOS, and CAT activity in the temporoparietal cortex in the CCAO group might reflect a late postischemic sequel in this region that can account for the reduced free mobility in the open field and its resistance to treatment with the subacute prophylactic zinc administration combined with swimming at 30 days postreperfusion. Preliminary studies show that 2.5 mg/kg subacute prophylactic administration in the absence of swimming caused severe cerebral damage after CCAO at 24 h and 7 days postreperfusion (data not shown). This harmful effect can be caused by the higher zinc concentration accumulated in the brain [49] due to the zinc treatment and the released zinc from presynaptic vesicles following long times of artery occlusion, thus leading to excitotoxicity [72]. On this basis,

we utilized the zinc treatment combined with swimming exercise in a transient ischemic process of 30 min.

4.1. Swimming Exercise and Nitrosative Stress. Different modalities of swimming exercise are known to elicit a preconditioning effect [73, 74], able to attenuate or reverse cerebral injury in the early stage after ischemia [75], and improve cognition [76]. Furthermore, NO production from the three NOS isoforms [77] and increased hydroxyl radical rate [78] triggered by aerobic exercise participate in the formation of associative and spatial memory [79]. Our results in the temporoparietal cortex in the MWM group showed that swimming exercise during the late stage of ischemia increased lipid peroxidation, iNOS, and eNOS, events also associated with improved sensory and motor skills [80], spatial recognition, and long-term learning and memory [81]. Altogether, these findings support that NO plays a critical role in synaptic transmission, acting as a retrograde neurotransmitter [79], and that ROS are required in LTP formation, increasing memory acquisition and consolidation [82, 83].

We found that rats with 30 min CCAO submitted to swimming exercise presented learning and memory loss on day 12 postreperfusion, showing that swimming exercise alone was insufficient to avoid cerebral ischemic damage. In contrast, the prevention of cognitive deficits and tissue damage was achieved with the addition of subacute prophylactic zinc administration. eNOS likely mediates this beneficial effect since exercise prevents vascular endothelium dysfunction [77, 84, 85], reduces infarct volume [86], and promotes nerve repair after cerebral ischemia [77]. Furthermore, zinc stabilizing eNOS increases its enzymatic activity [87]. On the contrary, zinc deficiency increases O_2^- levels by eNOS, promoting cerebral damage [88], as could occur in the CCAO group.

An increasing number of reports have associated the protective effect of zinc with swimming exercise stimulation and improved cell functioning [89, 90]. Accordingly, swimming training using MWM protects hippocampal neurons against degenerative changes and improves learning and memory [51]. Furthermore, oral supplementation of 16 or 32 ppm $ZnSO_4$ [91, 92] and subacute intraperitoneal administration of 2.5 mg/kg of $ZnCl_2$ [41] or 0.2 mg/kg chronically administered [42] prevent memory loss in ischemia or TBI [41, 42, 51]. The protective effect of exercise and zinc is proposed to be mediated by increasing the expression of growth factors [41] through regulating CREB [67] and antioxidant enzymes, such as SOD [42] and CAT, in animal damage models [93, 94]. These neuroprotective events are shown to occur in the early stage (day 7) postreperfusion when ROS is elevated by the ischemic process [95, 96], as confirmed by unpublished results of our group. However, in the late stage (day 12), zinc and swimming exercise did not modify SOD and CAT activity in the hippocampus but decreased the CCAO-activated CAT activity in the temporoparietal cortex. These results suggest that the increased CAT activity in the ischemic group reflects a response to oxidative stress, which is prevented by zinc combined with swimming. In addition, zinc decreases CAT activity in neonate rats [69] through the regulation of ERK phosphorylation [97].

Furthermore, zinc can exert an anxiolytic effect [98] by decreasing the inflammatory process [99], nNOS [100], and cell damage [99]; increasing antioxidant enzymes [101], BDNF [102], and synaptic plasticity; modulating neurochemical transmission [103]; regulating the activity of NMDA receptors [103–105]; and reducing the ischemic damage [106].

In addition, several studies show that the administration of NMDA receptor antagonists prevented tissue damage [107, 108] and modified some aspects of behavior [108], which can be enhanced by hypothermia caused by anesthesia [109]. In this work, we used ketamine which has been useful in models of ischemia, being capable of reducing the damage when administered superacute and therapeutically mode [110, 111], due to its inhibitor effect on glutamate receptors [112].

Accordingly, subacute prophylactic zinc administration combined with swimming increased the entry to the open arms in the elevated plus maze, thus showing that the combined treatment prevented the CCAO-induced anxiety. However, the combined treatment could not improve motor skills in the open field, as reported in the TBI model [51]. These results show that the subacute prophylactic zinc administration combined with swimming zinc partially protects the sequel of ischemic damage on day 30 after reperfusion.

4.2. Zinc Administration Combined with Swimming Prevents Tissue Injury. The 30 min hypoxia-ischemia model causes neuronal death that remains until seven days in the infarct core [24], whereas in the penumbra zone, highly plastic events triggered lead to tissue regeneration 14 days postreperfusion [27]. Our results agree with both events. First, the CCAO group showed signs of infarct on day 12 postreperfusion, revealed by the decreased cell density mainly in DG and CA3 layers of the hippocampus that coincides with the reduced cell viability. Second, the recovery of cell density and viability in the hippocampus in the Zn+CCAO group indicates that the subacute prophylactic zinc administration induced potentiation of plastic events. A similar effect was observed in a 10 min CCAO model [11], thus showing that the zinc neuroprotector effect combined with swimming is still effective in a cerebral injury of 30 min CCAO, reported previously in a 10 min model [11, 41, 42].

Tissue recovery from CNS injury also involves the participation of microglia [113]. The CCAO group showed an increased Iba-1(+) cell number to the healthy group on day 12 postreperfusion, suggesting that the natural course of both neuroinflammation and tissue recovery has yet not terminated on day 12 postreperfusion. However, subacute prophylactic zinc administration combined with swimming increased the Iba-1 (+) cell population over that of the CCAO group on day 12 postreperfusion. This result agrees with the previous report showing that the Iba-1 (+) cell number is still high at this time and decreased at 14 days postreperfusion [27]. However, subacute prophylactic zinc administration combined with swimming decreased the protein levels of chemokines (CXCL1, CCL2, CXCL13, and CX3CL1), the three isoforms of NOS, and the tissue damage caused by CCAO, showing a decrease in the neuroinflammatory process. These results also suggest that the combined

treatment modulated the inflammation process, decreasing chemoattraction of leukocytes such as neutrophils by CXCL1 [114], macrophage/microglia by CCL2 [115] and CX3CL1 [116], and lymphocyte B, natural killer cells [117], and M1 microglia activation [118] by CXCL13 [119]. Therefore, the increase in microglial cells does not indicate a harmful effect but their participation in removing cell detritus.

In contrast, some reports have shown that these chemokines also have a neuroprotector effect in the late phase postreperfusion. For instance, CCL2 chemoattracts neuroblasts [120] and promotes neurogenesis [121] and synaptic plasticity in the hippocampus [122], thus decreasing the infarct size and recovering the cognitive function [41, 123]. In addition, CXCL1 promotes the remyelination process through the migration and maturation of oligodendrocytes [124]. Furthermore, CXCL13 induces proliferation and autophagy of mesenchymal stem cells [125] and has a chemoattractant action of neuroblast [126], and CX3CL1 causes the chemoattraction and differentiation of neural precursor cells [127] and reduces the microglia reactivity, decreasing neuroinflammation [128, 129]. However, the decrease in these chemokines by prophylactic zinc administration combined with zinc could affect those recovery processes in the long term.

The HSPEPS analysis reported previously [69] shows that in the CCAO+MWM group, the tissue damage correlates with the cognitive dysfunction, although biochemically; there are no differences with the MWM group. The MWM group showed a more beneficial effect on hippocampal cytoarchitecture and biochemical variables than the healthy control group. However, the subacute zinc prophylactic administration blocked the cognitive deficit and tissue damage caused by CCAO, and such effect was unmodified on the biochemical variables. In contrast, the score equality to the healthy control and MWM values observed in the Zn +CCAO+MWM in all the tests shows that the prophylactic zinc administration combined with swimming exercise prevented the 30 min CCAO-induced ischemic damage. In summary, HSPEPS analysis proves that the individual treatment did not cause the expected effect, i.e., a preconditioning effect by the prophylactic zinc administration or the therapeutic effect by swimming. However, effective neuroprotection against ischemic damage induced by 30 min CCAO in the rat was reached by combining the prophylactic and therapeutic strategies.

5. Conclusion

Prophylactic zinc administration combined with swimming exercise prevented ischemic damage in the 30 min CCAO model by decreasing neuroinflammation and nitrosative stress, preventing cell death, and improving the spatial learning-memory on day 12 postreperfusion and anxiety-like behavior on day 30 postreperfusion. These results suggest that subacute prophylactic zinc administration requires another complementary therapeutic approach to maintain the neuroprotector effect in the late phase of cerebral hypoxia-ischemia.

Data Availability

Data is included in this manuscript.

Conflicts of Interest

The authors declare that they have no conflicts of interest.

Authors' Contributions

Ana Karina Aguilar-Peralta and Alejandro Gonzalez-Vazquez were responsible for the methodology, formal analysis, investigation, writing original draft, review, and editing. Victor M. Blanco-Alvarez was responsible for the validation and investigation. Constantino Tomas-Sanchez was responsible for validation and investigation. Juan A. Gonzalez-Barrios was responsible for resources and funding acquisition. Daniel Martinez-Fong was responsible for animal supply, writing, review, and editing. Guadalupe Soto-Rodriguez was responsible for the methodology. Eduardo Brambila was responsible for formal statistical analysis. Lourdes Millán-Perez Peña was responsible for the resources. Viridiana Vargas-Castro helped in revision of article, Bertha Alicia Leon-Chavez was responsible for conceptualization, project administration, visualization, supervision, funding acquisition, writing, review, and editing.

Acknowledgments

Grant number VIEP-BUAP (100293600-2019) and Hospital 1° de Octubre, ISSSTE (ISSSTE-E015-RPI-033.2015), supported this work. AGV and AKAP received postgraduate scholarships from CONACYT. We thank the vivariums of CINVESTAV and BUAP for the care and maintenance of the test animals.

References

- [1] X. Hu, T. M. De Silva, J. Chen, and F. M. Faraci, "Cerebral vascular disease and neurovascular injury in ischemic stroke," *Circulation Research*, vol. 120, no. 3, pp. 449–471, 2017.
- [2] WHO, "Stroke, Cerebrovascular accident," <http://www.emro.who.int/health-topics/stroke-cerebrovascular-accident/index.html/>.
- [3] J. M. Wardlaw, C. Smith, and M. Dichgans, "Mechanisms of sporadic cerebral small vessel disease: insights from neuroimaging," *Lancet Neurology*, vol. 12, no. 5, pp. 483–497, 2013.
- [4] C. Xing, K. Arai, E. H. Lo, and M. Hommel, "Pathophysiologic cascades in ischemic stroke," *International Journal of Stroke*, vol. 7, no. 5, pp. 378–385, 2012.
- [5] J. C. Chavez, O. Hurko, F. C. Barone, and G. Z. Feuerstein, "Pharmacologic interventions for stroke: looking beyond the thrombolysis time window into the penumbra with biomarkers, not a stopwatch," *Stroke*, vol. 40, no. 10, pp. e558–e563, 2009.
- [6] Y. Shi, L. Zhang, H. Pu et al., "Rapid endothelial cytoskeletal reorganization enables early blood-brain barrier disruption and long-term ischaemic reperfusion brain injury," *Nature Communications*, vol. 7, no. 1, p. 10523, 2016.
- [7] I. Unal-Cevik, Y. Gursay-Ozdemir, M. Yemisci et al., "Alpha-synuclein aggregation induced by brief ischemia negatively impacts neuronal survival in vivo: a study in [A30P]alpha-synuclein transgenic mouse," *Journal of Cerebral Blood Flow and Metabolism*, vol. 31, no. 3, pp. 913–923, 2011.
- [8] Y. C. Liu, Y. D. Lee, H. L. Wang et al., "Anesthesia-induced hypothermia attenuates early-phase blood-brain barrier disruption but not infarct volume following cerebral ischemia," *PLoS One*, vol. 12, no. 1, article e0170682, 2017.
- [9] M. Franke, M. Bieber, P. Kraft, A. N. R. Weber, G. Stoll, and M. K. Schuhmann, "The NLRP3 inflammasome drives inflammation in ischemia/reperfusion injury after transient middle cerebral artery occlusion in mice," *Brain, Behavior, and Immunity*, vol. 92, pp. 221–231, 2021.
- [10] P. Aguilar-Alonso, D. Martinez-Fong, N. G. Pazos-Salazar et al., "The increase in zinc levels and upregulation of zinc transporters are mediated by nitric oxide in the cerebral cortex after transient ischemia in the rat," *Brain Research*, vol. 1200, pp. 89–98, 2008.
- [11] V. M. Blanco-Alvarez, P. Lopez-Moreno, G. Soto-Rodriguez et al., "Subacute zinc administration and L-NAME caused an increase of NO, zinc, lipoperoxidation, and caspase-3 during a cerebral hypoxia-ischemia process in the rat," *Oxidative Medicine and Cellular Longevity*, vol. 2013, Article ID 240560, 10 pages, 2013.
- [12] M. D. Ginsberg, D. I. Graham, and R. Busto, "Regional glucose utilization and blood flow following graded forebrain ischemia in the rat: correlation with neuropathology," *Annals of Neurology*, vol. 18, no. 4, pp. 470–481, 1985.
- [13] D. Tsuchiya, S. Hong, Y. Matsumori et al., "Overexpression of rat heat shock protein 70 reduces neuronal injury after transient focal ischemia, transient global ischemia, or kainic acid-induced seizures," *Neurosurgery*, vol. 53, no. 5, pp. 1179–1188, 2003.
- [14] W. D. Heiss, R. Graf, T. Fujita et al., "Early detection of irreversibly damaged ischemic tissue by flumazenil positron emission tomography in cats," *Stroke*, vol. 28, no. 10, pp. 2045–2052, 1997.
- [15] F. A. Welsh, M. D. Ginsberg, W. Rieder, and W. W. Budd, "Diffuse cerebral ischemia in the cat: II. Regional metabolites during severe ischemia and recirculation," *Annals of Neurology*, vol. 3, no. 6, pp. 493–501, 1978.
- [16] H. A. Awooda, M. F. Lutfi, G. G. Sharara, and A. M. Saeed, "Oxidative/nitrosative stress in rats subjected to focal cerebral ischemia/reperfusion," *Int J Health Sci (Qassim)*, vol. 9, no. 1, pp. 17–24, 2015.
- [17] F. Liu and L. D. McCullough, "The middle cerebral artery occlusion model of transient focal cerebral ischemia," *Methods in Molecular Biology*, vol. 1135, pp. 81–93, 2014.
- [18] T. R. Sairanen, P. J. Lindsberg, M. Brenner, and A. L. Siren, "Global forebrain ischemia results in differential cellular expression of interleukin-1beta (IL-1beta) and its receptor at mRNA and protein level," *Journal of Cerebral Blood Flow and Metabolism*, vol. 17, no. 10, pp. 1107–1120, 1997.
- [19] H. Pawluk, A. Wozniak, G. Grzesk et al., "The role of selected pro-inflammatory cytokines in pathogenesis of ischemic stroke," *Clinical Interventions in Aging*, vol. 15, pp. 469–484, 2020.
- [20] L. Pang, W. Ye, X. M. Che, B. J. Roessler, A. L. Betz, and G. Y. Yang, "Reduction of inflammatory response in the mouse brain with adenoviral-mediated transforming growth factor- α expression," *Stroke*, vol. 32, no. 2, pp. 544–552, 2001.
- [21] V. Supanc, Z. Biloglav, V. B. Kes, and V. Demarin, "Role of cell adhesion molecules in acute ischemic stroke," *Annals of Saudi Medicine*, vol. 31, no. 4, pp. 365–370, 2011.

- [22] W. Zhou, A. Liesz, H. Bauer et al., "Postischemic brain infiltration of leukocyte subpopulations differs among murine permanent and transient focal cerebral ischemia models," *Brain Pathology*, vol. 23, no. 1, pp. 34–44, 2013.
- [23] J. H. Park, J. H. Cho, J. H. Ahn et al., "Neuronal loss and gliosis in the rat striatum subjected to 15 and 30 minutes of middle cerebral artery occlusion," *Metabolic Brain Disease*, vol. 33, no. 3, pp. 775–784, 2018.
- [24] L. Buscemi, M. Price, P. Bezzi, and L. Hirt, "Spatio-temporal overview of neuroinflammation in an experimental mouse stroke model," *Scientific Reports*, vol. 9, no. 1, p. 507, 2019.
- [25] B. Y. Choi, S. J. Won, J. H. Kim et al., "EAAC1 gene deletion reduces adult hippocampal neurogenesis after transient cerebral ischemia," *Scientific Reports*, vol. 8, no. 1, p. 6903, 2018.
- [26] A. E. Dief, P. S. Hassan, O. Hartmut, and G. F. Jirikowski, "Neuronal and glial regeneration after focal cerebral ischemia in rat, an immunohistochemical and electron microscopical study," *Alexandria Journal of Medicine*, vol. 54, no. 4, pp. 699–704, 2018.
- [27] H. Li, N. Zhang, H. Y. Lin et al., "Histological, cellular and behavioral assessments of stroke outcomes after photothrombosis-induced ischemia in adult mice," *BMC Neuroscience*, vol. 15, no. 1, p. 58, 2014.
- [28] K. Wakayama, M. Shimamura, M. Sata et al., "Quantitative measurement of neurological deficit after mild (30 min) transient middle cerebral artery occlusion in rats," *Brain Research*, vol. 1130, no. 1, pp. 181–187, 2007.
- [29] T. Freret, L. Chazalviel, S. Roussel, M. Bernaudin, P. Schumann-Bard, and M. Boulouard, "Long-term functional outcome following transient middle cerebral artery occlusion in the rat: correlation between brain damage and behavioral impairment," *Behavioral Neuroscience*, vol. 120, no. 6, pp. 1285–1298, 2006.
- [30] K. M. Sicard, N. Henninger, M. Fisher, T. Q. Duong, and C. F. Ferris, "Long-term changes of functional MRI-based brain function, behavioral status, and histopathology after transient focal cerebral ischemia in rats," *Stroke*, vol. 37, no. 10, pp. 2593–2600, 2006.
- [31] W. Zhong, Y. Yuan, X. Gu et al., "Neuropsychological deficits chronically developed after focal ischemic stroke and beneficial effects of pharmacological hypothermia in the mouse," *Aging and Disease*, vol. 11, no. 1, pp. 1–16, 2020.
- [32] R. M. Umarova, C. Sperber, C. P. Kaller et al., "Cognitive reserve impacts on disability and cognitive deficits in acute stroke," *Journal of Neurology*, vol. 266, no. 10, pp. 2495–2504, 2019.
- [33] M. A. Hirsch and B. G. Farley, "Exercise and neuroplasticity in persons living with Parkinson's disease," *European Journal of Physical and Rehabilitation Medicine*, vol. 45, no. 2, pp. 215–229, 2009.
- [34] D. Pamplona-Santos, K. Lamarao-Vieira, P. C. Nascimento et al., "Aerobic physical exercise as a neuroprotector strategy for ethanol binge-drinking effects in the hippocampus and systemic redox status in rats," *Oxidative Medicine and Cellular Longevity*, vol. 2019, Article ID 2415243, 12 pages, 2019.
- [35] C. Wu, L. Yang, D. Tucker et al., "Beneficial effects of exercise pretreatment in a sporadic Alzheimer's rat model," *Medicine and Science in Sports and Exercise*, vol. 50, no. 5, pp. 945–956, 2018.
- [36] F. Chali, C. Desseille, L. Houdebine et al., "Long-term exercise-specific neuroprotection in spinal muscular atrophy-like mice," *The Journal of Physiology*, vol. 594, no. 7, pp. 1931–1952, 2016.
- [37] L. Marais, D. J. Stein, and W. M. Daniels, "Exercise increases BDNF levels in the striatum and decreases depressive-like behavior in chronically stressed rats," *Metabolic Brain Disease*, vol. 24, no. 4, pp. 587–597, 2009.
- [38] L. Just-Borrás, E. Hurtado, V. Cilleros-Mane et al., "Running and swimming prevent the deregulation of the BDNF/TrkB neurotrophic signalling at the neuromuscular junction in mice with amyotrophic lateral sclerosis," *Cellular and Molecular Life Sciences*, vol. 77, no. 15, pp. 3027–3040, 2020.
- [39] D. M. Camera, W. J. Smiles, and J. A. Hawley, "Exercise-induced skeletal muscle signaling pathways and human athletic performance," *Free Radical Biology & Medicine*, vol. 98, pp. 131–143, 2016.
- [40] I. Kwon, W. Song, Y. Jang, M. D. Choi, D. M. Vinci, and Y. Lee, "Elevation of hepatic autophagy and antioxidative capacity by endurance exercise is associated with suppression of apoptosis in mice," *Annals of Hepatology*, vol. 19, no. 1, pp. 69–78, 2020.
- [41] V. M. Blanco-Alvarez, G. Soto-Rodriguez, J. A. Gonzalez-Barrios et al., "Prophylactic subacute administration of zinc increases CCL2, CCR2, FGF2, and IGF-1 expression and prevents the long-term memory loss in a rat model of cerebral hypoxia-ischemia," *Neural Plasticity*, vol. 2015, Article ID 375391, 15 pages, 2015.
- [42] C. Tomas-Sanchez, V. M. Blanco-Alvarez, D. Martinez-Fong et al., "Prophylactic zinc and therapeutic selenium administration increases the antioxidant enzyme activity in the rat temporoparietal cortex and improves memory after a transient hypoxia-ischemia," *Oxidative Medicine and Cellular Longevity*, vol. 2018, Article ID 9416432, 17 pages, 2018.
- [43] R. Aquilani, P. Baiardi, M. Scocchi et al., "Normalization of zinc intake enhances neurological retrieval of patients suffering from ischemic strokes," *Nutritional Neuroscience*, vol. 12, no. 5, pp. 219–225, 2009.
- [44] K. Matsushita, K. Kitagawa, T. Matsuyama et al., "Effect of systemic zinc administration on delayed neuronal death in the gerbil hippocampus," *Brain Research*, vol. 743, no. 1–2, pp. 362–365, 1996.
- [45] Y. J. Zhao, G. Y. Yang, and E. F. Domino, "Zinc protoporphyrin, zinc ion, and protoporphyrin reduce focal cerebral ischemia," *Stroke*, vol. 27, no. 12, pp. 2299–2303, 1996.
- [46] G. K. Helal, "Systemic administration of Zn²⁺ during the reperfusion phase of transient cerebral ischaemia protects rat hippocampus against iron-catalysed postischaemic injury," *Clinical and Experimental Pharmacology & Physiology*, vol. 35, no. 7, pp. 775–781, 2008.
- [47] C. Tomas-Sanchez, V. M. Blanco-Alvarez, J. A. Gonzalez-Barrios et al., "Prophylactic chronic zinc administration increases neuroinflammation in a hypoxia-ischemia model," *Journal of Immunology Research*, vol. 2016, Article ID 4039837, 15 pages, 2016.
- [48] B. L. Sun, W. An, Z. L. Xia et al., "Zinc protoporphyrin aggravates cerebral ischemic injury following experimental subarachnoid hemorrhage," *Clinical Hemorheology and Microcirculation*, vol. 34, no. 1–2, pp. 241–246, 2006.
- [49] J. Y. Koh, S. W. Suh, B. J. Gwag, Y. Y. He, C. Y. Hsu, and D. W. Choi, "The role of zinc in selective neuronal death after transient global cerebral ischemia," *Science*, vol. 272, no. 5264, pp. 1013–1016, 1996.

- [50] D. R. Morris and C. W. Levenson, "Zinc in traumatic brain injury," *Current Opinion in Clinical Nutrition and Metabolic Care*, vol. 16, no. 6, pp. 708–711, 2013.
- [51] E. C. Cope, D. R. Morris, A. G. Scrimgeour, J. W. VanLandingham, and C. W. Levenson, "Zinc supplementation provides behavioral resiliency in a rat model of traumatic brain injury," *Physiology & Behavior*, vol. 104, no. 5, pp. 942–947, 2011.
- [52] E. C. Cope, D. R. Morris, and C. W. Levenson, "Improving treatments and outcomes: an emerging role for zinc in traumatic brain injury," *Nutrition Reviews*, vol. 70, no. 7, pp. 410–413, 2012.
- [53] C. T. Anderson, R. J. Radford, M. L. Zastrow et al., "Modulation of extrasynaptic NMDA receptors by synaptic and tonic zinc," *Proceedings of the National Academy of Sciences of the United States of America*, vol. 112, no. 20, pp. E2705–E2714, 2015.
- [54] F. Jalali-Yazdi, S. Chowdhury, C. Yoshioka, and E. Gouaux, "Mechanisms for zinc and proton inhibition of the GluN1/GluN2A NMDA receptor," *Cell*, vol. 175, no. 6, pp. 1520–1532, 2018.
- [55] M. Jarosz, M. Olbert, G. Wyszogrodzka, K. Mlyniec, and T. Librowski, "Antioxidant and anti-inflammatory effects of zinc. Zinc-dependent NF- κ B signaling," *Inflammopharmacology*, vol. 25, no. 1, pp. 11–24, 2017.
- [56] Y. Zhao, Y. Tan, J. Dai et al., "Exacerbation of diabetes-induced testicular apoptosis by zinc deficiency is most likely associated with oxidative stress, p38 MAPK activation, and p53 activation in mice," *Toxicology Letters*, vol. 200, no. 1–2, pp. 100–106, 2011.
- [57] A. Travaglia and D. La Mendola, "Zinc interactions with brain-derived neurotrophic factor and related peptide fragments," *Vitamins and Hormones*, vol. 104, pp. 29–56, 2017.
- [58] Y. Z. Huang, E. Pan, Z. Q. Xiong, and J. O. McNamara, "Zinc-mediated transactivation of TrkB potentiates the hippocampal mossy fiber-CA3 pyramid synapse," *Neuron*, vol. 57, no. 4, pp. 546–558, 2008.
- [59] M. Galvez-Peralta, Z. Wang, S. Bao, D. L. Knoell, and D. W. Nebert, "Tissue-specific induction of mouse ZIP8 and ZIP14 divalent cation/bicarbonate symporters by, and cytokine response to, inflammatory signals," *International Journal of Toxicology*, vol. 33, no. 3, pp. 246–258, 2014.
- [60] J. Zhan, W. Qin, Y. Zhang et al., "Upregulation of neuronal zinc finger protein A20 expression is required for electroacupuncture to attenuate the cerebral inflammatory injury mediated by the nuclear factor- κ B signaling pathway in cerebral ischemia/reperfusion rats," *Journal of Neuroinflammation*, vol. 13, no. 1, p. 258, 2016.
- [61] V. von Bulow, S. Dubben, G. Engelhardt et al., "Zinc-dependent suppression of TNF- α production is mediated by protein kinase A-induced inhibition of Raf-1, I κ B kinase β , and NF- κ B," *Journal of Immunology*, vol. 179, no. 6, pp. 4180–4186, 2007.
- [62] E. C. Cope, D. R. Morris, S. D. Gower-Winter, N. C. Brownstein, and C. W. Levenson, "Effect of zinc supplementation on neuronal precursor proliferation in the rat hippocampus after traumatic brain injury," *Experimental Neurology*, vol. 279, pp. 96–103, 2016.
- [63] B. Y. Choi, I. Y. Kim, J. H. Kim et al., "Zinc plus cyclo-(His-Pro) promotes hippocampal neurogenesis in rats," *Neuroscience*, vol. 339, pp. 634–643, 2016.
- [64] M. Yang, D. Bao, A. Shi et al., "Zinc promotes patient-derived induced pluripotent stem cell neural differentiation via ERK-STAT signaling," *Stem Cells and Development*, vol. 29, no. 13, pp. 863–875, 2020.
- [65] D. Li, W. Lang, C. Zhou et al., "Upregulation of microglial ZEB1 ameliorates brain damage after acute ischemic stroke," *Cell Reports*, vol. 22, no. 13, pp. 3574–3586, 2018.
- [66] Y. Chu, M. F. Mouat, R. B. Harris, J. A. Coffield, and A. Grider, "Water maze performance and changes in serum corticosterone levels in zinc-deprived and pair-fed rats," *Physiology & Behavior*, vol. 78, no. 4–5, pp. 569–578, 2003.
- [67] X. Li, L. Wang, S. Zhang, X. Hu, H. Yang, and L. Xi, "Timing-dependent protection of swimming exercise against d-galactose-induced aging-like impairments in spatial learning/memory in rats," *Brain Sciences*, vol. 9, no. 9, p. 236, 2019.
- [68] S. S. Park, H. S. Park, T. W. Kim, and S. J. Lee, "Effects of swimming exercise on social isolation-induced memory impairment and apoptosis in old rats," *J Exerc Rehabil*, vol. 16, no. 3, pp. 234–241, 2020.
- [69] A. Gonzalez-Vazquez, A. K. Aguilar-Peralta, C. Tomas-Sanchez et al., "Taurine increases zinc preconditioning-induced prevention of nitrosative stress, metabolic alterations, and motor deficits in young rats following intrauterine ischemia," *Oxidative Medicine and Cellular Longevity*, vol. 2021, Article ID 6696538, 20 pages, 2021.
- [70] Z. Liu, Y. Cai, X. Zhang, Z. Zhu, and J. He, "High serum levels of malondialdehyde and antioxidant enzymes are associated with post-stroke anxiety," *Neurological Sciences*, vol. 39, no. 6, pp. 999–1007, 2018.
- [71] H. Schottke and C. M. Giabbiconi, "Post-stroke depression and post-stroke anxiety: prevalence and predictors," *International Psychogeriatrics*, vol. 27, no. 11, pp. 1805–1812, 2015.
- [72] B. Pochwat, G. Nowak, and B. Szewczyk, "Relationship between Zinc (Zn²⁺) and Glutamate Receptors in the Processes Underlying Neurodegeneration," *Neural Plasticity*, vol. 2015, Article ID 591563, 9 pages, 2015.
- [73] T. Terashi, S. Otsuka, S. Takada et al., "Neuroprotective effects of different frequency preconditioning exercise on neuronal apoptosis after focal brain ischemia in rats," *Neurological Research*, vol. 41, no. 6, pp. 510–518, 2019.
- [74] Z. Zhang, R. Li, X. Zhang et al., "Voluntary exercise promotes neurotrophic factor and suppresses apoptosis in hippocampal ischemia," *Journal of Integrative Neuroscience*, vol. 18, no. 1, pp. 65–70, 2019.
- [75] Y. Xing, S. D. Yang, F. Dong, M. M. Wang, Y. S. Feng, and F. Zhang, "The beneficial role of early exercise training following stroke and possible mechanisms," *Life Sciences*, vol. 198, pp. 32–37, 2018.
- [76] F. Farokhi-Sisakht, S. Sadigh-Eteghad, G. Mohaddes, A. Ebrahimi-Kalan, P. Karimi, and M. Farhoudi, "Physical and cognitive training attenuate hippocampal ischemia-induced memory impairments in rat," *Brain Research Bulletin*, vol. 155, pp. 202–210, 2020.
- [77] L. Sun, L. P. Zhuang, and W. F. Wu, "Aerobic exercise repairs neurological function after cerebral ischaemia by regulating the nitric oxide," *Anais da Academia Brasileira de Ciências*, vol. 91, no. 3, p. e20190068, 2019.
- [78] Q. Chen and D. S. Xiao, "Long-term aerobic exercise increases redox-active iron through nitric oxide in rat hippocampus," *Nitric Oxide*, vol. 36, pp. 1–10, 2014.

- [79] C. A. Massaad and E. Klann, "Reactive oxygen species in the regulation of synaptic plasticity and memory," *Antioxidants & Redox Signaling*, vol. 14, no. 10, pp. 2013–2054, 2011.
- [80] H. R. Wang, J. S. Li, J. Chen, and H. Zhang, "Effects of zinc on activity of NOS and expression of nNOS in hippocampus of acute hypoxic mice," *Zhongguo Ying Yong Sheng Li Xue Za Zhi*, vol. 22, no. 4, pp. 395–398, 2006.
- [81] A. Garthe and G. Kempermann, "An old test for new neurons: refining the Morris water maze to study the functional relevance of adult hippocampal neurogenesis," *Frontiers in Neuroscience*, vol. 7, p. 63, 2013.
- [82] R. De Pasquale, T. F. Beckhauser, M. S. Hernandez, and L. R. Giorgetti Britto, "LTP and LTD in the visual cortex require the activation of NOX2," *The Journal of Neuroscience*, vol. 34, no. 38, pp. 12778–12787, 2014.
- [83] F. Serrano and E. Klann, "Reactive oxygen species and synaptic plasticity in the aging hippocampus," *Ageing Research Reviews*, vol. 3, no. 4, pp. 431–443, 2004.
- [84] M. Leardini-Tristao, J. P. Borges, F. Freitas et al., "The impact of early aerobic exercise on brain microvascular alterations induced by cerebral hypoperfusion," *Brain Research*, vol. 1657, pp. 43–51, 2017.
- [85] A. Ally and T. J. Maher, "Endothelial NOS expression within the ventrolateral medulla can affect cardiovascular function during static exercise in stroked rats," *Brain Research*, vol. 1196, pp. 33–40, 2008.
- [86] D. M. Arrick, S. Yang, C. Li, S. Cananzi, and W. G. Mayhan, "Vigorous exercise training improves reactivity of cerebral arterioles and reduces brain injury following transient focal ischemia," *Microcirculation*, vol. 21, no. 6, pp. 516–523, 2014.
- [87] F. M. Abregú, M. N. Gobetto, L. V. Juriol et al., "Developmental programming of vascular dysfunction by prenatal and postnatal zinc deficiency in male and female rats," *The Journal of Nutritional Biochemistry*, vol. 56, pp. 89–98, 2018.
- [88] A. V. Santhanam, L. V. d'Uscio, L. A. Smith, and Z. S. Katusic, "Uncoupling of eNOS causes superoxide anion production and impairs NO signaling in the cerebral microvessels of hph-1 mice," *Journal of Neurochemistry*, vol. 122, no. 6, pp. 1211–1218, 2012.
- [89] M. Bicer, M. Akil, A. Sivrikaya, E. Kara, A. K. Baltaci, and R. Mogulkoc, "Effect of zinc supplementation on the distribution of various elements in the serum of diabetic rats subjected to an acute swimming exercise," *Journal of Physiology and Biochemistry*, vol. 67, no. 4, pp. 511–517, 2011.
- [90] T. I. Chen and M. Y. Chen, "Zinc is indispensable in exercise-induced cardioprotection against intermittent hypoxia-induced left ventricular function impairment in rats," *PLoS One*, vol. 11, no. 12, p. e0168600, 2016.
- [91] A. Piechal, K. Blecharz-Klin, J. Pyrzanowska, and E. Widy-Tyszkiewicz, "Influence of long-term zinc administration on spatial learning and exploratory activity in rats," *Biological Trace Element Research*, vol. 172, no. 2, pp. 408–418, 2016.
- [92] A. Piechal, K. Blecharz-Klin, J. Pyrzanowska, and E. Widy-Tyszkiewicz, "Maternal zinc supplementation improves spatial memory in rat pups," *Biological Trace Element Research*, vol. 147, no. 1–3, pp. 299–308, 2012.
- [93] S. A. E. Bashandy, A. Alaamer, S. A. A. Moussa, and E. A. Omara, "Role of zinc oxide nanoparticles in alleviating hepatic fibrosis and nephrotoxicity induced by thioacetamide in rats," *Canadian Journal of Physiology and Pharmacology*, vol. 96, no. 4, pp. 337–344, 2018.
- [94] M. Sefi, M. Chaabane, A. Elwej et al., "Zinc alleviates maneb-induced kidney injury in adult mice through modulation of oxidative stress, genotoxicity, and histopathological changes," *Environmental Science and Pollution Research International*, vol. 27, no. 8, pp. 8091–8102, 2020.
- [95] E. Candelario-Jalil, N. H. Mhadu, S. M. Al-Dalain, G. Martinez, and O. S. Leon, "Time course of oxidative damage in different brain regions following transient cerebral ischemia in gerbils," *Neuroscience Research*, vol. 41, no. 3, pp. 233–241, 2001.
- [96] S. Matsuda, M. Umeda, H. Uchida, H. Kato, and T. Araki, "Alterations of oxidative stress markers and apoptosis markers in the striatum after transient focal cerebral ischemia in rats," *Journal of Neural Transmission (Vienna)*, vol. 116, no. 4, pp. 395–404, 2009.
- [97] N. Patrushev, B. Seidel-Rogol, and G. Salazar, "Angiotensin II requires zinc and downregulation of the zinc transporters ZnT3 and ZnT10 to induce senescence of vascular smooth muscle cells," *PLoS One*, vol. 7, no. 3, article e33211, 2012.
- [98] J. Samardzic, K. Savic, N. Stefanovic et al., "Anxiolytic and antidepressant effect of zinc on rats and its impact on general behavioural parameters," *Vojnosanitetski Pregled*, vol. 70, no. 4, pp. 391–395, 2013.
- [99] C. L. Cavalcanti, M. C. R. Goncalves, A. F. Alves et al., "Anti-depressant, anxiolytic and neuroprotective activities of two zinc compounds in diabetic rats," *Frontiers in Neuroscience*, vol. 13, p. 1411, 2020.
- [100] H. R. Wang, J. S. Li, J. Chen, and H. Zhang, "Effects of taurine and zinc on activity of NOS and expression of nNOS in cerebral cortex of acute hypoxic mice," *Wei Sheng Yan Jiu*, vol. 35, no. 1, pp. 97–99, 2006.
- [101] H. Famatafreshi and M. Karimian, "Modulation of catalase, copper and zinc in the hippocampus and the prefrontal cortex in social isolation-induced depression in male rats," *Acta Neurobiologiae Experimentalis (Wars)*, vol. 79, no. 2, pp. 184–192, 2019.
- [102] K. Mlyniec, G. Starowicz, M. Gawel, E. Frackiewicz, and G. Nowak, "Potential antidepressant-like properties of the TC G-1008, a GPR39 (zinc receptor) agonist," *Journal of Affective Disorders*, vol. 201, pp. 179–184, 2016.
- [103] U. Doboszewska, P. Wlaz, G. Nowak, M. Radziwon-Zaleska, R. Cui, and K. Mlyniec, "Zinc in the monoaminergic theory of depression: its relationship to neural plasticity," *Neural Plasticity*, vol. 2017, Article ID 3682752, 18 pages, 2017.
- [104] J. Zhu, C. Y. Shao, W. Yang et al., "Chronic zinc exposure decreases the surface expression of NR2A-containing NMDA receptors in cultured hippocampal neurons," *PLoS One*, vol. 7, no. 9, article e46012, 2012.
- [105] B. Szewczyk, E. Poleszak, P. Wlaz et al., "The involvement of serotonergic system in the antidepressant effect of zinc in the forced swim test," *Progress in Neuro-Psychopharmacology & Biological Psychiatry*, vol. 33, no. 2, pp. 323–329, 2009.
- [106] J. C. Sorensen, B. Mattsson, A. Andreasen, and B. B. Johansson, "Rapid disappearance of zinc positive terminals in focal brain ischemia," *Brain Research*, vol. 812, no. 1–2, pp. 265–269, 1998.
- [107] G. Yu, F. Wu, and E. S. Wang, "BQ-869, a novel NMDA receptor antagonist, protects against excitotoxicity and attenuates cerebral ischemic injury in stroke," *International Journal of Clinical and Experimental Pathology*, vol. 8, no. 2, pp. 1213–1225, 2015.

- [108] T. Gerriets, E. Stolz, M. Walberer, M. Kaps, G. Bachmann, and M. Fisher, "Neuroprotective effects of MK-801 in different rat stroke models for permanent middle cerebral artery occlusion: adverse effects of hypothalamic damage and strategies for its avoidance," *Stroke*, vol. 34, no. 9, pp. 2234–2239, 2003.
- [109] C. W. Liu, K. H. Liao, H. Tseng, C. M. Wu, H. Y. Chen, and T. W. Lai, "Hypothermia but not NMDA receptor antagonism protects against stroke induced by distal middle cerebral arterial occlusion in mice," *PLoS One*, vol. 15, no. 3, article e0229499, 2020.
- [110] Z. Xiong, L. Chang, Y. Qu et al., "Neuronal brain injury after cerebral ischemic stroke is ameliorated after subsequent administration of R-ketamine, but not S-ketamine," *Pharmacology, Biochemistry, and Behavior*, vol. 191, p. 172904, 2020.
- [111] I. A. Abdoulaye, S. S. Wu, E. Chibaatar et al., "Ketamine induces lasting antidepressant effects by modulating the NMDAR/CaMKII-mediated synaptic plasticity of the hippocampal dentate gyrus in depressive stroke model," *Neural Plasticity*, vol. 2021, Article ID 6635084, 17 pages, 2021.
- [112] L. R. Aleksandrova, A. G. Phillips, and Y. T. Wang, "Antidepressant effects of ketamine and the roles of AMPA glutamate receptors and other mechanisms beyond NMDA receptor antagonism," *Journal of Psychiatry & Neuroscience*, vol. 42, no. 4, pp. 222–229, 2017.
- [113] X. Li, S. Chen, L. Mao et al., "Zinc improves functional recovery by regulating the secretion of granulocyte colony stimulating factor from microglia/macrophages after spinal cord injury," *Frontiers in Molecular Neuroscience*, vol. 12, p. 18, 2019.
- [114] J. Losy, J. Zaremba, and P. Skrobanski, "CXCL1 (GRO- α) chemokine in acute ischaemic stroke patients," *Folia Neuropathologica*, vol. 43, no. 2, pp. 97–102, 2005.
- [115] T. K. Roberts, E. A. Eugenin, L. Lopez et al., "CCL2 disrupts the adherens junction: implications for neuroinflammation," *Laboratory Investigation*, vol. 92, no. 8, pp. 1213–1233, 2012.
- [116] C. Lauro, G. Chece, L. Monaco et al., "Fractalkine modulates microglia metabolism in brain ischemia," *Frontiers in Cellular Neuroscience*, vol. 13, p. 414, 2019.
- [117] Y. Gan, Q. Liu, W. Wu et al., "Ischemic neurons recruit natural killer cells that accelerate brain infarction," *Proceedings of the National Academy of Sciences of the United States of America*, vol. 111, no. 7, pp. 2704–2709, 2014.
- [118] M. M. Pabon, A. D. Bachstetter, C. E. Hudson, C. Gemma, and P. C. Bickford, "CX3CL1 reduces neurotoxicity and microglial activation in a rat model of Parkinson's disease," *Journal of Neuroinflammation*, vol. 8, no. 1, p. 9, 2011.
- [119] F. Chen, X. Li, Z. Li, Y. Zhou, Z. Qiang, and H. Ma, "The roles of chemokine (C-X-C motif) ligand 13 in spinal cord ischemia-reperfusion injury in rats," *Brain Research*, vol. 1727, p. 146489, 2020.
- [120] Y. P. Yan, K. A. Sailor, B. T. Lang, S. W. Park, R. Vemuganti, and R. J. Dempsey, "Monocyte chemoattractant protein-1 plays a critical role in neuroblast migration after focal cerebral ischemia," *Journal of Cerebral Blood Flow and Metabolism*, vol. 27, no. 6, pp. 1213–1224, 2007.
- [121] R. H. Andres, R. Choi, A. V. Pendharkar et al., "The CCR2/CCL2 interaction mediates the transendothelial recruitment of intravascularly delivered neural stem cells to the ischemic brain," *Stroke*, vol. 42, no. 10, pp. 2923–2931, 2011.
- [122] J. G. Bray, K. C. Reyes, A. J. Roberts, R. M. Ransohoff, and D. L. Gruol, "Synaptic plasticity in the hippocampus shows resistance to acute ethanol exposure in transgenic mice with astrocyte-targeted enhanced CCL2 expression," *Neuropharmacology*, vol. 67, pp. 115–125, 2013.
- [123] A. M. Stowe, B. K. Wacker, P. D. Cravens et al., "CCL2 upregulation triggers hypoxic preconditioning-induced protection from stroke," *Journal of Neuroinflammation*, vol. 9, no. 1, p. 33, 2012.
- [124] P. Vora, P. Pillai, J. Mustapha et al., "CXCL1 regulation of oligodendrocyte progenitor cell migration is independent of calcium signaling," *Experimental Neurology*, vol. 236, no. 2, pp. 259–267, 2012.
- [125] J. Torrano, A. Al Emran, H. Hammerlindl, and H. Schaidler, "Emerging roles of H3K9me3, SETDB1 and SETDB2 in therapy-induced cellular reprogramming," *Epigenetics*, vol. 11, no. 1, p. 43, 2019.
- [126] K. Z. Chapman, R. Ge, E. Monni et al., "Inflammation without neuronal death triggers striatal neurogenesis comparable to stroke," *Neurobiology of Disease*, vol. 83, pp. 1–15, 2015.
- [127] A. Turbic, S. Y. Leong, and A. M. Turnley, "Chemokines and inflammatory mediators interact to regulate adult murine neural precursor cell proliferation, survival and differentiation," *PLoS One*, vol. 6, no. 9, article e25406, 2011.
- [128] S. Hulshof, E. S. van Haastert, H. F. Kuipers et al., "CX3CL1 and CX3CR1 expression in human brain tissue: noninflammatory control versus multiple sclerosis," *Journal of Neuro pathology and Experimental Neurology*, vol. 62, no. 9, pp. 899–907, 2003.
- [129] X. Chen, M. Jiang, H. Li et al., "CX3CL1/CX3CR1 axis attenuates early brain injury via promoting the delivery of exosomal microRNA-124 from neuron to microglia after subarachnoid hemorrhage," *Journal of Neuroinflammation*, vol. 17, no. 1, p. 209, 2020.

Research Article

The Improvement of Sepsis-Associated Encephalopathy by P2X7R Inhibitor through Inhibiting the Omi/HtrA2 Apoptotic Signaling Pathway

Kaifang Wang ¹, Meiyan Sun ¹, Zhaodong Juan ¹, Jianxin Zhang ², Yingui Sun ^{1,3}, Guizhi Wang ¹, Chunling Wang ¹, Yanjing Li ¹, Wenwen Kong ¹, Lulu Fan ¹, Yue Zhang ¹, Hongxiang Zhao ¹ and Xiaoyong Zhao ^{1,3}

¹Shandong Provincial Medicine and Health Key Laboratory of Clinical Anesthesia, School of Anesthesiology, Weifang Medical University, 261053 Weifang, Shandong, China

²Department of Anesthesiology, Suzhou Benkey Hospital, 215009 Suzhou, Jiangsu, China

³The Affiliated Hospital of Weifang Medical University, 261021 Weifang, Shandong, China

Correspondence should be addressed to Xiaoyong Zhao; zhaoxiaoyong@wfmw.edu.cn

Kaifang Wang and Meiyan Sun contributed equally to this work.

Received 27 July 2021; Revised 14 December 2021; Accepted 5 January 2022; Published 27 January 2022

Academic Editor: Yu Yo Sun

Copyright © 2022 Kaifang Wang et al. This is an open access article distributed under the Creative Commons Attribution License, which permits unrestricted use, distribution, and reproduction in any medium, provided the original work is properly cited.

The pathogenesis of sepsis-associated encephalopathy (SAE) involves many aspects, including intracellular peroxidative stress damage, mitochondrial dysfunction, and cell apoptosis. In this study, we mainly explored the influence of P2X7R on the cognitive function of SAE and its molecular mechanism. We established a sepsis model using lipopolysaccharide (LPS) stimulation, followed by an assessment of cognitive function using Morris water maze, and then Western Blot was used to analyze the expression of tight junction proteins ZO-1 and Occludin in the hippocampus of mice. TUNEL assay was used to analyze the apoptosis of brain cells in frozen brain slices of mice during sepsis. Human brain microvascular endothelial cells (HBMECs) were used to research the molecular mechanism of brain cell damage induced by P2X7R. The results showed that P2X7R inhibitors dramatically improved the survival rate of mice, relieved the cognitive dysfunction caused by LPS stimulation, and significantly reduced the brain cell apoptosis caused by LPS. In addition, the inhibition of P2X7R can also reduce the production and accumulation of reactive oxygen species (ROS) in HBMECs in vitro and inhibit the apoptosis signaling pathway associated with mitochondrial serine protease Omi/HtrA2 in HBMECs in vitro. These results suggest that P2X7R has strong value as a potential target for the treatment of SAE.

1. Introduction

SAE is an inflammatory infection that causes systemic sepsis to spread to the brain, but there is no evidence of direct infection in the brain, and this is one reason for long-term and short-term cognitive impairment and high mortality in sepsis patients in the ICU [1, 2]. More and more evidences show that SAE is closely related to peroxidation stress injury of brain cells, mitochondrial dysfunction, and apoptosis. Some researchers have found that 70% of severe sepsis survi-

vors are accompanied by cognitive impairment [3, 4], but the pathogenesis of SAE is still unclear.

As a member in the P2X family of ATP-sensitive purinergic receptors, P2X7R is unique in that it only functions in homomeric forms and is activated by high extracellular ATP levels [5]. Activation of P2X7R causes a large amount of Ca²⁺ and Na⁺ influx and K⁺ outflow, resulting in the imbalance of intracellular metabolism. P2X7R is primarily expressed on the surface of various brain cells, especially microglia and astrocytes [6, 7]. Many scholars regard P2X7R

as a receptor closely related to inflammatory injury, because P2X7R located in various organs of the body will be greatly activated when severe systemic infection occurs and the activation of P2X7R is also a damaging process [8]. In this regard, whether the brain damage caused by the activation of P2X7R in the brain can be considered as one of the mechanisms of SAE, and the molecular mechanisms in brain cells caused by the activation remain to be explored.

The blood-brain barrier (BBB) is a gateway through which the brain and the outside world exchange substances, allowing small molecules of nutrients and oxygen to enter the brain, while blocking harmful macromolecules from entering the brain [9]. It is well known that the BBB is mainly composed of cerebral capillary endothelial cells, basal membrane and foot processes of glial cells, and tight junction proteins produced by endothelial cells play a crucial role in the cell-cell connection of BBB and maintaining the integrity of BBB [10]. When harmful substances, such as lipopolysaccharide (LPS), arrive at BBB with blood flow, they will first damage endothelial cells, thereby inhibiting the expression of tight junction protein and damaging BBB [11]. However, it remains to be explored whether LPS-induced brain endothelial cell damage is related to P2X7R activation and whether inhibition of P2X7R has a protective effect.

Under normal physiology, the body's physiological metabolism will produce an appropriate amount of ROS, acting as a signal to regulate the physiological and biochemical reactions inside and outside cells of the body [12]. However, when the body suffers pathological injuries, such as invasion of external bacteria and reperfusion injury caused by ischemia and hypoxia of essential organs, the damaged organs will produce and accumulate ROS in large quantities. The accumulation of ROS in cells will destroy important organelles such as endoplasmic reticulum and mitochondria, even directly damage the DNA of cells [13, 14]. At present, many studies have found that the continuous production of ROS is closely associated with neurodegenerative diseases such as Parkinson's disease and Alzheimer's disease [15], as well as cell necrosis and apoptosis related to inflammation [16]. Although recent studies have found that the activation of P2X7R can induce ROS production in cardiomyocytes [17], the effect of P2X7R on the production of ROS in brain cells after severe sepsis-induced SAE remains to be explored. In addition, numerous studies have found that plenty of intracellular ROS can cause intracellular apoptosis related to caspase, Bcl-2, and cytochrome C [18]. However, whether ROS production can cause apoptosis related to mitochondrial serine protease Omi/HtrA2 remains unexplored.

Both apoptosis and programmed cell death occur in all organs of the body and maintain a balance between the removal of damaged cells and the renewal of new cells [19]. However, when the body is subjected to severe damaging stimuli, such as the disturbance of the body's internal environment caused by inflammation or biochemical stimulation, the cells of the body will undergo apoptosis caused by aspartate-specific cysteine proteases known as caspases. Cell apoptosis is closely related to mitochondria besides some signaling pathways in the cytoplasm [20]. Apoptosis caused by mitochondrial pathway is mainly related to the mito-

chondrial serine protease Omi/HtrA2, which exists in the inner and outer membrane of mitochondria under physiological conditions and is mainly involved in clarifying misfolded proteins in mitochondria [21, 22]. However, when cells are injured by various pathological factors such as external inflammation, biochemical and physiological changes will occur in the cells, thereby transferring Omi/HtrA2 from the mitochondrial intermembrane space into the cytoplasm [23, 24]. Nonetheless, it is still unclear whether the activation of P2X7R on the cell surface will affect the membrane potential of mitochondria and whether it will cause the transfer of Omi/HtrA2 from mitochondrial to cytoplasmic.

Apoptosis-related proteins XIAP, Caspase9, and Caspase3 play a vital role in the process of cell apoptosis [25]. As a member in the evolutionarily conserved family of inhibitors of apoptosis proteins (IAPs), X-linked inhibitor of apoptosis protein (XIAP) can bind and inhibit caspase-related apoptosis in cells [26]. When Omi/HtrA2 enters the cytoplasm from mitochondria, XIAP will be degraded, thus, inhibiting the degradation of caspase-9 by XIAP [27–29], and increased expression of caspase-9 activates caspase-3, ultimately causing intracellular DNA damage. It has been proved that cell apoptosis induced by external damaging stimuli is significantly reduced after mitochondrial serine protease Omi/HtrA2 is knocked down [30]. Therefore, the effect of P2X7R activation on XIAP and caspase-3-related apoptosis needs further exploration.

2. Materials and Methods

2.1. Reagents. Chemicals: P2X7R antagonist A-438079 and LPS were purchased from Sigma-Aldrich. Antibodies: Rabbit anti-cleaved-caspase-3, rabbit anti-cleaved-caspase-9, mouse anti-XIAP, mouse anti-P2X7R, Rabbit anti-ZO-1, Rabbit anti-Occludin, and mouse anti-HtrA2 were from Santa Cruz Biotechnology (Santa Cruz, CA, USA).

2.2. Animal Feeding and Animal Experiment. After obtaining the male C57BL/6 (8–10 weeks) mice from Medical Laboratory Animal Center of Weifang Medical University, they were allowed to adapt for seven days. The mice lived in a quiet room, with the rotation of dark and light every 12 hours, the room temperature of 25°C, and free access to food and water every day in the cage. All animal operations were conducted following ethical regulations and laboratory guidelines. To test whether A-438079 could affect LPS-induced SAE and cognitive function in mice, LPS was dissolved in PBS, and A-438079 was dissolved with 25% dimethyl sulfoxide (DMSO) (Sigma-Aldrich, USA). Then, the mice were divided into four groups. Control group mice were intraperitoneally injected with PBS of the same volume as LPS group. LPS group was injected intraperitoneally LPS (5 mg/kg), LPS + A-438079 group was intraperitoneally injected with A-438079 (30 mg/kg) after one hour of pre-treatment with LPS (5 mg/kg), LPS + DMSO group was intraperitoneally injected with DMSO after one hour of pre-treatment with LPS (5 mg/kg). Body weight and the survival rate of the mice were recorded daily for 7 days (each group

contained five mice), after that, the mice were decapitated and their brains were taken under pentobarbital anesthesia, and proteins were extracted from their hippocampal tissues for subsequent experiments. However, for behavioral tests, three days after the injection, behavioral tests were performed on each group of mice to determine the success of the model and the changes in cognitive function (each group contained ten mice). After the behavioral test (day 7 after LPS injection), the mice were placed under pentobarbital anesthesia with a heart infused with normal saline followed by 4% paraformaldehyde fixation and decapitated. Mouse brain tissue was immobilized in 4% paraformaldehyde for 4 h and then placed in 15% sucrose solution until the brain tissue sank to the bottom. The brain tissue was taken out, and frozen sections were performed after OTC embedding. The brain slices were stored at -20°C .

2.3. Cell Culture and Experiment. HBMEC (HUM-CELL-0101) cells were purchased from PriCells (Wuhan, China). The cells were cultured in DMEM medium of 30 mg/ml endothelial growth factor, 10% fetal bovine serum, and 10 mg/ml penicillin/streptomycin. Cells were cultured at 5% CO_2 and 37°C . The culture medium was changed every 24 hours, and it was passed after 48 hours. Before LPS treatment, the cells were inoculated in a six-well plate at a density of 1×10^5 cells/well and placed in an incubator overnight. On the second day, cells were pretreated with A-438079 ($2.5 \mu\text{g/ml}$) or DMSO, and LPS ($5 \mu\text{g/ml}$) was added one hour later in each group. After 12 hours of culture, the cells were collected for Western Blot analysis.

2.4. ROS Assay. The production of ROS in HBMEC was analyzed by DCFH-DA staining. According to the protocol of the manufacturer, DCFH-DA and DMEM are configured in quantities of 1:1000. The cells were inoculated in a six-well plate at a density of 1×10^5 cells/well, and drugs are treated in line with the above cell treatment protocol, then, each well was added with 1 ml and incubated at 37°C for 40 minutes. Finally, ROS production in each group of cells was filmed by fluorescence microscopy (Olympus, Japan).

2.5. Mitochondrial Membrane Potential Analysis. We used Mito-Tracker Red CMXRos aggregation in mitochondria which depends on the characteristics of mitochondrial membrane potential to analyze the changes of mitochondrial membrane potential in different groups of cells. Briefly, HBMECs were inoculated in a six-well plate with preplaced circular slides overnight, followed by abandoning culture and adding 1:1000 Mito-Tracker Red CMXRos (purchased from Beyotime) working fluid to the preprepared medium at 37°C for 15-30 minutes, and finally, DAPI was added, with each group of cells filmed by fluorescence microscopy (Olympus, Japan).

2.6. Western Blot Analyses. Western Blot was roughly divided into four steps. The first step was electrophoresis. After adding the sample of each group to the electrophoresis tank, the electrophoretic liquid was added, and the electrophoresis is performed at 80 V for 30 minutes first, then, at 120 V for 60 minutes. In the second step of membrane trans-

fer, the separation gel after electrophoresis was placed in a membrane transfer clamp with sponge and filter paper to transfer the membrane for 90 minutes in a transfer tank with the transfer solution at 300 mA. The third step was seal and incubation. After membrane transfer, the nitocellulose membrane was transferred to 5% skim milk powder for sealing for 2 hours, then, incubated overnight in the primary antibody at 4°C and in the secondary antibody at room temperature for 1-1.5 hours the next day. Fourth, ECL solution (purchased from Beyond) was added to the immunoreactive membrane and developed using Enhanced Chemiluminescent Detection. Results analysis: ImageJ software was used to analyze the gray value of the strip.

2.7. TUNEL Assay. The TUNEL fluorescence assay kit was used to detect apoptosis in frozen brain sections, i.e., a well-preserved frozen brain section was placed in a citrate solution in a microwave oven on high heat for 5 minutes, followed by medium heat for 10 minutes for percolation. Then, the section was washed three times with PBS solution and incubated for 60 min at 37°C under darkroom conditions after adding preconfigured TUNEL working solution (I solution : II solution = 1 : 9), followed by being washed three times with PBS and added DAPI to seal. TUNEL-positive cells were counted using image analysis software (Image-Pro Plus 6.0) under identical conditions, and each group of cells was recorded by fluorescence microscopy (Olympus, Japan).

2.8. Morris Water Maze. An operator who was not aware of each treatment group detected the cognitive function of mice by Morris water maze (MWM). The MWM consisted of a circular steel pool (125 cm in mice by Morris water maze (MWM)). The MWM consisted of a circular steel pool (125 cm in diameter, 60 cm in depth) with water depth below 1 cm above the top of the platform (10 cm in diameter, 30 cm in height). The pool was surrounded by a gray curtain and placed in a quiet room at 25°C with titanium dioxide to make the water turbid. MWM testing began on the third day after LPS or A-438079 treatment and lasted for five days, with the first 4 days (3-6 days) being a training period. The mice were released from various locations and given 60 seconds to find the platform, and they were artificially led to the platform and stayed there for 15 seconds if they failed to find the platform. A video surveillance system was used to record and track the escape latency of mice (i.e., the time taken from being placed in the water to finding the platform). On the 5th day (day 7), the mice were subjected to the space exploration experiment. The platform was removed, and the mice were released from the opposite side of the platform and swam free for 120 seconds, with the number of target crossings recorded.

2.9. Statistical Analyses. All data are presented in the mean-standard deviation, with their validation analyses were performed by SPSS24.0 (SPSS Inc., Chicago, IL). $P < 0.05$ was considered statistically significant. Differences among the groups were examined by one-way analysis of variance.

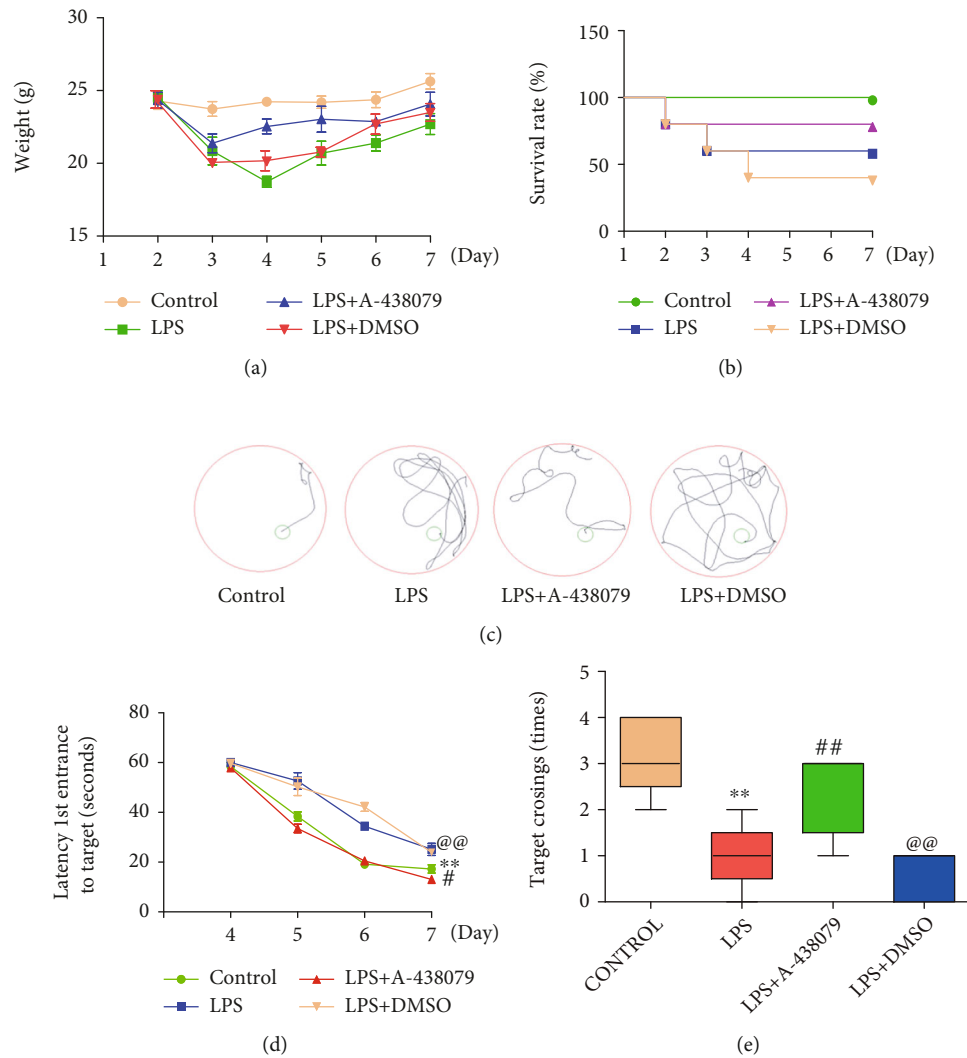


FIGURE 1: Treatment with P2X7R inhibitor A-438079 improved LPS-induced cognitive dysfunction and SAE in mice. (a) A-438079 treatment rescued LPS-induced weight loss. (b) Treatment of A-438079 significantly alleviated the reduced survival rate in mice caused by LPS. (c) The distance traveled by each group to reach the platform during the training period. Mice traveling distance was significantly reduced after treatment with A-438079 compared with the LPS and LPS+ DMSO groups. (d) Mice in LPS groups and LPS + DMSO groups expressed a signally longer escape latency than the control group. Treatment with A-438079 significantly reduced the extension of the escape latency after LPS treatment, $n = 5$. All data are expressed as mean \pm SD. ** $P < 0.01$ vs. control, # $P < 0.05$ vs. LPS group, and @@ $P < 0.01$ vs. LPS + A - 438079 group. (e) The number of times the mice crossed the platform was significantly reduced in the LPS group compared with the control group but increased after treatment with A-438079 compared with the LPS group, moreover, the number of mice crossing the platform in the LPS + DMSO group was significantly decreased compared with the LPS + A - 438079 group; $n = 5$. All data are expressed as mean \pm SD. ** $P < 0.01$ vs. control, ## $P < 0.01$ vs. LPS group, and @@ $P < 0.01$ vs. LPS + A - 438079 group.

3. Results

3.1. P2X7R Inhibitors Can Increase the Survival Rate and Improve Cognitive Dysfunction in Mice with SAE. At present, little is known about the pathogenesis of SAE. Many studies have found that cells in the brain undergo apoptosis under the stimulation of inflammatory factors, which is crucial for the pathogenesis of SAE. Since P2X7R is a receptor closely associated with inflammation and amplifies inflammatory damage, we investigated the influence of P2X7R inhibitor A-438079 on cognitive function in mice after severe sepsis was induced by LPS.

The results showed a significant weight loss after treatment with LPS compared to the control group, whereas the pretreated LPS group treated with A-438079 did not indicate a significant weight loss (Figure 1(a)). Similarly, we found a significant decrease in survival in mice after several weeks of LPS treatment compared to the control group, but pretreatment with A-438079 could reverse the LPS-induced low survival in mice (Figure 1(b)). When mice were trained for MWM (3-6 days), we found that the distance to the platform was significantly longer after LPS or LPS + DMSO treatment compared to the control group, while the distance was dramatically shortened after A-438079

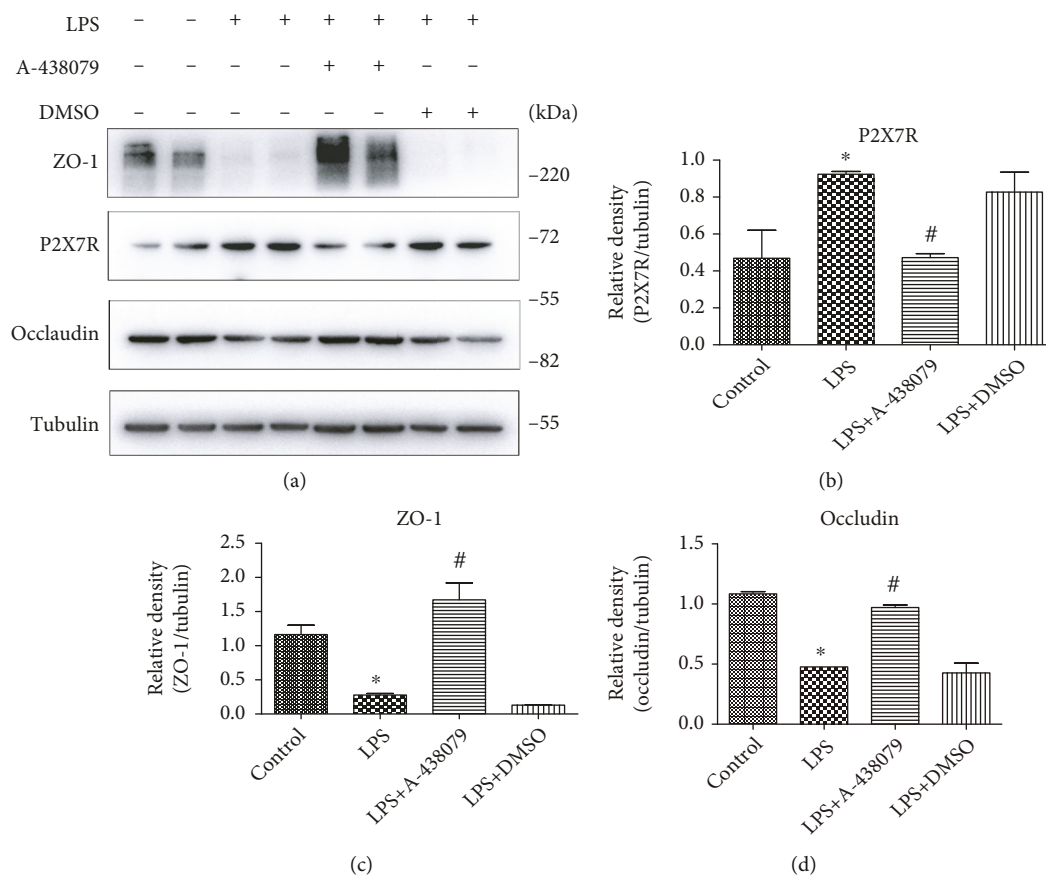


FIGURE 2: Treatment with the P2X7R inhibitor A-438079 improved LPS-induced decline in tight junction protein expression in the mouse hippocampus. (a) The expression levels of ZO-1, P2X7R, and Occludin were detected by Western Blot. Respective bands with Tubulin as loading controls are shown. (b) The expression of P2X7R was significantly increased in the hippocampus of mice after intraperitoneal injection of LPS. All data are expressed as mean \pm SD. * $P < 0.05$ vs. control. (c) and (d) LPS significantly inhibited the expression of tight junction proteins ZO-1 and Occludin in the hippocampal tissues of mice, while A-438079 reversed this effect. All data are expressed as mean \pm SD. * $P < 0.05$ vs. control, and # $P < 0.05$ vs. LPS group.

treatment compared with those in LPS and LPS + DMSO groups (Figure 1(c)). Moreover, mice in the LPS treatment group and the LPS + DMSO group took notably longer to reach the platform during the training period than those in the control group, and the result was reversed after A-438079 treatment (Figure 1(d)). Then, the spatial memory test was performed on day 7 by removing the platform, releasing the mice from the quadrant facing the platform, and recording the number of times the mice crossed the platform area within 120 seconds. We found that the number of platform crossings was significantly reduced in the LPS group and the LPS + DMSO group compared with the control group, while the number in the A-438079 group was higher than that in the LPS and LPS + DMSO groups (Figure 1(e)).

From the above findings, we can find that LPS injection does cause cognitive impairment and lead to SAE in mice, while treatment with P2X7R inhibitor can improve the loss of spatial memory and directional learning abilities in mice. These results suggest that P2X7R plays a crucial role in the pathogenesis of SAE.

3.2. P2X7R Inhibitors Ameliorate LPS-Induced Tight Junction Protein Reduction in the Mouse Hippocampus. In

order to verify the protective effect of P2X7R inhibitor on BBB in the hippocampal area of mice after LPS treatment, we extracted the protein from the hippocampal tissue of mice and detected the expression of tight junction protein in each group by Western Blot. The results showed that LPS treatment significantly increased the expression of P2X7R in the hippocampus of mice (Figures 2(a) and 2(b)), and compared with the control group, LPS treatment significantly reduced the expression of tight junction protein Occludin and ZO-1, while LPS + A-438079 group reversed this effect (Figures 2(a), 2(c), and 2(d)). From these results, it is clear that P2X7R plays a key role in LPS-induced BBB damage in mice.

3.3. P2X7R Inhibitors Can Attenuate the ROS Production and Changes in Mitochondrial Membrane Potential in HBMECs Induced by LPS Stimulation In Vitro.

As the activation of P2X7R will lead to a large increase in intracellular Ca^{2+} level, HBMEC cells cultured in vitro were selected and given LPS or P2X7R inhibitor A-438079 to research the effect of P2X7R activation on intracellular mitochondrial membrane potential and ROS production. Then, the production of ROS in HBMECs was analyzed by DCFH-DA

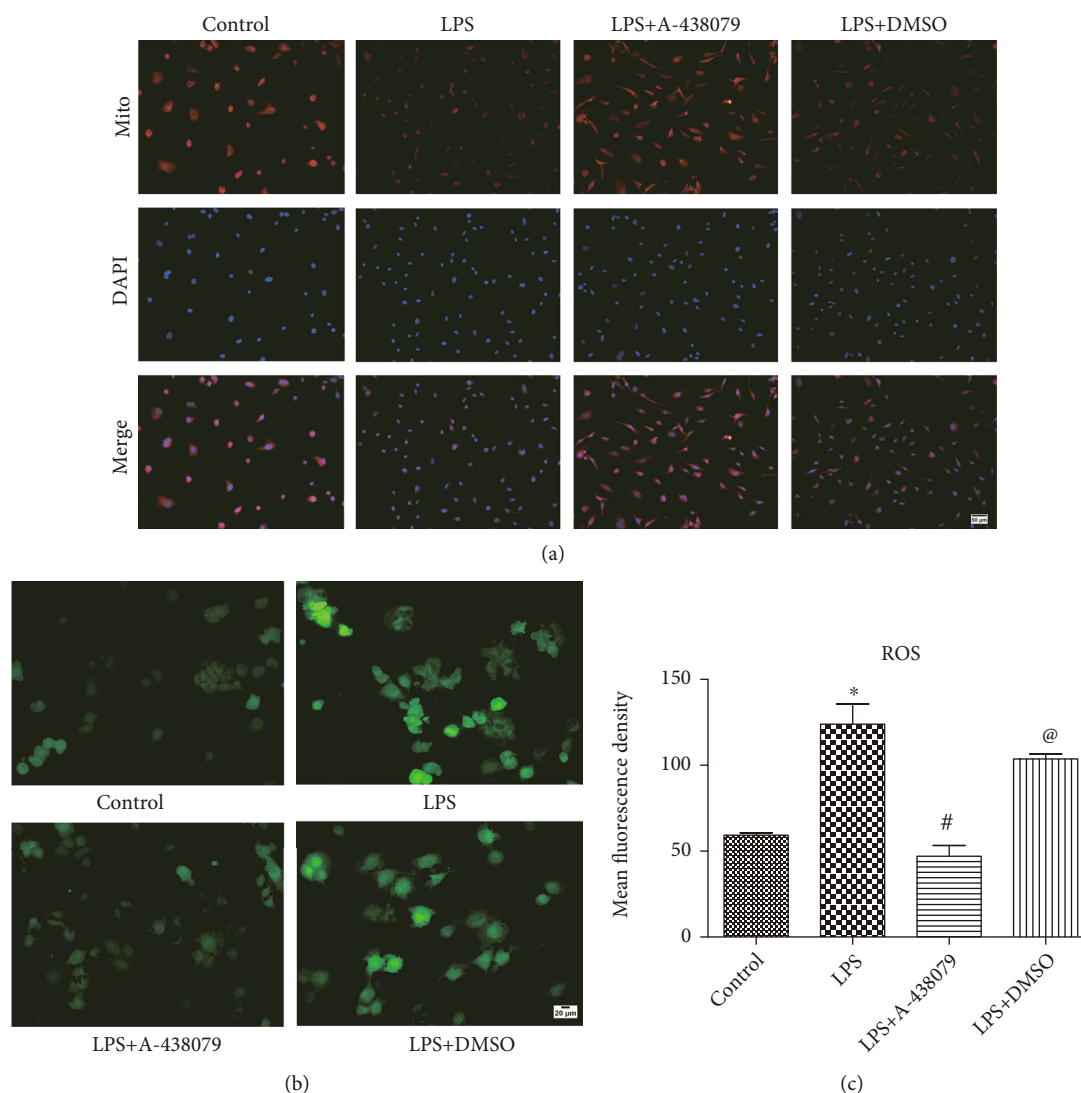


FIGURE 3: Effects of LPS or A-438079 on ROS production and mitochondrial membrane potential in HBMECs in vitro. (a) The adherent HBMECs in the LPS + A - 438079 group were treated with A-438079 for an hour and then treated with LPS for 12 hours. The same cells in the LPS + DMSO group were treated with DMSO for an hour and then treated with LPS for 12 hours. The LPS group was treated with LPS one hour after the addition of the same amount of normal saline for 12 hours. Mito-tracker Red CMXRos was used to evaluate the mitochondrial membrane potential in each group, and the intensity of red fluorescence signal in each group indicated the change of mitochondrial membrane potential. Scale bars = 50 μ m. (b) A fluorescence microscope was used to observe the production of ROS in each group. Scale bars = 20 μ m. (c) The fluorescence signals of different groups were analyzed using ImageJ. All data are expressed as mean \pm SD. * P < 0.05 vs. control group, # P < 0.05 vs. LPS group, and @ P < 0.05 vs. LPS + A - 438079 group.

staining, and the fluorescence intensity of each group was analyzed by ImageJ. The results showed that HBMECs produced more ROS when stimulated by LPS than by normal saline alone, and this phenomenon was reversed by P2X7R inhibitor A-438079 (Figures 3(b) and 3(c)). Since A-438079 was dissolved in DMSO, we found that the LPS + DMSO group was not statistically significant compared with the LPS group.

Since the fluorescence emitted by Mito-tracker Red CMXRos is dependent on mitochondrial membrane potential, we then used Mito-tracker Red CMXRos in HBMECs in vitro to evaluate the intracellular mitochondrial membrane potential. We found that the fluorescence signal intensity of the LPS stimulation group alone or the LPS + DMSO

group was observably decreased than that of the control group and the LPS + A - 438079 group (Figure 3(a)). It can be seen that when brain cells are stimulated by inflammation, P2X7R inhibitors can reduce intracellular ROS production and have a protective effect on mitochondria.

3.4. LPS Stimulation Induced the Transfer of Omi/HtrA2 from Mitochondria to the Cytoplasm In Vitro and P2X7R Inhibitors Inhibited This Process. We speculated that the large influx of calcium ions caused by P2X7R activation would lead to the apoptosis of mitochondrial pathways, i.e., the Omi/HtrA2 protease generally presented in the mitochondria probably be transferred into the cytoplasm under the inflammation stimuli. Therefore, we explored the

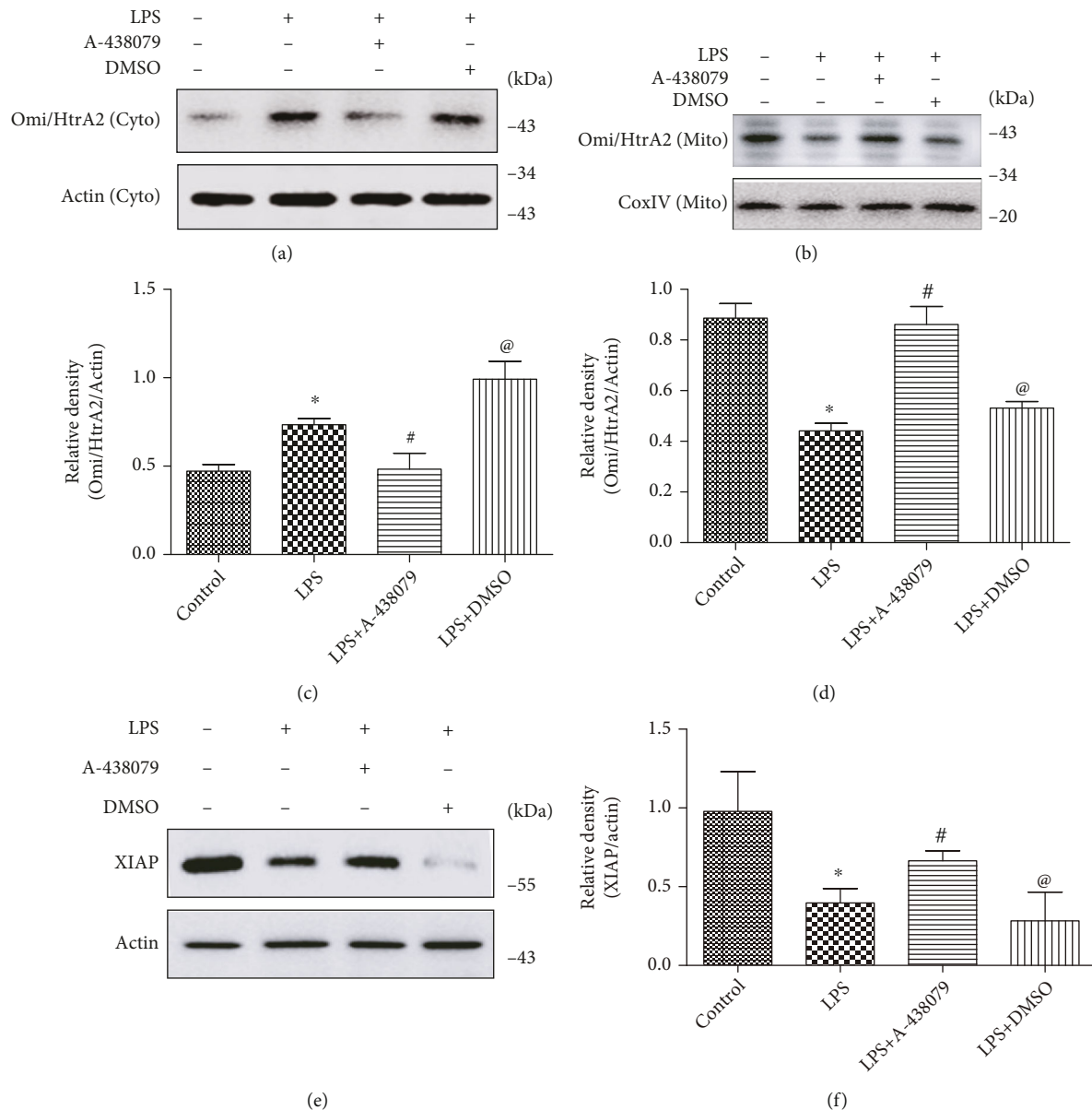


FIGURE 4: A-438079 treatment decreased LPS-induced transposition of Omi/HtrA2 from mitochondria to cytoplasm and reversed the decrease in XIAP expression. (a) and (c) A-438079 reduced LPS-induced increase of Omi/HtrA2 in the cytoplasm of HBMECs in vitro. All data are expressed as mean \pm SD. * $P < 0.05$ compared with control, # $P < 0.05$ compared with LPS, and @ $P < 0.05$ compared with LPS + A - 438079. (b) and (d) Under the effect of LPS, the mitochondrial Omi/HtrA2 of HBMECs in vitro was significantly decreased compared with the control group, and this reduction could be inhibited by A-438079. All data are expressed as mean \pm SD. * $P < 0.05$ compared with control, # $P < 0.05$ compared with LPS, and @ $P < 0.05$ compared with LPS + A - 438079. (e) and (f) Western Blot showed that LPS treatment could inhibit the expression of the apoptosis inhibitor protein XIAP and could be reversed by A-438079. All data are expressed as mean \pm SD. * $P < 0.05$ compared with control, # $P < 0.05$ compared with LPS, and @ $P < 0.05$ compared with LPS + A - 438079.

influence of P2X7R on the intracellular localization of Omi/HtrA2 cells under inflammatory conditions. We extracted the proteins in the cytoplasm and mitochondria of HBMECs cells by the mitochondrial extraction kit and found that under the action of LPS, there was the evident translocation of Omi/HtrA2 into the cytoplasm from mitochondria in HBMECs. However, when P2X7R inhibitor A-438079 was given in advance and then treated with LPS, reversal of

Omi/HtrA2 translocation was observed (Figures 4(a) and 4(c)). Nevertheless, the LPS-induced transfer of Omi/HtrA2 to the cytoplasm was reversed after the treatment of A-438079. (Figures 4(a)–4(d)).

These results indicate that P2X7R expression in cells is significantly increased under inflammatory stimulation, and P2X7R inhibitors can alleviate the cytoplasmic translocation of apoptosis-related protein Omi/HtrA2 in mitochondria

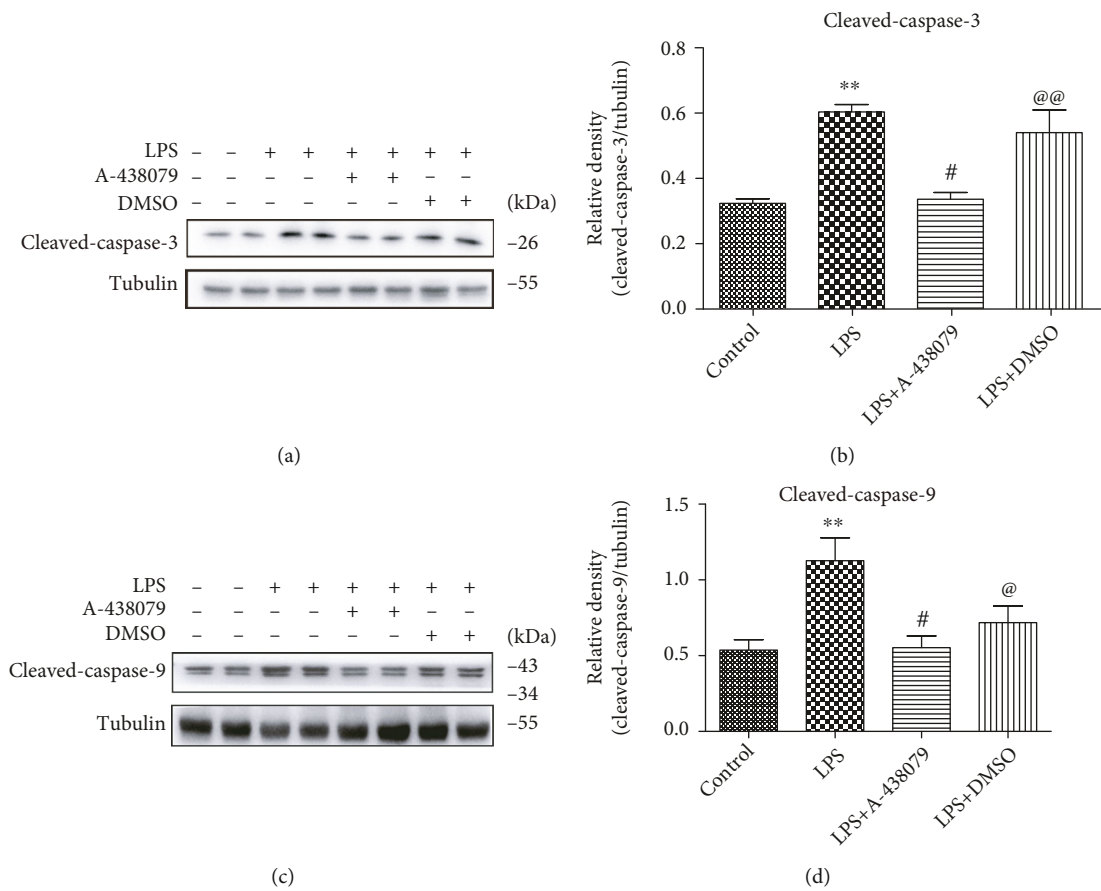


Figure 5 Continued.

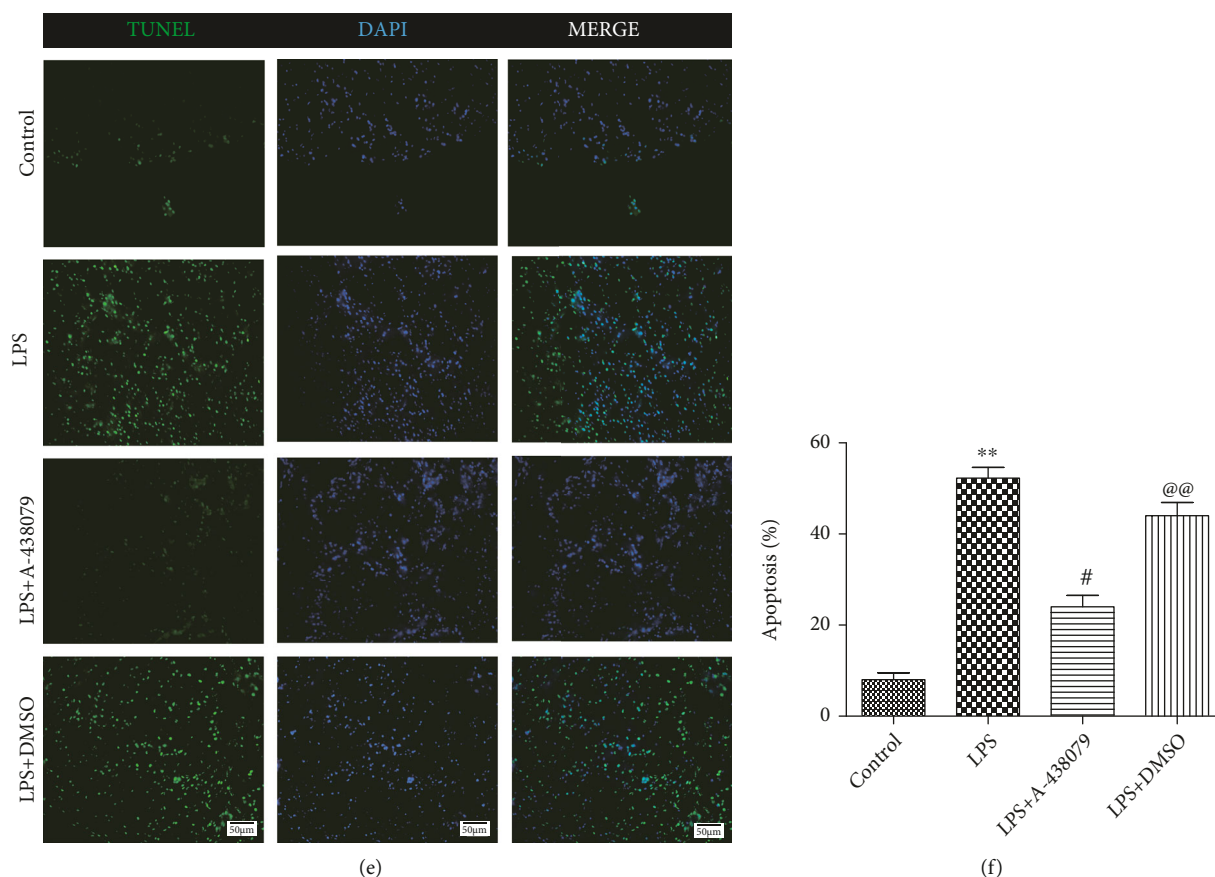


FIGURE 5: A-438079 inhibited Cleaved caspase-9 and Cleaved caspase-3 expression upregulation induced by LPS stimulation and LPS-induced apoptosis of brain cells in mice. (a)–(d) LPS-induced the increasing of Cleaved caspase-9 and Cleaved caspase-3 expression was inhibited by A-438079. All data are expressed as mean \pm SD. ** $P < 0.01$ compared with control, # $P < 0.05$ compared with LPS, @@ $P < 0.01$ compared with LPS + A-438079. (e) and (f) TUNEL fluorescence staining shows apoptosis of cells in the brain of mice. Scale bars = 50 μ m. All data are expressed as mean \pm SD. ** $P < 0.01$ compared with control, # $P < 0.05$ compared with LPS, and @@ $P < 0.01$ compared with LPS + A-438079.

induced by LPS. Therefore, we further researched the effect of A-438079 on the downstream signaling pathway of Omi/HtrA2-induced apoptosis.

Previous studies have shown that XIAP can inhibit apoptosis by degrading apoptotic protein caspase-3 and caspase-9, while Omi/HtrA2 protease mainly degrades XIAP and thus leading to increased activation of caspase-3 and caspase-9. Therefore, in sepsis-associated encephalopathy caused by LPS, P2X7R activation may induce the brain cell apoptosis through the Omi/HtrA2 protease signaling pathway.

In order to identify the impact of P2X7R inhibitor on apoptosis-related proteins, the expression of apoptosis inhibiting protein XIAP was detected by Western Blot. As previously predicted, the level of XIAP in HBMECs was significantly higher in the inhibitor A-438079 group than in the LPS (Figures 4(e) and 4(f)).

3.5. P2X7R Inhibitors A-438079 Alleviated Apoptosis of Brain Cells after LPS Stimulation In Vivo and Reduced Cleaved Caspase-3 and Cleaved Caspase-9 Expression. Caspases are a class of cysteine proteases that exist in the cytoplasm and play an important role in the upstream and downstream of

cell death signaling pathways. Caspase-9, for example, is activated by self-shearing in response to a stimulus signal, which in turn activates downstream apoptotic agents such as Caspase-3.

In order to explore the molecular mechanism of P2X7R induced apoptosis of brain cells by LPS stimulation, we first pretreated microglia with P2X7R inhibitor A-438079 in vitro, followed by LPS stimulation. The expression of cleaved-Caspase-9 and cleaved-Caspase-3 in the LPS + A-438079 groups was decreased compared with the LPS and LPS + DMSO groups (Figures 5(a)–5(d)), while these two indicators were not statistically significant in the inhibitor A-438079 group compared with the control group (Figures 5(a)–5(d)). In order to observe the effect of LPS and A-438079 on the brain cell apoptosis in mice, we further selected frozen brain sections of mice for TUNEL staining. The results demonstrated that a large number of brain cell apoptosis occurred in mice after the administration of LPS 5 mg/kg compared with the control group. However, the number of apoptotic cells in the brain of mice treated with A-438079 after LPS injection was significantly reduced comparing with the LPS group and the LPS + DMSO group. (Figures 5(e) and 5(f)). These results suggest that P2X7R

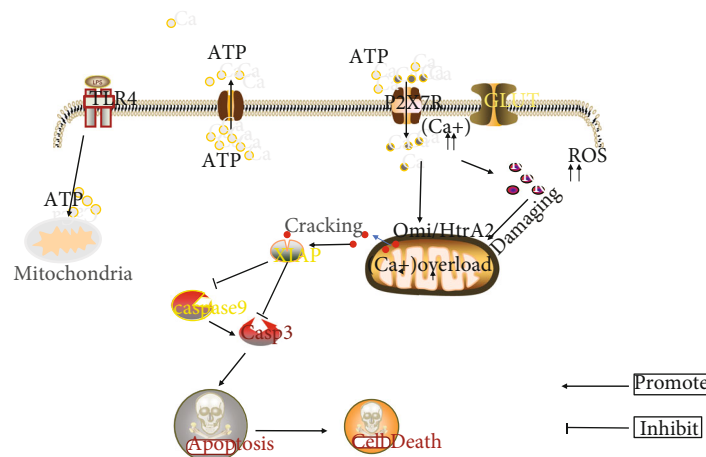


FIGURE 6: LPS stimulated cells to induce the P2X7R-mediated intracellular Omi/HtrA2 apoptosis signaling pathway. Under the stress stimulation of LPS, mitochondria in cells will produce a large amount of ATP and activate P2X7R on the cell surface. The activated P2X7R will cause a large amount of Ca²⁺ influx, and then the imbalance of intracellular Ca²⁺ homeostasis will lead to the production of a large amount of intracellular ROS and further cause mitochondrial damage. However, Ca²⁺ overload in mitochondria will further increase the production of ROS and cause the transfer of OMI/HtrA2 in the damaged mitochondrial membrane space into the cytoplasm. Omi/HtrA2 in the cytoplasm can crack the apoptosis inhibiting protein XIAP, which leads to the decrease of XIAP inhibiting caspase-3 and caspase-9 in cells, and promotes cell apoptosis.

inhibitor A-438079 can reduce intracellular Cleaved Caspase-9 and Cleaved Caspase-3 protein content and also curb the brain cell apoptosis during sepsis in mice.

4. Discussion

Being a syndrome involved multiple brain disorders, SAE is defined by many studies as cognitive impairment caused by severe peripheral sepsis or direct damage to brain tissue without evidence of direct infection in the brain (e.g., hepatic or renal encephalopathy) [31]. Cerebral dysfunction caused by septicemia has been a vital cause of delirium or altered mental state in critically ill patients [32]. Moreover, SAE can dramatically increase the mortality rate of sepsis patients [33, 34]. The destruction of the blood-brain barrier is crucial in SAE, and it leads to the activation of a series of cell surface receptors (especially the P2X7R) in the brain, resulting in the damage of reactive oxygen species and the occurrence of apoptosis and necrosis in the brain [35].

Among the components of BBB, tight junction protein plays an important role in promoting the tight binding between cells and the transmission of information between cells. The relatively common tight junction proteins mainly include transmembrane proteins, such as Occludin, Claudin, and JAM-1, and cytoplasmic attachment proteins, such as ZO-1 [36]. Our study found that LPS-induced inflammatory stimulation activated P2X7R in the hippocampus of mice and further reduced tight junction protein expression, whereas when we used P2X7R inhibitor A-438079, the expression of ZO-1 and Occludin was significantly improved. Therefore, inhibition of P2X7R can protect the integrity of the blood-brain barrier to some extent and reduce the damage of brain cells.

Previous studies have found that the mitochondrial serine protease Omi/HtrA2 plays a critical role in the pathogen-

esis of SAE [29, 35], but their study was limited to Omi/HtrA2 itself. In this study, we found that P2X7R is crucial for cytoplasmic translocation of Omi/HtrA2 under inflammatory stimulation, and there are two possible reasons. First, our experiment found that after activation of P2X7R, plenty of ROS would be produced in cells, causing severe damage to mitochondria in cells. This damage causes the opening of mitochondrial outer membrane channels (especially mPTP) [37], allowing Omi/HtrA2 to enter the cytoplasm. However, as a critical ROS producer, mitochondria also produce bountiful ROS when stimulated, thus, amplifying this effect. Second, as a nonselective cation channel on the cell surface, P2X7R will cause numerous cation influx after activation, break the ion balance inside and outside the cell, and also destroy the membrane potential of mitochondria, leading to cell apoptosis.

In this study, we found that after intraperitoneal injection of LPS, mice had significant cognitive dysfunction in the short term, especially spatial memory and directional sense, and all of them could be alleviated by the treatment of P2X7R inhibitor A-438079. Studies have found that the activation of P2X7R in the brain under inflammatory stimulation can not only result in the release of inflammatory factors (such as IL-6 and TNF- α) [6], but also activate some signaling pathways (such as NLRP3/IL-1 β and STAT3) [38, 39]. However, few studies have been conducted on the role of P2X7R in mediating apoptosis of brain cells under inflammatory conditions. Our study found a mitochondria-related apoptosis pathway caused by P2X7R activation, providing some clues to the possible pathogenesis of SAE.

To sum up, our data demonstrate that P2X7R plays a damaging role in the pathogenesis of SAE. Besides, we provided some valuable evidence, for example, P2X7R activates brain cells to produce a lot of ROS in vivo sepsis, mediates mitochondrial damage and Omi/HtrA2 translocation from

mitochondria to cytoplasm, thereby promoting the cleavage of the intracellular apoptosis-inhibiting protein XIAP through Omi/HtrA2, and increases the expression of proapoptotic protein such as cleaved-Caspase-3 (Figure 6), ultimately leading to cognitive impairment. These findings provide potential therapeutic targets for the treatment of encephalopathy caused by severe infectious diseases and probably reduce the clinical mortality of SAE patients in the future.

5. Conclusion

In this study, we found that P2X7R inhibitors can protect the blood-brain barrier in mice and alleviate the ROS production in brain cells induced by LPS stimulation. In addition, A-438079 also inhibits cell apoptosis by blocking mitochondrial serine protease transfer from mitochondria into the cytoplasm. Moreover, we also demonstrated that P2X7R inhibitors can significantly treat short-term cognitive dysfunction caused by LPS in mice. These findings further demonstrate the great importance of P2X7R in the clinical treatment of SAE.

Data Availability

The data used to support the findings of this study are available from the corresponding author upon request.

Conflicts of Interest

All the authors declare that there are no financial or nonfinancial competing interests regarding the publication of this paper.

Authors' Contributions

Kaifang Wang and Meiyang Sun generated the hypothesis and experimental design. Xiaoyong Zhao contributed to the experimental design. Kaifang Wang and Meiyang Sun conducted the experiments and helped with the data analysis. All the authors reviewed and edited the final manuscript. All authors read and approved the final manuscript. Kaifang Wang and Meiyang Sun are co-first authors.

Acknowledgments

This study was supported by grants from the Shandong Provincial Natural Science Foundation (ZR2016HP06), the Shandong Province Medical and Health Science and Technology Development Plan Project Fund (2019WS605 and 202104110334), Weifang Science and Technology Development plan project (2021YX028), and the Weifang Medical College Students Innovation and Entrepreneurship Training Program Project (X2021523, X2021514 and X2021520).

References

- [1] T. E. Gofton and G. B. Young, "Sepsis-associated encephalopathy," *Nature Reviews. Neurology*, vol. 8, no. 10, pp. 557–566, 2012.
- [2] H. Rabee, R. Tanbour, Z. Nazzal et al., "Epidemiology of sepsis syndrome among intensive care unit patients at a tertiary University Hospital in Palestine in 2019," *Indian Journal of Critical Care Medicine*, vol. 24, no. 7, pp. 551–556, 2020.
- [3] M. Ji, L. L. Qiu, H. Tang et al., "Sepsis-induced selective parvalbumin interneuron phenotype loss and cognitive impairments may be mediated by NADPH oxidase 2 activation in mice," *Journal of Neuroinflammation*, vol. 12, no. 1, p. 182, 2015.
- [4] D. Lowes, A. M. Almawash, N. R. Webster, V. L. Reid, and H. F. Galley, "Melatonin and structurally similar compounds have differing effects on inflammation and mitochondrial function in endothelial cells under conditions mimicking sepsis," *British Journal of Anaesthesia*, vol. 107, no. 2, pp. 193–201, 2011.
- [5] F. Di Virgilio, G. Schmalzing, and F. Markwardt, "The elusive P2X7 macropore," *Trends in Cell Biology*, vol. 28, no. 5, pp. 392–404, 2018.
- [6] G. Burnstock and G. E. Knight, "The potential of P2X7 receptors as a therapeutic target, including inflammation and tumour progression," *Purinergic Signal*, vol. 14, no. 1, pp. 1–18, 2018.
- [7] Y. He, N. Taylor, L. Fourgeaud, and A. Bhattacharya, "The role of microglial P2X7: modulation of cell death and cytokine release," *Journal of Neuroinflammation*, vol. 14, no. 1, p. 135, 2017.
- [8] F. Di Virgilio, D. Dal Ben, A. C. Sarti, A. L. Giuliani, and S. Falzoni, "The P2X7 receptor in infection and inflammation," *Immunity*, vol. 47, no. 1, pp. 15–31, 2017.
- [9] A. Gupta, K. R. Rarick, and R. Ramchandran, "Established, new and emerging concepts in brain vascular development," *Frontiers in Physiology*, vol. 12, p. 73, 2021.
- [10] D. C. Nwafor, A. L. Brichacek, A. S. Mohammad et al., "Targeting the blood-brain barrier to prevent sepsis-associated cognitive impairment," *Journal of Central Nervous System Disease*, vol. 11, article 117957351984065, 2019.
- [11] M. D. Sweeney, A. P. Sagare, and B. V. Zlokovic, "Blood-brain barrier breakdown in Alzheimer disease and other neurodegenerative disorders," *Nature Reviews Neurology*, vol. 14, no. 3, pp. 133–150, 2018.
- [12] F. M. Munoz, R. Gao, Y. Tian, B. A. Henstenburg, J. E. Barrett, and H. Hu, "Neuronal P2X7 receptor-induced reactive oxygen species production contributes to nociceptive behavior in mice," *Scientific Reports*, vol. 7, no. 1, p. 3539, 2017.
- [13] S. Stojilkovic, E. Leiva-Salcedo, M. B. Rokic, and C. Coddou, "Regulation of ATP-gated P2X channels: from redox signaling to interactions with other proteins," *Antioxidants & Redox Signaling*, vol. 21, no. 6, pp. 953–970, 2014.
- [14] L. Zhang, K. Wang, Y. Lei, Q. Li, E. C. Nice, and C. Huang, "Redox signaling: potential arbitrator of autophagy and apoptosis in therapeutic response," *Free Radical Biology & Medicine*, vol. 89, pp. 452–465, 2015.
- [15] E. Tonnes and E. Trushina, "Oxidative stress, synaptic dysfunction, and Alzheimer's disease," *Journal of Alzheimer's Disease*, vol. 57, no. 4, pp. 1105–1121, 2017.
- [16] H. Blaser, C. Dostert, T. W. Mak, and D. Brenner, "TNF and ROS crosstalk in inflammation," *Trends in Cell Biology*, vol. 26, no. 4, pp. 249–261, 2016.
- [17] W. Cheng, Y. Sun, Q. Wu et al., "Paraventricular nucleus P2X7 receptors aggravate acute myocardial infarction injury via ROS-induced vasopressin-V1b activation in rats," *Neuroscience Bulletin*, vol. 37, no. 5, pp. 641–656, 2021.

- [18] H. Wang, T. Zhang, W. Sun et al., "Erianin induces G2/M-phase arrest, apoptosis, and autophagy via the ROS/JNK signaling pathway in human osteosarcoma cells *in vitro* and *in vivo*," *Cell Death & Disease*, vol. 7, no. 6, article e2247, 2016.
- [19] S. Kumar and D. Vaux, "A cinderella caspase takes center stage," *Science*, vol. 297, no. 5585, pp. 1290-1291, 2002.
- [20] Y. Fang and K. Peng, "Regulation of innate immune responses by cell death-associated caspases during virus infection," *The FEBS Journal*, 2021.
- [21] S. M. Kilbride and J. H. Prehn, "Central roles of apoptotic proteins in mitochondrial function," *Oncogene*, vol. 32, no. 22, pp. 2703-2711, 2013.
- [22] Q. B. Liu, L. L. Liu, Y. M. Lu et al., "The induction of reactive oxygen species and loss of mitochondrial Omi/HtrA2 is associated with S-nitrosoglutathione-induced apoptosis in human endothelial cells," *Toxicology and Applied Pharmacology*, vol. 244, no. 3, pp. 374-384, 2010.
- [23] Y. Suzuki, K. Takahashi-Niki, T. Akagi, T. Hashikawa, and R. Takahashi, "Mitochondrial protease Omi/HtrA2 enhances caspase activation through multiple pathways," *Cell Death and Differentiation*, vol. 11, no. 2, pp. 208-216, 2004.
- [24] S. Srinivasula, S. Gupta, P. Datta et al., "Inhibitor of Apoptosis Proteins Are Substrates for the Mitochondrial Serine Protease Omi/HtrA2*," *The Journal of Biological Chemistry*, vol. 278, no. 34, pp. 31469-31472, 2003.
- [25] P. J. Jost and D. Vucic, "Regulation of cell death and immunity by XIAP," *Cold Spring Harbor Perspectives in Biology*, vol. 12, no. 8, article a036426, 2020.
- [26] E. Varfolomeev and D. Vucic, "Inhibitor of apoptosis proteins: fascinating biology leads to attractive tumor therapeutic targets," *Future Oncology*, vol. 7, no. 5, pp. 633-648, 2011.
- [27] G. van Loo, M. Van Gurp, B. Depuydt et al., "The serine protease Omi/HtrA2 is released from mitochondria during apoptosis. Omi interacts with caspase-inhibitor XIAP and induces enhanced caspase activity," *Cell Death and Differentiation*, vol. 9, no. 1, pp. 20-26, 2002.
- [28] J. Althaus, M. D. Siegelin, F. Dehghani, L. Cilenti, A. S. Zervos, and A. Rami, "The serine protease Omi/HtrA2 is involved in XIAP cleavage and in neuronal cell death following focal cerebral ischemia/reperfusion," *Neurochemistry International*, vol. 50, no. 1, pp. 172-180, 2007.
- [29] P. Wang, Y. Hu, D. Yao, and Y. Li, "Omi/HtrA2 regulates a mitochondria-dependent apoptotic pathway in a murine model of septic encephalopathy," *Cellular Physiology and Biochemistry*, vol. 49, no. 6, pp. 2163-2173, 2018.
- [30] A. Catarina, G. Branchini, L. Bettoni, J. R. de Oliveira, and F. B. Nunes, "Sepsis-associated encephalopathy: from pathophysiology to progress in experimental studies," *Molecular Neurobiology*, vol. 58, no. 6, pp. 2770-2779, 2021.
- [31] B. Atterton, M. C. Paulino, P. Pova, and I. Martin-Loeches, "Sepsis associated delirium," *Medicina*, vol. 56, no. 5, p. 240, 2020.
- [32] M. Yu, C. Qin, P. Li et al., "Hydrogen gas alleviates sepsis-induced neuroinflammation and cognitive impairment through regulation of DNMT1 and DNMT3a-mediated BDNF promoter IV methylation in mice," *International Immunopharmacology*, vol. 95, article 107583, 2021.
- [33] R. Luo, C. Luo, F. Zhong et al., "ProBDNF promotes sepsis-associated encephalopathy in mice by dampening the immune activity of meningeal CD4 T cells," *Journal of Neuroinflammation*, vol. 17, no. 1, p. 169, 2020.
- [34] H. Wang, L. J. Hong, J. Y. Huang et al., "P2RX7 sensitizes Mac-1/ICAM-1-dependent leukocyte-endothelial adhesion and promotes neurovascular injury during septic encephalopathy," *Cell Research*, vol. 25, no. 6, pp. 674-690, 2015.
- [35] Y. Hu, Y. Bi, D. Yao, P. Wang, and Y. Li, "Omi/HtrA2 protease associated cell apoptosis participates in blood-brain barrier dysfunction," *Frontiers in Molecular Neuroscience*, vol. 12, p. 48, 2019.
- [36] Q. Sun, X. Xu, T. Wang et al., "Neurovascular units and neural-glia networks in intracerebral hemorrhage: from mechanisms to translation," *Translational Stroke Research*, vol. 12, pp. 447-460, 2021.
- [37] K. Ma, G. Chen, W. Li, O. Kepp, Y. Zhu, and Q. Chen, "Mitophagy, mitochondrial homeostasis, and cell fate," *Frontiers in Cell and Development Biology*, vol. 8, p. 467, 2020.
- [38] L. E. Savio, M. G. Andrade, P. de Andrade Mello et al., "P2X7 receptor signaling contributes to sepsis-associated brain dysfunction," *Molecular Neurobiology*, vol. 54, no. 8, pp. 6459-6470, 2017.
- [39] E. Beamer, F. Göllöncsér, G. Horváth et al., "Purinergic mechanisms in neuroinflammation: an update from molecules to behavior," *Neuropharmacology*, vol. 104, pp. 94-104, 2016.

Research Article

Initial Clinical Experience of Repeat Thrombectomy with a Retrieval Stent (RTRS) with Continuous Proximal Flow Arrest by Balloon Guide Catheter for Acute Intracranial Carotid Occlusion

Wen-huo Chen , Tingyu Yi , Yan-Min Wu , Zhi-nan Pan , Xiu-fen Zheng ,
Xiao-hui Lin , Ding-lai Lin , and Rong-cheng Chen 

Department of Neurointervention, Zhangzhou Affiliated Hospital of Fujian Medical University, Fujian, China

Correspondence should be addressed to Tingyu Yi; siyuyufen@163.com

Received 27 September 2021; Accepted 29 November 2021; Published 31 December 2021

Academic Editor: Muh-Shi Lin

Copyright © 2021 Wen-huo Chen et al. This is an open access article distributed under the Creative Commons Attribution License, which permits unrestricted use, distribution, and reproduction in any medium, provided the original work is properly cited.

Background. Balloon guide catheters (BGCs) have good performance in terms of radiological outcomes in acute ischemic thrombectomy. It is not uncommon for BGCs to be blocked by thrombi, especially in cases with acute intracranial internal carotid artery (ICA) occlusion. Our initial experience using repeat thrombectomy with a retrieval stent (RTRS) with continuous proximal flow arrest by BGC for acute intracranial ICA occlusion is presented. **Methods.** In patients with acute intracranial ICA occlusion treated with RTRS, clinical data, including the National Institutes of Health Stroke Scale (NIHSS) score at admission and modified Rankin Scale (mRS) score at 90 days, and procedural data, including the Extended treatment in Cerebral Infarction (eTICI) score, procedural time, and complications, were analyzed. **Results.** Thirty-two consecutive patients (12 men (37.5%); mean age: 73 years) were treated with RTRS using a BGC. The median NIHSS score was 19. The median puncture-to-reperfusion time was 46 minutes (range: 22-142 minutes). All patients were successfully revascularized; eTICI 2c or better recanalization was achieved in 30 (93.8%) patients. No procedure-related complications or symptomatic intracranial hemorrhage occurred. Two cases (6.3%) had distal emboli, but none had emboli to the anterior cerebral artery. Fourteen patients (43.8%) achieved a good outcome with an mRS score of 0-2 at 90 days, and 8 patients (25.0%) died. **Conclusions.** In patients with intracranial ICA occlusion, RTRS with proximal flow arrest by BGC is effective and safe, achieving good clinical and angiographic outcomes. This method may reduce the incidence of distal emboli in thrombectomy with stent retrievers.

1. Introduction

Acute intracranial internal carotid artery (ICA) occlusion, especially carotid T occlusion, is often associated with a large clot burden, low clot burden score, poor collateral flow, and poor outcome, resulting in a large ICA territory infarction [1]. Its overall mortality is up to 51% [1]. Endovascular therapy is the standard treatment for acute large intracranial artery occlusion [2-8]. Despite major strides in reducing disability from large vessel occlusion strokes with stent retrievers (SRs), 72% of patients with intracranial ICA occlusion remain physically disabled [1]. A high first-pass complete reperfusion rate [9], short puncture-to-reperfusion time (PRT) [10], and

low incidence of distal emboli [11] are associated with improved functional neurological recovery.

Balloon guide catheters (BGCs) offer reliable blood flow arrest and flow reversal in combination with aspiration via syringes or high-flow pump systems [12]. Nonrandomized studies suggest that BGC use during mechanical thrombectomy for acute ischemic stroke is associated with superior clinical and angiographic outcomes [13]. However, in the setting of acute intracranial ICA occlusion with a large clot burden, it is very possible that BGCs is blocked by thrombi. In the clinical setting, when the guide catheter is blocked by a thrombus, no blood flow comes out of the catheter, and the guide catheter will be retracted to clear the thrombus in it.

However, such an operation wastes time and may increase the possibility of distal emboli occurrence, which may influence patients' clinical outcome.

The purpose of our study was to assess the feasibility of repeat thrombectomy with a retrieval stent (RTRS) with continuous proximal flow arrest by BGC and to evaluate whether the use of this technique improves reperfusion and clinical outcomes in acute intracranial ICA occlusion.

2. Methods

2.1. Study Patients. The study included patients identified from our prospective registry database of acute stroke patients treated with endovascular therapy between January 1, 2015, and November 30, 2020. The selected patients met the following criteria: (1) ischemic stroke resulting from acute intracranial ICA occlusion confirmed by digital subtraction angiography (DSA); (2) patient age greater than 18 years; (3) prestroke modified Rankin Scale (mRS) score of 0–1; and (4) receiving endovascular therapy with the use of a BGC.

The exclusion criteria for this study were thrombectomies performed for (1) ipsilateral stenosis or acute extracranial occlusions, (2) previously deployed stents, and (3) dissections and in settings in which (4) the BGC was not blocked by a thrombus during the procedure and (5) the BGC was blocked by a thrombus but the RTRS technique was not used.

2.2. Endovascular Procedure: RTRS Technique. The RTRS technique is shown in Figure 1.

All procedures were performed under general anesthesia or conscious sedation. After femoral puncture with an 8F sheath, 2500 units or less of intravenous (IV) heparin was injected. An 8F BGC (Merci/Flowgate 2, Stryker Products, Boston, USA) was advanced with a 4F/5F MPA catheter or via the exchange technique and placed distal to the carotid bifurcation. After the presence of acute intracranial ICA occlusion was confirmed by injection of contrast through the BGC and in some cases a distal access catheter (Catalyst, Stryker Products, Boston, USA; Navein, ev3 Inc., Plymouth, MN, USA) was applied, a 0.014-inch microwire (Transcend; Stryker, Kalamazoo, MI) was passed through the intracranial ICA occluded segment, and a microcatheter (ev3 Inc., Plymouth, MN, USA) was advanced over the microwire through the occlusion site. Microcatheter injection was performed to verify the microcatheter's position distal to the thrombus; then, a Solitaire AB 6–30 mm (ev3 Inc., Plymouth, MN, USA) was unsheathed at the occlusion site. After at least 3 minutes, the balloon was inflated to arrest the anterograde flow from the ICA, and the fully deployed Solitaire stent was partially resheathed by microcatheter or distal access catheter. Together with the delivery microcatheter and distal access catheter if used, the stent was gently pulled back under continuous suction achieved with a syringe (Figure 1(a), named as primary clot retrieve). If the BGC was blocked by a thrombus and there was no blood flow through the BGC, the BGC was kept inflated and continuous suction was applied via a syringe (Figure 1(b)). Then, the microcatheter together with stent was advanced directly into

the site, which was close to the distal tip of the BGC (Figure 1(c)), and unsheathed at the site. The stent together with the delivery microcatheter was then retrieved under continuous suction (Figure 1(d), called rescue clot retrieval). Steps C and D were repeated (i.e., the repeat thrombectomy with a retrieval stent (RTRS) technique) with continuous inflation of the balloon until there was blood flow through the BGC without a thrombus (Figure 1(e)). Contrast was injected via the BGC to confirm successful reperfusion was achieved; then, the BGC was deflated (Figure 1(e)).

2.3. Outcome Measures

2.3.1. Clinical Outcomes. The primary clinical efficacy outcome was the rate of good prognosis at 90 days postprocedure, as defined by an mRS score of 0 to 2. Safety was evaluated by the incidence of symptomatic intracranial hemorrhage (sICH) and all-cause mortality \leq 90 days postprocedure.

2.3.2. Angiographic and Procedural Outcomes. The primary angiographic outcome was the rate of achieving successful reperfusion ($eTICI \geq 2b$, $eTICI \geq 2c$, and $eTICI 3$), [14] after a single pass of primary clot retrieval. Achievement of complete reperfusion ($eTICI 3$) after a single pass of primary clot retrieval no matter how many passes of rescue clot retrieval was adopted, is called the first-pass effect (FPE) [15].

Secondary outcome measures included the incidence of distal emboli, the incidence of emboli in the anterior cerebral artery (ACA), and the final successful reperfusion rate. Successful reperfusion was defined as an $eTICI$ grade of 2b, 2c, or 3 after endovascular treatment. The PRT was defined as the time from puncture to achieving $eTICI \geq 2b$ or procedure completion.

2.4. Data Availability. Access to patient records for data collection and analysis was approved by our local medical ethics committee, and informed consent was not obtained because of the retrospective nature of the study. We will share the identified data of participants in our study upon request.

2.5. Statistical Analysis. The data for categorical variables are described in absolute and relative frequencies. The data for continuous variables are given as the median and range or the mean and standard deviation. All statistical analyses were performed with IBM SPSS Statistics 22.0 (IBM, Inc., Armonk, NY).

3. Results

From 1 January 2015 to 1 November 2020, there were 426 patients with acute intracranial ICA occlusion, and BGCs were used in 116 patients. The BGC was blocked by a thrombus after the first pass of SR, allowing no blood flow out of the BGC, in 40 patients (36 cases with 8F Merci, 4 cases with 8F Flowgate 2), and the RTRS technique was applied in 32 patients. An illustration of the cases is shown in Figure 2.

Baseline characteristics, clinical features, and preprocedural radiological features are shown in Table 1. There were 12 (12/32, 37.5%) male patients, the age of onset was 73 ± 11

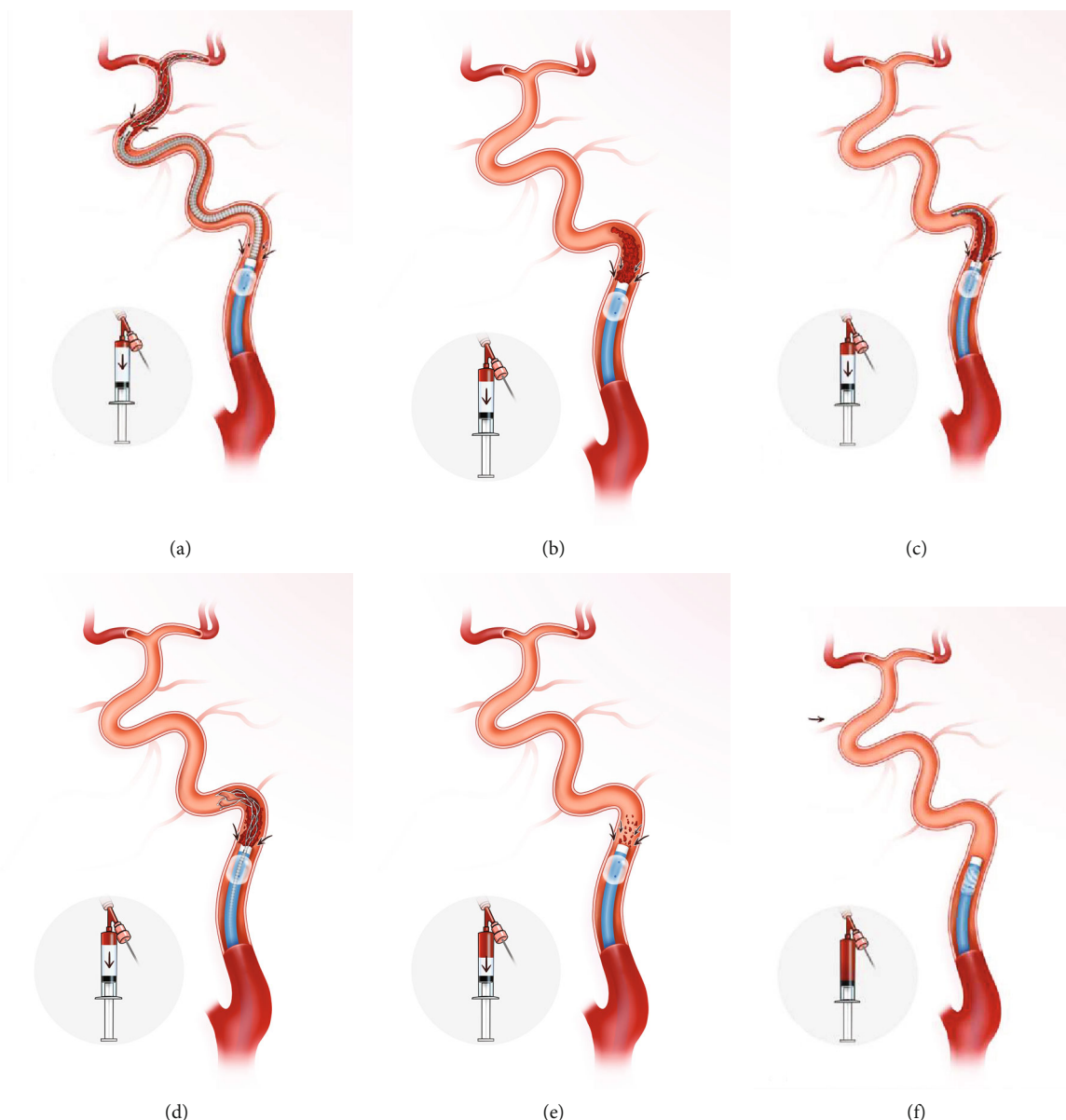


FIGURE 1: Illustration of the repeat thrombectomy with a retrieval stent (RTRS) technique with continuous proximal flow arrest by a balloon guide catheter for acute intracranial ICA occlusion. (a) DSA shows ICA terminus occlusion involving the MCA and ACA. The retrieval stent is unsheathed at the occlusion site. After at least 3 minutes, the balloon is inflated to arrest the anterograde flow from the ICA, and then the fully deployed Solitaire stent is partially resheathed. Together with the delivery microcatheter and distal access catheter, the stent is gently pulled back under continuous suction achieved with a syringe. This procedure is called primary clot retrieval. (b) The BGC was blocked by a thrombus, and there was no blood flow through the BGC. The BGC was kept inflated, and continuous suction was achieved via a syringe. (c) The microcatheter and stent were advanced together directly into the site, which was close to the distal tip of the BGC. (d) The stent is unsheathed at the site close to the distal tip of the BGC, and then the stent together with the delivery microcatheter is retrieved back under continuous suction. This procedure is called rescue clot retrieval. (e) Blood flow without a thrombus comes out of BGC, and gentle injection contrast via the BGC was performed to confirm successful reperfusion. (f) The BGC was deflated. ICA: internal carotid artery; DSA: digital subtraction angiography; BGC: balloon guide catheter.

years, and the mean admission NIHSS score was 19. Regarding vascular risk factors, 23/32 (71.9%) patients had hypertension, 6/32 (18.8%) had diabetes mellitus, 3/32 (9.4%) had hyperlipidemia, 21/32 (65.6%) had atrial fibrillation, and 7/32 (21.9%) were smokers.

Procedure details and radiological and clinical outcomes are shown in Table 2. Regarding procedural details, all patients underwent one pass of primary clot retrieval, the

median number of rescue clot retrieval passes was 1 (range from 1 to 8), the mean PRT was 61.2 ± 24.0 minutes, the median PRT was 46 minutes, and the range was from 22 minutes to 142 minutes. After one primary clot retrieval pass, eTICI $\geq 2b$ reperfusion was achieved in all patients, eTICI $\geq 2c$ reperfusion was achieved in 30/32 (93.8%) patients, eTICI 3 reperfusion was achieved in 27/32 (84.4%) patients, distal emboli occurred in 2/32 (6.3%)

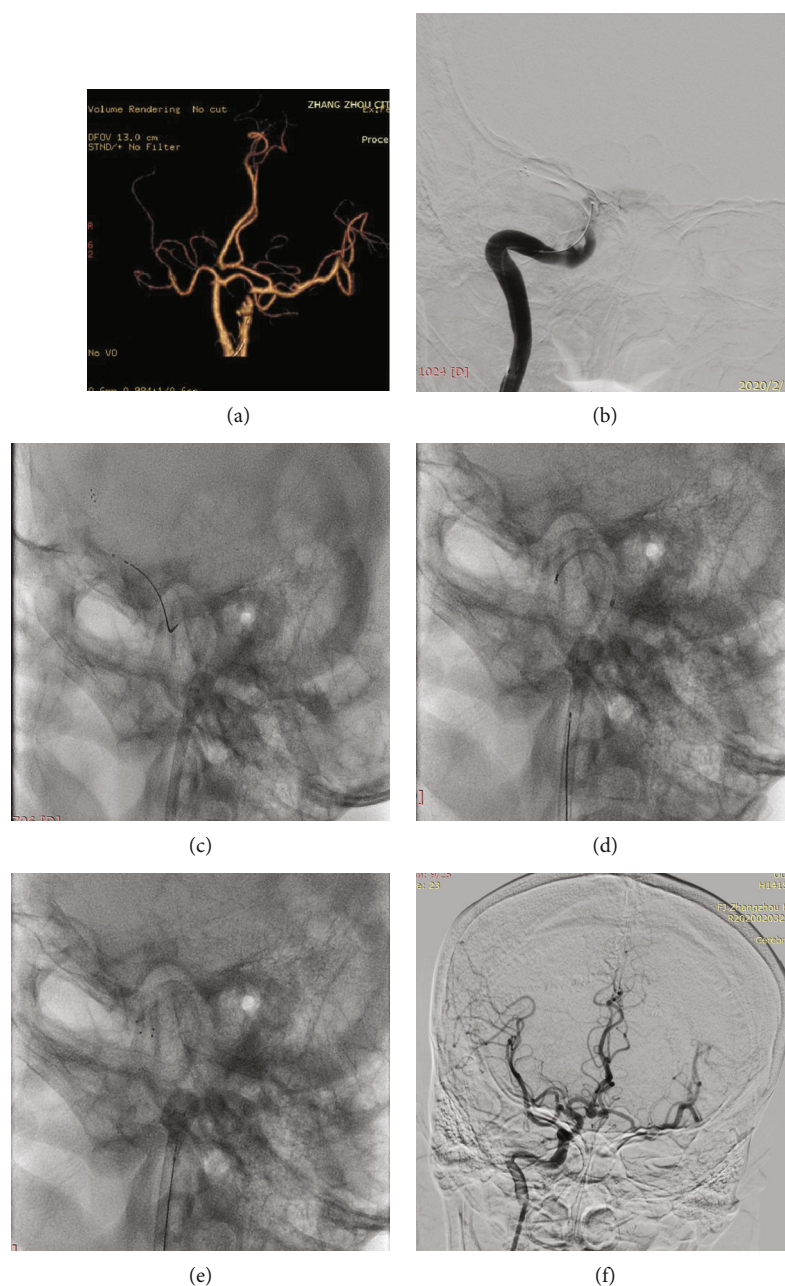


FIGURE 2: An elderly presented with left hemiparesis and a history of atrial fibrillation postcardiac valve replacement. The patient regularly took warfarin, and admission NIHSS was 18. (a) Computed tomography angiography (CTA) shows total occlusion of the right ICA occlusion and the anterior communicating artery open; the right anterior cerebral artery is supplied by the left ICA. (b) A Solitaire 6-30 mm stent was unsheathed at the occlusion site (shown as a black arrow). DSA showed ICA intracranial segment occlusion with a large clot burden, and the CBS was 3. (c) After at least 3 minutes, the balloon (shown as a black arrow) was inflated to arrest the anterograde flow from the ICA. Then, the fully deployed Solitaire stent was partially resheathed, and together with the delivery microcatheter, it was gently pulled back under continuous suction achieved with a syringe. This procedure is called primary clot retrieval. (d) The BGC remained inflated for there is no blood out of BGC, and continuous suction was applied via a syringe; the microcatheter and stent are advanced together directly into the site, which is close to the distal tip of the BGC. (e) The stent is unsheathed at the site close to the distal tip of the BGC, and then the stent together with the delivery microcatheter is retrieved back under continuous suction. This procedure is called rescue clot retrieval. (f) Rescue clot retrieval is repeated until there is blood flow without a thrombus through the BGC; contrast is gently injected via the BGC to confirm that successful reperfusion is achieved. The balloon is deflated, and DSA shows that the right ICA is totally patent and the anterior communicating artery is open; the bilateral MCA and ACA are supplied by the right ICA. NIHSS: NIH stroke scale; CTA: CT angiography; DSA: digital subtraction angiography; ICA: internal carotid artery; BGC: balloon guide catheter; CBS: clot burden score; MCA: middle cerebral artery; ACA: anterior cerebral artery.

TABLE 1: Baseline characteristics, clinical features, and preprocedural radiological features of the 32 patients who underwent RTRS.

Item		
Clinical features	Male sex, <i>n</i> (%)	12 (37.5%)
	Age, mean \pm SD (y)	73 \pm 11
	OPT, mean \pm SD (min)	382.0 \pm 325.9
	TOAST-CE	21 (65.6%)
	TOAST-undetermined: cryptogenic embolism	11 (34.4%)
Admission NIHSS, IQR		
19 (17, 21)		
Vascular risk factors	Hypertension, <i>n</i> (%)	23 (71.9%)
	Diabetes mellitus, <i>n</i> (%)	6 (18.8%)
	Atrial fibrillation, <i>n</i> (%)	21 (65.6%)
	Hyperlipidemia, <i>n</i> (%)	3 (9.4%)
	History of smoking, <i>n</i> (%)	7 (21.9%)
Preprocedural radiological features		
CBS, IQR		
4.5 (3, 5)		

SD: standard deviation; OPT: onset-to-presentation time; TOAST: Trial of Org 10172 in Acute Stroke Treatment; CE: cardioembolism; NIHSS: NIH stroke scale; IQR: interquartile range; CBS: clot burden score.

TABLE 2: Procedure details and radiological and clinical outcomes of the 32 patients who underwent RTRS.

Item		
Procedure detail	One pass of primary clot retrieval, <i>n</i> (%)	32 (100%)
	Passes of rescue clot retrieval, IQR	1 (1.3)
	Passes of rescue clot retrieval, median (min, max)	1 (1.8)
	PRT, mean \pm SD (min)	59.8 \pm 23.1
	PRT, median (min, max) (min)	46 (22.142)
Radiological outcome	One pass of primary clot retrieval achieves	
	\geq eTICI 2b reperfusion, <i>n</i> (%)	32 (100%)
	\geq eTICI 2c reperfusion, <i>n</i> (%)	30 (93.8%)
	PPE: eTICI3 reperfusion, <i>n</i> (%)	27 (84.4%)
	Distal emboli, <i>n</i> (%)	2 (6.3%)
	Emboli to the ACA	0 (0%)
sICH		
0 (0%)		
Clinical outcome	Good prognosis	14 (43.8%)
	Mortality	8 (25.0%)

IQR: interquartile range; SD: standard deviation; OPT: onset-to-presentation time; eTICI: Extended treatment in Cerebral Infarction (eTICI) score; ACA: anterior cerebral artery; PPE: first-pass effect; sICH: symptomatic intracranial hemorrhage; PRT: puncture-to-reperfusion time; FPE: first-pass effect.

patients, and no cases of emboli to the anterior cerebral artery or sICH occurred.

Regarding clinical outcome, the good prognosis rate was 43.8% (14/32), and the mortality rate was 25.0% (8/32).

4. Discussion

RTRS is a modification of the conventional SR thrombectomy technique. The modifications of conventional SR thrombectomy are (1) the use of a BGC with the SR thrombectomy technique, (2) continuous inflation of the balloon when removing the retrieval stent and distal access catheter from the guide catheter, and, most importantly, (3) the inclusion of a procedure for when the BGC is blocked by a thrombus and no blood flows out of the BGC. In RTRS,

the balloon is kept inflated, and then repeated thrombectomy with a retrieval stent is performed at the site near the distal tip of the BGC until blood flows out of the BGC. Angiography is performed via the BGC by gentle manual injection of contrast agent to ensure that the thrombus is cleared, and then, the balloon is deflated.

The use of RTRS when the BGC is blocked by a thrombus has three useful advantages. First, it is time saving. The BGC does not need to be retracted out of the sheath and reestablished the route. During the rescue clot retrieval procedure, we did not need to advance a microcatheter with a microwire into the middle cerebral artery. We just advanced the microcatheter together with the stent into the site that was close to the distal tip of the BGC and unsheathed the stent at that site, and such an operation was very quick,

simple, and convenient. Our study showed that the mean time of PRT was shorter than that in a previous study, which was also about endovascular therapy for intracranial artery occlusion (59 minutes vs. 120 minutes) [1]. Second is the high rate of successful reperfusion. Acute intracranial ICA occlusion, especially carotid T occlusion, is usually associated with high clot burden and low CBS [16], and the successful reperfusion rate ranges from 60.5% [1] to 86.9% [17]. In our study, all patients achieved successful reperfusion, and approximately 90.9% of patients achieved nearly complete successful reperfusion after one primary clot retrieval pass. Third is high FPE occurrence. FPE is associated with significantly higher rates of good clinical outcome [9, 15]. A previous study showed that FPE was observed in 33% of patients with intracranial artery occlusion who underwent SR thrombectomy with 8F Flowgate 2BGC in which the inner lumen was larger than that of 8F Merci. In our study, FPE was observed in 81.8% of patients. Fourth, there was a low occurrence of distal emboli and emboli into the ACA. Distal emboli are a troublesome event during mechanical thrombectomy and is usually associated with increased mortality and disability rates, regardless of the success of reperfusion [18]. Distal emboli are a controllable event. Acute intracranial ICA occlusion, which is associated with a high clot burden, had a higher rate of distal emboli (15.3%) than middle cerebral artery (MCA) occlusion (4.8%) [18]. The use of mechanical thrombectomy (MT) techniques can decrease the incidence of distal emboli. For example, the use of distal access catheters in association with SR, which is common in clinical practice, can decrease the distal emboli incidence from 5% to 11% [19]. The use of BGCs can also decrease the incidence of distal emboli [20, 21]. Regarding intracranial ICA occlusion, the incidence of distal emboli is as high as 75% in patients who underwent MT with conventional guide catheters [20], but the incidence decreases to 0% when MT is combined with BGCs [20]. In our study, the incidence of distal emboli was 6.3%, with no emboli to the ACA. Regarding cases with distal emboli, the thrombus is very small, so it causes only very remote branches to become occluded, which may minimize the influence on functional outcome.

There are three important technical points of the RTRS technique. The first point is continuous inflation of the balloon when there is no blood flow coming out of the BGC and never performing angiography with contrast during this step because of the risk of moving the thrombus into a distal territory with the injection pressure. Second, repeat thrombectomy with a retrieval stent should not be stopped at the site near the tip of the BGC until blood is flowing out of the BGC and no thrombus is trapped by the stent. Third, when the blood flow from the BGC is not fluent and no thrombus is trapped by the stent, two situations should be considered. One is that the tip of the BGC is completely or partially covered by the vessel wall, and the other is that there is a thrombus in the ICA terminus. Therefore, we needed to partly unsheath the stent at the ICA terminus, deflate the balloon, gently retract the BGC slightly, and then perform angiography via the BGC to check what happened. If complete recanalization is

achieved, the procedures terminated; if there is thrombus in the culprit artery, the balloon is reinflated, and the thrombectomy was repeated.

There is one concern about cerebral ischemia caused by continuous proximal blood flow arrest using balloon occlusion, which has also been reported with the TSAT technique [21]. However, we only adopt this technique in patients with intracranial ICA occlusion, so we do not need to worry about this problem because the vessel is initially occluded and there is no blood supply downstream territory. Another concern is the formation of fresh thrombi secondary to continuous proximal blood flow arrest. Therefore, the procedure should be performed as soon as possible, and proper heparinization is also needed during the procedure.

Due to the excellent performance of the RTRS technique on radiological outcomes, the clinical outcome of the patients in our study was acceptable and even better than that of those in a previous study, although the thrombus burden was large in our included cases, which is usually associated with poor clinical outcomes. The clinical outcome is poor in patients with intracranial ICA occlusion [17, 22, 23], the rate of good outcomes ranges from 21.4% [1] to 40% [17], and the mortality rate ranges from 29.3% [22] to 55.2% [1]. In our study, the incidence of good outcomes was 43.8%, and the mortality rate was 25.0%.

This study is limited by being a single-center study. Despite this limitation, our study is the first series with relatively numerous cases that attempted to examine an endovascular strategy in the setting of the BGC being blocked by a thrombus. Second, the 8F Flowgate2 BGC inner lumen (0.084 inches) of which is larger than that of the 8F Merci (0.078 inches), was not used in all cases in our study. However, we only present the technique to address the circumstance of the BGC being blocked by a thrombus, which could also occurred in cases with 8F Flowgate 2 BGCs or even those with larger inner lumens (0.090 inches) [24], so this usage of this technique is not influenced.

5. Conclusion

RTRS with proximal flow arrest using a BGC is effective for the treatment of acute ischemic stroke due to acute intracranial ICA occlusion. This approach has allowed us to achieve excellent clinical and angiographic outcomes and shorten the PRT time, and it may reduce the incidence of distal emboli in acute ischemic thrombectomy. This technique should be considered in cases of acute intracranial ICA occlusion when the BGC is blocked by a thrombus during the procedure. However, our findings should be confirmed by future multicenter, large-sample studies.

Data Availability

We declare that we can make data available on request through institutional review board once it is needed.

Conflicts of Interest

The authors declare that they have no conflicts of interest.

Acknowledgments

This study was supported by the National Health Commission Capacity Building and Continuing Education Center (grant number GWJJ2021100203). We thank the team of American Journal Expert for editing the English text of a draft of this manuscript (<https://secure.aje.com>).

References

- [1] D. S. Liebeskind, A. C. Flint, R. F. Budzik et al., "Carotid I's, L's and T's: collaterals shape the outcome of intracranial carotid occlusion in acute ischemic stroke," *Journal of NeuroInterventional Surgery*, vol. 7, no. 6, pp. 402–407, 2015.
- [2] O. A. Berkhemer, P. S. S. Fransen, D. Beumer et al., "A randomized trial of intraarterial treatment for acute ischemic stroke," *The New England Journal of Medicine*, vol. 372, no. 1, pp. 11–20, 2015.
- [3] B. C. V. Campbell, P. J. Mitchell, T. J. Kleinig et al., "Endovascular therapy for ischemic stroke with perfusion-imaging selection," *The New England Journal of Medicine*, vol. 372, no. 11, pp. 1009–1018, 2015.
- [4] M. Goyal, A. M. Demchuk, B. K. Menon et al., "Randomized assessment of rapid endovascular treatment of ischemic stroke," *The New England Journal of Medicine*, vol. 372, no. 11, pp. 1019–1030, 2015.
- [5] J. L. Saver, M. Goyal, A. Bonafe et al., "Stent-retriever thrombectomy after intravenous t-PA vs. t-PA alone in stroke," *The New England Journal of Medicine*, vol. 372, no. 24, pp. 2285–2295, 2015.
- [6] T. G. Jovin, A. Chamorro, E. Cobo et al., "Thrombectomy within 8 hours after symptom onset in ischemic stroke," *The New England Journal of Medicine*, vol. 372, no. 24, pp. 2296–2306, 2015.
- [7] R. G. Nogueira, A. P. Jadhav, D. C. Haussen et al., "Thrombectomy 6 to 24 hours after stroke with a mismatch between deficit and infarct," *The New England Journal of Medicine*, vol. 378, no. 1, article NEJMoa1706442, pp. 11–21, 2018.
- [8] G. W. Albers, M. P. Marks, S. Kemp et al., "Thrombectomy for stroke at 6 to 16 hours with selection by perfusion imaging," *The New England Journal of Medicine*, vol. 378, no. 8, pp. 708–718, 2018.
- [9] O. Nikoubashman, S. Dekeyser, A. Riabikin et al., "True first-pass Effect," *Stroke*, vol. 50, no. 8, pp. 2140–2146, 2019.
- [10] M. Mazighi, S. A. Chaudhry, M. Ribo et al., "Impact of onset-to-reperfusion time on stroke Mortality," *Circulation*, vol. 127, no. 19, pp. 1980–1985, 2013.
- [11] A. Todo, A. Minaeian, R. Sahni, and K. H. Chao, "Incidence and outcome of procedural distal emboli using the penumbra thrombectomy for acute stroke," *Journal of NeuroInterventional Surgery*, vol. 5, no. 2, pp. 135–138, 2013.
- [12] O. Nikoubashman, D. Wischer, H. M. Hennemann et al., "Balloon-guide catheters are needed for effective flow reversal during mechanical thrombectomy," *American Journal of Neuroradiology*, vol. 39, no. 11, pp. 2077–2081, 2018.
- [13] W. Brinjikji, R. M. Starke, M. H. Murad et al., "Impact of balloon guide catheter on technical and clinical outcomes: a systematic review and meta-analysis," *Journal of NeuroInterventional Surgery*, vol. 10, no. 4, pp. 335–339, 2018.
- [14] D. S. Liebeskind, S. Bracard, F. Guillemin et al., "ETICI reperfusion: defining success in endovascular stroke therapy," *Journal of NeuroInterventional Surgery*, vol. 11, no. 5, pp. 433–438, 2019.
- [15] O. O. Zaidat, A. C. Castonguay, I. Linfante et al., "First pass Effect," *Stroke*, vol. 49, no. 3, pp. 660–666, 2018.
- [16] I. Derraz, R. Bourcier, M. Soudant et al., "Does clot burden score on baseline T2*-MRI impact clinical outcome in acute ischemic stroke treated with mechanical thrombectomy?," *Journal of Stroke*, vol. 21, no. 1, pp. 91–100, 2019.
- [17] T. Ota, K. Shigeta, T. Amano, and J. Kaneko, "Endovascular treatment for acute carotid T and carotid non-T occlusion: a retrospective multicentre study of 81 patients," *Interventional Neuroradiology*, vol. 25, no. 5, pp. 497–501, 2019.
- [18] V. Chalumeau, R. Blanc, H. Redjem et al., "Anterior cerebral artery embolism during thrombectomy increases disability and mortality," *Journal of NeuroInterventional Surgery*, vol. 10, no. 11, pp. 1057–1062, 2018.
- [19] R. A. McTaggart, E. L. Tung, S. Yaghi et al., "Continuous aspiration prior to intracranial vascular embolectomy (CAPTIVE): a technique which improves outcomes," *Journal of NeuroInterventional Surgery*, vol. 9, no. 12, pp. 1154–1159, 2017.
- [20] S. H. Kim, J. H. Choi, M. J. Kang et al., "Efficacy of combining proximal balloon guiding catheter and distal access catheter in thrombectomy with stent retriever for anterior circulation ischemic stroke," *Journal of Korean Neurosurgical Association*, vol. 62, no. 4, pp. 405–413, 2019.
- [21] H. Matsumoto, H. Nishiyama, Y. Tetsuo, H. Takemoto, and N. Nakao, "Initial clinical experience using the two-stage aspiration technique (TSAT) with proximal flow arrest by a balloon guiding catheter for acute ischemic stroke of the anterior circulation," *Journal of NeuroInterventional Surgery*, vol. 9, no. 12, pp. 1160–1165, 2017.
- [22] D. Frahm, S. Wunderlich, M. I. Schubert, H. Poppert, J. F. Kleine, and S. Prothmann, "Mechanical thrombectomy in acute occlusion of the carotid-T: a retrospective single centre study in 51 patients," *Clinical Neuroradiology*, vol. 26, no. 1, pp. 23–29, 2016.
- [23] G. B. Bradac, F. Venturi, G. Bosco et al., "Acute occlusion of the distal internal carotid Artery," *Clinical Neuroradiology*, vol. 30, no. 1, pp. 67–76, 2020.
- [24] A. Okamura, K. Kuroki, K. Shinagawa, and N. Yamada, "Simple aspiration with balloon catheter technique (simple ABC technique) against proximal internal carotid artery occlusion in cases of cardiogenic cerebral embolism," *Interventional Neuroradiology*, vol. 24, no. 3, pp. 317–321, 2018.

Research Article

The Parkinson's Disease Progression Neuroimaging Initiative

Shiyi Zhu ¹, Zizhao Ju ², Ping Wu ², Fengtao Liu ³, Jingjie Ge ², Huiwei Zhang ²,
Jiaying Lu ², Ling Li ², Min Wang ¹, Jiehui Jiang ⁴, Jian Wang ³,
and Chuantao Zuo ²

¹School of Communication and Information Engineering, Shanghai University, Shanghai, China

²PET Center and National Research Center for Aging and Medicine & National Center for Neurological Disorders, Huashan Hospital, Fudan University, Shanghai, China

³Department of Neurology and National Research Center for Aging and Medicine & National Center for Neurological Disorders, Huashan Hospital, Fudan University, Shanghai, China

⁴School of Life Science, Shanghai University, Shanghai, China

Correspondence should be addressed to Jian Wang; wangjian_hs@fudan.edu.cn and Chuantao Zuo; zuochuantao@fudan.edu.cn

Received 12 October 2021; Accepted 29 November 2021; Published 30 December 2021

Academic Editor: Muh-Shi Lin

Copyright © 2021 Shiyi Zhu et al. This is an open access article distributed under the Creative Commons Attribution License, which permits unrestricted use, distribution, and reproduction in any medium, provided the original work is properly cited.

The Parkinson's Disease Progressive Neuroimaging Initiative (PDPNI) is a longitudinal observational clinical study. In PDPNI, the clinical and imaging data of patients diagnosed with Parkinsonian syndromes and Idiopathic rapid eye movement sleep behavior disorder (RBD) were longitudinally followed every two years, aiming to identify progression biomarkers of Parkinsonian syndromes through functional imaging modalities including FDG-PET, DAT-PET imaging, ASL MRI, and fMRI, as well as the treatment conditions, clinical symptoms, and clinical assessment results of patients. From February 2012 to March 2019, 224 subjects (including 48 healthy subjects and 176 patients with confirmed PDS) have been enrolled in PDPNI. The detailed clinical information and clinical assessment scores of all subjects were collected by neurologists from Huashan Hospital, Fudan University. All subjects enrolled in PDPNI were scanned with ¹⁸F-FDG PET, ¹¹C-CFT PET, and MRI scan sequence. All data were collected in strict accordance with standardized data collection protocols.

1. Introduction

Parkinsonian syndromes are a group of diseases featured by symptoms of parkinsonism, including bradykinesia, rigidity, tremor, and postural instability [1]. Parkinsonian syndromes include at least dozens of diseases, including MSA, PSP, and CBD. Parkinson's disease (PD) is the most common neurodegenerative parkinsonian syndrome, affecting approximately 2% to 3% of adults over the age of 65 [2]. The main pathological manifestations of PD are the degeneration of dopaminergic neurons in the substantia nigra, the reduction of striatal dopamine, and the abnormal aggregation of α -synuclein. Aside from PD, there are a number of other diseases, which also present with Parkinsonian features, but its further clinical manifestations are atypical for PD. It has been named as atypical parkinsonian syndromes (APS) or

atypical parkinsonism. APS mainly include multisystem atrophy (MSA), progressive supranuclear palsy (PSP), corticobasal degeneration (CBD), and dementia with Lewy bodies (DLB). The pathogenesis, clinical manifestations, and treatment methods of PD and APS are different. APS are synucleinopathies and tauopathies, and its clinical characteristics depend on the site of abnormal protein α -synuclein and tau deposition [3]. Several studies have demonstrated that RBD, a rapid eye movement sleep- (REM-) phase-associated parasomnia with the loss of muscle atonia and the occurrence of abnormal movements during REM [4], is a prodromal phase of synucleinopathies disease including PD, DLB, and MSA, which has up to 30% estimated risk of synucleinopathy at 3 years of disease duration, increasing to 76% at 10 years and coming to about 91% at 14 years [5, 6]. RBD patients can also present with clinical features

of synucleinopathies, such as deficits in motor, cognitive, olfaction, color discrimination, and autonomic functions [7]. Up to now, the prediction of the risk and time course of individual subsequent phenoconversion is still challenging, thus an increasing number of neuroimaging researches have been carried out, for the purpose of improving the understanding of the development and progression of RBD and related neurodegenerative diseases.

The diagnosis of Parkinsonian syndromes relies mostly on clinical criteria. However, in lack of specific clinical signs initially, it can be difficult in the differential diagnosis among these diseases especially at an early phase. Moreover, the clinical symptoms could develop heterogeneously during the progression of these diseases. Therefore, it is necessary to establish a clinical database for parkinsonian syndromes, which can manage and analyze medical records for Parkinsonian syndromes patients, including clinical, imaging, and biospecimen data and clinical scale evaluation; individualized therapies enhance the diagnosis and treatment trials on PDS, find the novel imaging manifestations and clinical biomarkers of PDS, promote the accuracy of the diagnosis and differentiation, and enhance the development of PD treatment. There are several databases of PD and Parkinsonian syndrome have been established worldwide, and the most widely used one is the international multicenter study called PPMI (the Parkinson's progression markers initiative), which was a multicenter study enrolled in 24 sites, which started in June 2010. The cohort included 423 untreated PD patients, 196 healthy control (HC) subjects, and 64 SWEDD (scans without evidence of dopaminergic deficit) subjects. The study established standardized protocols for the acquisition of clinical and neuroimaging data, which can provide basis for further PD research [8]. And PPMI's clinical research data and standardized protocols can be obtained on their official website (<http://www.ppmi-info.org>). Parkinson's Disease and Movement Disorders Multicenter Database and Collaboration Network in China (PD-MDCNC) (<http://pd-mdcnc.com/zh-cn/normal.html>) is a database comprised of several cohorts of PD and other movement disorders, established by Xiangya Hospital Central South University in 2018, and has already enrolled over 100000 cases from 100 sites until 2020, including the Chinese Parkinson's disease registry (CPDR), the Chinese familial Parkinson's disease registry (CFPDR), the early onset Parkinson's disease registry (CEOPDR), the Chinese Parkinson's disease with GBA Variants registry (PD-GBAR), the Chinese Parkinson's disease with LRRK2 Variants (CPD-LRRK2R), the Chinese Parkinson's disease with parkin Variants registry (CPD-PARKINR), the Chinese essential tremor registry (CETR), Dystonia, PSP, MSA, CBD, and health control. The data contains demographic characteristics, clinical symptoms, environmental factors, family history, comorbid phenomena, brain imaging, genomics, treatment options, neuropsychology, and quality of life assessment. PD-MDCNC mainly focuses on the clinical features, comorbidities, progression and prognosis of PD, and other movement disorders among Chinese people. But the summarized data of the PSP/MSA/CBD cohort is still unavailable on the website. These cohorts are helpful to the diagnosis and differentiation of PD at early phase.

In the past decades, researchers conducted dopaminergic or metabolic PET imaging to assist in the diagnosis of PD in several studies, and ^{11}C -CFT and ^{18}F -FDG PET scans have been proved to be objective tools for the evaluation of disease severity and treatment efficacy [9, 10]. Meanwhile, previous studies have illustrated the correlations between functional imaging measures and clinical ratings [11, 12]. Thus, with the combination of dopaminergic, metabolic imaging, MRI, and clinical ratings and examining the correlations between them, the interaction among neuroimaging and clinical manifestations may be further illuminated, and it may provide credible biomarkers for the diagnosis and curative effect evaluation.

Here, the details of the design of PDPNI were summarized. This is an ongoing longitudinal observational study launched by PET Center and Department of Neurology, Huashan Hospital, Fudan University. The main aim of PDPNI is to identify PDS progression biomarkers, help the diagnosis result more accurate in patients with uncertain Parkinsonism, and provide new clues for the treatment of Parkinsonism. The study included the PD\RBD\PSP\MSA cohort for long-term longitudinal follow-up. Patients enrolled in this study all went through functional imaging modalities including FDG-PET, DAT-PET imaging, ASL MRI, and fMRI, as well as cognitive assessment and motor function assessment. All of the data was sorted and uploaded to the database. The database was able to classify and sort patient data and download the corresponding category to meet needs.

2. Methods

2.1. Study Organization and Governance. PDPNI was launched by PET Center and Department of Neurology, Huashan Hospital, Fudan University. The neuroradiologists of PET Center were responsible for scanning, imaging interpretation, and reporting; the neurologists of Huashan Hospital were responsible for the enrolment, diagnosis, and clinical assessment of subjects; and students from the School of Communication and Information Engineering of Shanghai University were in charge of the construction and maintenance of website. The database construction were shown in Figure 1. The enrolment of all subjects was based on the China-US Biomedical Collaborative Research Program (No. 81361120393).

PDPNI was a prospective cohort comprised of healthy middle-aged and elderly patients and Parkinson's syndrome patients. The figure above is an overview of the PDPNI study, each of which has subdivision test items (Table 1) to indicate cognitive assessment, pathology detailed inspection items of information, and image data. After ten years of longitudinal tracking, four cohorts were obtained.

2.2. PDPNI Study Design. Subjects have been enrolled in this research since February 2010. PDS subjects will be recruited at disease threshold. All the patients were diagnosed by a movement disorder specialist in Huashan Hospital affiliated to Fudan University based on the clinical diagnostic criteria [13–17]. Those subjects screened as potential PDS subjects

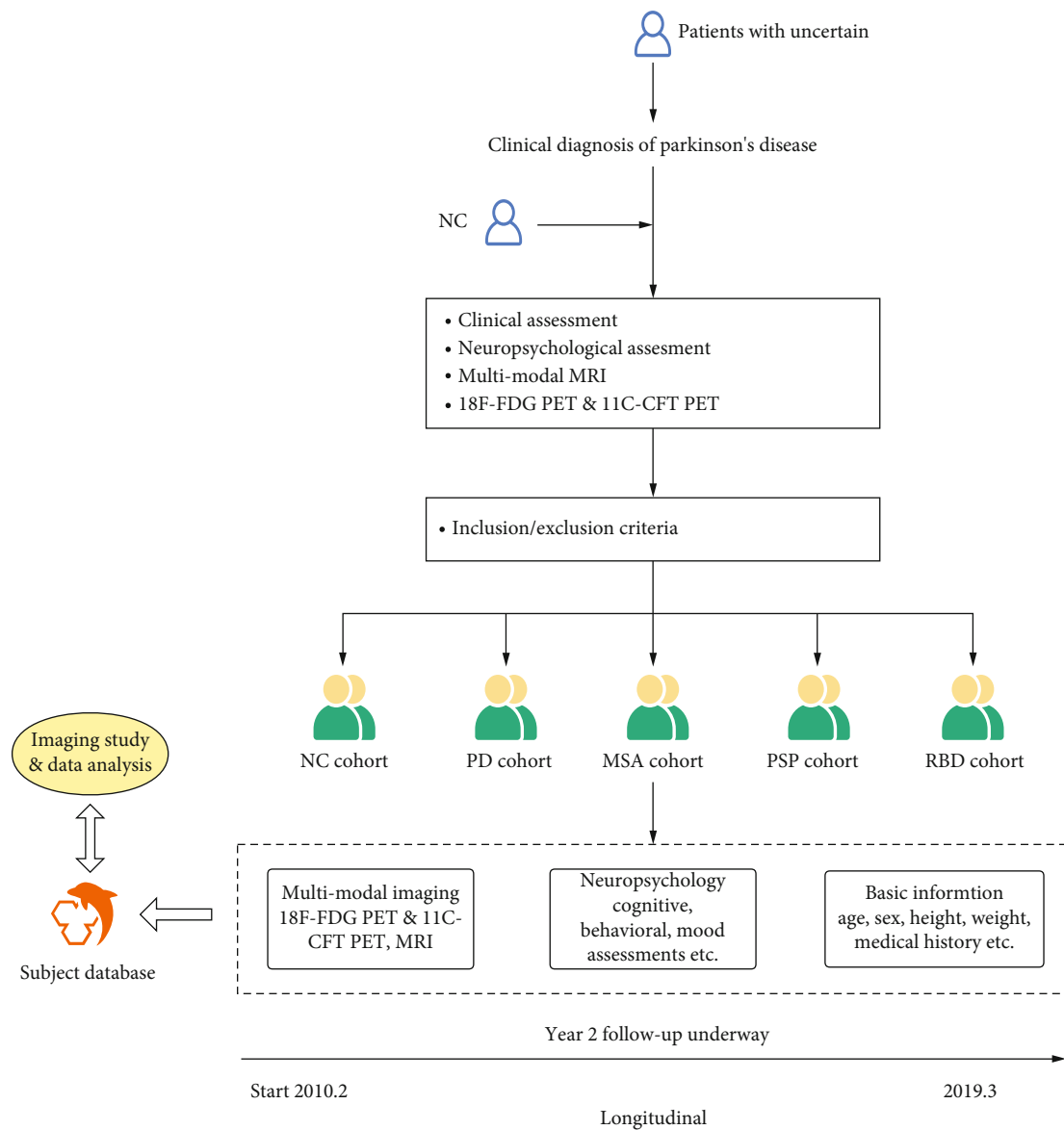


FIGURE 1: Overview of PDPNI study process.

who were ineligible due to DAT scan without evidence of dopaminergic deficit (SWEDD) were eligible to be enrolled in a SWEDD cohort. However, no one was enrolled in this cohort so far. All of them were scanned with 18F-fluorodeoxyglucose positron emission tomography (¹⁸F-FDG PET) for glucose metabolism assessment and ¹¹C-2-β-carbomethoxy-3-β-(4-fluorophenyl) tropane positron emission tomography (¹¹C-CFT PET) for presynaptic dopaminergic binding assessment, and part of them (these subjects all voluntarily undergo MRI examinations) were scanned with multimodal MRI including structural MRI (sMRI), arterial spin labelling perfusion (ASL), and functional MRI (fMRI). The detailed clinical scores of cognitive assessment and motor function assessment evaluated with clinical scales (Unified Parkinson's Disease Rating Scale (UPDRS), Montreal Cognitive Assessment (MoCA), Self-Rating Anxiety Scale (SAS), Self-Rating Depression Scale

(SDS), and Progressive Supranuclear Palsy Rating Scale (PSPRS); Table 1) were collected in all patients. All subjects were longitudinally followed every two years. Subjects underwent clinical assessment and imaging modalities according to established standardized protocols. During the period of follow-up, if subjects in the health control group developed Parkinsonism symptoms, they would be excluded from the cohort. If the RBD patients developed PD or MSA, they would be enrolled into the corresponding cohort. If the RBD patients developed DLB, the follow-up would be terminated. The PD database was established in November 2020, by the School of Communication and Information Engineering, Shanghai University, and both clinical and imaging data would be uploaded into the specific database and are open to registered users. The enrollment is still underway; meanwhile, the follow-up of enrolled subjects will continue and the data will be available through the PDPNI web.

TABLE 1: Clinical examination items of PDPNI.

	Clinical assessments	Clinical information	Imaging data
Data collection	MoCA total score	Sex, age	FDG PET
	Rey-O copy test	Symptoms	CFT PET
	Similarity test	Medication compliance	ASL
	Clock test	MDS-UPDRS III	fMRI
	Stroop Color Word Test	HY classification	Structural MRI
	Wired Test	MSA	
	Sign to digit conversion test	PSPRS	
	Rey-O delayed imitation test	NMSS	
	Auditory word learning test	RBD self-evaluation	
	Boston Naming Test	ESS self-evaluation	
	Fluency test	PDQ39	
	Semantic similarity test	SAS	
		SDS	

2.3. Inclusion/Exclusion Criteria. Patients participating in the PDPNI project all met the following criteria: (1) patients with uncertain clinical diagnosis of parkinsonism; (2) ≥ 45 years old; (3) Hoehn and Yahr ≤ 1 ; and (4) time interval between imaging and the final clinical diagnosis ≤ 2 years. HC subjects were excluded if they had chief complaint and objective evidence on cardiovascular, respiratory, hematological, and neurological diseases or participated in radiopharmaceutical clinical trial research in the past 2 years. All subjects were excluded with following characteristics: (1) treated with antipsychotics, atypical antipsychotics, antiemetics, or other anti-PD drugs (tetra-benzoxazine, diarrhea, etc.) within 12 months; (2) women might not be pregnant; (3) with history of stroke, brain trauma, or other possible factors which may result in structural brain injury; (4) with the presence of pacemakers, aneurysm clips, artificial heart valves, ear implants, metal fragments, or foreign objects in the eyes, skin, or body or any other known contraindication; (5) and characteristics of atypical Parkinson's syndrome (MSA, PSP, etc.), such as excessive autonomic symptoms, and abnormal eye movements.

2.4. Cognitive Assessment. The project mainly focused on the clinical and neuroimaging signs of PDS patients. Clinical evaluation was performed every 2 years by 2 senior specialists of movement disorders from Huashan hospital. Clinical assessments contained motor function assessment and cognitive assessment, including Movement Disorders Society-Unified Parkinson Disease Rating Scale (MDS-UPDRS) and Hoehn and Yahr scales, the Montreal Cognitive Assessment (MoCA), Rey-O copy test, Similarity test, Clock test, Stroop Color Word Test, Wired Test, Sign to digit conversion test, Rey-O delayed imitation test, Auditory word learning test, Boston Naming Test, Fluency test, and Semantic similarity test. Besides, Epworth Sleepiness Scale and a REM sleep behavior disorder (RBD) questionnaire for sleep behavior assessing were also included. All of the clinical and imaging data were integrated into the PDPNI database by professionals after training. PDPNI will serve as a sustain-

able source of information management of standardization research, research progress, and results.

2.5. PET Imaging

- (1) The scanning equipment used is Siemens Biograph 64 HD PET/CT (Siemens, Erlangen, Germany)
- (2) In preparation before scanning, all subjects should fast over 6 hours and withdrew anti-Parkinsonian and antipsychotics drugs for more than 12 hours before clinical assessment and each imaging acquisition. And other drugs that may affect glucose metabolism also need to withdraw over 12h before the ^{18}F -FDG PET imaging
- (3) The acquisition protocols of PET imaging are shown in Table 2.

Acquisition for patients was performed in a resting state in a quiet and dimly lit room to avoid sensory, auditory, and motor stimulation to the patient.

2.6. Magnetic Resonance Imaging (MRI)

- (1) The scanning equipment used is a 3-tesla GE Discovery MR750 Scanner (Milwaukee, WI, USA)
- (2) Precautions before scanning as follows: ensure that no metal objects are implanted or left in/on the patient's body. Ask the participants if they suffered from claustrophobia since claustrophobic may be anxious or even prone to have panic attacks during the scanning. Inform the participants that loud noises would occur during the scanning and not to move their body during the long-time examination
- (3) The acquisition protocols of MRI are shown in Table 3.

2.7. Statistical Analysis. All analyses were performed using SPSS 20 (SPSS Inc., Chicago, IL), and a 2-tailed P value of less than 0.05 was considered significant.

TABLE 2: Acquisition protocols of PET imaging.

	11C-CFT PET imaging	18F-FDG PET imaging
Inject dose	350–400 MBq	150–200 MBq
Time duration between injection and scan	60–80 minutes	45–55 minutes
Scan mode	3D mode	3D mode
Reconstruction	OSEM method	OSEM method
Attenuation correction	CTAC	CTAC

OSEM: ordered subset expectation maximization; CTAC: computed tomography attenuation correction.

TABLE 3: Acquisition protocols of MRI.

	FOV	Slice thickness	Repetition time (TR)	Echo time (TE)	Inversion time (TI)	Flip angle
T1 Bravo	25.6 cm	1 mm	8.2 ms	3.2 ms	450 ms	12°
T2 Flair	24 cm	6 mm	2000 ms	28.4 ms	2100 ms	111°
fMRI	24 cm	3 mm	8800 ms	145 ms	/	77°
ASL	24 cm	4 mm	4844 ms	10.5 ms	/	/

2.8. Data Storage. A very important part of the PDPNI research is to achieve a cloud storage of PDS patient data and rapid data sharing. The PDPNI website is an essential component of the study as shown in Figure 2 (after hiding the patient's private information). The website will provide PDPNI data, including clinical and imaging data obtained during the long-term follow-up.

This website can help administrators realize the functions of uploading and downloading data of subjects and can make accurate queries based on characteristics and manage patient information more conveniently. Users requesting to query or download data need to register an account; fill in the name, gender, unit, email address, registration password, and mobile phone number to complete the registration; and then jump to the login page and enter the account password to login. Continuously update the data of the subjects in the cloud by connecting to the database, while uploading the image files for follow-up and directly downloading them remotely when needed, realizing intelligent management, which is safer and more efficient.

3. Results

The Parkinson's Disease Progression Neuroimaging Initiative (PDPNI) was launched in February 2010, enrolling 176 PDS patients (both inpatients and outpatients in Huashan Hospital affiliated to Fudan University). The tables below illustrate the sample distribution of the four cohorts and the characteristics of subjects (Tables 4 and 5). 48 healthy control subjects and 149 patients were followed up every two years, including 71/83 PD patients, 19/19 PSP patients, 23/23 MSA patients, and 36/51 RBD patients. A total of 295 cases of follow-up have been completed, including 134 cases of PD patients, 23 PSP, 31 MSA, 107 RBD, and 43 health control. All the patients were diagnosed by a movement disorder specialist in Huashan Hospital affiliated to Fudan University based on the clinical diagnostic criteria.

4. Discussion

The Parkinson's Disease Progression Neuroimaging Initiative (PDPNI) was launched in February 2010, by PET Centre Huashan Hospital affiliated to Fudan University, aiming at identifying PDS progression biomarkers through innovative techniques such as DAT PET imaging and MRI, therapeutic conditions, and clinical symptoms, hoping to promote the accuracy of diagnose in patients with uncertain Parkinsonism especially at early stage and promote the development of PD disease-modifying treatment trials and inform PD treatment. Four cohorts were established in this study, including PD, MSA, PSP, RBD, and health control (HC). The study has enrolled 224 subjects (176 PDS patients and 48 healthy subjects) from February 2010 to March 2019, and a total of 338 cases of follow-up were conducted. The follow-up is still ongoing, and more subjects will be enrolled in this project. Through statistical analysis of the age and gender of subjects in the four cohorts and healthy subjects, there are significant statistical differences between the HC cohort and the cohorts of PD/RBD/MSA. The follow-up of these four cohorts is still ongoing; we will supplement the data of these three cohorts in order to make the age and gender of each group of patients matched. All subjects went through the 18F-FDG PET and 11C-CFT PET scanning, and part of them were scanned with multimodal MRI. The detailed clinical scores of cognitive assessment and motor function assessment were collected and evaluated by neurologists of Huashan Hospital affiliated to Fudan University with clinical scales (UPDRS, MoCA, etc.). All of the study data was integrated into the database and collected strictly in accordance with standardized data collection protocols. Data was tracked vertically in strict accordance with standardized data collection protocols.

PDPNI may be of benefit to the research related to Parkinsonian syndromes. Several studies have been carried out based on PDPNI; the findings of these studies may provide novel perspectives in understanding the specific manifestations in PDS, provide new insights in the correlation

The screenshot shows the PDPNI website interface. On the left is a sidebar menu with a user profile 'root' and a 'Management' section containing 'Add Patient', 'Patient List', 'Query', and 'Add Questionnaire'. The main content area is titled 'Patient List' and shows a table of 10 patients. The table columns are: #, PatientID, Name, Sex, IDCard, Height, Weight, Education, BirthDate, Follow-up, and Operate. Each row has a checkbox, a 'QCheck' button with a count in parentheses, and three buttons: 'Revise', 'Delete', and 'Download'. The table is paginated, showing Page 10 of 100.

#	PatientID	Name	Sex	IDCard	Height	Weight	Education	BirthDate	Follow-up	Operate
1	98888		M	3	6				QCheck (2)	Revise Delete Download
2	99549		M	3	2				QCheck (2)	Revise Delete Download
3	102930		M	3	7				QCheck (2)	Revise Delete Download
4	96807		F	3	9				QCheck (2)	Revise Delete Download
5	97204		M	3	5				QCheck (2)	Revise Delete Download
6	97499		M	3	8				QCheck (2)	Revise Delete Download
7	97504		M	3	5				QCheck (2)	Revise Delete Download
8	89755		M	3	3				QCheck (3)	Revise Delete Download
9	90544		F	3	9				QCheck (2)	Revise Delete Download
10	90953		M	3	9				QCheck (1)	Revise Delete Download

FIGURE 2: PDPNI website interface-patient information list.

TABLE 4: Sample distribution of research cohorts and healthy subjects.

Cohort	Number	Subjects were followed up	Cases of follow-up	Cases of only one follow-up	Cases of over twice follow-up
PSP	19	19	23	15	4
MSA	23	23	31	16	7
PD	83	71	134	32	39
RBD	51	36	107	5	31
HC	48	23	43	9	14

TABLE 5: Characteristics of subjects.

	HC (n = 48)	PD (n = 83)	PSP (n = 19)	MSA (n = 23)	RBD (n = 51)
Male (%)	24 (50.0)	53 (63.9)	16 (84.2)	15 (65.2)	40 (78.4)
Female (%)	24 (50.0)	30 (36.1)	3 (15.8)	8 (34.8)	11 (21.6)
Age (year \pm SD)	61.9 \pm 7.2	58.8 \pm 9.5	64.7 \pm 7.6	57.6 \pm 8.0	66.1 \pm 6.7
P value	NS	0.034*	0.211	0.036*	0.011*

* $P < 0.05$. NS: not significant. Data are given as the mean \pm standard deviation (SD) values.

between brain dysfunction and clinical features, and enhance the understanding of the pathological mechanism of PDS [18–23]. Thus, we believe these clinical evaluation data and image information of different types of patients can help develop more studies in the domain of Parkinsonian syndromes. It has already been demonstrated that regional changes in brain metabolism vary among parkinsonism and the differentiation among APS can be carried out by 18F-FDG-PET [24–28]. MRI technology can clearly show the anatomical structure of the substantia nigra and can reflect the pathological changes of PD through quantitative analysis [29]. Therefore, PDPNI data may be helpful in

the studies of differential diagnosis. With the collection of treatment condition of patients with Parkinsonian syndromes, PDPNI may also be conducive to the update of the treatment plan for PD. Besides, the evaluation of cognitive assessment scales can help medical researchers evaluate the progression of the disease and further develop better treatment options. Except improving understanding of the pathophysiology and treatment of PD, PDPNI can also establish a standardized protocol for the acquisition, transmission, and analysis of clinical and image data for PD research. Continuous longitudinal follow-up of PD from the preclinical stage to the prodromal symptom stage, and

finally to the stage of cognitive impairment, will provide a more profound understanding of the disease progression.

The PDPNI study is aimed at identifying PDS progression biomarkers through innovative techniques such as DAT PET imaging and MRI, therapeutic conditions and clinical symptoms, promoting the development of PD disease-modifying treatment trials, and providing new clues for PD treatment. At the same time, other Parkinson's syndromes such as PSP, MSA, and RBD, which are different from PD, are diagnosed on the basis of the clinical evaluation and images collected by PET and MRI. The follow-up of the clinical assessment and imaging of PDS patients and HC have been carried out, and all data was uploaded to the PDPNI database. It is a longitudinal study which has been running for over ten years, and the enrollment is still underway. A large amount of data could generate during long-term clinical monitoring of PD patients, which is not convenient for data management and statistical analysis. However, with the use of database, the collected data can be organized, processed, and sorted in a desired way. Integrating the basic clinical information, image data, and pathological information of different disease stages of patients into the database, doctors can obtain targeted clinical data of all patients. The database included the assessment scale data obtained from long-term follow-up and the DICOM images of PET and MRI, and all of the data can be downloaded and viewed directly and conveniently when needed. Besides, the follow-up of enrolled subjects will continue and the data will be available through the PDPNI website. The database can enhance the efficiency of the management and analysis of clinical imaging, clinical scale evaluation, individualized therapies, and other data for PD patients and make it convenient to observe the pathophysiological changes longitudinally. Therefore, PDPNI is a collaborative effort of specialists in the department of neurology, radiology, and nuclear medicine and IT technicians. In this paper, we comprehensively summarized the study methods, as well as the baseline data and follow-up data of the cohort obtained by advanced imaging techniques and professional clinical evaluation.

Different from other studies, the PDPNI study enrolled MSA, PSP, and RBD patients beside the PD cohort and conducted longitudinal cohort studies on them. In order to conduct a longitudinal study, all subjects of the project will be followed up for several years in PET center, Huashan Hospital. The same group of clinical assessment and functional imaging modalities were conducted every two years. Since PDPNI is a single center study, the sample size of PDPNI is small compared to the PPMI and PD-MDCNC study. But the follow-up is still ongoing, and more subjects will be enrolled in this project. We will update the data to form a more systematic PDS database. Another limitation is the sex ratio of the subjects and the age significance between cohorts. In the study, there were 224 subjects including healthy subjects, of which 150 were males and 74 were females. Apparently, there were more male volunteer researchers than females. In the follow-up study, we will consider the age range between different cohorts and the balance of the proportion of male and female volunteers when

recruiting subjects. Thirdly, it is clear that biomarkers with a focus ranging from clinical symptoms to PD pathobiology to molecular genetic mechanisms are necessary for fully mapping PD progression. However, serum/CSF biomarkers such as α -synuclein, tau, and pathological biomarkers were not included in PDPNI so far. In the next phase of the study, we plan to collect the biospecimens including blood, CSF for plasma and CSF α -synuclein, and tau and conduct tau PET imaging in new subjects enrolled in this study after ethical approval, to provide useful and novel insights for PDS progression and diagnosis [30].

In summary, PDPNI is a cohort-rich longitudinal study. The subjects are healthy middle-aged people and people with Parkinson's syndrome. For the included subjects, follow-up data is collected every 1-2 years, and it is committed to advance the research progress of PD disease through the systematic analysis of a large amount of data. This process can also help each medical team complete the latest academic research and provide a large amount of clinical data.

The samples included in the clinical study are still being updated. In order to achieve better patient selection and stratification and to advance the research progress of Parkinson's syndrome, it is necessary to expand the cohort and further follow-up. In order to achieve the above goals, we will continue the follow-up data collection work and expand the sample size of baseline data and follow-up data.

Data Availability

Due to restrictions on privacy, confidentiality, etc., all the pictures of the subject's information in the article have been encrypted. Due to various constraints, a "data sharing agreement" is required before the data is released. In terms of data sharing of PDPNI research, further review and approval may be required according to the specific research project request, and the data will be shared on the basis of the reviewed project.

Ethical Approval

Ethical approval of this has been obtained from the Federal-wide Assurance (FWA00017396) and Institutional Review Board of the Huashan Hospital, Fudan University (IORG0006909).

Conflicts of Interest

All the contributing authors declare no conflict of interest.

Authors' Contributions

Shiyi Zhu and Zizhao Ju contributed equally to this work.

Acknowledgments

This work was supported by grants (No. 82021002, 81971641, 81771483, 81671239, and 81902282) from the National Natural Science Foundation of China, the research project of Shanghai Health Commission (2020YJZX0111), the Clinical Research Plan of SHDC (SHDC2020CR1038B),

the Youth Medical Talents-Medical Imaging Practitioner Program by Shanghai Municipal Health Commission and Shanghai Medical and Health Development Foundation (No. SHWRS (2020)_087), and the Medical Innovation Research Project funded by Shanghai Science and Technology Commission (No. 21Y11903300).

References

- [1] S. Morbelli, G. Esposito, J. Arbizu et al., "EANM practice guideline/SNMMI procedure standard for dopaminergic imaging in Parkinsonian syndromes 1.0," *European Journal of Nuclear Medicine and Molecular Imaging*, vol. 47, no. 8, pp. 1885–1912, 2020.
- [2] W. Poewe, K. Seppi, C. M. Tanner et al., "Parkinson Disease," *Nature Reviews Disease Primers*, vol. 3, no. 1, 2017.
- [3] L. Johannes, K. Alexander, A. Thomas, G. Armin, and G. U. Höglinger, "The differential diagnosis and treatment of atypical Parkinsonism," *Deutsches Arzteblatt international*, vol. 113, no. 5, pp. 61–69, 2016.
- [4] T. H. Michele, "REM sleep behavior disorder (RBD)," *Neurobiology of Disease*, vol. 143, 2020.
- [5] P. A. Bourgooin, S. Rahayel, M. Gaubert et al., "Neuroimaging of rapid eye movement sleep behavior disorder," *International Review of Neurobiology*, vol. 144, pp. 185–210, 2019.
- [6] A. Iranzo, A. Fernández-Arcos, E. Tolosa et al., "Neurodegenerative disorder risk in idiopathic REM sleep behavior disorder: study in 174 patients," *PLoS One*, vol. 9, no. 2, p. e89741, 2014.
- [7] B. F. Boeve, "Idiopathic REM sleep behaviour disorder in the development of Parkinson's disease," *Lancet Neurology*, vol. 12, no. 6, pp. 469–482, 2013.
- [8] K. Marek, S. Chowdhury, A. Siderowf et al., "The Parkinson's progression markers initiative (PPMI) – establishing a PD biomarker cohort," *Annals of Clinical and Translational Neurology*, vol. 5, no. 12, pp. 1460–1477, 2018.
- [9] S. Hirano, T. Eckert, T. Flanagan, and D. Eidelberg, "Metabolic networks for assessment of therapy and diagnosis in Parkinson's disease," *Movement Disorders*, vol. 24, no. S2, pp. S725–S731, 2009.
- [10] T. Eckert, C. Tang, and D. Eidelberg, "Assessment of the progression of Parkinson's disease: a metabolic network approach," *Lancet Neurology*, vol. 6, pp. 926–932, 2007.
- [11] C. Huang, C. Tang, A. Feigin et al., "Changes in network activity with the progression of Parkinson's disease," *Brain*, vol. 130, no. 7, pp. 1834–1846, 2007.
- [12] F. Holtbernd, Y. Ma, S. Peng et al., "Dopaminergic correlates of metabolic network activity in Parkinson's disease," *Human brain mapping*, vol. 36, no. 9, pp. 3575–3585, 2015.
- [13] A. J. Hughes, S. E. Daniel, L. Kilford, and A. J. Lees, "Accuracy of clinical diagnosis of idiopathic Parkinson's disease: a clinico-pathological study of 100 cases," *Journal of Neurology, Neurosurgery, and Psychiatry*, vol. 55, no. 3, pp. 181–184, 1992.
- [14] S. Gilman, G. K. Wenning, P. A. Low et al., "Second consensus statement on the diagnosis of multiple system atrophy," *Neurology*, vol. 70, no. 11, pp. A229–A229, 2008.
- [15] I. Litvan, Y. Agid, D. Calne et al., "Clinical research criteria for the diagnosis of progressive supranuclear palsy (Steele-Richardson-Olszewski syndrome): report of the NINDS-SPSP international workshop," *Neurology*, vol. 47, no. 1, pp. 1–9, 1996.
- [16] H. W. Duchna, "Sleep-related breathing disorders—a second edition of the International Classification of Sleep Disorders (ICSD-2) of the American Academy of Sleep Medicine (AASM)," *Pneumologie*, vol. 60, no. 9, pp. 568–575, 2006.
- [17] T. M. Ellmore, A. J. Hood, R. J. Castriotta, E. F. Stimming, R. J. Bick, and M. C. Schiess, "Reduced volume of the putamen in REM sleep behavior disorder patients," *Parkinsonism & related disorders*, vol. 16, pp. 645–649, 2010.
- [18] F. Liu, J. Ge, J. Wu et al., "Clinical, dopaminergic, and metabolic correlations in Parkinson disease: a dual-tracer PET study," *Clinical Nuclear Medicine*, vol. 43, no. 8, pp. 562–571, 2018.
- [19] C. Liu, J. Jiang, H. Zhou et al., "Brain functional and structural signatures in Parkinson's disease," *Frontiers in aging neuroscience*, vol. 12, 2020.
- [20] X. Han, X. Li, W. Tang et al., "Assessing gray matter volume in patients with idiopathic rapid eye movement sleep behavior disorder," *Neural Regeneration Research*, vol. 14, no. 5, pp. 868–875, 2019.
- [21] Y. Yang, J. Ge, F. Liu et al., "Preserved caudate function in young-onset patients with Parkinson's disease: a dual-tracer PET imaging study," *Therapeutic Advances in Neurological Disorders*, vol. 12, p. 175628641985140, 2019.
- [22] Z. Huang, C. Jiang, L. Li et al., "Correlations between dopaminergic dysfunction and abnormal metabolic network activity in REM sleep behavior disorder," *Journal of Cerebral Blood Flow and Metabolism: Official Journal of the International Society of Cerebral Blood Flow and Metabolism*, vol. 40, no. 3, pp. 552–562, 2020.
- [23] J. Ge, P. Wu, S. Peng et al., "Assessing cerebral glucose metabolism in patients with idiopathic rapid eye movement sleep behavior disorder," *Journal of Cerebral Blood Flow and Metabolism*, vol. 35, no. 11, p. 1902, 2015.
- [24] Z. Walker, F. Gandolfo, S. Orini et al., "Clinical utility of FDG PET in Parkinson's disease and atypical parkinsonism associated with dementia," *European Journal of Nuclear Medicine and Molecular Imaging*, vol. 45, no. 9, pp. 1534–1545, 2018.
- [25] Y. Chiba, E. Iseki, H. Fujishiro et al., "Early differential diagnosis between Alzheimer's disease and dementia with Lewy bodies: Comparison between ¹⁸F-FDG PET and ¹²³I-IMP SPECT," *Psychiatry Research: Neuroimaging*, vol. 249, pp. 105–112, 2016.
- [26] C. Jiang, G. E. Jingjie, X. Shi et al., "Characteristics of cerebral glucose metabolism on 18F-FDG PET imaging in patients with Parkinson's disease," *Chinese Journal of Nuclear Medicine and Molecular Imaging*, vol. 37, no. 4, pp. 193–197, 2017.
- [27] P. Wu, C. Lin, H. Zhang et al., "Metabolic brain networks in patients with Parkinson's disease based on 18F-FDG PET imaging," *Chinese Journal of Nuclear Medicine and Molecular Imaging*, vol. 33, no. 4, pp. 275–278, 2013.
- [28] L. Li, P. Wu, Q. Xu et al., "The value of statistical parameter map analysis of 18 F-FDG PET imaging in the differential diagnosis of Parkinson's syndrome," *Chinese Journal of Nuclear Medicine and Molecular Imaging*, vol. 6, pp. 331–336, 2019.
- [29] X. Liu, J. Lu, Y. Li, C. Zuo, and D. Geng, "Research progress of substantia nigra in patients with Parkinson's disease in magnetic resonance imaging," *Chinese Clinical Neuroscience*, vol. 27, pp. 98–104, 2019.
- [30] C. Klein and M. G. Schlossmacher, "Parkinson disease, 10 years after its genetic revolution: multiple clues to a complex disorder," *Neurology*, vol. 69, no. 22, pp. 2093–2104, 2007.

Review Article

Advances regarding Neuroinflammation Biomarkers with Noninvasive Techniques in Epilepsy

Hongrui Ma  and Hua Lin 

Department of Neurology, Xuanwu Hospital, Capital Medical University, Beijing, China 100053

Correspondence should be addressed to Hua Lin; linhua@ccmu.edu.cn

Received 16 July 2021; Revised 16 November 2021; Accepted 17 November 2021; Published 22 December 2021

Academic Editor: Jan Aasly

Copyright © 2021 Hongrui Ma and Hua Lin. This is an open access article distributed under the Creative Commons Attribution License, which permits unrestricted use, distribution, and reproduction in any medium, provided the original work is properly cited.

A rapidly growing body of evidence supports that neuroinflammation plays a major role in epileptogenesis and disease progression. The capacity to identify pathological neuroinflammation in individuals with epilepsy is a crucial step on the timing of anti-inflammatory intervention and patient selection, which will be challenging aspects in future clinical studies. The discovery of noninvasive biomarkers that are accessible in the blood or molecular neuroimaging would facilitate clinical translation of experimental findings into humans. These innovative and noninvasive approaches have the advantage of monitoring the dynamic changes of neuroinflammation in epilepsy. Here, we will review the available evidence for the measurement of neuroinflammation in patients with epilepsy using noninvasive techniques and critically analyze the major scientific challenges of noninvasive methods. Finally, we propose the potential for use in clinical applications.

1. Introduction

Epilepsy is a common heterogeneous disease with a complex pathophysiology. Increasing evidence suggests that dynamic changes of neuroinflammation processes in epilepsy with a range of etiologies lead to the development and progression of this disease. Activation of microglia and astroglia triggers the release of inflammatory mediators including cytokines and chemokines. Initiation of inflammatory pathways exacerbates blood-brain barrier damage (BBBD) and fuels the innate and adaptive immune response within the brain and the periphery. These inflammatory processes often occur and last throughout the development of epilepsy, which contribute to the progression and severity of epilepsy. Recurrent epilepsy can also exacerbate brain inflammation. The causal and reciprocal link between neuroinflammation and epilepsy may contribute to neuronal hyperexcitability and drug resistance [1].

Modulation of these inflammation mechanisms could be a potential therapeutic target for epilepsy, which fostered interest in developing drugs targeting pathologic inflammatory pathways for selected epilepsy syndromes [2]. Identifi-

cation of biomarkers of pathological neuroinflammation could help to define the patient population that is likely to benefit and the best treatment time for specific anti-inflammatory drugs [3]. Thus, there is an urgent need to develop clinically useful biomarkers that can predict the progression of neuroinflammation in patients with epilepsy and treatment response. How to measure and quantify brain inflammation in humans? The neuropathological observations of brain tissue from epilepsy surgery are the gold standard, but these samples are not routinely available. The biomarkers of cerebrospinal fluid (CSF) represent neuroinflammatory, but CSF obtained by lumbar puncture is invasive. Importantly, patients often reject invasive examination. Therefore, research has focused on the search for noninvasive biomarkers of neuroinflammation in various neurological disorders, including epilepsy [4].

Inflammatory mediator measurement in the blood sample and brain imaging of neuroinflammation could provide noninvasive methodologies to detect and quantify brain inflammation in humans. Blood samples and molecular neuroimaging are accessible and can be monitored repeatedly. Preclinical and clinical studies have developed potential

biomarkers of neuroinflammation in epilepsy [3]. In this article, we will review the existing evidence measuring neuroinflammation with noninvasive techniques in epilepsy and critically analyze the major scientific challenges of non-invasive methodologies. Finally, we will address the suggestion that multidimensional biomarker panels can be used to identify brain inflammation in humans.

2. Blood Biomarkers

Immune cell subset distribution and inflammatory molecules in peripheral blood are candidate biomarkers. These biomarkers can be quantitatively measured and be used to evaluating brain inflammation progression or reaction to intervention. Mounting evidence has been made in identifying circulating neuroinflammatory biomarkers in animal models of epilepsy [5]. However, a major scientific challenge is to define valid and useful biomarkers in human epilepsy with efforts to ensure that individuals can benefit from immunomodulatory therapies.

2.1. Immune Cell Subset Distribution in Peripheral Blood. Changes in the immune cell subtypes indicate the activation of the immune system [6]. BBBB mediates the reciprocal brain-to-blood communication. Experimental studies of status epilepticus have demonstrated a pathogenic role of infiltrating monocytes [7]. Previous studies found infiltration of monocytes and lymphocytes in human brain tissue from epilepsy surgery with various etiologies [8–11]. In resected brain tissues from pediatric epilepsy patients, Xu et al. observed significant brain infiltration of peripherally derived T lymphocytes [12]. A recent work has shown that monocyte infiltration can contribute to the recurrence of epileptic seizures [13]. As the availability of brain specimens in epilepsy surgery is limited, blood provides the most easily accessible specimens for detecting the role of the immune system.

Flow cytometry remains a relatively popular method to investigate monocyte populations. Several cohorts reported differences in the profile of peripheral immune cells in epilepsy patients by cell sorting measurements of leukocytes [14, 15]. Decreased CD4⁺ T cells and increased NK cells were pronounced postictally in mesial temporal lobe epilepsy with hippocampal sclerosis [14]. Some studies showed an activation of classical monocytes [16] or an increase of the frequency of all monocytes [15]. A recent finding showed that the blood CD4⁺/CD8⁺ T cell ratio was elevated in patients with epilepsy due to limbic encephalitis compared to temporal lobe epilepsy (TLE) patients [17]. Compared with the control group, patients with TLE revealed distinct shifts in monocyte and lymphocyte subsets in the peripheral blood and CSF by flow cytometry. Changes in blood immune signatures were the most robust parameters that differentiated TLE from controls [18], including a shift toward immature CD14^{low}CD16⁺ cells within monocytes, increased proportions of granulocytes, and decreased CD8⁺ T lymphocytes, while there was a weak negative correlation between CSF leukocyte count and time since the last seizure. Differently, the correlation of immune signatures with dis-

ease duration was not found. The clinical evidence supports that immune cell signatures may persist shift and the immune signature of TLE appears to manifest early in the disease course.

As studies on immune cells in the peripheral blood in patients with epilepsy syndrome are lacking, little is known about monocyte function in epileptogenesis. More information is still needed to understand whether these changes could be used as meaningful and reliable biomarkers of neuroinflammatory traits in epileptic syndromes [5].

2.2. Cytokine Levels in Peripheral Blood. Evidences from experimental and clinical research have supported that neuroinflammation is a hallmark of the epileptic focus in refractory epilepsy [5]. Cytokines are critical in immune regulation. Activation of cytokines and multiple pathways plays important roles in the development of chronic neuroinflammation during epilepsy [19]. Recent studies have shown a crucial contribution of glial cells (astrocyte and microglia) in the production of proinflammatory cytokines. The most commonly studied IL-1 β , IL-6, and TNF- α tend to be potential mediators in the neuropathology of epilepsy [20]. Thus, considerable effort has been invested in the noninvasive identification of these neuroinflammation biomarkers.

It is interesting to note that the expression level of inflammatory cytokines varies with the cause and period of epilepsy. For example, serum proinflammatory cytokines increased after repetitive seizures, especially in cases of new-onset refractory status epilepticus or febrile infection-related epilepsy syndrome. Serum levels of IL-6 and TNF- α were detected with increased expression within 48 h in pediatric patients with acute afebrile seizures. The increased expression of cytokine levels (IFN- γ , IL-1 β , and IL-6) in acute seizures was associated with younger patients at disease onset. The result suggested that younger patients showed stronger inflammatory responses to seizures. Correlation analysis showed that serum levels of IL-1 β were significantly associated with disease severity in children with epilepsy. This set of evidence highlights that serum IL-1 β may represent a biomarker for epilepsy as an ongoing neuroinflammation [21]. An observational study [22] reported that IL-6 levels in both serum and CSF were elevated in refractory status epilepticus and acute seizures. IL-6 levels normalized after tocilizumab treatment and clinical symptoms improved [23]. This phenomenon supports that IL-6 is a potential useful biomarker of inflammation and a measure of therapeutic response in this clinical entity.

An in vitro study suggested that after epilepsy, IL-1 β mRNA, IL-6 mRNA, and TNF- α mRNA were expressed by microglia and astrocyte. The expression of IL-1 β increases epilepsy susceptibility and neuronal excitability by directly inhibiting GABA_A receptor and promoting the phosphorylation of NR2B subunit of NMDA receptor. Low concentrations of IL-1 β may exert antiepileptic effects by limiting intracellular Ca²⁺ and enhancing GABAergic transmission. The complex of IL-6 and IL-6 receptor can trigger gp130 signaling, which may disrupt cholinergic and GABAergic transmission of hippocampal neurons. Lowering extracellular Ca²⁺ levels can block the overexpression of IL-6. TNF- α can activate two

receptors (p55 and p75). Low concentrations of TNF- α trigger apoptosis signal-regulating kinase 1 through the p55 pathway and induce neuronal apoptosis following seizures. High concentrations of TNF- α can play an antiepileptic role through the p75 pathway that associated with activation of the nuclear factor Kappa B (NF- κ B) system [20, 24]. However, these results are based on animal studies while cytokines in human epilepsy remain to be studied because cytokines can only be detected in blood or CSF. Further questions to be addressed are the extent to which cytokines are associated with human epilepsy and whether these pathways can be blocked by immunomodulatory therapy.

As the structurally related members of the immunoglobulin supergene family, intercellular adhesion molecules (ICAMs) organize a variety of junctions between cells and extracellular matrix, which mediate the cell signaling cascades on inflammation [25, 26]. Of the five ICAMs identified, soluble intercellular adhesion molecule 1 (sICAM-1) is the most widely studied inflammatory mediator and is activated in epileptic patients. Compared with drug-responsive epilepsy, serum sICAM-1 level was elevated in drug-refractory epilepsy. sICAM-5 is a kind of neuron-specific anti-inflammatory protein that plays an important immunosuppressive role in neuronal inflammatory diseases [27]. sICAM-5 can also be found in the blood that it can be a biomarker to detect the inflammatory response of epilepsy. Blood concentrations of sICAM-5 are reduced in epilepsy patients. T thymus and activation-regulated chemokine (TARC) levels have a growing trend in epilepsy. The ratio of TARC to sICAM-5 provides candidate blood biomarkers for refractory epilepsy and can be used for distinguishing epilepsy from normal controls [28].

Another cell adhesion molecule in the immunoglobulin superfamily, vascular cell adhesion molecule (VCAM), is a marker mainly expressed on the surface of endothelial cells that majorly regulate leukocyte adhesion and transendothelial migration, which mediates the process of vascular inflammation [29]. Soluble vascular adhesion molecules (sVCAM) mirror parenchymal inflammation in epilepsy. Clinical studies have demonstrated the upregulation of sVCAM in the serum and CSF of patients with epilepsy. CSF sVCAM-1 and serum sVCAM-1 levels were higher in the epilepsy group than in the neurosis group [30]. Moreover, there are higher CSF sVCAM-1 and serum sVCAM-1 concentrations in drug-refractory epilepsy compared to drug-responsive epilepsy. CSF and serum sVCAM-1 implied the possibility of drug resistance epilepsy and might be prognostic biomarkers for epilepsy.

Promising developments have been made in blood cytokines as biomarkers reflecting neuroinflammation in epilepsy, but caution should be taken. There are several drawbacks in these types of measurements. First, it is difficult to demonstrate that blood biomarkers meaningfully represent the degree and extent of brain inflammation. Second, seizures affect serum levels of cytokines, which may show seizure-dependent increase or decrease [31]. Third, since the half-life of many inflammatory cytokines is rapid, the blood levels vary considerably and it is difficult to be accurately detected. CSF measurements of the inflammatory

molecules would directly reflect brain inflammation released from the epileptic zone. However, these samples are not routinely available. Therefore, analysis of serum extracellular vesicles (EVs) derived from neuron and glia cells has received considerable attention as they can be measured through a noninvasive approach [32].

2.3. Serum Inflammatory Exosomes. Brain-derived EVs cross the BBB and can also be found in the peripheral blood [32]. Neuron-, astrocyte-, and microglia-derived EVs (NDEVs, ADEVs, and MDEVs) are enriched with several disease-specific proteins and/or microribonucleic acids (miRNAs). Therefore, serum EVs are a set of valuable biomarkers which noninvasively detect brain function and the progression of brain diseases [33]. Such a liquid biopsy approach makes it easier to repeat measures in clinical trials, convenient for testing the molecular mechanisms of the disease, the progression of the disease, and efficacy of treatment.

There have been only a few studies on the analysis of blood EVs in epilepsy [34, 35]. Yan and colleagues examined plasma miRNA-derived EVs in 40 patients with mesial temporal lobe epilepsy with hippocampal sclerosis (mTLE-HS) and 40 normal controls [36]. Expressions of over 50 EV miRNAs were abnormal in the plasma of these patients compared with healthy controls. In EVs from patients with mTLE-HS, miR-3613-5p and miR-6511b increased as much as 11-fold and 2-fold, respectively. Other 48 miRNAs showed downregulation. Five candidate EV miRNAs significantly decreased, including miR-4668-5p, miR-8071, miR-197-5p, miR-4322, and miR-6781-5p. Evidence indicated that they were involved in seizure development in mTLE-HS. Among these miRNAs, plasma EV miR-8071 differentiated mTLE-HS from healthy controls with a sensitivity of 83.3% and a specificity of 96.7%. In addition, miR-8071 was well associated with seizure severity. Therefore, plasma EV miR-8071 could represent a key diagnostic and prognostic marker for TLE-HS. Other clinical reports [35] have shown plasma miR-27a-3p, miR-328-3p, and miR-654-3p in exosomes as diagnostic markers with favorable sensitivity and specificity in patients with temporal lobe epilepsy. Specifically, the targets of the three miRNAs were associated with signaling pathways of neuronal apoptosis and growth factors involved in inflammation.

Notably, subtype analysis of astrocyte-derived exosomes in the serum has received considerable attention for evaluating brain inflammation [37]. Upregulation of inflammatory A1-type astrocyte exosomes, glial fibrillary acidic protein (GFAP-) positive, plays an essential role in human inflammatory and neurodegenerative diseases of the CNS [38]. New findings support that A1-type astrocytes secrete neuronal toxic mediators which are pathogenically critical in human neurodegenerative diseases. Multiple studies have demonstrated that activated inflammatory A1-type astrocytes generate proinflammatory cytokines in the epileptic hippocampus [39–41]. However, little has been done to examine the A1 and A2 subtypes of astrocyte-derived exosomes in patients with epilepsy. The subtype studies of astrocyte-derived exosomes in the blood of patients with epilepsy could further help in evaluating the occurrence or

progression of neuroinflammation and monitoring the effects of anti-inflammatory treatment. More studies are required on the role of exosomes in the pathophysiology of epilepsy.

2.4. Inflammasome Complex. As growing body of evidence suggests that complex signaling pathways are involved in neuronal excitotoxicity and cell loss progress during epilepsy, such as transforming growth factor- (TGF-) β , interleukin- (IL-) 1 receptor/Toll-like receptor (TLR), and cyclooxygenase-2 (COX-2) signaling pathways. Major research in recent years focuses on the expression of inflammasome complex and the influence on induced seizures in animal models of epilepsy, as well as findings in human studies [42]. Inflammasome is a multiprotein complex that has been understudied as a new target to neuroinflammation in epilepsy. It is mainly composed of NOD-like receptor protein (NLRP), apoptosis speck-like protein (ASC), and caspase 1 (CASP1), which are considered key platforms of inflammatory signaling pathway [42]. The NLRP3 inflammasome components, the most widely studied one, is mainly activated and expressed in the microglia and astrocytes after oxidative stress, hypoxia, or acidosis [43]. CASP1 can be activated by the interaction between NLRP3 and ASC, resulting in production of inflammatory cytokines such as IL-1 β , IL-18, and TNF- α , which trigger a cascade of inflammatory response [24, 44]. The NLRP3/ASC/caspase 1 inflammation pathway leads to epileptic neuronal apoptosis, thereby promoting epileptogenesis, and ultimately developed into seizures and recurrence. In contrast to NLRP3, the NLRP1 mainly expressed in neuron. The activation of NLRP1 inflammasome component generates caspase 1 and leads to programmed cell death termed “pyroptotic death” [45]. Clinical studies have shown that in patients with TLE, NLRP3 and NLRP1 inflammasomes are upregulated and they are associated with the increased hippocampal expression of caspase 1 and IL-1 β . Pharmacological inhibition of NLRP1, NLRP3, or caspase 1 can reduce seizure frequency and severity in TLE rats [46–48]. Components of the inflammasome pathway might be useful as biomarkers in neuroinflammation epilepsy and new targets of antiepileptogenic strategies in TLE patient while the transformation from animal studies to clinical trials needs further exploration considering that the drug treatment of human epilepsy is more complicated than animal models [44].

Overall, these studies are promising and imply that clinical translations of such noninvasive blood approaches are attractive for periodic analyses in different phases and types of epilepsy. However, several limitations remain. For example, lacking critical spatial information of the brain inflammation, indirectly reflecting the brain phenomenon, and the variability of peripheral blood reports are still considerable. Therefore, the combination of multiple blood biomarkers and brain imaging markers may enhance the diagnostic potential of neuroinflammation in epilepsy.

3. Brain Imaging Markers

3.1. TSPO PET. Translocator protein 18kDa (TSPO), the peripheral benzodiazepine receptor on the outer mitochon-

drial membrane of microglia and reactive astrocytes [49], is upregulated by activated microglia [50] and reactive astrocytes, which is a promising biomarker of neuroinflammation [51]. TSPO positron emission tomography (PET) is the most widely studied noninvasive imaging to better characterize the neuroinflammatory processes underlying epilepsy [49, 52, 53].

TSPO has been shown to be upregulated in patients with TLE, neocortical epilepsy, and drug-resistant epilepsy, as well as in animal models [54–56]. Alterations in its expression indicate a different state of epilepsy. TSPO expression increases peak in the subacute phase (1–2 weeks) after the onset of epilepsy and maintains a certain concentration level in the chronic phase [57], which suggests microglia-mediated inflammation is involved in the occurrence and persistence of epilepsy, which could be further investigated by PET imaging [50, 52, 58]. For example, the study of patients with neocortical frontal epilepsy using the ^{11}C -PK11195 TSPO PET tracer showed that inflammatory responses in brain lasted approximately 36 hours after seizure and the inflammatory areas were colocalized with the frontal epileptogenic zone [58]. Using ^{11}C -PBR28 tracer, a study revealed that increased brain uptake of the tracer was evident in the ipsilateral hippocampus to the seizure focus than contralateral in TLE patients, including patients with mesial temporal sclerosis (MTS) [55]. In a rat model of status epilepticus (SE), TSPO PET using ^{18}F -DPA-714 tracer showed increased uptake within the limbic system even in the hippocampus and reached its maximum at 7 days after SE, while TSPO binding declined to the baseline levels at 14–16 weeks post-SE. It demonstrated that TSPO binding changed over time in epilepsy with neuroinflammation [59].

To be more precise, TSPO PET could in vivo quantify the spatial temporal profile of microglial activation in patients with epilepsy and SE-induced rat models [60], which has the potential for determine the therapeutic windows in epilepsy and monitoring the response to anti-inflammatory treatment [58]. In rat models, early TSPO upregulation is associated with epileptogenesis, while chronic TSPO overexpression is related to seizure frequency [61]. TSPO PET can be used to ascertain spontaneous recurrent seizure frequency and reflect the severity of related comorbidities such as depression-like and sensorimotor-related disorders [52]. Meanwhile, TSPO PET also serves as an auspicious tool for temporal monitoring and quantification of anti-inflammatory effects of different drugs during epileptogenesis [62].

These findings further support the idea that TSPO PET might also be a valid biomarker for assessing epileptogenesis-associated brain inflammatory processes, and it would be particularly valuable that other imaging modalities are unrevealing [54–56]. However, there are still certain limitations to measure reliably neuroinflammation by PET imaging. PET tracer is one of the most important factors that affect the sensitivity of TSPO PET. The first-generated tracer ^{11}C -PK11195 has several disadvantages such as limited brain entrance, poor signal-to-noise ratio, and labeling with the impractically rapidly decaying isotope that affects the specificity of TSPO detection [63]. Novel

radiotracers have improved the ability to measure TSPO in vivo [64]. The second-generated tracers, such as ^{18}F -DPA-714, ^{11}C -PBR28, and ^{18}F -PBR111, with better enhanced pharmacological and pharmacokinetic properties, offer more appropriate tools for in vivo TSPO-PET imaging [52]. In recent years, ^{18}F -GE-180, the third-generated TSPO PET tracer, has been rapidly translated into human clinical research due to the advantages of higher signal-to-noise ratio and lower nonspecific binding. However, the current dispute refutes this view. The insensitive genotype seems to be blamed on poor quality of images, and higher signal-to-noise ratio is only because of the broken BBB. Thus, ^{18}F -GE-180 is considered to have low credibility, even if it failed for TSPO protein detection [65].

Besides, TSPO signal in the brain varies between the normal intrasubject and a true reference region which is absent; it is difficult to accurately calculate the sample size for an anti-neuroinflammatory treatment study [58]. Increased TSPO expression signals may also be observed in nonepileptic lesions due to BBBD or due to more radiotracer availability in the blood, which may reduce the specificity [55]. Interestingly, TSPO was identified in both proinflammatory and anti-inflammatory tissues. Besides, TSPO binding should not be assumed to reflect specific microglial activation, as it is also expressed by astrocyte and vascular endothelium [62]. Future research should pay more attention to further screening novel PET radiotracers that will provide fascinating insights into the ability to measure TSPO in vivo and improve understanding of the meaning of the TSPO-PET results.

3.2. Gadolinium- (Gd-) Enhanced MRI. Besides microglia and astrocytes, BBBD, as well as named BBB leakage, is also tightly coupled to neuroinflammation [66]. In the experimental epilepsy model of animals, BBBD can promote epileptogenesis [3, 67]. Neuroinflammation may originate directly from the central nervous system or from the peripheral circulation due to the destruction of the BBB [68]. The leakage of plasma constituents to the extracellular neuronal environment leads to progression of neuroinflammation and enhanced cortical excitability [66, 67]. Noninvasive quantitative measures of BBBD are clinically required to reach a more accurate identification of neuroinflammation [69].

Increased vascular permeability ("leakiness") of the disrupted BBB can be measured using gadolinium- (Gd-) enhanced MRI [63]. Under normal circumstances, gadolinium-based contrast agents do not cross the intact BBB. However, it may extravasate from the blood into the brain tissue even when BBBD occurs [70]. Thus, the contrast agents leaked from the circulation can be detected and quantified with high spatial resolution [71]. Breuer et al. [72] reported that the BBB leakage was detected by gadolinium- (Gd-) enhanced MRI at 1 day and 6 weeks after SE. BBB leakage is measured with Gd-enhanced MRI during early epileptogenesis, which can be a potential biomarker of later emerging epileptic seizures. During the chronic phase, BBBD has received increasing attention because of evidence of its association with an increased risk of seizure frequency. Therefore, BBBD may be used as a biomarker to monitor

the efficacy of a potential therapeutic epilepsy treatment [73]. There is recent progress in the analysis of brain dynamic contrast-enhanced magnetic resonance imaging (DCE-MRI), in which the linear behavior of the contrast agents in the brain vasculature and parenchyma is used to evaluate BBB permeability [67, 74]. It showed higher values of DCE-MRI index in predicting lesions with a higher propensity to cause seizure recurrence [75].

For future studies, gadolinium- (Gd-) labeled contrast-enhanced MRI seems to be the most favorable modality to image BBB leakage with epilepsy [71, 72]. However, most of the research on Gd-enhanced MRI stays in animal models because of the duration and frequency of seizures, as well as patient characteristics (age, medication, and concomitant conditions) may affect BBB permeability [72]. Besides, Gd-enhanced MRI measurements in clinical use are currently limited to measuring paracellular leakage of low molecular weight gadolinium contrast agents. Due to the low amplitude of signal change detected using these methods, some factors can confound the results of measurements, such as partial volume errors, Gibbs ringing, signal drift, patient motion, arterial input function definition errors, and kinetic model inaccuracy [76]. Of note, gadolinium- (Gd-) labeled contrast-enhanced MRI is characterized by potential toxicity. A large number of clinical and animal experiments have shown that multiple exposures to gadolinium-based contrast agent have health effects such as nephrotoxicity [77]. Thus, the current thinking regarding the permeability of the BBB may be greatly oversimplified and limited to animal models [70]. Additional investigations in the future are needed to clarify the relationship among different factors for neuroinflammation due to BBBD.

3.3. Magnetic Resonance Spectroscopy (MRS). MRS can assess the neurochemical changes in given brain regions of interest and provide metabolic or inflammatory information of neurons and neuroglial cells in vivo without invasive intervention [78]. Proton MRS (^1H -MRS) is one of the most common methods for MRS, and it can detect and quantify endogenous metabolites including N-acetyl aspartate (NAA, a marker for neuronal status and integrity), choline (Cho, a marker for membrane integrity and turnover), creatine (Cr, a marker for energy metabolism), myo-inositol (Ins, a marker for glial cell integrity), and glutamate⁺ glutamine (Glx, related to excitatory neurotransmission) [79]. ^1H -MRS can be used to measure neuroinflammation, and its molecular biochemical detection principle can be used to assist to detect neuroinflammation in epileptic patients [63].

MRS could in vivo monitor the inflammation of epileptogenic foci in patients with epilepsy. A study has demonstrated significant reductions in the NAA/Cr and NAA/(Cr⁺Cho) ratios in the hippocampus ipsilateral to the epileptic zone in structured MRI-negative TLE patients [80]. The pathological outcome of the resected hippocampus suggested neuroinflammation. Magnetic resonance spectroscopy and thermometry (MRS-t) is a temperature imaging which is currently under study, and this technique can be used to monitor the inflammatory response of epileptic lesions. At the same time of neuroinflammation, the metabolic demand

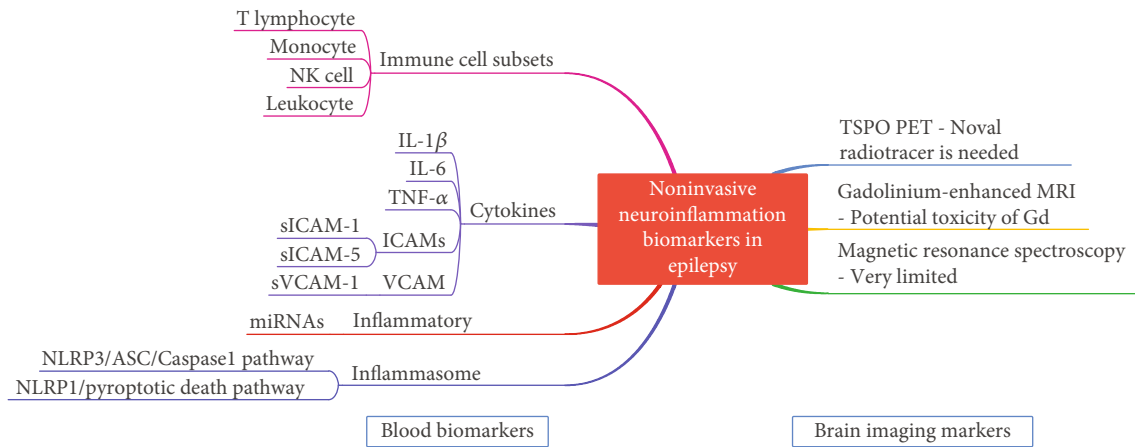


FIGURE 1: Graphical abstract showing the main blood biomarkers and brain imaging markers suggesting neuroinflammation in epilepsy. IL: interleukin; TNF- α : tumor necrosis factor- α ; ICAM: intercellular cell adhesion molecule; VCAM: vascular cell adhesion molecule; NLRP: NOD-like receptor protein; ASC: apoptosis speck-like protein; TSPO PET: translocator protein positron emission computed tomography; MRI: magnetic resonance imaging.

of brain tissue increases correspondingly, which may inhibit the cooling mechanism of brain and make the temperature of brain tissue 1–2°C higher than the core temperature. Therefore, MRS-t can be used to monitor the neuroinflammation of epilepsy and its response to treatment [63, 80].

However, the practicability of MRS in detecting epileptogenic inflammation is mainly limited by the intensity and power of the magnetic field, which affects the accurate quantification of different neurotransmitters [81]. It has been reported that ^1H -MRS is applied to detect epilepsy ranging from TLE [82] to idiopathic generalized epilepsy while it seems to be of little value for monitoring insular epilepsy [83]. In addition, antiepileptic drugs also have a confounding effect on nerve metabolism and affect the monitoring effect of MRS [84]. To date, there are a few studies on detecting the dynamic changes of neuroinflammation by MRS in epilepsy and it has very limited resolution for the practical technical support [83, 85, 86].

4. Conclusion

A graphical abstract showing the main conclusions of this review is shown in Figure 1. The discovery of noninvasive biomarkers of maladaptive neuroinflammation in epilepsy would facilitate clinical translation of anti-inflammatory treatments as they would enable the identification of patients who could benefit from the treatments and would provide pharmacodynamic markers of the therapeutic response. Despite the present evidence of seizure reduction by anti-inflammatory drugs in humans that relies mostly on case reports or small series, the association between the disease and biological markers of altered immunity has been still found in these cases. Numerous questions need to be answered. This effort might provide powerful tools for epileptologists to make complex decisions regarding the anti-inflammatory treatment of selected epilepsy patients.

Brain inflammation in epilepsy is based on multidimensional systems combining phenotypic, molecular variables,

neuroimaging, and neuropathology. Since various biomarkers from blood and neuroimaging may carry complementary information, the fusion of multidimensional and multimodal biomarker features may be a promising option to improve the identification accuracy of brain inflammation in humans. The complex assessment of multidimensional biomarker panels will provide a wealth of information and guide decision-making in patients with epilepsy.

Abbreviations

CSF:	Cerebrospinal fluid
BBBD:	Blood brain barrier dysfunction
TLE:	Temporal lobe epilepsy
ICAMs:	Intercellular adhesion molecules
sICAM-1:	Soluble intercellular adhesion molecule-1
TARC:	T thymus and activation-regulated chemokine
VCAM:	Vascular cell adhesion molecule
EVs:	Extracellular vesicles
miRNAs:	Microribonucleic acids
mTLE-HS:	Mesial temporal lobe epilepsy with hippocampal sclerosis
NLRP:	NOD-like receptor protein
ASC:	Apoptosis speck-like protein
CASP1:	Caspase 1
TSPO:	Translocator protein
PET:	Positron emission tomography
MTS:	Mesial temporal sclerosis
SE:	Status epilepticus
DCE-MRI:	Dynamic contrast-enhanced magnetic resonance imaging
MRS:	Magnetic resonance spectroscopy.

Conflicts of Interest

The authors declare that the research was conducted in the absence of any commercial or financial relationships that could be construed as a potential conflict of interest.

Authors' Contributions

Hongrui Ma is responsible for the writing—original draft preparation. Hua Lin is assigned to the writing, review, and editing.

Acknowledgments

This work was supported by the National Natural Science Foundation of China (81771909 and 81871438).

References

- [1] K. Kothur, S. Bandodkar, L. Wienholt et al., "Etiology is the key determinant of neuroinflammation in epilepsy: elevation of cerebrospinal fluid cytokines and chemokines in febrile infection-related epilepsy syndrome and febrile status epilepticus," *Epilepsia*, vol. 60, no. 8, pp. 1678–1688, 2019.
- [2] W. Löscher, H. Potschka, S. M. Sisodiya, and A. Vezzani, "Drug resistance in epilepsy: clinical impact, potential mechanisms, and new innovative treatment options," *Pharmacological Reviews*, vol. 72, no. 3, pp. 606–638, 2020.
- [3] A. Vezzani, S. Balosso, and T. Ravizza, "Neuroinflammatory pathways as treatment targets and biomarkers in epilepsy," *Nature Reviews Neurology*, vol. 15, no. 8, pp. 459–472, 2019.
- [4] A. Pitkänen, W. Löscher, A. Vezzani et al., "Advances in the development of biomarkers for epilepsy," *Lancet Neurology*, vol. 15, no. 8, pp. 843–856, 2016.
- [5] A. Vezzani and A. Friedman, "Brain inflammation as a biomarker in epilepsy," *Biomarkers in Medicine*, vol. 5, no. 5, pp. 607–614, 2011.
- [6] S. A. Sonar and G. Lal, "Differentiation and transmigration of CD4 T cells in neuroinflammation and autoimmunity," *Frontiers in Immunology*, vol. 8, p. 1695, 2017.
- [7] N. H. Varvel, J. J. Neher, A. Bosch et al., "Infiltrating monocytes promote brain inflammation and exacerbate neuronal damage after status epilepticus," *Proceedings of the National Academy of Sciences of the United States of America*, vol. 113, no. 38, pp. E5665–E5674, 2016.
- [8] H. Nakahara, Y. Konishi, G. T. Beach, N. Yamada, S. Makino, and I. Tooyama, "Infiltration of T lymphocytes and expression of icam-1 in the hippocampus of patients with hippocampal sclerosis," *Acta Histochemica et Cytochemica*, vol. 43, no. 6, pp. 157–162, 2010.
- [9] T. Ravizza, B. Gagliardi, F. Noé, K. Boer, E. Aronica, and A. Vezzani, "Innate and adaptive immunity during epileptogenesis and spontaneous seizures: evidence from experimental models and human temporal lobe epilepsy," *Neurobiology of Disease*, vol. 29, no. 1, pp. 142–160, 2008.
- [10] E. Volmering, P. Niehusmann, V. Peeva et al., "Neuropathological signs of inflammation correlate with mitochondrial DNA deletions in mesial temporal lobe epilepsy," *Acta Neuropathologica*, vol. 132, no. 2, pp. 277–288, 2016.
- [11] M. Zattoni, M. L. Mura, F. Deprez et al., "Brain infiltration of leukocytes contributes to the pathophysiology of temporal lobe epilepsy," *The Journal of Neuroscience*, vol. 31, no. 11, pp. 4037–4050, 2011.
- [12] D. Xu, A. P. Robinson, T. Ishii et al., "Peripherally derived T regulatory and $\gamma\delta$ T cells have opposing roles in the pathogenesis of intractable pediatric epilepsy," *The Journal of Experimental Medicine*, vol. 215, no. 4, pp. 1169–1186, 2018.
- [13] L. Feng, M. Murugan, D. B. Bosco et al., "Microglial proliferation and monocyte infiltration contribute to microgliosis following status epilepticus," *Glia*, vol. 67, no. 8, pp. 1434–1448, 2019.
- [14] S. Bauer, M. Köller, S. Cepok et al., "NK and CD4⁺ T cell changes in blood after seizures in temporal lobe epilepsy," *Experimental Neurology*, vol. 211, no. 2, pp. 370–377, 2008.
- [15] M. Nowak, S. Bauer, A. Haag et al., "Interictal alterations of cytokines and leukocytes in patients with active epilepsy," *Brain, Behavior, and Immunity*, vol. 25, no. 3, pp. 423–428, 2011.
- [16] H. Tumani, C. Jobs, J. Brettschneider, A. C. Hoppner, F. Kerling, and S. Fauser, "Effect of epileptic seizures on the cerebrospinal fluid - A systematic retrospective analysis," *Epilepsy Research*, vol. 114, pp. 23–31, 2015.
- [17] N. Hansen, K. Schwing, D. Önder et al., "Low CSF CD4/CD8⁺ T-cell proportions are associated with blood-CSF barrier dysfunction in limbic encephalitis," *Epilepsy & Behavior*, vol. 102, article 106682, 2020.
- [18] L. Langenbruch, L. Bleß, A. Schulte-Mecklenbeck et al., "Blood and cerebrospinal fluid immune cell profiles in patients with temporal lobe epilepsy of different etiologies," *Epilepsia*, vol. 61, no. 10, pp. e153–e158, 2020.
- [19] E. Nutma, H. Willison, G. Martino, and S. Amor, "Neuroimmunology - the past, present and future," *Clinical and Experimental Immunology*, vol. 197, no. 3, pp. 278–293, 2019.
- [20] G. Li, S. Bauer, M. Nowak et al., "Cytokines and epilepsy," *Seizure*, vol. 20, no. 3, pp. 249–256, 2011.
- [21] J. Choi, S. Y. Kim, H. Kim et al., "Serum α -synuclein and IL-1 β are increased and correlated with measures of disease severity in children with epilepsy: potential prognostic biomarkers?," *BMC Neurology*, vol. 20, no. 1, p. 85, 2020.
- [22] V. Cantarín-Extremuera, M. Jiménez-Legido, A. Duat-Rodríguez et al., "Tocilizumab in pediatric refractory status epilepticus and acute epilepsy: experience in two patients," *Journal of Neuroimmunology*, vol. 340, article 577142, 2020.
- [23] J. S. Jun, S. T. Lee, R. Kim, K. Chu, and S. K. Lee, "Tocilizumab treatment for new onset refractory status epilepticus," *Annals of Neurology*, vol. 84, no. 6, pp. 940–945, 2018.
- [24] S. Rong, D. Wan, Y. Fan et al., "Amentoflavone affects epileptogenesis and exerts neuroprotective effects by inhibiting NLRP3 inflammasome," *Frontiers in Pharmacology*, vol. 10, p. 856, 2019.
- [25] A. K. Hubbard and R. Rothlein, "Intercellular adhesion molecule-1 (ICAM-1) expression and cell signaling cascades," *Free Radical Biology & Medicine*, vol. 28, no. 9, pp. 1379–1386, 2000.
- [26] K. Shimizu and Y. Takai, "Roles of the intercellular adhesion molecule nectin in intracellular signaling," *Journal of Biochemistry*, vol. 134, no. 5, pp. 631–636, 2003.
- [27] C. G. Gahmberg, L. Ning, and S. Paetau, "ICAM-5: a neuronal dendritic adhesion molecule involved in immune and neuronal functions," *Cell Adhesion Molecules*, vol. 8, pp. 117–132, 2014.
- [28] J. R. Pollard, O. Eidelman, G. P. Mueller et al., "The TARC/sICAM5 ratio in patient plasma is a candidate biomarker for drug resistant epilepsy," *Frontiers in Neurology*, vol. 3, p. 181, 2012.
- [29] D. H. Kong, Y. Kim, M. Kim, J. Jang, and S. Lee, "Emerging roles of vascular cell adhesion molecule-1 (VCAM-1) in immunological disorders and cancer," *International Journal of Molecular Sciences*, vol. 19, no. 4, p. 1057, 2018.

- [30] J. Luo, W. Wang, Z. Xi et al., "Concentration of soluble adhesion molecules in cerebrospinal fluid and serum of epilepsy patients," *Journal of Molecular Neuroscience*, vol. 54, no. 4, pp. 767–773, 2014.
- [31] S. Bauer, S. Cepok, A. Todorova-Rudolph et al., "Etiology and site of temporal lobe epilepsy influence postictal cytokine release," *Epilepsy Research*, vol. 86, no. 1, pp. 82–88, 2009.
- [32] D. Upadhyay and A. K. Shetty, "Promise of extracellular vesicles for diagnosis and treatment of epilepsy," *Epilepsy & Behavior*, vol. 121, article 106499, 2021.
- [33] M. Xie, W. Xiong, Z. She et al., "Immunoregulatory effects of stem cell-derived extracellular vesicles on immune cells," *Frontiers in Immunology*, vol. 11, p. 13, 2020.
- [34] Q. Long, D. Upadhyay, B. Hattiangady et al., "Intranasal MSC-derived A1-exosomes ease inflammation, and prevent abnormal neurogenesis and memory dysfunction after status epilepticus," *Proceedings of the National Academy of Sciences of the United States of America*, vol. 114, no. 17, pp. E3536–e3545, 2017.
- [35] R. Raoof, S. Bauer, H. el Naggar et al., "Dual-center, dual-platform microRNA profiling identifies potential plasma biomarkers of adult temporal lobe epilepsy," *eBioMedicine*, vol. 38, pp. 127–141, 2018.
- [36] S. Yan, H. Zhang, W. Xie et al., "Altered microRNA profiles in plasma exosomes from mesial temporal lobe epilepsy with hippocampal sclerosis," *Oncotarget*, vol. 8, no. 3, pp. 4136–4146, 2017.
- [37] L. R. Liu, J. C. Liu, J. S. Bao, Q. Q. Bai, and G. Q. Wang, "Interaction of microglia and astrocytes in the neurovascular unit," *Frontiers in Immunology*, vol. 11, p. 1024, 2020.
- [38] E. J. Goetzl, J. B. Schwartz, E. L. Abner, G. A. Jicha, and D. Kapogiannis, "High complement levels in astrocyte-derived exosomes of Alzheimer disease," *Annals of Neurology*, vol. 83, no. 3, pp. 544–552, 2018.
- [39] B. Hattiangady, R. Kuruba, and A. K. Shetty, "Acute seizures in old age leads to a greater loss of CA1 pyramidal neurons, an increased propensity for developing chronic TLE and a severe cognitive dysfunction," *Aging and Disease*, vol. 2, no. 1, pp. 1–17, 2011.
- [40] M. Prinz and J. Priller, "Microglia and brain macrophages in the molecular age: from origin to neuropsychiatric disease," *Nature Reviews Neuroscience*, vol. 15, no. 5, pp. 300–312, 2014.
- [41] A. Vezzani, A. Friedman, and R. J. Dingledine, "The role of inflammation in epileptogenesis," *Neuropharmacology*, vol. 69, pp. 16–24, 2013.
- [42] P. Mohseni-Moghaddam, M. Roghani, H. Khaleghzadeh-Ahangar, S. S. Sadr, and C. Sala, "A literature overview on epilepsy and inflammasome activation," *Brain Research Bulletin*, vol. 172, pp. 229–235, 2021.
- [43] Y. Sun, J. Ma, D. Li et al., "Interleukin-10 inhibits interleukin-1 β production and inflammasome activation of microglia in epileptic seizures," *Journal of Neuroinflammation*, vol. 16, no. 1, p. 66, 2019.
- [44] C. Ulusoy, E. N. Vanlı-Yavuz, E. Şanlı et al., "Peripheral blood expression levels of inflammasome complex components in two different focal epilepsy syndromes," *Journal of Neuroimmunology*, vol. 347, article 577343, 2020.
- [45] C. C. Tan, J. G. Zhang, M. S. Tan et al., "NLRP1 inflammasome is activated in patients with medial temporal lobe epilepsy and contributes to neuronal pyroptosis in amygdala kindling-induced rat model," *Journal of Neuroinflammation*, vol. 12, no. 1, p. 18, 2015.
- [46] E. Cristina de Brito Toscano, É. L. Vieira, B. B. Dias et al., "NLRP3 and NLRP1 inflammasomes are up-regulated in patients with mesial temporal lobe epilepsy and may contribute to overexpression of caspase-1 and IL- β in sclerotic hippocampi," *Brain Research*, vol. 1752, article 147230, 2021.
- [47] X. F. Meng, L. Tan, M. S. Tan et al., "Inhibition of the NLRP3 inflammasome provides neuroprotection in rats following amygdala kindling-induced status epilepticus," *Journal of Neuroinflammation*, vol. 11, no. 1, p. 212, 2014.
- [48] H. Wang, P. Xu, D. Liao et al., "Association between NLRP1, NLRP3, and P2X7R gene polymorphisms with partial seizures," *BioMed Research International*, vol. 2017, Article ID 9547902, 6 pages, 2017.
- [49] L. Best, C. Ghadery, N. Pavese, Y. F. Tai, and A. P. Strafella, "New and old TSPO PET radioligands for imaging brain microglial activation in neurodegenerative disease," *Current Neurology and Neuroscience Reports*, vol. 19, no. 5, p. 24, 2019.
- [50] H. Amhaoul, J. Hamaide, D. Bertoglio et al., "Brain inflammation in a chronic epilepsy model: evolving pattern of the translocator protein during epileptogenesis," *Neurobiology of Disease*, vol. 82, pp. 526–539, 2015.
- [51] A. Nack, M. Brendel, J. Nedelcu et al., "Expression of translocator protein and [18F]-GE180 ligand uptake in multiple sclerosis animal models," *Cell*, vol. 8, no. 2, p. 94, 2019.
- [52] D. Bertoglio, J. Verhaeghe, E. Santermans et al., "Non-invasive PET imaging of brain inflammation at disease onset predicts spontaneous recurrent seizures and reflects comorbidities," *Brain, Behavior, and Immunity*, vol. 61, pp. 69–79, 2017.
- [53] A. A. Crawshaw and N. P. Robertson, "The role of TSPO PET in assessing neuroinflammation," *Journal of Neurology*, vol. 264, no. 8, pp. 1825–1827, 2017.
- [54] L. P. Dickstein, J. S. Liow, A. Austerluehle et al., "Neuroinflammation in neocortical epilepsy measured by PET imaging of translocator protein," *Epilepsia*, vol. 60, no. 6, pp. 1248–1254, 2019.
- [55] L. D. Gershen, P. Zanotti-Fregonara, I. H. Dustin et al., "Neuroinflammation in temporal lobe epilepsy measured using positron emission tomographic imaging of translocator protein," *JAMA Neurology*, vol. 72, no. 8, pp. 882–888, 2015.
- [56] L. D. Weidner, P. Kannan, N. Mitsios et al., "The expression of inflammatory markers and their potential influence on efflux transporters in drug-resistant mesial temporal lobe epilepsy tissue," *Epilepsia*, vol. 59, no. 8, pp. 1507–1517, 2018.
- [57] V. Bouilleret and S. Dedeurwaerdere, "What value can TSPO PET bring for epilepsy treatment?," *European Journal of Nuclear Medicine and Molecular Imaging*, 2021.
- [58] G. Scott, M. Mahmud, D. R. Owen, and M. R. Johnson, "Microglial positron emission tomography (PET) imaging in epilepsy: applications, opportunities and pitfalls," *Seizure*, vol. 44, pp. 42–47, 2017.
- [59] D. L. Nguyen, C. Wimberley, C. Truillet et al., "Longitudinal positron emission tomography imaging of glial cell activation in a mouse model of mesial temporal lobe epilepsy: toward identification of optimal treatment windows," *Epilepsia*, vol. 59, no. 6, pp. 1234–1244, 2018.
- [60] M. Brackhan, P. Bascuñana, J. M. Postema et al., "Serial quantitative TSPO-targeted PET reveals peak microglial activation up to 2 weeks after an epileptogenic brain insult," *Journal of Nuclear Medicine*, vol. 57, no. 8, pp. 1302–1308, 2016.
- [61] D. Bertoglio, H. Amhaoul, J. Goossens et al., "TSPO PET upregulation predicts epileptic phenotype at disease onset

- independently from chronic TSPO expression in a rat model of temporal lobe epilepsy,” *NeuroImage: Clinical*, vol. 31, article 102701, 2021.
- [62] M. M. Alam, J. Lee, and S. Y. Lee, “Recent Progress in the development of TSPO PET ligands for Neuroinflammation imaging in neurological diseases,” *Nuclear Medicine and Molecular Imaging*, vol. 51, no. 4, pp. 283–296, 2017.
 - [63] A. A. Sharma and J. P. Szaflarski, “In vivo imaging of neuroinflammatory targets in treatment-resistant epilepsy,” *Current Neurology and Neuroscience Reports*, vol. 20, no. 4, p. 5, 2020.
 - [64] K. J. Langen and A. Willuweit, “TSPO PET using 18F-GE-180: a new perspective in neurooncology?,” *European Journal of Nuclear Medicine and Molecular Imaging*, vol. 44, no. 13, pp. 2227–2229, 2017.
 - [65] P. Zanotti-Fregonara, B. Pascual, R. C. Rostomily et al., “Anatomy of 18F-GE180, a failed radioligand for the TSPO protein,” *European Journal of Nuclear Medicine and Molecular Imaging*, vol. 47, no. 10, pp. 2233–2236, 2020.
 - [66] E. A. van Vliet, W. M. Otte, W. J. Wadman et al., “Blood-brain barrier leakage after status epilepticus in rapamycin-treated rats II: potential mechanisms,” *Epilepsia*, vol. 57, no. 1, pp. 70–78, 2016.
 - [67] E. Hanael, R. Veksler, A. Friedman et al., “Blood-brain barrier dysfunction in canine epileptic seizures detected by dynamic contrast-enhanced magnetic resonance imaging,” *Epilepsia*, vol. 60, no. 5, pp. 1005–1016, 2019.
 - [68] A. Rana and A. E. Musto, “The role of inflammation in the development of epilepsy,” *Journal of Neuroinflammation*, vol. 15, no. 1, p. 144, 2018.
 - [69] E. Swissa, Y. Serlin, U. Vazana, O. Prager, and A. Friedman, “Blood-brain barrier dysfunction in status epileptics: mechanisms and role in epileptogenesis,” *Epilepsy & Behavior*, vol. 101, article 106285, Part B, 2019.
 - [70] W. Löscher and A. Friedman, “Structural, molecular, and functional alterations of the blood-brain barrier during epileptogenesis and epilepsy: a cause, consequence, or both?,” *International Journal of Molecular Sciences*, vol. 21, no. 2, p. 591, 2020.
 - [71] H. Han, A. Mann, D. Ekstein, and S. Eyal, “Breaking bad: the structure and function of the blood-brain barrier in epilepsy,” *The AAPS Journal*, vol. 19, no. 4, pp. 973–988, 2017.
 - [72] H. Breuer, M. Meier, S. Schneefeld et al., “Multimodality imaging of blood-brain barrier impairment during epileptogenesis,” *Journal of Cerebral Blood Flow and Metabolism*, vol. 37, no. 6, pp. 2049–2061, 2017.
 - [73] E. A. van Vliet, W. M. Otte, W. J. Wadman et al., “Blood-brain barrier leakage after status epilepticus in rapamycin-treated rats I: magnetic resonance imaging,” *Epilepsia*, vol. 57, no. 1, pp. 59–69, 2016.
 - [74] A. Varatharaj, M. Liljeroth, A. Darekar, H. B. W. Larsson, I. Galea, and S. P. Cramer, “Blood-brain barrier permeability measured using dynamic contrast-enhanced magnetic resonance imaging: a validation study,” *The Journal of Physiology*, vol. 597, no. 3, pp. 699–709, 2019.
 - [75] A. K. Singh, R. K. Garg, R. K. Gupta et al., “Dynamic contrast-enhanced (DCE) MRI derived kinetic perfusion indices may help predicting seizure control in single calcified neurocysticercosis,” *Magnetic Resonance Imaging*, vol. 49, pp. 55–62, 2018.
 - [76] B. R. Dickie, G. J. M. Parker, and L. M. Parkes, “Measuring water exchange across the blood-brain barrier using MRI,” *Progress in Nuclear Magnetic Resonance Spectroscopy*, vol. 116, pp. 19–39, 2020.
 - [77] M. Rogosnitzky and S. Branch, “Gadolinium-based contrast agent toxicity: a review of known and proposed mechanisms,” *Biometals*, vol. 29, no. 3, pp. 365–376, 2016.
 - [78] R. Abedi-Firouzjah, A. Rostamzadeh, A. Banaei, M. Shafiee, Z. Masoumi Moghaddam, and H. Vafapour, “Exploring changes in thalamus metabolites as diagnostic biomarkers in idiopathic generalised epilepsy patients using magnetic resonance spectroscopy,” *The Malaysian Journal of Medical Sciences*, vol. 27, no. 1, pp. 78–86, 2020.
 - [79] B. C. Jobst, J. Gonzalez-Martinez, J. Isnard et al., “The insula and its epilepsies,” *Epilepsy Currents*, vol. 19, no. 1, pp. 11–21, 2019.
 - [80] D. Sone, N. Ikegaya, A. Takahashi et al., “Noninvasive detection of focal brain hyperthermia related to continuous epileptic activities using proton MR spectroscopy,” *Epilepsy Research*, vol. 138, pp. 1–4, 2017.
 - [81] Z. Tan, X. Long, F. Tian, L. Huang, F. Xie, and S. Li, “Alterations in brain metabolites in patients with epilepsy with impaired consciousness: a case-control study of Interictal Multivoxel 1H-MRS findings,” *American Journal of Neuroradiology*, vol. 40, no. 2, pp. 245–252, 2019.
 - [82] E. J. Park, M. C. G. Otaduy, K. P. Lyra et al., “Extratemporal abnormalities in phosphorus magnetic resonance spectroscopy of patients with mesial temporal sclerosis,” *Arquivos de Neuro-Psiquiatria*, vol. 74, no. 2, pp. 93–98, 2016.
 - [83] Y. Aitouche, S. A. Gibbs, G. Gilbert, O. Boucher, A. Bouthillier, and D. K. Nguyen, “Proton MR spectroscopy in patients with nonlesional insular cortex epilepsy confirmed by invasive EEG recordings,” *Journal of Neuroimaging*, vol. 27, no. 5, pp. 517–523, 2017.
 - [84] J. Detour, C. Bund, C. Behr et al., “Metabolomic characterization of human hippocampus from drug-resistant epilepsy with mesial temporal seizure,” *Epilepsia*, vol. 59, no. 3, pp. 607–616, 2018.
 - [85] O. M. Gonen, B. A. Moffat, P. M. Desmond, E. Lui, P. Kwan, and T. J. O’Brien, “Seven-tesla quantitative magnetic resonance spectroscopy of glutamate, γ -aminobutyric acid, and glutathione in the posterior cingulate cortex/precuneus in patients with epilepsy,” *Epilepsia*, vol. 61, no. 12, pp. 2785–2794, 2020.
 - [86] L. Zhang, H. Li, P. Hong, and X. Zou, “Proton magnetic resonance spectroscopy in juvenile myoclonic epilepsy: a systematic review and meta-analysis,” *Epilepsy Research*, vol. 121, pp. 33–38, 2016.

Research Article

Choline Intake Correlates with Cognitive Performance among Elder Adults in the United States

Lu Liu,¹ Song Qiao,¹ Liying Zhuang,¹ Shanhu Xu,¹ Linhui Chen,¹ Qilun Lai¹ ,¹ and Wenfeng Wang² 

¹Department of Neurology, Zhejiang Hospital, Hangzhou, Zhejiang 310013, China

²School of Science, Shanghai Institute of Technology, Shanghai 201418, China

Correspondence should be addressed to Qilun Lai; laiql665@outlook.com

Received 5 August 2021; Accepted 11 October 2021; Published 29 October 2021

Academic Editor: Muh-Shi Lin

Copyright © 2021 Lu Liu et al. This is an open access article distributed under the Creative Commons Attribution License, which permits unrestricted use, distribution, and reproduction in any medium, provided the original work is properly cited.

Objective. This research attempted to explore the neuroprotective effect of choline and establish evidence for future dietary recommendations and nutritional interventions to maintain a proper cognitive function among elders aged >60 years in the US. **Method.** This cross-sectional study retrieved data of 2,393 eligible elderly participants from the 2011-2014 National Health and Nutrition Examination Survey. Combining dietary and supplement choline intake, total choline intake was evaluated using the 24-hour dietary recall method and the dietary supplement questionnaire. Total choline intake was categorized into tertiles, which ranged at <187.60 mg/day (T1), 187.60-399.50 mg/day (T2), and >399.50 mg/day (T3). The Consortium to Establish a Registry for Alzheimer's Disease (CERAD) Word Learning subtest, Animal Fluency (AF) test, and Digit Symbol Substitution test (DSST) was used to measure cognitive function. Participants who scored the lowest 25th percentile in each cognitive test were classified in the low cognitive function (LC) group. Logistic regression models were implemented to examine the association between total choline intake and the incidence of LC. **Results.** In the CERAD test, the risk of LC was significantly lower in T2 than T1 (OR: 0.668, 95% CI: 0.493-0.904, and $P=0.006$) when adjusted for age, gender, BMI, alcohol consumption, and hypertension. Similarly, T2 was associated with a significantly lower risk of LC when assessed by the AF test (OR: 0.606, 95% CI: 0.580-0.724, and $P<0.001$) and DSST (0.584, 95% CI: 0.515-0.661, and $P<0.001$). In all three cognitive measures, the T3 of the total choline intake was not associated with cognitive function compared to T1. **Conclusion.** Total choline intake at 187.06-399.50 mg/day reduces the risk of LC by approximately 50% compared to intake at <187.6 mg/day. The findings of this research may be used to establish dietary recommendations and nutritional interventions to optimize the cognitive function among elders.

1. Introduction

Aging is the most prominent risk factor of cognitive function declines, including processing speed, attention, certain memories, language, visuospatial abilities, and executive functioning [1]. The diagnostic criteria of several cognitive disorders are defined by the Diagnostic and Statistical Manual of Mental Disorders (DSM-5) [2]. Globally, the size of the elderly population is projected to reach 2 billion by 2050, accounting for 22% of the world population [3]. The substantial growth of the elderly population has raised considerable attention regarding cognitive changes or deficits, impacting the quality of life and leading to medical and

social burdens [4, 5]. Current treatment for cognitive impairment is limited. Thus, the prevention and management of age-related cognitive decline have become a global imperative.

Choline is a water-soluble micronutrient crucial for the structural integrity of cell membrane, methyl metabolism, cholinergic neurotransmission, transmembrane signaling, and lipid-cholesterol metabolism [6]. As the precursor of acetylcholine and phospholipids, choline plays a pivotal role in neurotransmission and cell signaling [7, 8]. Dysregulation of cholinergic neurotransmission is linked to several cognitive disorders, such as Alzheimer's disease (AD), the most prevalent age-related neurodegenerative disease [9]. A

reduction in acetylcholine, an essential neurotransmitter for memory and learning, has been observed among patients with AD [10].

Previous researches have proposed the neuroprotective effect of choline consumption [11, 12]. In an animal study, lifelong supplementation of choline significantly improves spatial memory [13]. Maternal choline supplementation during prenatal and perinatal periods decreases the risk of cognitive disorders of the fetus in the mice model [14, 15]. In humans, choline supplementation is also associated with improved cognitive function among young and middle-aged adults [16]. However, limited human studies have investigated the effect of choline consumption on cognitive performance.

Moreover, previous studies mainly examined the therapeutic effect of choline supplementation while ignoring the dietary choline intake. Therefore, the primary purpose of this research is to examine the relationship between total choline intake, combining dietary and supplement choline intake, and cognitive performance among elders in the US.

2. Methods

2.1. Study Design. The National Health and Nutrition Examination Survey (NHANES) is a nationwide ongoing survey consisting of a household interview and a physical examination in a mobile examination center (MEC) [17]. The Center for Disease Prevention and Control has been conducting the survey on a 2-year basis since the 1960s, intending to assess the health and nutritional status of the noninstitutionalized US civilian population. The collected data was deidentified and released for public use on the NHANES official website (<https://www.cdc.gov/nchs/nhanes/index.htm>). The National Center for Health Statistics Ethics Review Board approved all the NHANES protocols, and informed consent was obtained from all study participants [18].

The 2011-2012 and 2013-2014 NHANES cycles evaluated the cognitive performance of the study participants and were therefore retrieved in this cross-sectional study. In this study, participants aged 60 years or older who participated in the cognitive function assessments and reported complete information were included. Participants who reported incomplete or missing data in age, gender, body mass index (BMI), race, poverty income ratio (PIR), education level, choline intake, alcohol consumption, diabetic status, hypertension status, and smoking status were excluded. Participants who indicated extreme dietary consumption (male: <500 kcal or >8000 kcal and female: <500 kcal or >5000 kcal) were excluded. Underweight people with BMI < 18.5 kg/m² were also excluded. In total, 2,393 participants were eligible for the analyses in this study, as shown in Figure 1.

2.2. Total Choline Intake. The choline intake in this research combined the dietary and supplement intake. The total choline intake of participants with missing supplement intake is equivalent to their dietary intake. The total choline intake was categorized into the low-intake group (<25th percentile), medium-intake group (25th-75th percentile), and high-intake

group (>75th percentile), corresponding to choline intake at <187.60 mg/day, 187.60-399.50 mg/day, and >399.50 mg/day.

The dietary intake was collected during the MEC examination using the 24-hour dietary recall method and a USDA validated Automated Multiple-Pass Method [19]. The quantified dietary choline intake was obtained from the Dietary datasets, Dietary Interview-Total Nutrient Intakes file.

The Dietary Supplement and Prescription Medication Questionnaire (DSQ) was used to determine the supplement choline intake. The DSQ collected the total supplement intake of the participants in the past 30 days. The average daily supplement intake was calculated by averaging the total 30-day supplement intake. The Dietary Supplement Use 30 day-Total Dietary Supplements data file was accessed to obtain the total supplement choline consumption.

2.3. Cognitive Performance. Cognitive performance was assessed in the MEC using three cognitive function tests, the Consortium to Establish a Registry for Alzheimer's Disease (CERAD) Word Learning subset, the Animal Fluency (AF) test, and the Digit Symbol Substitution Test (DSST). Data on cognitive function was retrieved from the cognitive functioning questionnaire (CFQ).

The CERAD tested the immediate and delayed learning ability for new verbal information [20]. After visually or auditorily presenting ten words to the participants, the designated research instructed the participants to read aloud the words and recall the words immediately and after completing the AF test and DSST. Participants were asked to recall the words as many and possible. Categorical verbal fluency was assessed by the AF test [21]. Participants were asked to name as many animals as possible within 1 minute. Each named animal was counted as one point. The DSST estimated the processing speed, sustained attention, and working memory [22]. Participants were provided with a piece of paper with a key at the top and 133 boxes that adjoined numerical numbers at the bottom of the paper. The key presented the pair relationship of 9 numbers and symbols. The participants were asked to match the corresponding symbols for the 133 boxes in two minutes.

Although there was no consensus definition of low cognitive function, previous studies using the NHANES database defined participants who scored the lowest 25th percentile in the cognitive tests as having low cognitive function [23, 24]. Thus, this research adopted <25th percentile as the cutoff of low cognitive performance. Participants who scored CERAD < 5, AF < 13, and DSST < 34 were classified into the low cognitive function (LC) group, otherwise categorized into the normal cognitive function (NC) group.

2.4. Potential Covariates. This study accommodated potential covariates identified in previous studies [25, 26], containing diabetes, hypertension, weight, education level, race, social-economic status, alcohol consumption, and smoking.

Age groups were categorized on a 10-year basis, 60-69 years old, 70-79 years old, and ≥80 years old. The BMI was categorized into the normal weight group (BMI 18.5-24.9 kg/m²), overweight group (BMI 25-29.9 kg/m²), and

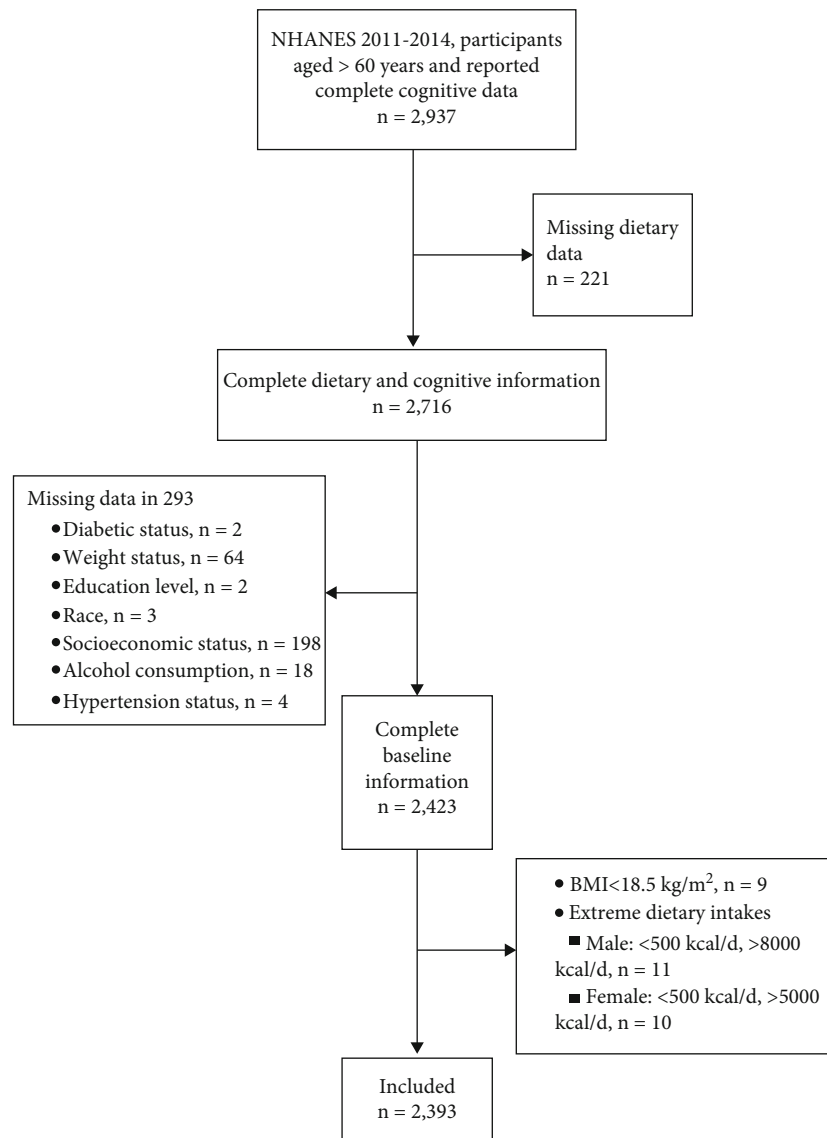


FIGURE 1: Flow chart of selecting eligible participants.

obese group ($\text{BMI} \geq 30 \text{ kg/m}^2$) based on the WHO standard [27]. Social-economic status was evaluated using the PIR, which was available in the Demographic Variables & Sample Weight (DEMO) data file. The PIR is the ratio of family income to poverty, calculated by dividing family income by the poverty guidelines. The $\text{PIR} < 1$ was defined as the low-income group. The Alcohol Use Questionnaire (ALQ) was used to identify alcohol consumers. Participants who answered “yes” to question ALQ101, “Had at least 12 alcohol drinks/1 yr.,” were considered alcohol consumers.

Hypertension patients were determined based on the laboratory data and Blood Pressure & Cholesterol Questionnaire (BPQ). Participants were classified as hypertension patients if their systolic pressure $\geq 140 \text{ mmHg}$ and diastolic pressure $\geq 90 \text{ mmHg}$. The BPQ question 020 asked, “[Have you/Has SP] ever been told by a doctor or other health professional that {you/s/he} had hypertension, also called high blood pressure?”. Participants who answered “yes” were defined as having hypertension.

Question DIQ010 of the Diabetes Questionnaire (DIQ) asked, “The next questions are about specific medical conditions. {Other than during pregnancy, {have you/has SP}/{Have you/Has SP}} ever been told by a doctor or health professional that {you have/{he/she/SP} has} diabetes or sugar diabetes?” Participants who answered “yes” were considered diabetic. Additionally, participants with a fasting blood glucose level $\geq 7.0 \text{ mmol/L}$ or a hemoglobin A1c $\geq 6.5\%$ were identified as diabetic.

2.5. Statistical Analysis. All statistical tests were two-sided tests in this study. A P value less than 0.05 was considered significant. SAS 9.4 (SAS Institute, Inc., Cary, NC, USA) was used for all the statistical analyses. R 4.02 was used to generate all the graphics in this study. The distribution of variables was tested for normality by the Shapiro normality test. Nonnormally distributed continuous variables were categorized into groups. Summary statistics presented the mean and standard deviation for continuous variables (mean \pm SD).

) while displayed frequencies and percent distributions for categorical variables (N %). Baseline characteristics were compared using the independent samples t -test, the Pearson's chi-square test (χ^2), and the Fisher's exact test when appropriate. The unadjusted and multivariate logistic regression models were implemented to acquire the odds ratio (OR), 95% confidence interval (95% CI), and P value when investigating the association between dietary choline intake and cognitive function. The 2011-2012 and 2013-2014 NHANES cycle purposely oversampled non-Hispanic black persons, non-Hispanic non-black Asian persons, Hispanic persons, and low- and nonlow-income groups to increase the sample's representativeness in the US. Sample weights (full sample 2-year MEC examination weight) were applied to all the statistical analyses in this study. The power analysis was used to assess the statistical power ($1-\beta$) by the PASS 15.0 software. We found that the power values ($1-\beta$) of the CERAD test, the Animal Fluency (AF) test, and the Digit Symbol Substitution Test (DSST) were all 0.9, indicating that the sample size could support the multiple regression results and our findings performed well reliability.

3. Results

3.1. Study Population. The baseline characteristics were summarized and compared in Table 1. Of the included 2,393 participants, 49.02% were male, and 50.98% were female. The study population was mainly composed of non-Hispanic whites (50.02%). The PIR of most study participants was ≥ 1 (83.95%). More participants were obese (39.16%) than overweight (35.65%) and normal weight (25.20%). A larger percentage of alcohol consumers (69.62%) than nonconsumers (30.38%) were included in the study. Diabetic participants contributed to 23.36% of the study population. Most participants (95.45%) were not consuming dietary supplements. The total choline intake was divided into tertiles. The range of each tertile was <187.06 mg/day in T1, 187.06-399.50 mg/day in T2, and >399.50 mg/day in T3.

In all three cognition measures, the intragroup comparisons of the LC group and NC group revealed significant differences in age ($P < 0.001$), gender ($P < 0.001$), race ($P < 0.001$), an education level ($P < 0.001$), marital status ($P < 0.001$), PIR ($P < 0.001$), BMI ($P < 0.001$), alcohol consumption ($P < 0.001$), diabetes ($P < 0.001$), hypertension ($P < 0.001$), and smoking ($P < 0.001$).

In the CERAD test, of the LC group, 38.41% were 60-69 years old, 31.66% were 70-79 years old, and 29.93% were ≥ 80 years old; 60.73% were male, and 39.27% were female; 24.74% were normal weight (BMI 18.5 – 24.9 kg/m²), 41.25% were overweight (BMI 25 – 29.9 kg/m²), and 33.91% were obese (BMI ≥ 30 kg/m²); 68.17% were alcohol consumers; 65.92% had hypertension; patients with low choline intake (<187.60 mg/day) were 23.18%, medium choline intake (187.60-399.50 mg/day) were 53.81%, and high choline intake were 23.01%. In the AF test, of the LC group, 44.05% were 60-69 years old, 33.78% were 70-79 years old, and 21.82% were ≥ 80 years old; 48.77% were male, and 51.23% were female; 27.13% were normal weight

(BMI 18.5 – 24.9 kg/m²), 33.97% were overweight (BMI 25 – 29.9 kg/m²), and 38.90% were obese (BMI ≥ 30 kg/m²); 63.95% were alcohol consumers; 70.40% had hypertension; patients with low choline intake (<187.60 mg/day) were 31.69%, medium choline intake (187.60-399.50 mg/day) were 46.68%, and high choline intake were 21.63%. In the DSST, of the LC group, 42.70% were 60-69 years old, 34.23% were 70-79 years old, and 23.06% were ≥ 80 years old; 56.22% were male, and 43.78% were female; 25.05% were normal weight (BMI 18.5 – 24.9 kg/m²), 35.31% were overweight (BMI 25 – 29.9 kg/m²), and 39.64% were obese (BMI ≥ 30 kg/m²); 63.06% were alcohol consumers; 71.71% had hypertension; patients with low choline intake (<187.60 mg/day) were 31.71%, medium choline intake (187.60-399.50 mg/day) were 47.93%, and high choline intake were 20.36%.

3.2. Choline Intake and Cognitive Performance. Three logistic regression models were implemented in this research. The crude model did not adjust for any potential covariates, while model 1 controlled for age and gender. Model 2 adjusted for age, gender, BMI, alcohol consumption, and hypertension. T1, the first tertile (<187.06 mg/day) of the total choline intake, was set as the reference group in all the logistic regression analyses. The risks of low cognitive performance in T2 (187.06-399.50 mg/day) and T3 (>399.50 mg/day) were compared with T1.

In the CERAD test (Table 2 and Figure 2), T2 of the total choline intake was associated with a significantly lower incidence of declined learning ability than T1 (OR: 0.414, 95% CI: 0.304-0.564, and $P < 0.001$). The risk of low cognitive function was not statistically different in T3 compared to T1 (OR: 0.752, 95% CI: 0.499-1.133, and $P = 0.272$). Model 1, adjusting for age and gender, uncovered similar results, with the risk of impaired learning ability being the lowest in T2 (OR: 0.563, 95% CI: 0.414-0.765, and $P < 0.001$). The results of model 2 (OR: 0.668, 95% CI: 0.493-0.904, and $P = 0.006$) were allied with the crude model and model 1.

When analyzing categorical verbal fluency using the AF test (Table 3 and Figure 3), total choline intake level at 187.06-399.50 mg/day indicated reduced odds of low categorical verbal fluency (OR: 0.493, 95% CI: 0.433-0.560, and $P < 0.001$) compared to the intake level at <187.06 mg/day. Nevertheless, no significant difference was found between the intake level >399.50 mg/day and the intake level <187.06 mg/day (OR: 1.043, 95% CI: 0.866-1.256, and $P = 0.660$). After adjusting for covariates, the relationship remained in model 1, revealing significantly lower odds of impaired categorical verbal fluency in T2 when compared to T1 (OR: 0.548, 95% CI: 0.464-0.646, and $P < 0.001$). When further controlling for BMI, alcohol consumption, and hypertension in model 2, T2 still showed a decreased occurrence of low categorical verbal fluency (OR: 0.606, 95% CI: 0.580-0.724, and $P < 0.001$).

As demonstrated in Table 4 and Figure 4, the risk of declined processing speed, sustained attention, and working memory in the T2 of total choline intake was significantly lower than that of the T1 when evaluating the cognitive performance by the DSST (OR: 0.476, 95% CI: 0.402-0.542, and

TABLE 1: Baseline characteristics of the 2,393 study participants, 2011-2014 NHANES.

Variables	Total (<i>n</i> = 2,393)	CERAD		<i>P</i>	AF		<i>P</i>	DSST		<i>P</i>
		LC (<i>n</i> = 578)	NC (<i>n</i> = 1,815)		LC (<i>n</i> = 527)	NC (<i>n</i> = 1,866)		LC (<i>n</i> = 555)	NC (<i>n</i> = 1,838)	
Age, <i>n</i> (%)				<0.001			<0.001			<0.001
60-69	1,322 (55.24)	222 (38.41)	1,100 (60.61)		237 (44.05)	1,098 (58.22)		237 (42.70)	1,085 (59.03)	
70-79	703 (29.38)	183 (31.66)	520 (28.65)		178 (33.78)	531 (28.15)		190 (34.23)	513 (27.91)	
≥80	368 (15.38)	173 (29.93)	195 (10.74)		115 (21.82)	257 (13.63)		128 (23.06)	240 (13.06)	
Gender, <i>n</i> (%)				<0.001			<0.001			<0.001
Male	1,173 (49.02)	351 (60.73)	822 (45.29)		257 (48.77)	924 (48.99)		312 (56.22)	861 (46.84)	
Female	1,220 (50.98)	227 (39.27)	993 (54.71)		270 (51.23)	962 (51.01)		243 (43.78)	977 (53.16)	
Race, <i>n</i> (%)				<0.001			<0.001			<0.001
Mexican American	206 (8.61)	57 (9.86)	149 (8.21)		37 (7.02)	169 (8.96)		75 (13.51)	131 (7.13)	
Other Hispanic	238 (9.95)	64 (11.07)	174 (9.59)		68 (12.90)	170 (9.01)		102 (18.38)	136 (7.40)	
Non-Hispanic white	1,197 (50.02)	286 (49.48)	911 (50.19)		185 (35.10)	1,025 (54.35)		169 (30.45)	1,028 (55.93)	
Non-Hispanic black	560 (23.40)	145 (25.09)	415 (22.87)		185 (35.10)	379 (20.10)		190 (34.23)	370 (20.13)	
Other	192 (8.02)	26 (4.50)	166 (9.15)		52 (9.87)	143 (7.58)		19 (3.42)	173 (9.41)	
Education level, <i>n</i> (%)				<0.001			<0.001			<0.001
Less than 9th grade	244 (10.20)	109 (18.86)	135 (7.44)		102 (19.35)	142 (7.53)		188 (33.87)	56 (3.05)	
9-11th grade	319 (13.33)	89 (15.40)	230 (12.67)		100 (18.98)	222 (11.77)		118 (21.26)	201 (10.94)	
High school graduate	557 (23.28)	148 (25.61)	409 (22.53)		148 (28.08)	412 (21.85)		128 (23.06)	429 (23.34)	
Some college	704 (29.42)	128 (22.15)	576 (31.74)		116 (22.01)	593 (31.44)		87 (15.68)	617 (33.57)	
College graduate	569 (23.78)	104 (17.99)	465 (25.62)		61 (11.57)	517 (27.41)		34 (6.13)	535 (29.11)	
Marital status, <i>n</i> (%)				<0.001			<0.001			<0.001
Married	1,333 (55.70)	308 (53.29)	1,025 (56.47)		267 (50.66)	1,074 (56.95)		258 (46.49)	1,075 (58.49)	
Widowed	440 (18.39)	138 (23.88)	302 (16.64)		133 (25.24)	312 (16.54)		147 (26.49)	293 (15.94)	
Divorced	358 (14.96)	66 (11.42)	292 (16.09)		72 (13.66)	291 (15.43)		72 (12.97)	286 (15.56)	
Separated	65 (2.72)	20 (3.46)	45 (2.48)		21 (3.98)	45 (2.39)		33 (5.95)	32 (1.74)	
Never married	132 (5.52)	27 (4.67)	105 (5.79)		24 (4.55)	109 (5.78)		29 (5.23)	103 (5.60)	
Living with partner	65 (2.72)	19 (3.29)	46 (2.53)		10 (1.90)	55 (2.92)		16 (2.88)	49 (2.67)	
PIR, <i>n</i> (%)				<0.001			<0.001			<0.001
<1	384 (16.05)	109 (18.86)	275 (15.15)		135 (25.62)	256 (13.57)		171 (30.81)	213 (11.59)	
≥1	2,009 (83.95)	469 (81.14)	1,540 (84.85)		392 (74.38)	1,630 (86.43)		384 (69.19)	1,625 (88.41)	
BMI, <i>n</i> (%)				<0.001			<0.001			<0.001
18.5 to <25	603 (25.20)	143 (24.74)	460 (25.34)		143 (27.13)	460 (24.39)		139 (25.05)	464 (25.24)	
25 to <30	853 (35.65)	239 (41.35)	614 (33.83)		179 (33.97)	674 (35.74)		196 (35.32)	657 (35.75)	
≥30	937 (39.16)	196 (33.91)	741 (40.83)		205 (38.90)	732 (38.81)		220 (39.64)	717 (39.01)	
Alcohol consumption, <i>n</i> (%)				<0.001			<0.001			<0.001
Yes	1,666 (69.62)	394 (68.17)	1,272 (70.08)		337 (63.95)	1,343 (71.21)		350 (63.06)	1,316 (71.60)	
No	727 (30.38)	184 (31.83)	543 (29.92)		190 (36.05)	543 (28.79)		205 (36.94)	522 (28.40)	

TABLE 1: Continued.

Variables	Total (<i>n</i> = 2,393)	CERAD		<i>P</i>	AF		<i>P</i>	DSST		<i>P</i>
		LC (<i>n</i> = 578)	NC (<i>n</i> = 1,815)		LC (<i>n</i> = 527)	NC (<i>n</i> = 1,866)		LC (<i>n</i> = 555)	NC (<i>n</i> = 1,838)	
Diabetes, <i>n</i> (%)				<0.001			<0.001			<0.001
Yes	559 (23.36)	149 (25.78)	410 (22.59)		158 (29.98)	401 (21.26)		180 (32.43)	379 (20.62)	
No	1,721 (71.92)	400 (69.20)	1,321 (72.78)		347 (65.84)	1,394 (73.91)		352 (63.42)	1,369 (74.48)	
Borderline	113 (4.72)	29 (5.02)	84 (4.63)		22 (4.17)	91 (4.83)		23 (4.14)	90 (4.90)	
Hypertension, <i>n</i> (%)				<0.001			<0.001			<0.001
Yes	1,502 (62.77)	381 (65.92)	1,121 (61.76)		371 (70.40)	1,139 (60.39)		398 (71.71)	1,104 (60.07)	
No	891 (37.23)	197 (34.08)	694 (38.24)		156 (29.60)	747 (39.61)		157 (28.29)	734 (39.93)	
Smoking, <i>n</i> (%)				<0.001			<0.001			<0.001
Yes	1,230 (51.40)	291 (50.35)	939 (51.74)		276 (52.37)	966 (51.22)		300 (53.10)	936 (50.92)	
No	1,163 (48.60)	287 (49.65)	876 (48.26)		251 (47.63)	920 (48.78)		265 (46.90)	902 (49.08)	
Supplement use, <i>n</i> (%)				<0.001			<0.001			<0.001
Yes	109 (4.55)	22 (3.81)	87 (4.79)		13 (2.47)	101 (5.36)		11 (1.98)	98 (5.33)	
No	2,284 (95.45)	556 (96.19)	1,728 (95.21)		514 (97.53)	1,785 (94.64)		544 (98.02)	1,740 (94.67)	
Choline intake tertiles (mg)				<0.001			<0.001			<0.001
<187.60	598 (24.99)	134 (23.18)	464 (25.56)		167 (31.69)	436 (23.12)		176 (31.71)	422 (22.96)	
187.60 to <399.50	1,197 (50.02)	311 (53.81)	886 (48.82)		246 (46.68)	961 (50.95)		266 (47.93)	931 (50.65)	
≥ 399.50	598 (24.99)	133 (23.01)	465 (25.62)		114 (21.63)	489 (25.93)		113 (20.36)	485 (26.39)	

CERAD: the Consortium to Establish a Registry for Alzheimer's Disease; AF: Animal Fluency test; DSST: the Digit Symbol Substitution Test; LC: low cognitive function group; NC: normal cognitive function group; PIR: poverty income ratio; BMI: body mass index.

TABLE 2: The association between choline intake and cognitive performance assessed by the CERAD test.

Variables	Crude		<i>P</i>	Model 1		Model 2	
	OR (95% CI)			OR (95% CI)	<i>P</i>	OR (95% CI)	<i>P</i>
Total choline intake (mg/day)							
T1 (<187.06)	Ref			Ref		Ref	
T2 (187.06-399.50)	0.414 (0.304-0.564)	<0.001		0.563 (0.414-0.765)	<0.001	0.668 (0.493-0.904)	0.006
T3 (>399.50)	0.752 (0.499-1.133)	0.272		0.765 (0.540-1.082)	0.881	0.865 (0.602-1.242)	0.719

Crude: unadjusted logistic regression model; model 1: logistic regression model adjusted for age and gender; model 2: logistic regression model adjusted for age, gender, BMI, alcohol consumption, and hypertension; OR: odds ratio; CI: confidence interval.

$P < 0.001$). There was no significant difference when comparing the risk of low cognitive performance in T3 to the reference (OR: 1.009, 95% CI: 0.852-1.194, and $P = 0.920$). A similar pattern was observed when adjusting for age and gender, with the risk of low cognitive performance being the lowest in T2 (OR: 0.525, 95% CI: 0.457-0.605, and $P < 0.001$), while no significant difference between T1 and T3 (OR: 0.765, 95% CI: 0.802-1.176, and $P = 0.766$). After further controlling for BMI, alcohol consumption, and hypertension, the results were consistent with the crude model and model 1 (OR: 0.584, 95% CI: 0.515-0.661, and $P < 0.001$).

4. Discussion

This research analyzed the combined data of the 2011-2012 and 2013-2014 NHANES datasets. Compared to choline intake at <187.6 mg/day, intake at 187.6-399.5 mg/day

decreases the risk of low cognitive performance in learning ability, categorical verbal fluency, working memory, processing speed, and sustained attention. The risk of low cognitive performance reduces approximately 40% in all three cognition measures when the participants consume 187.6-399.5 mg choline per day.

Although choline intake at 187.6-399.5 mg/day indicates a beneficial effect, no change in the cognitive performance was observed when choline intake reached greater than 399.5 mg/day. The relationship assembles a "U" shape risk as choline consumption increases, implying there might be an optimal level of choline consumption to attenuate age-related cognitive declines. The good dietary choline sources are mainly from animal products, such as beef liver (3 oz provides 356 mg) and egg (1 large egg provides 147 mg) [28]. Although it remains controversial, consumption of red meat may increase the risk of AD by elevating brain iron

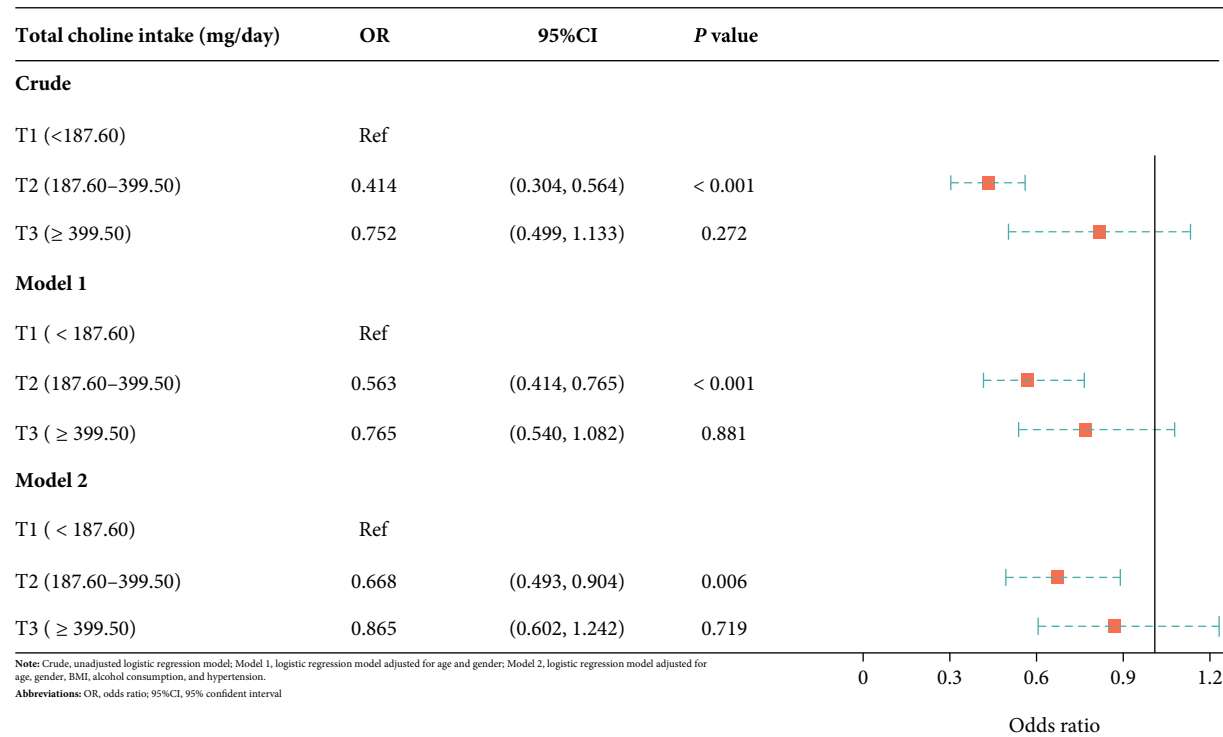


FIGURE 2: Forest plot-association between choline intake and cognitive performance assessed by the CERAD test.

TABLE 3: The association between choline intake and cognitive performance assessed by the AF test.

Variables	Crude		Model 1		Model 2	
	OR (95% CI)	P	OR (95% CI)	P	OR (95% CI)	P
Total choline intake (mg/day)						
T1 (<187.06)	Ref		Ref		Ref	
T2 (187.06-399.50)	0.493 (0.433-0.560)	<0.001	0.548 (0.464-0.646)	<0.001	0.606 (0.508-0.724)	<0.001
T3 (>399.50)	1.043 (0.866-1.256)	0.660	1.062 (0.882-1.276)	0.529	1.083 (0.905-1.295)	0.390

Crude: unadjusted logistic regression model; model 1: logistic regression model adjusted for age and gender; model 2: logistic regression model adjusted for age, gender, BMI, alcohol consumption, and hypertension; OR: odds ratio; CI: confidence interval.

levels [29]. As dietary choline intake increases, the consumption of animal products also rises, which may explain the unchanged risk of low cognitive performance when the choline consumption achieves >399.5 mg/day in our study.

Currently, the tolerable upper limit of choline intake is 3.5 g/day. The recommended daily allowance (RDA) and estimated average requirement (EAR) of choline intake have not been established due to insufficient evidence. The adequate intake (AI) is developed when insufficient data is available. The AI of choline for adults is 425 mg/day for women and 550 mg/day for men [8]. Nevertheless, our findings suggest that the optimal level of choline intake to prevent the progression of cognitive decline is lower than the AI. Therefore, results of our study may be used for the evidence-based dietary recommendation for the elders, aiming to achieve a proper cognitive function.

The underlying mechanism of choline influencing cognition has been investigated in some previous studies. Patients with AD display a reduced level of acetylcholine [30], which activates microglia in the hippocampus and leads to cascade

reaction of brain inflammation and neuronal death [13]. The epigenetic mechanism has also been proposed, demonstrating the essential role of choline as an epigenetic modifier [31]. As a critical methyl donor that involves DNA and histone methylation, choline may alter brain function by modulating neuronal gene expression, such as influencing the availability of S-adenosylmethionine. Thus, identifying effective nutritional strategies is a cost-effective approach to optimize cognitive function among elders.

The Framingham Heart Study Offspring Study, a cohort study conducted in the US, measured the total choline intake using the Harvard FFQ and examined its relationship to cognitive impairment among participants aged 36-83 years [32]. Cognitive function was evaluated by a neuropsychological test battery, consisting of verbal memory, visual memory, verbal learning, and executive function assessments, and the brain MRI, evaluating the white-matter hyperintensity. The study revealed that choline consumption at midlife acted as a neuroprotective agent by decreasing the white-matter hyperintensity volume. The effectiveness of choline

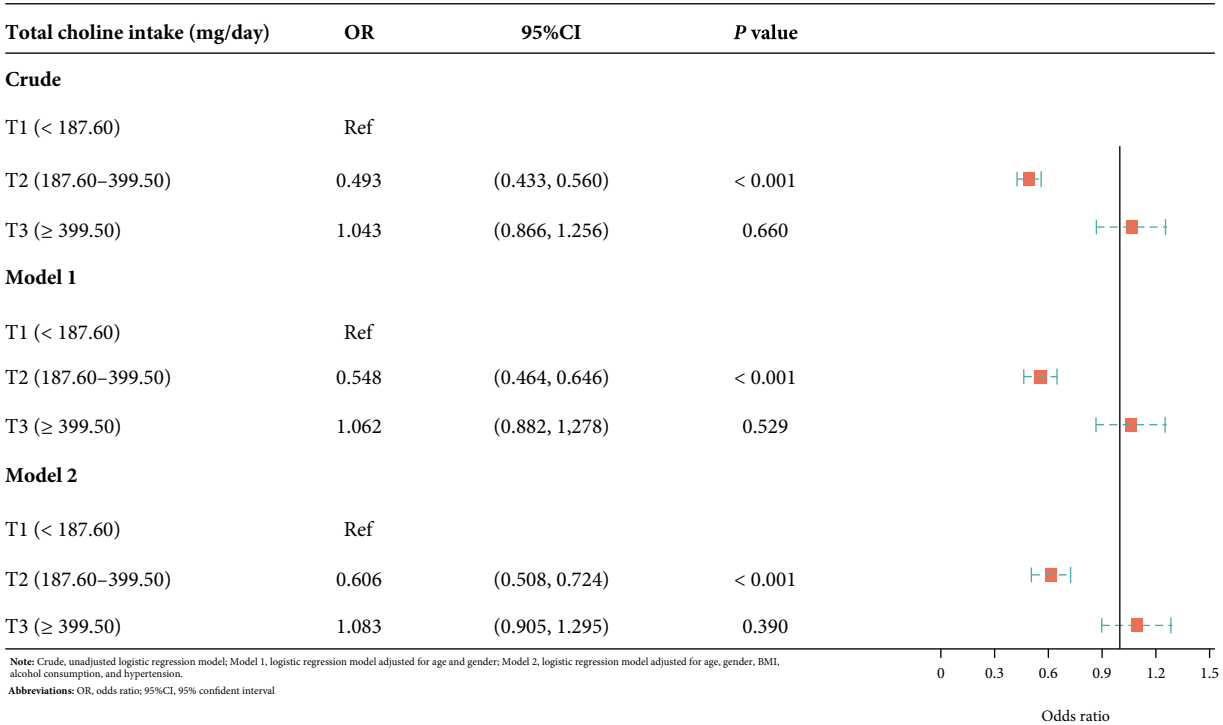


FIGURE 3: Forest plot-association between choline intake and cognitive performance assessed by the AF test.

TABLE 4: The association between choline intake and cognitive performance assessed by the DSST.

Variables	Crude		Model 1		Model 2	
	OR (95% CI)	P	OR (95% CI)	P	OR (95% CI)	P
Total choline intake (mg/day)						
T1 (<187.06)	Ref		Ref		Ref	
T2 (187.06-399.50)	0.476 (0.402-0.542)	<0.001	0.526 (0.457-0.605)	<0.001	0.584 (0.515-0.661)	<0.001
T3 (>399.50)	1.009 (0.852-1.194)	0.920	0.765 (0.802-1.176)	0.786	0.997 (0.826-1.203)	0.974

Crude: unadjusted logistic regression model; model 1: logistic regression model adjusted for age and gender; model 2: logistic regression model adjusted for age, gender, BMI, alcohol consumption, and hypertension; OR: odds ratio; CI: confidence interval.

intake in the Framingham Heart Study was allied with the findings of our study. However, the Framingham Heart Study investigated the effectiveness of choline intake at mid-life, while the consumption at elder life was not evaluated.

Low plasma choline concentration was also found to associate with poor cognitive performance. Nurk et al. conducted a cross-sectional study, attempting to research the relationship between plasma-free choline and cognitive performance [33]. The cognitive tests were administered to 2,195 participants aged 70-74 years. Nonfasting blood was collected to obtain the plasma choline concentration. High plasma choline concentration was associated with better sensorimotor speed, perceptual speed, and executive function. Many reports have shown that supplementing the maternal (during gestation and lactation) diet with additional choline benefits cognition [34–36]. A recent study showed that Chinese ischemic stroke patients with higher choline and betaine levels had a lower risk of cognitive impairment, using data derived from CATIS (China Antihypertensive Trial in

Acute Ischemic Stroke) [37]. The effectiveness of choline intake was allied with the findings of our study.

In the elderly population, the neuroprotective effect on the age-related cognitive decline has not been ascertained due to limited research. The findings of our study provide evidence to establish the protective effect of choline intake on cognitive performance. Nevertheless, there are several limitations of this research. The cross-sectional design of this research cannot establish a causal relationship between choline intake and cognitive performance. Furthermore, this retrospective study could not control all behavioral, medical, and environmental factors influencing cognitive functioning. The plasma choline level related to the baseline plasma choline status was not available for consideration in this study. Thus, the therapeutic effect of choline may not be fully uncovered in this research. Finally, it is well known that food intake changes daily, and as such, a 24 h recall is not necessarily representative of usual food intake [38]. However, we have excluded underweight participants and

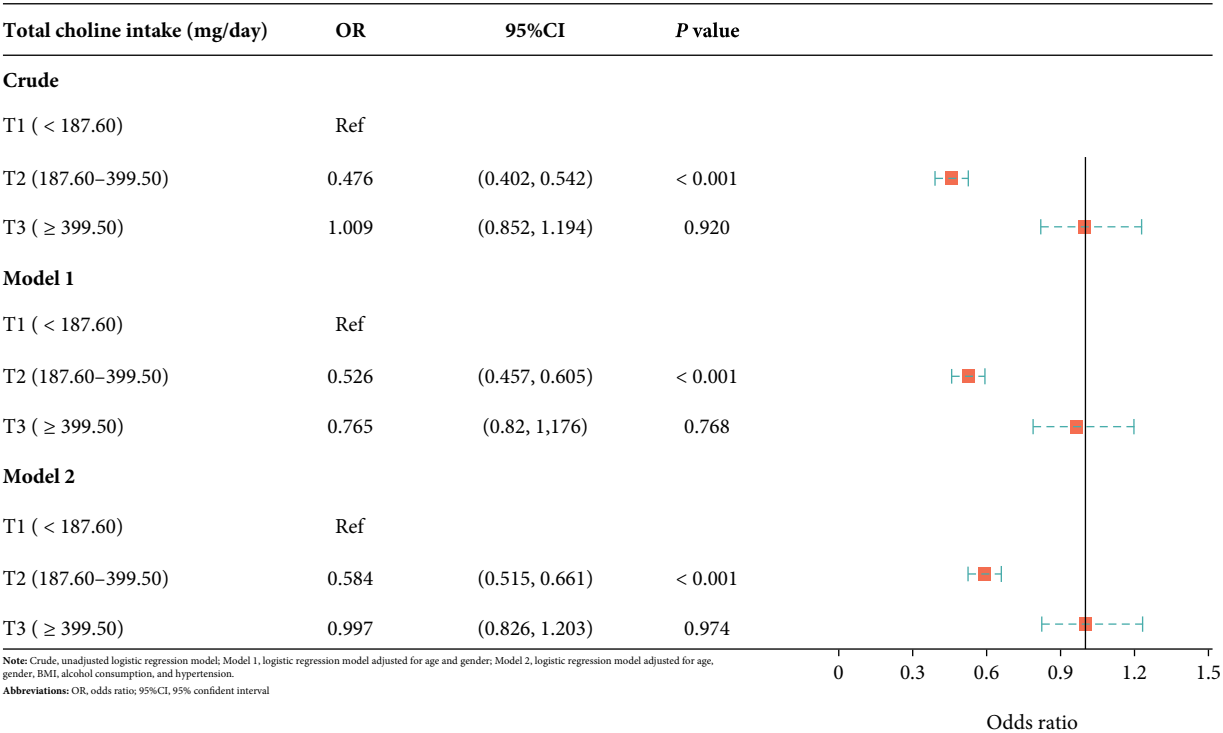


FIGURE 4: Forest plot-association between choline intake and cognitive performance assessed by the DSST.

participants with extreme intakes to reduce the incidence of potential choline deficiency or extremely low choline intake. Future research may administer nutrition interventions considering the baseline choline status to explore the ideal choline intake to maintain healthy physiological functions and proper cognitive performance.

5. Conclusion

Compared to <187.6 mg/day, the total choline intake at 187.06–399.50 mg/day illustrates a protective effect on cognitive function, including learning ability, categorical verbal fluency, processing speed, sustained attention, and working memory. The results of this study may provide evidence to support and establish dietary choline recommendations for the elders and identify ideal dietary interventions to prevent age-related cognitive decline and maintain a proper cognitive function.

Abbreviations

- AD: Alzheimer’s disease
- NHANES: National Health and Nutrition Examination Survey
- MEC: Mobile examination center
- DSQ: Dietary Supplement and Prescription Medication Questionnaire
- CERAD: Consortium to Establish a Registry for Alzheimer’s Disease
- DSST: Digit Symbol Substitution test
- CFQ: Cognitive functioning questionnaire
- LC: Low cognitive function

- NC: Normal cognitive function
- BMI: Body mass index
- PIR: Poverty income ratio
- OR: Odds ratio
- 95% CI: 95% confidence interval
- AI: Adequate intake.

Data Availability

The data utilized to support the findings are available from the corresponding authors upon request.

Conflicts of Interest

The authors declare that there is no conflict of interest.

Authors’ Contributions

Lu Liu and Song Qiao are co-first authors.

Acknowledgments

This work was supported by the Natural Science Foundation of Zhejiang Province under Grant (No. LQ19H090006).

References

[1] C. N. Harada, M. C. Natelson Love, and K. Triebel, “Normal cognitive aging,” *Clinics in Geriatric Medicine*, vol. 29, no. 4, pp. 737–752, 2013.

[2] Association AP, *Diagnostic and Statistical Manual of Mental Disorders*, American Psychiatric Publishing, Fifth edition, 2013.

- [3] World Health Organization, *Ageing and health*, 2020, <https://www.who.int/news-room/fact-sheets/detail/ageing-and-health>.
- [4] H. Bárrios, S. Narciso, M. Guerreiro, J. Maroco, R. Logsdon, and A. de Mendonça, "Quality of life in patients with mild cognitive impairment," *Aging & Mental Health*, vol. 17, no. 3, pp. 287–292, 2013.
- [5] R. A. Lawson, A. J. Yarnall, G. W. Duncan et al., "Cognitive decline and quality of life in incident Parkinson's disease: the role of attention," *Parkinsonism & Related Disorders*, vol. 27, pp. 47–53, 2016.
- [6] S. H. Zeisel, "Choline: an essential nutrient for humans," *Nutrition*, vol. 16, no. 7-8, pp. 669–671, 2000.
- [7] B. Vitamin, *National Institute of Diabetes and Digestive and Kidney Diseases*, 2016, <https://www.ncbi.nlm.nih.gov/books/NBK548710/>.
- [8] Institute of Medicine (US) Standing Committee on the Scientific Evaluation of Dietary Reference Intakes and its Panel on Folate, Other B Vitamins, and Choline. *Dietary Reference Intakes for Thiamin, Riboflavin, Niacin, Vitamin B6, Folate, Vitamin B12, Pantothenic Acid, Biotin, and Choline*, National Academies Press (US), 1998, <http://www.ncbi.nlm.nih.gov/books/NBK114310/>.
- [9] H. Hampel, M. M. Mesulam, A. C. Cuello et al., "The cholinergic system in the pathophysiology and treatment of Alzheimer's disease," *Brain*, vol. 141, no. 7, pp. 1917–1933, 2018.
- [10] W. M. McDonald and C. B. Nemeroff, "Neurotransmitters and neuropeptides in Alzheimer's disease," *Psychiatric Clinics of North America*, vol. 14, no. 2, pp. 421–442, 1991.
- [11] R. A. Bekdash, "Neuroprotective effects of choline and other methyl donors," *Nutrients*, vol. 11, no. 12, 2019.
- [12] J. K. Blusztajn, B. E. Slack, and T. J. Mellott, "Neuroprotective actions of dietary choline," *Nutrients*, vol. 9, no. 8, 2017.
- [13] R. Velazquez, E. Ferreira, S. Knowles et al., "Lifelong choline supplementation ameliorates Alzheimer's disease pathology and associated cognitive deficits by attenuating microglia activation," *Aging Cell*, vol. 18, no. 6, 2019.
- [14] R. Velazquez, J. A. Ash, B. E. Powers et al., "Maternal choline supplementation improves spatial learning and adult hippocampal neurogenesis in the Ts65Dn mouse model of Down syndrome," *Neurobiology of Disease*, vol. 58, pp. 92–101, 2013.
- [15] B. J. Strupp, B. E. Powers, R. Velazquez et al., "Maternal choline supplementation: a potential prenatal treatment for down syndrome and Alzheimer's disease," *Current Alzheimer Research*, vol. 13, no. 1, pp. 97–106, 2016.
- [16] C. Poly, J. M. Massaro, S. Seshadri et al., "The relation of dietary choline to cognitive performance and white-matter hyperintensity in the Framingham Offspring Cohort1234," *The American Journal of Clinical Nutrition*, vol. 94, no. 6, pp. 1584–1591, 2011.
- [17] National Center for Health Statistics, *NHANES - About the National Health and Nutrition Examination Survey*, 2020, https://www.cdc.gov/nchs/nhanes/about_nhanes.htm.
- [18] National Center for Health Statistics, *NHANES - NCHS Research Ethics Review Board Approval*, 2019, <https://www.cdc.gov/nchs/nhanes/irba98.htm>.
- [19] C. A. Blanton, A. J. Moshfegh, D. J. Baer, and M. J. Kretsch, *The USDA Automated Multiple-Pass Method accurately estimates group total energy and nutrient intake*, 2006, <https://pubag.nal.usda.gov/catalog/10039>.
- [20] J. C. Moms, A. Heyman, R. C. Mohs et al., "The Consortium to Establish a Registry for Alzheimer's Disease (CERAD). Part I. Clinical and neuropsychological assessment of Alzheimer's disease," *Neurology*, vol. 39, no. 9, pp. 1159–1165, 1989.
- [21] E. Strauss, E. M. S. Sherman, and O. Spreen, "A Compendium of Neuropsychological Tests: Administration," in *Norms, and Commentary*, Oxford University Press, 3rd edition, 2006.
- [22] J. J. Ryan and S. J. Lopez, "Wechsler Adult Intelligence Scale-III," in *Understanding Psychological Assessment*, W. I. Dorfman and M. Hersen, Eds., pp. 19–42, Perspectives on Individual Differences, Springer US, 2001.
- [23] D. J. Brody, E. A. Kramarow, C. A. Taylor, and L. C. McGuire, "Cognitive performance in adults aged 60 and over: National Health and Nutrition Examination Survey, 2011–2014," *National Health Statistics Reports*, vol. 126, pp. 1–23, 2019.
- [24] L. Arab and A. Ang, "A cross sectional study of the association between walnut consumption and cognitive function among adult us populations represented in NHANES," *The Journal of Nutrition, Health & Aging*, vol. 19, no. 3, pp. 284–290, 2015.
- [25] M. A. Beydoun, H. A. Beydoun, A. A. Gamaldo, A. Teel, A. B. Zonderman, and Y. Wang, "Epidemiologic studies of modifiable factors associated with cognition and dementia: systematic review and meta-analysis," *BMC Public Health*, vol. 14, p. 643, 2014.
- [26] K. M. Langa and D. A. Levine, "The diagnosis and management of mild cognitive impairment: a clinical review," *Journal of the American Medical Association*, vol. 312, no. 23, pp. 2551–2561, 2014.
- [27] World Health Organization, *Obesity and overweight* <https://www.who.int/news-room/fact-sheets/detail/obesity-and-overweight>.
- [28] National Institutes of Health Office of Dietary Supplements, *Choline-Fact Sheet for Health Professionals* <https://ods.od.nih.gov/factsheets/Choline-HealthProfessional/>.
- [29] E. P. Raven, P. H. Lu, T. A. Tishler, P. Heydari, and G. Bartzokis, "Increased iron levels and decreased tissue integrity in hippocampus of Alzheimer's disease detected in vivo with magnetic resonance imaging," *Journal of Alzheimer's Disease*, vol. 37, no. 1, pp. 127–136, 2013.
- [30] P. T. Francis, "The interplay of neurotransmitters in Alzheimer's disease," *CNS Spectrums*, vol. 10, 11 Suppl 18, pp. 6–9, 2005.
- [31] S. H. Zeisel, "Choline, other methyl-donors and epigenetics," *Nutrients*, vol. 9, no. 5, 2017.
- [32] C. Poly, J. M. Massaro, S. Seshadri et al., "The relation of dietary choline to cognitive performance and white-matter hyperintensity in the Framingham Offspring Cohort," *The American Journal of Clinical Nutrition*, vol. 94, no. 6, pp. 1584–1591, 2011.
- [33] E. Nurk, H. Refsum, I. Bjelland et al., "Plasma free choline, betaine and cognitive performance: the Hordaland Health Study," *The British Journal of Nutrition*, vol. 109, no. 3, pp. 511–519, 2013.
- [34] X. Jiang, A. A. West, and M. A. Caudill, "Maternal choline supplementation: a nutritional approach for improving offspring health?," *Trends in Endocrinology and Metabolism*, vol. 25, no. 5, pp. 263–273, 2014.
- [35] C. M. Kelley, J. A. Ash, B. E. Powers et al., "Effects of maternal choline supplementation on the septohippocampal cholinergic system in the Ts65Dn mouse model of Down syndrome," *Current Alzheimer Research*, vol. 13, no. 1, pp. 84–96, 2016.

- [36] R. Velazquez, E. Ferreira, W. Winslow et al., “Maternal choline supplementation ameliorates Alzheimer's disease pathology by reducing brain homocysteine levels across multiple generations,” *Molecular Psychiatry*, vol. 25, no. 10, pp. 2620–2629, 2020.
- [37] C. Zhong, Z. Lu, B. Che et al., “Choline pathway nutrients and metabolites and cognitive impairment after acute ischemic stroke,” *Stroke*, vol. 52, no. 3, pp. 887–895, 2021.
- [38] K. Zuniga and E. McAuley, “Considerations in selection of diet assessment methods for examining the effect of nutrition on cognition,” *The Journal of Nutrition, Health & Aging*, vol. 19, no. 3, pp. 333–340, 2015.

Research Article

Association between Serum 25-Hydroxyvitamin D Level and Stroke Risk: An Analysis Based on the National Health and Nutrition Examination Survey

Lan Wang,¹ Shu Li,² G. H. Anuja Sanika,³ Jinsheng Zhao,⁴ Hui Zhang,⁵ Lin Zhao^{ID},³ and Wenfeng Wang^{ID}⁶

¹School of Nursing, Tianjin Medical University, Tianjin 300070, China

²School of Public Health, Tianjin Medical University, Tianjin 300070, China

³International Medical School, Tianjin Medical University, Tianjin 300070, China

⁴Department of Acupuncture, Tianjin Nankai Hospital, Tianjin 300100, China

⁵Department of Nephrology, Tianjin Hospital, Tianjin 300210, China

⁶School of Science, Shanghai Institute of Technology, Shanghai 201418, China

Correspondence should be addressed to Lin Zhao; linzhaodc@outlook.com

Received 5 August 2021; Accepted 8 October 2021; Published 29 October 2021

Academic Editor: Hua Lin

Copyright © 2021 Lan Wang et al. This is an open access article distributed under the Creative Commons Attribution License, which permits unrestricted use, distribution, and reproduction in any medium, provided the original work is properly cited.

Background. To analyze the association between serum 25-hydroxyvitamin D level (25(OH)D) and stroke risk based on the National Health and Nutrition Examination Survey (NHANES). **Methods.** Between 2007 and 2018, the baseline information of participants from NHANES was collected. Univariate analysis was used to identify the covariates. Multivariate logistic regression model was used to analyze the association between serum 25(OH)D level and the stroke risk. **Results.** Of the 8,523 participants, there were 310 participants with stroke and 8,213 participants without stroke. The multivariate logistic analysis showed that serum 25(OH)D deficiency (odds ratio (OR): 1.993, 95% confidence intervals (CI): 1.141-3.481, and $P=0.012$) was the significant risk factors for stroke. Subgroup analysis showed that non-Hispanic whites with serum 25(OH)D deficiency (OR: 2.501, 95% CI: 1.094-5.720, and $P=0.001$) and insufficiency (OR: 1.853, 95% CI: 1.170-2.934, and $P=0.006$) were associated with a higher risk of stroke than those with normal 25(OH)D levels. **Conclusions.** Serum 25(OH)D deficiency may be associated with an increased risk of stroke.

1. Introduction

Stroke remains the third most common cause of disability and the second most common cause of death worldwide [1]. In the United States, there were an estimated 795,000 new or recurrent stroke with approximately 130,000 deaths due to stroke each year [2]. The prevalence increases with age in both females and males. By 2030, an additional 3,400,000 adults are estimated to have a stroke in the United States, which increased by 20.5% with 2012 [3]. Stroke is associated with modifiable risk factors (hypertension, hyper-

glycemia, obesity, hyperlipidemia, and renal dysfunction) and behavioral risk factors (sedentary lifestyle, cigarette smoking, and unhealthy diet) [2, 4]. Interestingly, vitamin D (25-hydroxyvitamin D, 25(OH)D), a hormone mainly regulating calcium homeostasis, is found to be associated with the development of various nonskeletal chronic diseases, including stroke [5], cardiovascular disease [6], cancer [7], metabolic disorder [8], autoimmune disease [9], and infectious diseases [10].

In recent years, several studies have been conducted on the association between 25(OH)D level and stroke risk, but

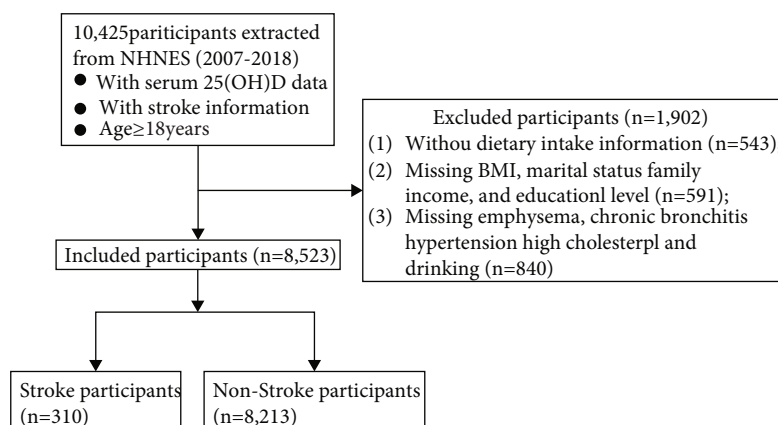


FIGURE 1: Flow chart of study population inclusion.

the results are inconsistent. Zhou et al. reported that 25(OH)D levels were associated with ischemic stroke (relative risk: 2.45) [11]. Berghout et al. also found a correlation between 25(OH)D level and prevalent stroke (adjusted odds ratio (OR): 1.31), but only extremely low 25(OH)D level was related to incident stroke (hazard ratio (HR): 1.25), showing that low 25(OH)D level may not increase the risk of stroke [12]. There is another evidence suggesting no association between 25(OH)D levels and incidence of stroke (HR: 1.00) [13]. In view of the inconsistent results, in this study, we used a pooled cross-sectional data from the National Health and Nutrition Examination Survey (NHANES) (2007-2018) to further analyze the association of serum 25(OH)D level with stroke risk.

2. Methods

2.1. Data Sources. NHANES, a nationally representative survey for noninstitutionalized civilians in the United States, is conducted in two-year cycles, with approximately 10,000 persons in each cycle [14]. Participants aged over 18 years who had serum 25(OH)D level measured during the survey were enrolled in this study. Pregnant women and participants who did not respond to the question on stroke history and had missing information (e.g., age, sex, marital status, family income, educational level, and condition of complications) were excluded from the study.

The data used in this study were accessed from NHANES, a continuous program performed by the National Center for Health Statistics. The approval from the Institutional Review Board of Tianjin Medical University was not required because the data from NHANES were freely available.

The baseline characteristics of participants were collected, including age, gender, body mass index (BMI), race (Mexican Americans, non-Hispanic whites, non-Hispanic blacks, other races), marital status (married, widowed/divorced, unmarried, and living with partner), family income (<20,000\$ and ≥20,000\$), educational level (<high school, high school, and >high school), dietary intake (dietary fiber, total fat, fruits, vegetables, and vitamins A, B, C, and E), total cholesterol (TC), glycated hemoglobin (GHb), high-density

lipoprotein (HDL), C-reactive protein (CRP), and 25(OH)D levels (deficiency: <30 nmol/L, insufficiency: 30-50 nmol/L, normal: 50-125 nmol/L, and adequacy: >125 nmol/L), as well as presence or absence of drinking, emphysema, chronic bronchitis, hypertension, high cholesterol, and diabetes mellitus.

The stroke was determined based on the Medical Condition Questionnaire (MCQ). Question MCQ160f “Has a doctor or other health professional ever told you that you had a stroke?” was asked by interviews. The participants answered “yes” were deemed to have stroke.

Diabetes mellitus was identified through the Diabetes Questionnaire (DIQ). Question DIQ010 is “Other than during pregnancy, have you ever been told by a doctor or health professional that you have diabetes or sugar diabetes?” Participants who answered “yes” were considered as diabetic.

The Blood Pressure & Cholesterol Questionnaire (BPQ) question BPQ080 is “Have you ever been told by a doctor or other health professional that your blood cholesterol level was high?” Participants who answered “yes” were considered as with high cholesterol level.

Hypertension was determined according to the question BPQ020, “Have you ever been told by a doctor or other health professional that you had hypertension, also called high blood pressure?” Participants who answered “yes” were considered with hypertension.

Dietary intake was estimated by two 24-hour dietary recall, a validated Automated Multiple-Pass Method jointly completed by the United States Department of Agriculture (USDA) and the United States Department of Health and Human Services (DHHS) [15]. The specific intake of each nutrient was available in the Dietary Interview-Total Nutrients Intakes. Consumptions of dietary fiber, total fat, fruits, vegetables, vitamin A, vitamin B, vitamin C, and vitamin E were retrieved from the dietary data.

2.2. Measurement of Serum 25(OH)D Level. Serum 25(OH)D level (ng/mL) was thought to be the optimal indicator to assess vitamin D status [16]. In the NHANES (2001-2006), the serum 25(OH)D level in approximately 88% of the adult participants was measured using radioimmunoassay kits (DiaSorin Inc., Stillwater, MN). An independent calibration

TABLE 1: Baseline characteristics of participants after multiple imputation.

Variables	Description (<i>n</i> = 8,523)
Age, years, mean \pm SE	46.96 \pm 0.35
Gender, <i>n</i> (%)	
Male	4,201 (48.60)
Female	4,322 (51.40)
BMI, kg/m ² , mean \pm SE	28.79 \pm 0.10
Race, <i>n</i> (%)	
Mexican Americans	1,519 (8.31)
Other races	1,199 (9.87)
Non-Hispanic whites	4,294 (71.57)
Non-Hispanic blacks	1,511 (10.25)
Marital status, <i>n</i> (%)	
Married	4562 (57.47)
Widowed/divorced	1913 (17.89)
Unmarried	1377 (16.93)
Living with partner	671 (7.71)
Educational level, <i>n</i> (%)	
<high school	2408 (18.46)
High school	2010 (23.56)
>high school	4105 (57.98)
Family income, <i>n</i> (%)	
<20,000\$	2100 (16.96)
\geq 20,000\$	6423 (83.04)
Drinking, <i>n</i> (%)	2337 (23.04)
Emphysema, <i>n</i> (%)	203 (1.91)
Chronic bronchitis, <i>n</i> (%)	474 (5.15)
Hypertension, <i>n</i> (%)	3022 (30.53)
High cholesterol, <i>n</i> (%)	3547 (39.33)
Diabetes mellitus, <i>n</i> (%)	1045 (8.63)
Dietary intake, mean \pm SE	
Dietary fiber	16.68 \pm 0.28
Total fat	82.96 \pm 0.81
Fruits	1.00 \pm 0.02
Vegetables	1.58 \pm 0.03
Vitamin A	632.18 \pm 10.22
Vitamin B	2.23 \pm 0.02
Vitamin C	84.52 \pm 1.96
Vitamin E	7.90 \pm 0.12
TC, nmol/L, mean \pm SE	196.89 \pm 0.71
GHb, nmol/L, mean \pm SE	5.60 \pm 0.02
HDL, nmol/L, mean \pm SE	52.72 \pm 0.37
CRP, nmol/L, mean \pm SE	0.38 \pm 0.01
25(OH)D, nmol/L, <i>n</i> (%)	
Deficiency (<30)	749 (6.24)
Insufficiency (30-50)	2,026 (18.71)
Normal (50-125)	5,585 (72.40)
Adequacy (\geq 125)	163 (2.65)

TABLE 1: Continued.

Variables	Description (<i>n</i> = 8,523)
Stroke, <i>n</i> (%)	
Yes	8,213 (97.20)
No	310 (2.80)

Notes: BMI: body mass index; TC: total cholesterol; GHb: glycated hemoglobin; HDL: high-density lipoprotein; CRP: C-reactive protein; 25(OH)D: 25-hydroxyvitamin D. Values were presented as mean \pm standard error (SE) or median and quartile (M (Q1 and Q3)) for continuous variables and *n* (%) for categorical variables. In the NHANES 2007–2018 study, exam weight was taken into account.

was conducted for radioimmunoassay kits against high-performance liquid chromatography-purified 25(OH)D. Since 2007, the serum 25(OH)D level was measured using ultrahigh performance liquid chromatography-tandem mass spectrometry. Due to the differences in the results of these two measurement methods, this study only analyzed data from 2007 to 2018. The detailed measurement methods and quality assurance for serum 25(OH)D level could be found in the survey laboratory data [17]. The Institute of Medicine (IOM) and United State Preventive Services Task Force define vitamin D sufficiency as a total 25(OH)D level greater than 50 nmol/L [18, 19]. In this study, serum 25(OH)D level < 30 nmol/L is thought as deficiency, 30–50 nmol/L as insufficiency, 50–125 nmol/L as the normal value, and >125 nmol/L as adequacy.

2.3. Statistical Analysis. The SAS software (version 9.4, SAS Institute Inc., NC, USA) was employed to analyze the data. Normally, distributed data were represented as mean \pm standard error (SE) and compared using *t* test, while non-normal data was presented as median and quartile (M (Q1 and Q3)) and compared using Mann-Whitney *U* rank-sum test. χ^2 test or Fisher's exact test was used to compare the enumeration data which were described as *n* (%). In the NHANES 2007–2018 study, exam weight was taken into account.

All included data from 2007 to 2018 were not missing. The covariates with significant difference in the univariate analysis were enrolled into the multivariate logistic regression model to analyze the association between serum 25(OH)D levels and the stroke risk. The difference was significant at *P* < 0.05.

3. Results

3.1. Basic Characteristics of Participants. A total of 10,425 participants with serum 25(OH)D data, stroke information, and age \geq 18 years were retrieved from the NHANES between 2007 and 2018. After excluding 543 participants without dietary intake data and 1,359 participants with other missing information (BMI, marital status, drinking, emphysema, chronic bronchitis, etc.), 8,523 participants were finally eligible for the study. The process of inclusion and exclusion of participants is shown in Figure 1. Of these 8,523 participants, the mean age was 46.96 \pm 0.35 years, 4,201 (48.60%) were males, and 4,322 (51.40%) were

TABLE 2: Comparison of the baseline characteristics between stroke and nonstroke groups.

Variables	Nonstroke group ($n = 8,213$)	Stroke group ($n = 310$)	Statistic	P
Age, years, mean \pm SE	46.47 \pm 0.35	63.93 \pm 1.28	$t = -13.62$	<0.001
Gender, n (%)			$\chi^2 = 1.246$	0.264
Male	4045 (48.74)	156 (44.01)		
Female	4168 (51.26)	154 (55.99)		
BMI, kg/m ² , mean \pm SE	28.75 \pm 0.10	30.16 \pm 0.36	$t = -3.60$	0.001
Race, n (%)			$\chi^2 = 12.177$	0.007
Mexican Americans	1492 (8.44)	27 (3.78)		
Other races	1172 (9.96)	27 (6.68)		
Non-Hispanic whites	4108 (71.44)	186 (76.23)		
Non-Hispanic blacks	1441 (10.16)	70 (13.31)		
Marital status, n (%)			$\chi^2 = 25.660$	<0.001
Married	4396 (57.59)	166 (53.30)		
Widowed/divorced	1804 (17.48)	109 (32.20)		
Unmarried	1353 (17.20)	24 (7.71)		
Living with partner	660 (7.74)	11 (6.80)		
Educational level, n (%)			$\chi^2 = 37.712$	<0.001
<high school	2291 (18.13)	117 (29.97)		
High school	1931 (23.40)	79 (29.04)		
>high school	3991 (58.47)	114 (40.99)		
Family income, n (%)			$\chi^2 = 14.866$	<0.001
<20,000\$	1989 (16.68)	111 (26.77)		
$\geq 20,000$ \$	6224 (83.32)	199 (73.23)		
Drinking, n (%)	2228 (22.66)	109 (36.32)	$\chi^2 = 25.510$	<0.001
Emphysema, n (%)	179 (1.75)	24 (7.22)	$\chi^2 = 42.304$	<0.001
Chronic bronchitis, n (%)	431 (4.79)	43 (17.71)	$\chi^2 = 61.132$	<0.001
Hypertension, n (%)	2773 (29.23)	249 (75.83)	$\chi^2 = 194.882$	<0.001
High cholesterol, n (%)	3364 (38.86)	183 (55.70)	$\chi^2 = 28.263$	<0.001
Diabetes mellitus, n (%)	939 (8.00)	106 (30.64)	$\chi^2 = 168.476$	<0.001
Dietary intake, mean \pm SE				
Dietary fiber	16.74 \pm 0.28	14.48 \pm 0.71	$t = 3.36$	0.002
Total fat	83.32 \pm 0.76	70.44 \pm 4.55	$t = 3.04$	0.005
Fruits	1.00 \pm 0.03	0.93 \pm 0.08	$t = 0.92$	0.366
Vegetables	1.59 \pm 0.03	1.38 \pm 0.07	$t = 3.14$	0.004
Vitamin A	633.17 \pm 10.04	597.84 \pm 41.66	$t = 0.89$	0.381
Vitamin B	2.24 \pm 0.02	1.89 \pm 0.09	$t = 4.06$	<0.001
Vitamin C	84.80 \pm 1.97	74.84 \pm 5.03	$t = 2.00$	0.054
Vitamin E	7.93 \pm 0.11	6.71 \pm 0.41	$t = 3.28$	0.003
TC, nmol/L, mean \pm SE	197.05 \pm 0.72	191.52 \pm 3.95	$t = 1.37$	0.179
GHb, nmol/L, mean \pm SE	5.58 \pm 0.01	6.09 \pm 0.08	$t = -6.67$	<0.001
HDL, nmol/L, mean \pm SE	52.81 \pm 0.37	49.53 \pm 1.05	$t = 2.97$	0.006
CRP, nmol/L, mean \pm SE	0.37 \pm 0.01	0.67 \pm 0.09	$t = -3.55$	0.001

TABLE 2: Continued.

Variables	Nonstroke group (n = 8,213)	Stroke group (n = 310)	Statistic	P
25(OH)D, nmol/L, n (%)			$\chi^2 = 9.357$	0.025
Deficiency (<30)	715 (6.11)	34 (11.01)		
Insufficiency (30-50)	1957 (18.64)	69 (21.00)		
Normal (50-125)	5385 (72.59)	200 (65.66)		
Adequacy (≥ 125)	156 (2.66)	7 (2.34)		

Notes: BMI: body mass index; TC: total cholesterol; GHb: glycated hemoglobin; HDL: high-density lipoprotein; CRP: C-reactive protein; 25(OH)D: 25-hydroxyvitamin D. Values were presented as mean \pm standard error (SE) or median and quartile (M (Q1 and Q3)) for continuous variables and n (%) for categorical variables. In the NHANES 2007–2018 study, exam weight was taken into account.

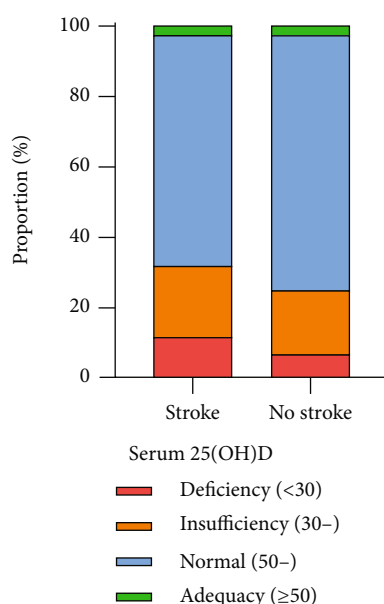


FIGURE 2: The serum 25(OH)D level distribution of stroke and no stroke groups.

females. Among included participants, 1,519 (8.31%) were Mexican Americans, 4,294 (71.57%) were non-Hispanic whites, 1,511 (10.25%) were non-Hispanic blacks, and 1,199 (9.87%) were other races. In addition, there were 749 (6.24%) participants of serum 25(OH)D deficiency, 2,026 (18.71%) participants of serum 25(OH)D insufficiency, 5,585 (72.40%) participants of serum 25(OH)D normal, and 163 (2.65%) participants of serum 25(OH)D adequacy. There were 310 participants of stroke and 8,213 participants of no stroke. More detailed characteristics of participants are shown in Table 1.

3.2. Comparison of the Baseline Characteristics between the Stroke and No Stroke Groups. Univariable analyses are shown in Table 2. The results indicated that age ($t = -13.62$, $P < 0.001$), BMI ($t = -3.60$, $P < 0.001$), GHb ($t = -6.67$, $P < 0.001$), CRP ($t = -3.55$, $P < 0.001$), and the proportion of drinking ($\chi^2 = 25.510$, $P < 0.001$), emphysema ($\chi^2 = 42.304$, $P < 0.001$), chronic bronchitis ($\chi^2 = 61.132$, $P < 0.001$), hypertension ($\chi^2 = 194.882$, $P < 0.001$), high cholesterol ($\chi^2 = 28.263$, $P < 0.001$), and diabetes mellitus

($\chi^2 = 168.476$, $P < 0.001$) of participants in the stroke group were higher than those in the no stroke group. However, participant's education level ($\chi^2 = 37.712$, $P < 0.001$), HDL ($t = 2.97$, $P = 0.006$), serum 25(OH)D ($\chi^2 = 9.357$, $P = 0.025$), the proportion of family income ($\chi^2 = 14.866$, $P < 0.001$), intake of dietary fiber ($t = 3.36$, $P = 0.002$), total fat ($t = 3.04$, $P = 0.005$), vegetables ($t = 3.14$, $P = 0.004$), vitamin B ($t = 4.06$, $P < 0.004$), and vitamin E ($t = 3.28$, $P = 0.003$) were lower in the stroke group compared with the no stroke group. In addition, there were statistical differences in the race ($\chi^2 = 12.177$, $P = 0.007$) and marital status ($\chi^2 = 25.660$, $P < 0.001$) between the two groups. The serum 25(OH)D level distribution of stroke and no stroke groups is shown in Figure 2, and the results indicated that the proportion of patients with serum 25(OH)D deficiency and insufficiency in the stroke group was higher in the stroke group than that in the no stroke group.

3.3. Relationship between Serum 25(OH)D Level and Stroke Risk. Multivariate logistic regression analysis results of the association between serum 25(OH)D levels and the stroke risk are summarized in Figure 3. As is shown, in the univariate serum 25(OH)D logistic regression analysis (model 1), the patients with serum 25(OH)D deficiency (OR: 1.993, 95% confidence interval (95% CI): 1.141-3.481, and $P = 0.012$) had an increased risk of stroke in contrast to those with normal 25(OH)D levels. After adjustment for covariates of age and gender (model 2), the risk of stroke was increased by 1.369- and 0.523-fold, respectively, in patients with serum 25(OH)D deficiency (OR: 2.369, 95% CI: 1.404-3.995, and $P < 0.023$) and insufficiency (OR: 1.523, 95% CI: 1.044-2.222, and $P = 0.023$) when compared with those with normal serum 25(OH)D levels. After the adjustment of all the covariates (model 3), such as age, gender, BMI, educational level, hypertension, vitamin E, and CRP levels, serum 25(OH)D deficiency (OR: 1.770, 95% CI: 1.023-3.065, and $P = 0.034$) was still the independent risk factors for stroke.

3.4. Further Analysis of the Relationship between Serum 25(OH)D Level and Stroke Risk Based on Race. Further analysis results of the relationship between serum 25(OH)D levels and stroke risk based on race are shown in Table 3. Except for non-Hispanic whites, the association between serum 25(OH)D level and stroke risk was not statistically significant among Mexican Americans, non-Hispanic

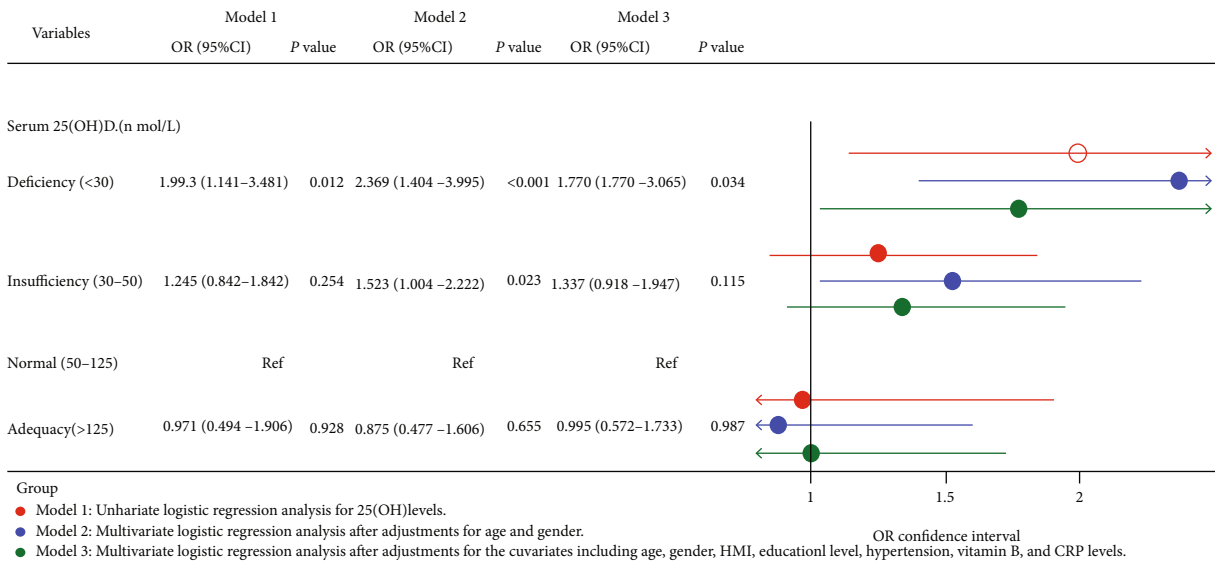


FIGURE 3: Multivariate logistic regression forest plot of the association between serum 25(OH)D levels and the stroke risk.

blacks, and other races (all $P > 0.05$). In the univariate serum 25(OH)D logistic regression analysis, the non-Hispanic whites with serum 25(OH)D deficiency (OR: 4.651, 95% CI: 1.908–11.338, and $P < 0.001$) and insufficiency (OR: 1.957, 95% CI: 1.257–3.047, and $P = 0.002$) had a higher risk of stroke than those with normal 25(OH)D levels. After adjustment for part covariates, the risk of stroke was increased by 2.087- and 0.982-fold, respectively, in patients with serum 25(OH)D deficiency (OR: 3.087, 95% CI: 1.390–6.856, and $P = 0.004$) and insufficiency (OR: 1.982, 95% CI: 1.246–3.153, and $P = 0.003$) as compared with participants with normal serum 25(OH)D levels. After adjustment for all the covariates, the risk of stroke in patients with serum 25(OH)D deficiency (OR: 2.501, 95% CI: 1.094–5.720, and $P = 0.001$) and insufficiency (OR: 1.853, 95% CI: 1.170–2.934, and $P = 0.006$) was 2.501 times and 1.853 times that of patients with normal serum 25(OH)D levels, respectively.

4. Discussion

A total of 8,523 eligible participants were involved into the present study, among whom 310 participants were subjected to stroke, while 8,213 participants were not. The multivariate logistic analysis showed that serum 25(OH)D deficiency was the significant risk factor for stroke. All these findings suggested that the patients with serum 25(OH)D deficiency (<30 nmol/L) might have an increased risk of stroke. Sub-group analysis showed that non-Hispanic whites with serum 25(OH)D deficiency and insufficiency were associated with a high risk of stroke.

As a fat-soluble vitamin, vitamin D, can affect cardiomyocytes, endothelial cells, vascular smooth muscle cells, and inflammatory cells by binding vitamin D receptors (VDR) and exert the effects of inhibiting myocardial hypertrophy, protecting vascular endothelium, and regulating inflammatory responses, consequently decreasing the onset risk of cardiovascular and cerebrovascular diseases and

improving patients' prognosis [20–22]. 25(OH)D, a major circulation form of vitamin D in the body, can better reflect vitamin D status. Several studies reported vitamin D deficiency, whether in serum or in intake, may be associated with an increased risk of ischemic stroke [11, 23]. In the present study, a pooled cross-sectional data from NHANES were used to identify the association of serum 25(OH)D level with the stroke risk. The risk of stroke was found to significantly increase in patients with serum 25(OH)D deficiency and insufficiency. However, vitamin D status is under the influence of various factors including age, living areas, exposure to sunlight, and vitamin D daily dietary intake [24, 25]. After adjustment for multiple covariates, our results still showed that serum 25(OH)D deficiency is related to an increased risk of stroke.

The impact of serum 25(OH)D level-related stroke risk between different races is controversial. The study of Judd et al. indicated that lower 25(OH)D level is a significant risk factor for incident stroke, and no statistically significant difference was observed between blacks and whites [26]. However, Michos et al. found that serum 25(OH)D deficiency was associated with a higher risk of stroke in whites but not in blacks (hazard ratios 2.13 vs. 0.93) [27]. Our results showed that a lower serum 25(OH)D level was related to an increased risk of stroke in non-Hispanic whites. Robinson-Cohen et al. also demonstrated that lower serum 25(OH)D level was related to an increased risk of incident coronary heart disease among participants who were Hispanic [28]. In addition, several studies indicated that both low and high serum 25(OH)D levels have increased the risk of stroke [29, 30]. However, the relationship between high 25(OH)D levels and stroke risk was not observed in this study. The possible explanation was that the sample size of participants with higher high 25(OH)D levels is not large, and no statistically significant results can be obtained.

At present, the effect of 25(OH)D level on the stroke risk can be explained by several mechanisms below. Inappropriate activation of the renin-angiotensin system (RAS) may be

TABLE 3: Subgroup analysis of the association between serum 25(OH)D levels and the stroke risk based on race.

Race	N (%)	Model 1 OR (95% CI)	P	Model 2 OR (95% CI)	P	Model 3 OR (95% CI)	P
Mexican Americans							
25(OH)D, nmol/L							
Deficiency (<30)	115 (7.75)	0.762 (0.230-2.524)	0.643	1.015 (0.310-3.320)	0.979	0.868 (0.282-2.671)	0.798
Insufficiency (30-50)	524 (34.98)	0.676 (0.308-1.484)	0.309	0.786 (0.364-1.697)	0.522	0.778 (0.351-1.727)	0.520
Normal (50-125)	878 (57.17)	Ref		Ref		Ref	
Adequacy (≥125)	2 (0.10)	-		-		-	
Non-Hispanic whites							
25(OH)D, nmol/L							
Deficiency (<30)	108 (10.62)	4.651 (1.908-11.338)	<0.001	3.087 (1.390-6.856)	0.004	2.501 (1.094-5.720)	0.024
Insufficiency (30-50)	353 (29.13)	1.957 (1.257-3.047)	0.002	1.982 (1.246-3.153)	0.003	1.853 (1.170-2.934)	0.006
Normal (50-125)	731 (59.69)	Ref		Ref		Ref	
Adequacy (≥125)	7 (0.56)	0.954 (0.456-1.995)	0.897	0.922 (0.481-1.767)	0.800	1.011 (0.574-1.781)	0.969
Non-Hispanic blacks							
25(OH)D, nmol/L							
Deficiency (<30)	123 (2.40)	0.746 (0.437-1.273)	0.262	1.009 (0.550-1.851)	0.976	0.837 (0.470-1.492)	0.528
Insufficiency (30-50)	567 (12.43)	0.555 (0.209-1.473)	0.218	0.739 (0.276-1.977)	0.529	0.702 (0.264-1.864)	0.459
Normal (50-125)	3461 (81.65)	Ref		Ref		Ref	
Adequacy (≥125)	143 (3.53)	1.739 (0.185-16.329)	0.613	0.819 (0.097-6.899)	0.848	1.298 (0.145-11.605)	0.808
Other races							
25(OH)D, nmol/L							
Deficiency (<30)	403 (27.69)	0.615 (0.135-2.798)	0.513	1.050 (0.298-3.695)	0.937	0.828 (0.267-2.571)	0.734
Insufficiency (30-50)	582 (39.36)	0.334 (0.089-1.261)	0.092	0.408 (0.107-1.555)	0.172	0.379 (0.095-1.502)	0.151
Normal (50-125)	515 (32.36)	Ref		Ref		Ref	
Adequacy (≥125)	11 (0.60)	-		-		-	

Notes: model 1 is the univariate logistic regression analysis for 25(OH)D levels; model 2 is the multivariate logistic regression analysis after adjustments for age and gender; model 3 is the multivariate logistic regression analysis after adjustment for the covariates including age, gender, BMI, educational level, hypertension, vitamin B, and CRP levels.

a major risk factor for stroke [31]. 25(OH)D, a negative endocrine regulator of the renin-angiotensin system (RAS), may influence the stroke risk through RAS regulation [31, 32]. A previous experiment showed that by regulating cholesterol efflux and macrophage polarization through elevated CYP27A1 activation, vitamin D played a protective role against atherosclerosis in hypercholesterolemic swine [33]. Activated vitamin D may defer atherosclerosis by inhibiting the formation of foam cells and the process of macrophage cholesterol absorption, consequently reducing the risk of developing stroke [34]. There is another study showing that vitamin D deficiency contributes to facilitating secondary hyperparathyroidism, while the increased levels of parathyroid hormone may accelerate the inflammatory response in atherosclerosis [35, 36]. In addition, activated vitamin D plays a crucial role in preventing thrombosis, which may explain why the low vitamin D level is associated with an increased risk of ischemic stroke [37, 38].

The strength of the present study was that it was a large-scale, population-based study, providing strong evidence for assessing the relationship between vitamin D status and stroke risk. Compared with the single-center studies, our

research results may be more generalizable. Furthermore, we conducted a further analysis of the relationship between serum 25(OH)D level and stroke risk based on race. However, there existed some limitations. First, the data in our study were accessed from the NHNES database, which may be lack of some important variables, such as vitamin D supplementation, exposure to sunlight, living areas, and seasons of vitamin D measurement. Second, the stroke history was confirmed through self-reported data. Despite lack of verification for self-reporting stroke in NHANES, the stroke history from questionnaire was checked. In several studies, the self-reported data from NHANES were used to identify the risk factors for cardiovascular diseases [39–41].

5. Conclusions

The results suggested that serum 25(OH)D deficiency (<30 nmol/L) might be related to an increased risk of stroke. In addition, non-Hispanic whites with serum 25(OH)D deficiency (<30 nmol/L) and insufficiency (30-50 nmol/L) were associated with a high risk of stroke than those with normal 25(OH)D levels.

Data Availability

The data utilized to support the findings are available from the corresponding authors upon request.

Conflicts of Interest

The authors declare that they have no competing interests in this study.

Authors' Contributions

Lan Wang and Shu Li contributed equally to this work.

Acknowledgments

This study was funded by the Natural Science Foundation of Tianjin (Project number: 18JCQNJC11500).

References

- [1] V. L. Feigin, M. H. Forouzanfar, R. Krishnamurthi et al., "Global and regional burden of stroke during 1990-2010: findings from the Global Burden of Disease Study," *Lancet*, vol. 383, no. 9913, pp. 245–255, 2014.
- [2] E. J. Benjamin, P. Muntner, A. Alonso et al., "Heart disease and stroke statistics-2019 update: a report from the American Heart Association," *Circulation*, vol. 139, no. 10, pp. e56–e528, 2019.
- [3] P. A. Heidenreich, N. M. Albert, L. A. Allen et al., "Forecasting the impact of heart failure in the United States," *Circulation Heart Failure*, vol. 6, no. 3, pp. 606–619, 2013.
- [4] V. L. Feigin, G. A. Roth, M. Naghavi et al., "Global burden of stroke and risk factors in 188 countries, during 1990-2013: a systematic analysis for the Global Burden of Disease Study 2013," *The Lancet Neurology*, vol. 15, no. 9, pp. 913–924, 2016.
- [5] S. Pilz, H. Dobnig, J. E. Fischer et al., "Low vitamin d levels predict stroke in patients referred to coronary angiography," *Stroke*, vol. 39, no. 9, pp. 2611–2613, 2008.
- [6] A. Zittermann and S. Pilz, "Vitamin D and cardiovascular disease: an update," *Anticancer Research*, vol. 39, no. 9, pp. 4627–4635, 2019.
- [7] S. M. Jeon and E. A. Shin, "Exploring vitamin D metabolism and function in cancer," *Experimental & Molecular Medicine*, vol. 50, no. 4, pp. 1–14, 2018.
- [8] M. Grammatiki, E. Rapti, S. Karras, R. A. Ajjan, and K. Kotsa, "Vitamin D and diabetes mellitus: causal or casual association?," *Reviews in Endocrine & Metabolic Disorders*, vol. 18, no. 2, pp. 227–241, 2017.
- [9] J. Wang, S. Lv, G. Chen et al., "Meta-analysis of the association between vitamin D and autoimmune thyroid disease," *Nutrients*, vol. 7, no. 4, pp. 2485–2498, 2015.
- [10] R. R. Watkins, T. L. Lemonovich, and R. A. Salata, "An update on the association of vitamin D deficiency with common infectious diseases," *Canadian Journal of Physiology and Pharmacology*, vol. 93, no. 5, pp. 363–368, 2015.
- [11] R. Zhou, M. Wang, H. Huang, W. Li, Y. Hu, and T. Wu, "Lower vitamin D status is associated with an increased risk of ischemic stroke: a systematic review and meta-analysis," *Nutrients*, vol. 10, no. 3, p. 277, 2018.
- [12] B. P. Berghout, L. Fani, A. Heshmatollah et al., "Vitamin D status and risk of Stroke," *Stroke*, vol. 50, no. 9, pp. 2293–2298, 2019.
- [13] T. Skaaby, L. L. Husemoen, C. Pisinger et al., "Vitamin D status and incident cardiovascular disease and all-cause mortality: a general population study," *Endocrine*, vol. 43, no. 3, pp. 618–625, 2013.
- [14] J. A. Fain, "Nhanes," *Diabetes Educ*, vol. 43, no. 2, p. 151, 2017.
- [15] C. A. Blanton, A. J. Moshfegh, D. J. Baer, and M. J. Kretsch, "The USDA Automated Multiple-Pass Method accurately estimates group total energy and nutrient intake," 2006, June 2021, <https://pubag.nal.usda.gov/catalog/10039>.
- [16] X. Deng, Y. Song, J. E. Manson et al., "Magnesium, vitamin D status and mortality: results from US National Health and Nutrition Examination Survey (NHANES) 2001 to 2006 and NHANES III," *BMC Medicine*, vol. 11, p. 187, 2013.
- [17] "National Center for Health Statistics: Analytical note for 25-hydroxyvitamin D data analysis using NHANES III (1988-1994), NHANES 2001-2006, and NHANES 2007-2010," June 2021, https://wwwn.cdc.gov/nchs/nhanes/nhanes/vitaminD/analyticalnote.aspx?h=/nchs/data/nhanes/2007-2008/labmethods/VID_E_met_Vitamin_D.pdf&t=2007-2008%20Vitamin%20D%20Lab%20Method.
- [18] A. C. Ross, J. E. Manson, S. A. Abrams et al., "The 2011 report on dietary reference intakes for calcium and vitamin D from the Institute of Medicine: what clinicians need to know," *Journal of Clinical Endocrinology and Metabolism*, vol. 96, no. 1, pp. 53–58, 2011.
- [19] M. L. LeFevre and on behalf of the US Preventive Services Task Force, "Screening for vitamin D deficiency in adults: U.S. Preventive Services Task Force recommendation statement," *Annals of Internal Medicine*, vol. 162, no. 2, pp. 133–140, 2015.
- [20] S. S. Schleithoff, A. Zittermann, G. Tenderich, H. K. Berthold, P. Stehle, and R. Koerfer, "Vitamin D supplementation improves cytokine profiles in patients with congestive heart failure: a double-blind, randomized, placebo-controlled trial," *The American Journal of Clinical Nutrition*, vol. 83, no. 4, pp. 754–759, 2006.
- [21] F. Saponaro, C. Marcocci, and R. Zucchi, "Vitamin D status and cardiovascular outcome," *Journal of Endocrinological Investigation*, vol. 42, no. 11, pp. 1285–1290, 2019.
- [22] S. J. Wimalawansa, "Vitamin D and cardiovascular diseases: causality," *The Journal of Steroid Biochemistry and Molecular Biology*, vol. 175, pp. 29–43, 2018.
- [23] P. Brøndum-Jacobsen, B. G. Nordestgaard, P. Schnohr, and M. Benn, "25-hydroxyvitamin D and symptomatic ischemic stroke: an original study and meta-analysis," *Annals of Neurology*, vol. 73, no. 1, pp. 38–47, 2013.
- [24] S. Pilz, A. Tomaschitz, C. Drechsler, A. Zittermann, J. M. Dekker, and W. Marz, "Vitamin D supplementation: a promising approach for the prevention and treatment of strokes," *Current Drug Targets*, vol. 12, no. 1, pp. 88–96, 2011.
- [25] H. A. Sheerah, E. S. Eshak, R. Cui, H. Imano, H. Iso, and A. Tamakoshi, "Relationship between dietary vitamin D and deaths from stroke and coronary heart Disease," *Stroke*, vol. 49, no. 2, pp. 454–457, 2018.
- [26] S. E. Judd, C. J. Morgan, B. Panwar et al., "Vitamin D deficiency and incident stroke risk in community-living black and white adults," *International Journal of Stroke: official journal of the International Stroke Society*, vol. 11, no. 1, pp. 93–102, 2016.

- [27] E. D. Michos, J. P. Reis, W. S. Post et al., "25-Hydroxyvitamin D deficiency is associated with fatal stroke among whites but not blacks: the NHANES-III linked mortality files," *Nutrition*, vol. 28, no. 4, pp. 367–371, 2012.
- [28] C. Robinson-Cohen, A. N. Hoofnagle, J. H. Ix et al., "Racial differences in the association of serum 25-hydroxyvitamin D concentration with coronary heart disease events," *JAMA*, vol. 310, no. 2, pp. 179–188, 2013.
- [29] R. Y. Leung, Y. Han, C. W. Sing et al., "Serum 25-hydroxyvitamin D and the risk of stroke in Hong Kong Chinese," *Thrombosis and Haemostasis*, vol. 117, no. 1, pp. 158–163, 2017.
- [30] D. Durup, H. L. Jørgensen, J. Christensen et al., "A reverse J-shaped association between serum 25-hydroxyvitamin D and cardiovascular disease mortality: the CopD study," *The Journal of Clinical Endocrinology and Metabolism*, vol. 100, no. 6, pp. 2339–2346, 2015.
- [31] C. J. McMullan, L. Borgi, G. C. Curhan, N. Fisher, and J. P. Forman, "The effect of vitamin D on renin-angiotensin system activation and blood pressure," *Journal of Hypertension*, vol. 35, no. 4, pp. 822–829, 2017.
- [32] J. P. Forman, J. S. Williams, and N. D. Fisher, "Plasma 25-hydroxyvitamin D and regulation of the renin-angiotensin system in humans," *Hypertension*, vol. 55, no. 5, pp. 1283–1288, 2010.
- [33] K. Yin, Y. You, V. Swier et al., "Vitamin D protects against atherosclerosis via regulation of cholesterol efflux and macrophage polarization in hypercholesterolemic swine," *Arteriosclerosis, Thrombosis, and Vascular Biology*, vol. 35, no. 11, pp. 2432–2442, 2015.
- [34] P. Knekt, M. Laaksonen, C. Mattila et al., "Serum vitamin D and subsequent occurrence of type 2 diabetes," *Epidemiology*, vol. 19, no. 5, pp. 666–671, 2008.
- [35] A. Tomaschitz, E. Ritz, B. Pieske et al., "Aldosterone and parathyroid hormone interactions as mediators of metabolic and cardiovascular disease," *Metabolism: clinical and experimental*, vol. 63, no. 1, pp. 20–31, 2014.
- [36] J. L. Martín-Ventura, M. Ortego, P. Esbrit, M. A. Hernández-Presa, L. Ortega, and J. Egido, "Possible role of parathyroid hormone-related protein as a proinflammatory cytokine in atherosclerosis," *Stroke*, vol. 34, no. 7, pp. 1783–1789, 2003.
- [37] L. Moscarelli, M. Zanazzi, E. Bertoni et al., "Renin angiotensin system blockade and activated vitamin D as a means of preventing deep vein thrombosis in renal transplant recipients," *Clinical Nephrology*, vol. 75, no. 5, pp. 440–450, 2011.
- [38] W. X. Wu and D. R. He, "Low vitamin D levels are associated with the development of deep venous thromboembolic events in patients with ischemic stroke," *Clinical and Applied Thrombosis/Hemostasis: official journal of the International Academy of Clinical and Applied Thrombosis/Hemostasis*, vol. 24, 9^{suppl}, pp. 69s–75s, 2018.
- [39] D. H. Kim, S. Sabour, U. N. Sagar, S. Adams, and D. J. Whellan, "Prevalence of hypovitaminosis D in cardiovascular diseases (from the National Health and Nutrition Examination Survey 2001 to 2004)," *The American Journal of Cardiology*, vol. 102, no. 11, pp. 1540–1544, 2008.
- [40] J. Kendrick, G. Targher, G. Smits, and M. Chonchol, "25-Hydroxyvitamin D deficiency is independently associated with cardiovascular disease in the Third National Health and Nutrition Examination Survey," *Atherosclerosis*, vol. 205, no. 1, pp. 255–260, 2009.
- [41] S. S. Yoon, C. F. Dillon, K. Illoh, and M. Carroll, "Trends in the prevalence of coronary heart disease in the U.S.: National Health and Nutrition Examination Survey, 2001–2012," *American Journal of Preventive Medicine*, vol. 51, no. 4, pp. 437–445, 2016.

Research Article

Effect of the Interaction between Depression and Sleep Disorders on the Stroke Occurrence: An Analysis Based on National Health and Nutritional Examination Survey

Jia Li,¹ Leijun Li,² Yan Lv,³ Yanhai Kang,¹ Mingjin Zhu^{ID},⁴ and Wenfeng Wang^{ID}⁵

¹Department of Psychiatry and Psychology, Hainan General Hospital, Haikou, 570311 Hainan, China

²Department of Psychiatry, The Third Affiliated Hospital of Sun Yat-sen University, Guangzhou 510630, China

³Department of Neuorology, Hainan General Hospital, Haikou, 570311 Hainan, China

⁴Rehabilitation Department, Tongde Hospital of Zhejiang Province, Hangzhou, 310012 Zhejiang, China

⁵School of Science, Shanghai Institute of Technology, Shanghai 201418, China

Correspondence should be addressed to Mingjin Zhu; zhumingjindct@outlook.com
and Wenfeng Wang; wangwenfeng@nimte.ac.cn

Received 5 August 2021; Accepted 24 September 2021; Published 19 October 2021

Academic Editor: Muh-Shi Lin

Copyright © 2021 Jia Li et al. This is an open access article distributed under the Creative Commons Attribution License, which permits unrestricted use, distribution, and reproduction in any medium, provided the original work is properly cited.

Objective. To investigate the effect of the interaction between depression and sleep disorders on the stroke occurrence based on the data from the National Health and Nutritional Examination Survey (NHANES). **Methods.** Seven cycles of 2-year NHANES data (2005-2018) were analyzed in this study. Univariate analysis was first performed between the stroke and nonstroke patients, and then, multivariate logistic regression models were conducted to analyze the association of depression, sleep disorders, and their interactions with stroke occurrence. **Results.** A total of 30473 eligible participants were included in this study, including 1138 (3.73%) with stroke and 29335 (96.27%) with nonstroke. Except sex, the differences were all significant between the stroke and nonstroke patients in baseline information (all $P < 0.001$). Depression (odds ratio (OR): 2.494, 95% confidence interval (CI): 2.098-2.964), depression severity (moderate, OR: 2.013, 95% CI: 1.612-2.514; moderately severe, OR: 2.598, 95% CI: 1.930-3.496; severe, OR: 5.588, 95% CI: 3.883-8.043), and sleep disorders (OR: 1.677, 95% CI: 1.472-1.910) were presented to be associated with an increased risk of stroke after correcting all the confounders. The logistic regression analysis showed that there was a synergic, additive interaction between depression and sleep disorders on the stroke occurrence, and the proportion of stroke patients caused by this interaction accounted for 27.1% of all the stroke patients. **Conclusion.** Depression, depression severity, and sleep disorders are all independently associated with a high risk of stroke. The interaction between depression and sleep disorders can synergistically increase the stroke occurrence.

1. Introduction

Stroke is the second most common cause of deaths secondary to ischemic heart disease and a leading cause of disability worldwide [1]. As the population ages, its incidence increases significantly, especially in low- and middle-income countries. According to statistics, there were almost 6.5 million deaths from stroke and 25.7 million stroke survivors in 2013, while 12 million deaths and 70 million survivors would be estimated

by 2030 [2, 3]. Despite advances in prevention and treatment in recent years, stroke remains to be the important cause of long-term disability [4]. Stroke survivors are reported to be associated with a high risk of stroke recurrence and adverse events; they were not only at high risk of dementia, but also at high risk of depression, with the prevalence of 29%, which maintained stability up to 10 years following stroke [5-7]. In addition, the prevalence of sleep disorders after stroke was also estimated to be greater than 50% [8].

As a frequent complication of stroke, depression can worsen the course of poststroke neurological disorders, accelerate the patients' physical helplessness, decrease the quality of life, and affect the ability of patients to engage in rehabilitation therapies, consequently leading to an increased risk of death [3]. There is considerable evidence showing that stroke has a complicated bidirectional relationship with depression: stroke can increase the risk of depression occurrence, while depression is confirmed to be a significant risk factor for stroke and stroke mortality [9–12]. Moreover, sleep-disordered breathing and sleep-wake disturbances are also very common in stroke patients [13]. Previous studies indicated that preexisting sleep disorders were associated with an increased risk of stroke and depression and might aggravate after stroke onset, which exerted adverse effects on the outcomes of stroke patients [14–16]. Notably, hypersomnia or insomnia has been a key diagnostic criterion of depression [17]. However, relatively little is known about whether there exists a synergistic effect between sleep disorders and depression and how they interact on the stroke occurrence.

In this study, we attempted to assess the effect of the interaction between depression and sleep disorders on the stroke occurrence based on the data from the National Health and Nutritional Examination Survey (NHANES).

2. Materials and Methods

2.1. Data Source. The data used in this study were extracted from the NHANES, an ongoing cross-sectional survey representing a noninstitutionalized civilian United States (US) population. NHANES was conducted by the National Center for Health Statistics and Centers for Disease Control and Prevention, aiming at assessing the health status of the US population [18]. The interviews were performed by the study teams which were composed of medical and health technicians, multilingual physicians, and dietary health interviewers, and the information collected was designed to evaluate the incidence of major diseases and risk factors for diseases to promote health and prevent diseases [19].

In this study, seven cycles of 2-year NHANES data (2005–2018) including baseline demographic data and drug use questionnaire information were retrospectively analyzed. Both home interviews and comprehensive physical examinations in a mobile examination center were conducted for all the participants signing the informed consent forms. The participants without depression questionnaire data or sleep disorder data or those lacking other information were excluded. This study did not need to be approved by the Institutional Review Board of Hainan General Hospital because the data used were accessed from the NHANES, a publicly available database.

During the home interview, the demographic data were collected, including age, gender, body mass index (BMI), ethnicity, marital status, educational level, family income, and history of alcohol consumption and smoking. In addition, the presence or absence of sleep disorders, depression, diabetes mellitus, and stroke were also recorded. Sleep disorders were defined according to the item “have you ever told sleep disorders by doctors or professional health workers” from the NHANES. As a short, self-administered

questionnaire, the Patient Health Questionnaire 9 (PHQ-9) is widely employed to screen depression in primary care settings [20]. Regarding the severity, depression was classified into five categories based on total PHQ-9 scores, including no depressive symptoms (0–4), mild depressive symptoms (5–9), moderate depressive symptoms (10–14), moderately severe depressive symptoms (15–19), and severe depressive symptoms (20–27) [21]. In this study, depression was defined when the total PHQ-9 scores were equal to or greater than 10 [22].

2.2. Statistical Analysis. For the measurement data, a normality test was performed using the Shapiro-Wilk test. The normally distributed data were presented as the mean \pm standard deviation ($\bar{x} \pm s$), while abnormally distributed data were as the median and quartile ($M (Q_1, Q_3)$), and t -test and Mann-Whitney U rank-sum test were conducted, respectively. The enumeration data were compared using the χ^2 or Fisher's exact test, manifesting as cases and the constituent ratio (n (%)). The variables with statistical significance in the univariate analysis were enrolled into the multivariate logistic regression model for analyzing the association of depression, sleep disorders, and their interactions with stroke occurrence.

Three indexes including relative excess risk of interaction (RERI), attributable proportion of interaction (API), and synergy index (SI) were used to assess the interaction based on the additive model. No interactions were shown when 0 was comprised in the confidence interval (CI) of RERI and AP and 1 was involved in the CI of SI.

SAS software (SAS Institute Inc., Cary, NC, USA; version 9.4) was used to manage the data in both univariate and multivariate analyses. The forest plots and interaction schematic diagrams were drawn using R software (R Foundation for Statistical Computing, Vienna, Austria; version 4.2), and pictures of interactive odds ratio (OR) values were drawn using GraphPad Prism 8 software. All the statistical tests were two-sided, and the value of P less than 0.05 was statistically significant.

3. Results

3.1. Baseline Information of Participants. Between 2005 and 2018, there were 44,635 participants in the NHANES database. After excluding 8,411 participants with missing depression questionnaire data, 29 with missing sleep disorder data, and 5,722 with incomplete information, 30,473 participants including 15,043 males and 15,430 females were enrolled into the study, with the median age of 49 years.

Among the included 30,473 participants, 1,138 (3.73%) had stroke and 29,335 (96.27%) did not. The baseline information of the stroke and nonstroke patients was compared in Table 1. It could be observed that the patients with stroke had older age ($P < 0.001$) and higher BMI ($P < 0.001$), as well as higher proportions of smoking ($P < 0.001$), diabetes mellitus ($P < 0.001$), sleep disorders ($P < 0.001$), depression ($P < 0.001$), and depression severity ($P < 0.001$) than those without. Compared with nonstroke patients, stroke patients had lower proportions of alcohol consumption ($P < 0.001$),

TABLE 1: Comparison on the baseline information of the stroke and nonstroke patients.

Variables	Total (<i>n</i> = 30,473)	Grouping		<i>Z</i> / χ^2 / <i>t</i>	<i>P</i>
		Nonstroke (<i>n</i> = 29,335)	Stroke (<i>n</i> = 1,138)		
Age (years, <i>M</i> (<i>Q</i> ₁ , <i>Q</i> ₃))	49 (34, 64)	48 (34, 63)	68 (58, 77)	31.017	<0.001
Sex, <i>n</i> (%)				0.028	0.867
Male	15,043 (49.37)	14,484 (49.37)	559 (49.12)		
Female	15,430 (50.63)	14,851 (50.63)	579 (50.88)		
Body mass index (kg/m ² , $\bar{x} \pm s$)	29.25 \pm 7.00	29.23 \pm 7.01	29.97 \pm 6.77	-3.460	<0.001
Ethnicity, <i>n</i> (%)				97.628	<0.001
Chicanos	4,698 (15.42)	4,599 (15.68)	99 (8.70)		
Hispanics	2,753 (9.03)	2,691 (9.17)	62 (5.45)		
Non-Hispanic whites	13,533 (44.41)	12,950 (44.15)	583 (51.23)		
Non-Hispanic blacks	6,493 (21.31)	6,177 (21.06)	316 (27.77)		
Others	2,996 (9.83)	2,918 (9.95)	78 (6.85)		
Marital status, <i>n</i> (%)				382.769	<0.001
Married	15,834 (51.96)	15,289 (52.12)	545 (47.89)		
Widowed	2,368 (7.77)	2,130 (7.26)	238 (20.91)		
Divorced/separated	4,402 (14.45)	4,178 (14.24)	224 (19.68)		
Unmarried	7,869 (25.82)	7,738 (26.38)	131 (11.51)		
Education, <i>n</i> (%)				-7.480	<0.001
<High school	7,121 (23.37)	6,791 (23.15)	330 (29.00)		
High school	7,093 (23.28)	6,762 (23.05)	331 (29.09)		
> high school	16,259 (53.36)	15,782 (53.80)	477 (41.92)		
Family income, <i>n</i> (%)				164.030	<0.001
<20000\$	6,513 (21.37)	6,096 (20.78)	417 (36.64)		
\geq 20000\$	23,960 (78.63)	23,239 (79.22)	721 (63.36)		
History of alcohol consumption, <i>n</i> (%)	20,989 (68.88)	20,314 (69.25)	675 (59.31)	50.430	<0.001
History of smoking, <i>n</i> (%)	13,922 (45.69)	13,218 (45.06)	704 (61.86)	124.666	<0.001
Diabetes mellitus, <i>n</i> (%)	4,042 (13.26)	3,629 (12.37)	413 (36.29)	544.863	<0.001
Sleep disorders, <i>n</i> (%)	7,853 (25.77)	7,375 (25.14)	478 (42.00)	162.847	<0.001
Depression, <i>n</i> (%)	2,647 (8.69)	2,434 (8.30)	213 (18.72)	149.954	<0.001
Depression severity, <i>n</i> (%)				12.497	<0.001
No	27,826 (91.31)	26,901 (91.70)	925 (81.28)		
Moderate	1,649 (5.41)	1,540 (5.25)	109 (9.58)		
Moderately severe	713 (2.34)	651 (2.22)	62 (5.45)		
Severe	285 (0.94)	243 (0.83)	42 (3.69)		

educational levels ($P < 0.001$), and family income ($P < 0.001$). In addition, significant differences were also shown between the stroke and nonstroke patients in ethnicity ($P < 0.001$) and marital status ($P < 0.001$; Table 1).

3.2. Association of Depression and Its Severity with Stroke.

The association of depression and its severity with stroke was depicted in Figure 1. As shown, the risk of stroke in patients with depression was 2.545-fold than those without (OR: 2.545, 95% CI: 2.180-2.971, $P < 0.001$). The patients with depression had 3.077-fold of stroke risk than those without (OR: 3.077, 95% CI: 2.617-3.619, $P < 0.001$) after correction of age and sex, and this risk (OR: 2.494, 95% CI: 2.098-2.964, $P < 0.001$) was still present when all the confounders, such as age, sex, BMI, ethnicity, marital status,

educational levels, family income, diabetes mellitus, and history of alcohol consumption and smoking, were adjusted.

In terms of depression severity, the patients with moderate (OR: 2.058, 95% CI: 1.677-2.527, $P < 0.001$), moderately severe (OR: 2.770, 95% CI: 2.117-3.623, $P < 0.001$), and severe depressive symptoms (OR: 5.028, 95% CI: 3.601-7.022, $P < 0.001$) all had a markedly increased risk of stroke than those without. When the age and sex were adjusted, the risk of stroke was, respectively, increased by 1.438-fold in patients with moderate depressive symptoms (OR: 2.438, 95% CI: 1.970-3.017, $P < 0.001$), 2.314-fold in patients with moderately severe depressive symptoms (OR: 3.314, 95% CI: 2.504-4.387, $P < 0.001$), and 6.027-fold in patients with severe depressive symptoms (OR: 7.027, 95% CI: 4.938-9.999, $P < 0.001$) compared with those without. After adjusting all the

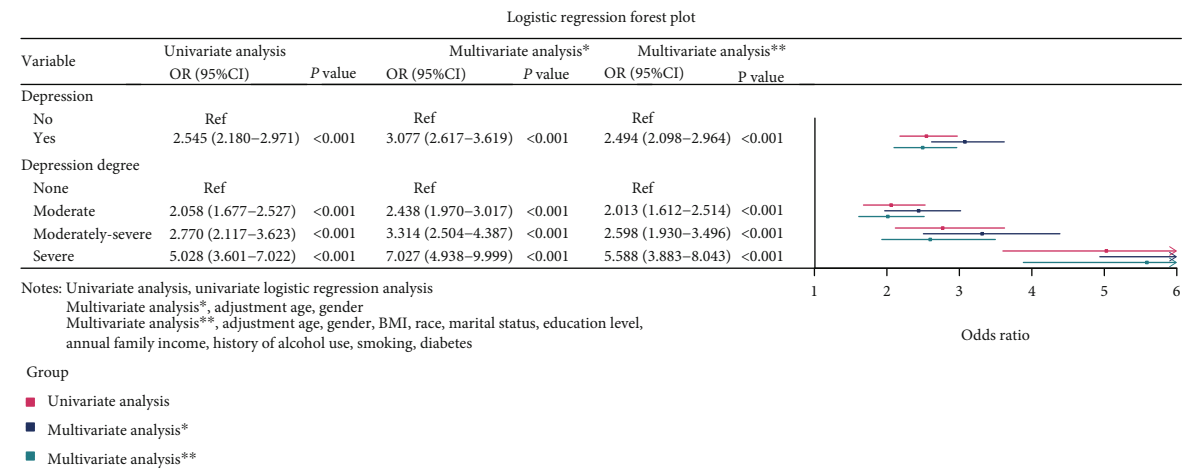


FIGURE 1: Logistic regression forest plot of the association of depression and its severity with stroke.

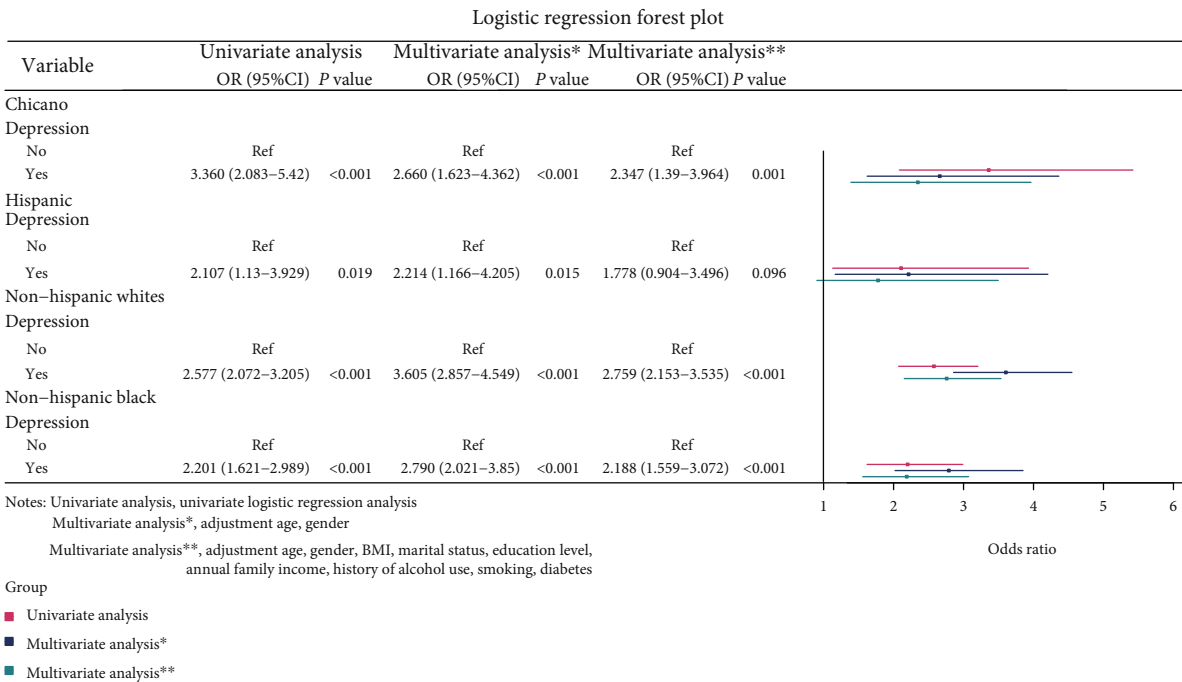


FIGURE 2: Logistic regression forest plot of the association between depression and stroke according to ethnicities.

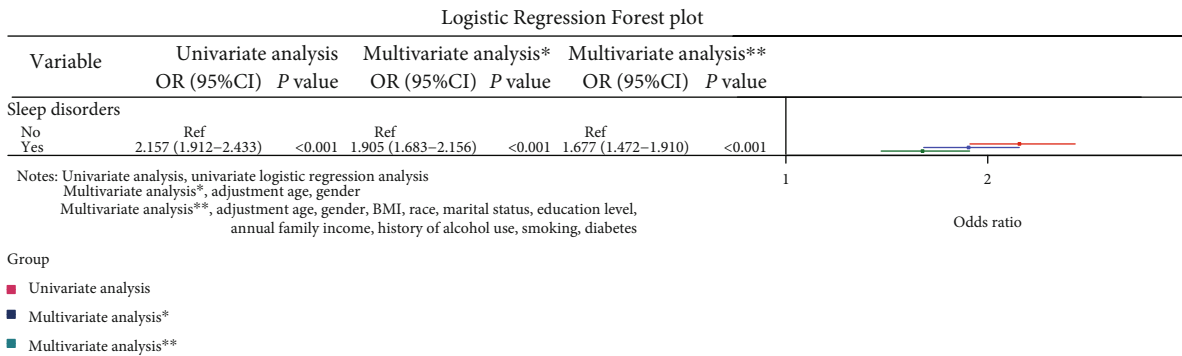


FIGURE 3: Logistic regression forest plot of the association between sleep disorders and stroke.

TABLE 2: The baseline information of participants according to interactive items between depression and sleep disorders.

Stroke	Depression		Sleep disorders	OR	
	Yes	No		Depression (yes)	Depression (no)
Yes	150	328	Yes	R11	R10
No	1,392	5,983			
Yes	63	597	No	R01	R00
No	1,042	20,918			

TABLE 3: Logistic regression analysis of the interactive items between depression and sleep disorders.

Sleep disorders	Depression	OR	Model 1		OR	Model 2		OR	Model 3	
			95% CI	P		95% CI	P		95% CI	P
0	0	Ref.			Ref.			Ref.		
0	1	2.118	1.622-2.767	<0.001	2.543	1.928-3.353	<0.001	2.020	1.512-2.699	<0.001
1	0	1.921	1.674-2.205	<0.001	1.628	1.414-1.875	<0.001	1.461	1.260-1.693	<0.001
1	1	3.776	3.132-4.552	<0.001	4.302	3.536-5.235	<0.001	3.405	2.766-4.190	<0.001
RERI (95% CI)			0.736 (-0.124-1.597)			1.131 (0.104-2.158)			0.924 (0.078-1.769)	
API (95% CI)			0.195 (-0.011-0.401)			0.263 (0.055-0.471)			0.271 (0.055-0.487)	
SI (95% CI)			1.361 (0.932-1.989)			1.521 (1.019-2.269)			1.624 (1.008-2.614)	

Notes: Model 1: univariate logistic regression analysis; Model 2: multivariate logistic regression analysis after correcting the age and sex; Model 3: multivariate logistic regression analysis after correcting the age, sex, body mass index, ethnicity, marital status, educational levels, family income, diabetes mellitus, and history of drinking alcohol and smoking.

confounders like age, sex, BMI, ethnicity, marital status, educational levels, family income, diabetes mellitus, and history of alcohol consumption and smoking, the risk of stroke was still higher in patients with moderate (OR: 2.013, 95% CI: 1.612-2.514, $P < 0.001$), moderately severe (OR: 2.598, 95% CI: 1.930-3.496, $P < 0.001$), and severe depressive symptoms (OR: 5.588, 95% CI: 3.883-8.043, $P < 0.001$) than those without.

Ethnicity-based subgroup analysis of the association between depression and stroke was presented in Figure 2. It could be found that after all the confounders, such as age, sex, BMI, ethnicity, marital status, educational levels, family income, diabetes mellitus, and history of alcohol consumption and smoking, were corrected, the risk of stroke was significantly higher in patients with depression in Chicano (OR: 2.347, 95% CI: 1.390-3.964, $P = 0.001$), non-Hispanic white (OR: 2.759, 95% CI: 2.153-3.535, $P < 0.001$), and non-Hispanic black populations (OR: 2.188, 95% CI: 1.559-3.072, $P < 0.001$) than those without, but not in Hispanic population (OR: 1.778, 95% CI: 0.904-3.496, $P = 0.096$).

3.3. Association between Sleep Disorders and Stroke. Univariate analysis indicated that the risk of stroke in patients with sleep disorders was 2.157-fold higher than those without (OR: 2.157, 95% CI: 1.912-2.433, $P < 0.001$; Figure 3). In multivariate analysis, the patients with sleep disorders were found to have a significantly elevated risk of stroke than those without after adjusting the age and sex (OR: 1.905, 95% CI: 1.683-2.156, $P < 0.001$), and this association still existed even though all the confounders were adjusted (OR: 1.677, 95% CI: 1.472-1.910, $P < 0.001$; Figure 3).

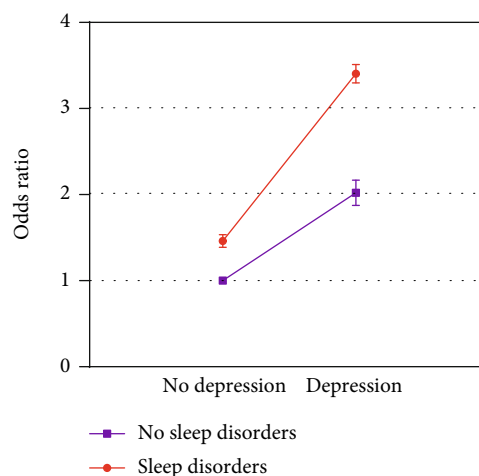


FIGURE 4: Visualization of odds ratio values and standard deviations in model 3.

3.4. Effect of the Interaction between Depression and Sleep Disorders on Stroke. The interactive items between depression and sleep disorders were established, including no sleep disorders and no depression, no sleep disorders and depression, sleep disorders and no depression, and no sleep disorders and no depression. According to these interactive items, the baseline information of participants was summarized in Table 2.

The logistic regression analysis revealed that after correcting all the confounders like age, sex, BMI, ethnicity, marital status, educational levels, family income, diabetes mellitus, and history of alcohol consumption and smoking, the CIs of interactive indexes $RERI_{model2}$ (1.131; 95% CI:

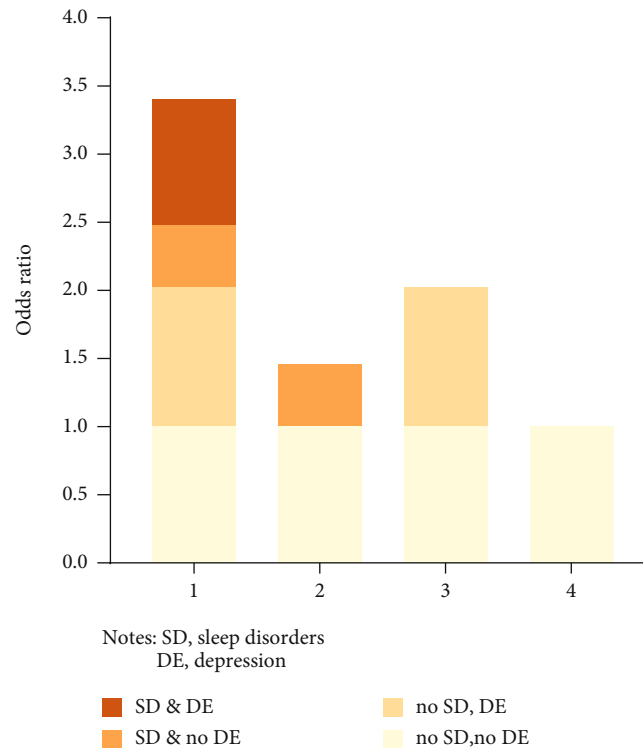


FIGURE 5: An interaction schematic diagram between depression and sleep disorders after correction of multiple confounders.

0.104-2.158), $RERI_{model3}$ (0.924; 95% CI: 0.078-1.769), API_{model2} (0.263; 95% CI: 0.055-0.471), and API_{model3} (0.271; 95% CI: 0.055-0.487) did not comprise 0, and 1 was not involved in the CIs of SI_{model2} (1.521; 95% CI: 1.019-2.269) and SI_{model3} (1.624; 95% CI: 1.008-2.614), suggesting that there was a synergic, additive interaction between depression and sleep disorders on the stroke occurrence. The API was equal to 0.271 after the variables with significant differences in the univariate analysis were adjusted, which indicated that the proportion of stroke patients caused by the interaction between depression and sleep disorders accounted for 27.1% of all the stroke patients included in this study (Table 3). The OR values and standard deviations in model 3 were visualized in Figure 4, and the interaction schematic diagram between depression and sleep disorders was shown in Figure 5.

4. Discussion

In the current study, 30,473 eligible participants were enrolled, containing 1,138 with stroke and 29,335 with non-stroke. We found that depression, depression severity, and sleep disorders were independently correlated with an elevated risk of stroke, and there was a synergic, additive interaction between depression and sleep disorders on the stroke occurrence. The proportion of patients with stroke caused by the interaction between depression and sleep disorders accounted for 27.1% of all the stroke patients.

As a frequent mental disorder, depression can occur repeatedly or for a long time, considerably affecting the capability of individuals to function in their daily life [23].

Amount of evidence has confirmed that depression is closely correlated with stroke occurrence [24–26]. In a meta-analysis, depression was identified to be associated with high risk of ischemic, fatal, and total stroke [27]. Our results showed that patients with depression had 3.077-fold of stroke risk than those without. Mai and Liang also supported that the risk of stroke was higher in patients with moderate, moderately severe, and severe depressive symptoms [28].

Depression may result in stroke through multiple mechanisms. First, depression may affect the risk of stroke through neuroendocrine and inflammation/immunological effects. There is a study showing that depression is positively correlated with interleukin- (IL-) 1, C-reactive protein (CRP), and IL-6 in community and clinical samples [29]. These inflammatory markers have been demonstrated to connect with the occurrence and prognosis of stroke [30]. Second, depression relates to obesity and poor health behaviors, such as smoking, physical inactivity, poor diet, and medication compliance [31, 32], which may raise the risk of stroke. Third, depression is associated with a variety of major comorbidities, including hypertension and diabetes mellitus which are considered to be significant risk factors for stroke [33, 34].

Sleep exerts a significant effect on the human life. Appropriate sleep duration (6-8 h) showed a protective effect on the stroke occurrence, while short or long sleep durations might significantly raise the risk of stroke [28, 35, 36]. Enormous studies have confirmed that sleep disorders are modifiable risk factors for stroke and have an impact on stroke outcome [37–39]. Our results revealed that patients with sleep disorders had 1.677-fold of stroke risk than those without, similar to 1.622 times reported by Mai and Liang [28].

It is well known that sleep disorders are the most dominant symptom in patients with depression and also generally considered the major secondary manifestations of depression. Nevertheless, there is evidence that insomnia is not only a prodromal manifestation of depression but also an independent risk factor for the development and recurrence of depression [15, 40]. There may be a complex bidirectional relationship between sleep disorders and depression, but not a cause-effect relationship [41]. In this study, we analyzed the effect of the interaction between sleep disorders and depression on the stroke occurrence and found that the interaction between sleep disorders and depression could increase the risk of stroke synergistically.

Although amount of evidence has shown that depression and sleep disorders are independent risk factors for stroke, few studies still report the association between their interactions and the risk of stroke. Our study first exhibited a synergic, additive interaction between depression and sleep disorders on the stroke occurrence. Moreover, our results might be more convincing due to the nationally representative nature of NHANES and a large sample size. However, the following limitations should be taken into consideration. First, the participants included in our study might have less severe stroke because noninstitutionalized participants were only involved in the NHANES. Second, some important factors like the stroke severity and stroke types were missing in the NHANES; thus, the stroke severity, a consistent predictor of poststroke depression, was not adjusted in the multivariate analysis. Third, the history of stroke in the NHANES was confirmed through self-reported data. Despite no validation for the self-reporting stroke in the NHANES, the history of stroke from questionnaires had been checked. In several studies, the risk factors for cardiovascular diseases had been identified through the self-reported data from NHANES [42–44].

5. Conclusions

Depression, depression severity, and sleep disorders were all independently related to an increased risk of stroke. The combination of depression and sleep disorders might play a synergistic role to increase the occurrence of stroke. In addition, evidence suggested that depression and sleep disorders may affect cardiovascular disease through multiple common pathways [45, 46]. Therefore, depression and sleep disorders may also have common pathways for the impact of stroke. In the future, more prospective studies should be conducted to further verify our results.

Data Availability

The data utilized to support the findings are available from the corresponding authors upon request.

Conflicts of Interest

The authors declare that they have no conflict of interests.

References

- [1] M. Katan and A. Luft, "Global burden of stroke," *Seminars in Neurology*, vol. 38, no. 2, pp. 208–211, 2018.
- [2] V. L. Feigin, B. Norrving, and G. A. Mensah, "Global burden of stroke," *Circulation Research*, vol. 120, no. 3, pp. 439–448, 2017.
- [3] R. F. Villa, F. Ferrari, and A. Moretti, "Post-stroke depression: mechanisms and pharmacological treatment," *Pharmacology & Therapeutics*, vol. 184, pp. 131–144, 2018.
- [4] L. B. Goldstein, C. D. Bushnell, R. J. Adams et al., "Guidelines for the primary prevention of stroke: a guideline for healthcare professionals from the American Heart Association/American Stroke Association," *Stroke*, vol. 42, no. 2, pp. 517–584, 2011.
- [5] M. L. Portegies, P. J. Koudstaal, and M. A. Ikram, "Cerebrovascular disease," *Handbook of Clinical Neurology*, vol. 138, pp. 239–261, 2016.
- [6] L. M. Allan, E. N. Rowan, M. J. Firbank et al., "Long term incidence of dementia, predictors of mortality and pathological diagnosis in older stroke survivors," *Brain*, vol. 134, no. 12, pp. 3716–3727, 2011.
- [7] L. Ayerbe, S. Ayis, C. D. Wolfe, and A. G. Rudd, "Natural history, predictors and outcomes of depression after stroke: systematic review and meta-analysis," *The British Journal of Psychiatry*, vol. 202, no. 1, pp. 14–21, 2013.
- [8] D. L. Brown, X. Jiang, C. Li et al., "Sleep apnea screening is uncommon after stroke," *Sleep Medicine*, vol. 59, pp. 90–93, 2019.
- [9] S. Kumar, M. H. Selim, and L. R. Caplan, "Medical complications after stroke," *Lancet Neurology*, vol. 9, no. 1, pp. 105–118, 2010.
- [10] A. J. Mitchell, B. Sheth, J. Gill et al., "Prevalence and predictors of post-stroke mood disorders: a meta-analysis and meta-regression of depression, anxiety and adjustment disorder," *General Hospital Psychiatry*, vol. 47, pp. 48–60, 2017.
- [11] A. Razmara, N. Valle, D. Markovic et al., "Depression is associated with a higher risk of death among stroke survivors," *Journal of Stroke and Cerebrovascular Diseases*, vol. 26, no. 12, pp. 2870–2879, 2017.
- [12] W. Cai, C. Mueller, Y. J. Li, W. D. Shen, and R. Stewart, "Post stroke depression and risk of stroke recurrence and mortality: a systematic review and meta-analysis," *Ageing Research Reviews*, vol. 50, pp. 102–109, 2019.
- [13] D. M. Hermann and C. L. Bassetti, "Role of sleep-disordered breathing and sleep-wake disturbances for stroke and stroke recovery," *Neurology*, vol. 87, no. 13, pp. 1407–1416, 2016.
- [14] D. M. Wallace, A. R. Ramos, and T. Rundek, "Sleep disorders and stroke," *International Journal of Stroke*, vol. 7, no. 3, pp. 231–242, 2012.
- [15] L. Zhai, H. Zhang, and D. Zhang, "Sleep duration and depression among adults: a meta-analysis of prospective studies," *Depression and Anxiety*, vol. 32, no. 9, pp. 664–670, 2015.
- [16] L. Dong, D. L. Brown, R. D. Chervin, E. Case, L. B. Morgenstern, and L. D. Lisabeth, "Pre-stroke sleep duration and post-stroke depression," *Sleep Medicine*, vol. 77, pp. 325–329, 2021.
- [17] R. G. Robinson and R. E. Jorge, "Post-stroke depression: a review," *The American Journal of Psychiatry*, vol. 173, no. 3, pp. 221–231, 2016.
- [18] J. A. Fain, "NHANES," *The Diabetes Educator*, vol. 43, no. 2, p. 151, 2017.

- [19] W. Mitchell, R. Bhatia, and N. Zebardast, "Retrospective cross-sectional analysis of the changes in marijuana use in the USA, 2005-2018," *BMJ Open*, vol. 10, no. 7, article e037905, 2020.
- [20] S. Kung, R. D. Alarcon, M. D. Williams, K. A. Poppe, M. Jo Moore, and M. A. Frye, "Comparing the Beck Depression Inventory-II (BDI-II) and Patient Health Questionnaire (PHQ-9) depression measures in an integrated mood disorders practice," *Journal of Affective Disorders*, vol. 145, no. 3, pp. 341-343, 2013.
- [21] K. Kroenke and R. L. Spitzer, "The PHQ-9: a new depression diagnostic and severity measure," *Psychiatric Annals*, vol. 32, no. 9, pp. 509-515, 2002.
- [22] D. Jorgensen, G. E. White, A. Sekikawa, and P. Gianaros, "Higher dietary inflammation is associated with increased odds of depression independent of Framingham Risk Score in the National Health and Nutrition Examination Survey," *Nutrition Research*, vol. 54, pp. 23-32, 2018.
- [23] G. Vilagut, C. G. Forero, G. Barbaglia, and J. Alonso, "Screening for depression in the general population with the Center for Epidemiologic Studies Depression (CES-D): a systematic review with meta-analysis," *PLoS One*, vol. 11, no. 5, article e0155431, 2016.
- [24] R. Ramasubbu and S. B. Patten, "Effect of depression on stroke morbidity and mortality," *Canadian Journal of Psychiatry*, vol. 48, no. 4, pp. 250-257, 2003.
- [25] A. J. Thomas, R. N. Kalaria, and J. T. O'Brien, "Depression and vascular disease: what is the relationship?," *Journal of Affective Disorders*, vol. 79, no. 1-3, pp. 81-95, 2004.
- [26] M. J. O'Donnell, D. Xavier, L. Liu et al., "Risk factors for ischaemic and intracerebral haemorrhagic stroke in 22 countries (the INTERSTROKE study): a case-control study," *Lancet*, vol. 376, no. 9735, pp. 112-123, 2010.
- [27] A. Pan, Q. Sun, O. I. Okereke, K. M. Rexrode, and F. B. Hu, "Depression and risk of stroke morbidity and Mortality," *JAMA*, vol. 306, no. 11, pp. 1241-1249, 2011.
- [28] X. Mai and X. Liang, "Risk factors for stroke based on the National Health and Nutrition Examination Survey," *The Journal of Nutrition, Health & Aging*, vol. 24, no. 7, pp. 791-795, 2020.
- [29] M. B. Howren, D. M. Lamkin, and J. Suls, "Associations of depression with C-reactive protein, IL-1, and IL-6: a meta-analysis," *Psychosomatic Medicine*, vol. 71, no. 2, pp. 171-186, 2009.
- [30] C. C. Esenwa and M. S. Elkind, "Inflammatory risk factors, biomarkers and associated therapy in ischaemic stroke," *Nature Reviews. Neurology*, vol. 12, no. 10, pp. 594-604, 2016.
- [31] Y. Milaneschi, W. K. Simmons, E. F. C. van Rossum, and B. W. Penninx, "Depression and obesity: evidence of shared biological mechanisms," *Molecular Psychiatry*, vol. 24, no. 1, pp. 18-33, 2019.
- [32] M. B. A. Barros, M. G. Lima, R. C. S. Azevedo et al., "Depression and health behaviors in Brazilian adults-PNS 2013," *Revista de Saude Publica*, vol. 51, suppl 1, p. 8s, 2017.
- [33] Y. Zhang, Y. Chen, and L. Ma, "Depression and cardiovascular disease in elderly: current understanding," *Journal of Clinical Neuroscience*, vol. 47, pp. 1-5, 2018.
- [34] Y. Zhang, J. R. He, H. B. Liang et al., "Diabetes mellitus is associated with late-onset post-stroke depression," *Journal of Affective Disorders*, vol. 221, pp. 222-226, 2017.
- [35] A. von Ruesten, C. Weikert, I. Fietze, and H. Boeing, "Association of sleep duration with chronic diseases in the European Prospective Investigation into Cancer and Nutrition (EPIC)-Potsdam study," *PLoS One*, vol. 7, no. 1, article e30972, 2012.
- [36] Q. He, H. Sun, X. Wu et al., "Sleep duration and risk of stroke: a dose-response meta-analysis of prospective cohort studies," *Sleep Medicine*, vol. 32, pp. 66-74, 2017.
- [37] D. M. Hermann and C. L. Bassetti, "Sleep-related breathing and sleep-wake disturbances in ischemic stroke," *Neurology*, vol. 73, no. 16, pp. 1313-1322, 2009.
- [38] S. P. Khot and L. B. Morgenstern, "Sleep and stroke," *Stroke*, vol. 50, no. 6, pp. 1612-1617, 2019.
- [39] S. B. Duss, A. K. Brill, P. Bargiotas et al., "Sleep-wake disorders in stroke-increased stroke risk and deteriorated recovery? An evaluation on the necessity for prevention and treatment," *Current Neurology and Neuroscience Reports*, vol. 18, no. 10, p. ???, 2018.
- [40] C. Baglioni, G. Battagliese, B. Feige et al., "Insomnia as a predictor of depression: a meta-analytic evaluation of longitudinal epidemiological studies," *Journal of Affective Disorders*, vol. 135, no. 1-3, pp. 10-19, 2011.
- [41] H. Fang, S. Tu, J. Sheng, and A. Shao, "Depression in sleep disturbance: a review on a bidirectional relationship, mechanisms and treatment," *Journal of Cellular and Molecular Medicine*, vol. 23, no. 4, pp. 2324-2332, 2019.
- [42] D. H. Kim, S. Sabour, U. N. Sagar, S. Adams, and D. J. Whellan, "Prevalence of hypovitaminosis D in cardiovascular diseases (from the National Health and Nutrition Examination Survey 2001 to 2004)," *The American Journal of Cardiology*, vol. 102, no. 11, pp. 1540-1544, 2008.
- [43] J. Kendrick, G. Targher, G. Smits, and M. Chonchol, "25-Hydroxyvitamin D deficiency is independently associated with cardiovascular disease in the Third National Health and Nutrition Examination Survey," *Atherosclerosis*, vol. 205, no. 1, pp. 255-260, 2009.
- [44] S. S. Yoon, C. F. Dillon, K. Illoh, and M. Carroll, "Trends in the prevalence of coronary heart disease in the U.S.: National Health and Nutrition Examination Survey," *American Journal of Preventive Medicine*, vol. 51, no. 4, pp. 437-445, 2016.
- [45] E. Tobaldini, E. M. Fiorelli, M. Solbiati, G. Costantino, L. Nobili, and N. Montano, "Short sleep duration and cardiometabolic risk: from pathophysiology to clinical evidence," *Nature Reviews. Cardiology*, vol. 16, no. 4, pp. 213-224, 2019.
- [46] C. B. Nemeroff and P. J. Goldschmidt-Clermont, "Heartache and heartbreak—the link between depression and cardiovascular disease," *Nature Reviews. Cardiology*, vol. 9, no. 9, pp. 526-539, 2012.

Research Article

Association between Congenital Cytomegalovirus Infection and Brain Injury in Neonates: A Meta-analysis of Cohort Studies

Li Zhang ¹, Zhankui Li,¹ Xiang Han,² Hongyan Du,³ Yingli Cao,² Yingmei Liu,⁴ and Wenfeng Wang ^{5,6,7,8}

¹Department of Neonatology, Northwest Women's and Children's Hospital, Xian 710061, China

²Department of Obstetrics, Northwest Women's and Children's Hospital, Xian 710061, China

³Department of Pathology, Northwest Women's and Children's Hospital, Xian 710061, China

⁴Xian Medical University, Xian 710021, China

⁵School of Science, Shanghai Institute of Technology, Shanghai 201418, China

⁶International Academy of Visual Art and Engineering, London E16 1AH, UK

⁷Interscience Institute of Management and Technology, Bhubaneswar 752054, India

⁸RCECA, Chinese Academy of Sciences, Urumqi 830011, China

Correspondence should be addressed to Li Zhang; zhangli2233@outlook.com

Received 5 August 2021; Revised 6 September 2021; Accepted 14 September 2021; Published 15 October 2021

Academic Editor: Horacio Soto

Copyright © 2021 Li Zhang et al. This is an open access article distributed under the Creative Commons Attribution License, which permits unrestricted use, distribution, and reproduction in any medium, provided the original work is properly cited.

Objective. To assess association between congenital cytomegalovirus (CMV) infection and brain injury in neonates. **Methods.** The literatures from inception to November 4, 2020, were searched through PubMed, Embase, Cochrane Library, and Web of Science. Heterogeneity test was conducted for each indicator and measured by I^2 statistics. If $I^2 \geq 50\%$, the random effects model was applied; otherwise, the fixed effects model was used. Sensitivity analysis was performed for all models. Weighted mean difference (WMD) was used as the effect size for measurement data, and risk ratio (RR) was as the effect indicator. **Results.** A total of 13 studies, including 4,262 congenital CMV infection neonates, were enrolled in this study. Our results showed that the rate of hearing impairment (RR: 2.105, 95% CI: (1.115, 3.971), $P = 0.002$), sensorineural hearing loss (SNHL) (RR: 17.051, 95% CI: (6.201, 46.886), $P < 0.001$), and microcephaly (RR: 2.283, 95% CI: (1.325, 3.935), $P = 0.003$) in neonates infected congenital CMV was higher than that in control group. **Conclusion.** The risks of hearing impairment, SNHL, and microcephaly in neonates during childhood may be associated with congenital CMV infection. It is necessary to establish neonatal screening programs and comprehensive diagnostic tests for patients to reduce the risk of adverse brain damage to the congenital CMV infection as early as possible and to improve the prognosis of the newborn.

1. Introduction

Congenital cytomegalovirus (CMV) infection refers to an infectious disease caused by vertical transmission of CMV in the fetus due to the mother's CMV infection during pregnancy, which causes damage to multiple organs of the fetus or newborn [1, 2]. After pregnant women are infected with CMV, the vertical transmission rate is as high as 32%-40%, with the prevalence of congenital CMV infection worldwide in live born newborns is 0.5%-3% [2]. CMV in pregnant congenital CMV infection women causes intrauterine infection of the fetus through the placenta, which is the most

important cause of congenital central nervous system damage caused by intrauterine infection. CMV infected infants may have severe brain damage, causing brain dysfunction, such as severe decreases in cognitive capacity, mental retardation, and seizures [3-5]. Insights into the risk of congenital CMV-associated impairment can help optimize care of neonates infected with congenital CMV and stimulate preventive measures to improve the prognosis.

Several studies showed congenital CMV infection patients develop long-term sequelae, including sensorineural hearing loss (SNHL) and neurodevelopmental damage, ranging up to severe decreases in cognitive capacity, which

is often irreversible [3, 4, 6–8]. Nevertheless, there is a study that shows that the risk of developing SNHL after age 5 years among case-patients was not different than in uninfected children [9]. A prospective follow-up study indicated that full-term infants with postnatal congenital CMV infection are often asymptomatic, without long-term sequelae or hearing problems [10].

There were studies attempting to investigate association between perinatal infections and neonatal brain injury [11, 12]. Nevertheless, studies estimating brain injury of congenital CMV infection in neonates were limited. Herein, we performed this meta-analysis to evaluate association between congenital CMV infection and brain injury in neonates so as to start a comprehensive screening of newborns with congenital CMV infection as soon as possible and achieve early intervention, comprehensive treatment, and dynamic monitoring to reduce the complications and sequelae caused by congenital CMV infection in newborns.

2. Methods

2.1. Search Strategy. The literatures from inception to November 4, 2020, were searched through PubMed, Embase, Cochrane Library, and Web of Science. The search words were as follows: “Virus Diseases” OR “Disease, Virus” OR “Diseases, Virus” OR “Virus Disease” OR “Virus Infections” OR “Infection, Virus” OR “Infections, Virus” OR “Virus Infection” OR “Viral Diseases” OR “Disease, Viral” OR “Diseases, Viral” OR “Viral Disease” OR “Viral Infections” OR “Infection, Viral” OR “Infections, Viral” OR “Viral Infection” OR “rubella virus” OR “cytomegalovirus” OR “hepatitis B virus” OR “herpesvirus” OR “human papilloma virus” OR “HPV” OR “Human parvovirus B19” OR “B19” OR “human immunodeficiency virus” OR “coxsackie virus” AND “Brain Injuries” OR “Injuries, Brain” OR “Brain Injury” OR “Injury, Brain” OR “Injuries, Acute Brain” OR “Acute Brain Injuries” OR “Acute Brain Injury” OR “Brain Injury, Acute” OR “Injury, Acute Brain” OR “Brain Injuries, Acute” OR “Brain Lacerations” OR “Brain Laceration” OR “Laceration, Brain” OR “Lacerations, Brain” OR “Brain Injuries, Focal” OR “Brain Injury, Focal” OR “Focal Brain Injury” OR “Injuries, Focal Brain” OR “Injury, Focal Brain” OR “Focal Brain Injuries” OR “Hearing Loss, Sensorineural” OR “Sensorineural Hearing Loss” OR “Hearing Loss, Cochlear” OR “Cochlear Hearing Loss” OR “SNHL” OR “brain” OR “Encephalon” OR “neurodevelopment” AND “Fetus” OR “Fetuses” OR “Fetal Structures” OR “Fetal Structure” OR “Structure, Fetal” OR “Structures, Fetal” OR “Mummified Fetus” OR “Fetus, Mummified” OR “Retained Fetus” OR “Fetus, Retained” OR “Fetal Tissue” OR “Fetal Tissues” OR “Tissue, Fetal” OR “Tissues, Feta” OR “Infant, Newborn” OR “Infants, Newborn” OR “Newborn Infant” OR “Newborn Infants” OR “Newborns” OR “Newborn” OR “Neonate” OR “Neonates.”

2.2. Inclusion and Exclusion Criteria. Inclusion criteria are as follows: (1) CMV group was neonates infected with congenital CMV, and healthy or noninfected newborns were as the control group; (2) cohort studies; and (3) English literatures.

Exclusion criteria are as follows: (1) animal experiments; (2) newborns treated after infection; and (3) meta-analyses, reviews, case reports, conference abstracts, and letters.

2.3. Quality Assessment and Data Extraction. Two researchers (Zhankui Li, Xiang Han) reviewed the identified literatures and extracted the research data according to inclusion and exclusion criteria. If a discrepancy existed, a third party (Li Zhang) would participate in the extraction of data. For each study, following information was extracted, including author, year, country, gender, gestation weeks or months, and birthweight. Newcastle-Ottawa Scale (NOS) was used to evaluate the literature quality. The scale has a total score of 10, with <5 as medium to low quality and ≥ 5 as high quality.

The association between congenital CMV infection and brain injury in neonates was assessed by hearing impairment, SNHL, microcephaly, neurodevelopmental delay, mental development index (MDI), and psychometric development index (PDI).

The Stata 15.0 software (Stata Corporation, College Station, TX, USA) was used for statistical analysis. Heterogeneity test was conducted for each indicator and measured by I^2 statistics. If $I^2 \geq 50\%$, the random effects model was applied; otherwise, the fixed effects model was used. Sensitivity analysis was performed for all models. Weighted mean difference (WMD) was used as the effect size for measurement data, and risk ratio (RR) was as the effect indicator. $P < 0.05$ was considered statistically significant.

3. Results

Initially, 11,532 potential literatures were searched through database; 11,146 articles were identified after duplicates removed. By checking the titles and abstracts, 236 studies were identified. Finally, 13 full-text articles were screened for eligibility in this meta-analysis, including 4,262 participants with 1,114 neonates in the CMV group and 3,148 neonates in the control group. The flow chart of literature search is shown in Figure 1. The basic characteristics of enrolled studies are summarized in Table 1.

3.1. Hearing Impairment. The hearing impairment was analyzed in 9 studies. The results of heterogeneity test showed that $I^2 = 65.3\%$, so the random effects model was adopted. The results showed that the rate of hearing impairment in CMV group was significantly higher than that in control group (RR: 2.105, 95% CI: (1.115, 3.971), $P = 0.002$) (Figure 2 and Table 2).

A total of 5 studies were enrolled to assess the association between SNHL and congenital CMV infection. Fixed-effect model was adopted ($I^2 = 0.0\%$). It showed that the SNHL rate in the CMV group was higher than that in the control group (RR: 17.051, 95% CI: (6.201, 46.886), $P < 0.001$), indicating SNHL was associated with congenital CMV infection (Figure 3 and Table 2).

There were 3 studies that were involved to investigate the potential association between microcephaly and

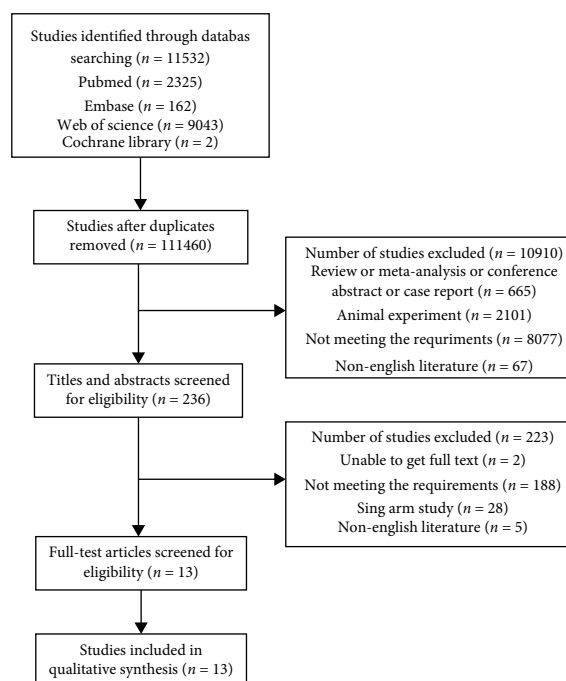


FIGURE 1: The flow chart of literature search.

congenital CMV infection. The pooled results showed that congenital CMV infection increased the risk of microcephaly in neonates infected with congenital CMV (RR: 2.283, 95% CI: (1.325, 3.935), $P = 0.003$) (Figure 4 and Table 2).

3.2. Neurodevelopmental Delay. The neurodevelopmental delay was identified in 3 studies to assess potential association between congenital CMV infection and neurodevelopmental delay. The results revealed that there was no significant difference in neurodevelopmental delay between the infection group and the control group ($I^2 = 54.0\%$, RR: 2.910, 95% CI: (0.417, 20.285), $P = 0.281$) (Figure 5 and Table 2).

Totally 3 studies were included in the analysis of association between MDI and congenital CMV infection. The fixed-effect model was used ($I^2 = 0.0\%$). It was shown that MDI in the infection group was no difference compared with the control group (WMD: -0.940, 95% CI: (-3.473, 1.593), $P = 0.467$) (Figure 6 and Table 2).

A total of 2 studies were enrolled to assess association between congenital CMV infection and PDI. The results revealed that congenital CMV infection could not increase the risk of PDI in newborns infected with congenital CMV (WMD: 2.717, 95% CI: (-1.068, 6.501), $P = 0.159$) (Figure 7 and Table 2).

Begg's test was used for the assessment of publication bias, and the results showed that there was no publication bias in hearing impairment ($t = 0.81$, $P = 0.441$). Moreover, the sensitivity analysis for each model was carried out. Sensitivity analysis result proves that the findings are trustworthy (Table 2).

4. Discussion

Brain injury often leads to developmental disorders such as motor function and intelligence in children and even leads to the death of children [13]. Neonatal brain injury causes lifelong morbidity for the survivors, with high emotional costs to the individual and the family plus a heavy economic burden for society. Scarce studies were conducted to investigate brain injury in congenital CMV infection. In this meta-analysis, we explored the association between congenital CMV infection and brain injury in neonates based on a comprehensive search of literatures from a variety of databases. A total of 13 studies involving 3855 participants were enrolled. The results indicated that the risk of hearing impairment, SNHL, and microcephaly in neonates infected congenital CMV were higher than that in the control group. Nevertheless, there was no significant difference in neurodevelopmental delay, MDI, and PDI between CMV group and the control group. The result suggested that congenital CMV infection in neonates is associated with the risk of hearing impairment, SNHL, and microcephaly in neonates.

Our results indicated that congenital CMV infection that increased the risk of hearing impairment in neonates is supported by multiple studies [8, 14, 15]. The exact mechanism of hearing impairment has not been clarified, but several studies have shown that the inflammatory response of the inner ear is more related to the hearing impairment of newborns than the direct damage caused by viruses [16, 17]. Goderis et al. found that the overall incidence of hearing loss in congenital CMV is 12.6%, with the majority of bilateral hearing loss in symptomatic children and unilateral losses predominated in asymptomatic group, indicating that the risk of hearing impairment in neonates is associated with congenital CMV infection [14]. Likewise, Yamamoto et al. [15] have found that congenital CMV is an important cause of permanent hearing impairment in childhood in all settings. A study has have shown that no matter what the cause of hearing impairment is and no matter the impairment is mild or severe, as long as it is found before 6 months after birth and the child's cognitive ability is normal, the child's language ability can basically reach the normal level after systematic and effective intervention [18]. Early detection of hearing impairment in children with CMV infection and systematic and effective clinical treatment are particularly important.

Some studies have suggested that congenital CMV infection is the leading nongenetic cause of SNHL during childhood [8, 19–21]. Our finding showed that SNHL in neonates infected congenital CMV was significantly higher than that in the control group. A meta-analysis by Vries et al. [21], which explore different type of maternal CMV infection during pregnancy, namely, primary (PI) versus nonprimary (NPI), found that the prevalence of SNHL was 13% in the PI group and 11% in the NPI group, respectively. Likewise, previous studies whose population based studies in Sweden [22], Canada [23], and USA [8, 24] have reported that between 9.3% and 17% of infants with congenital CMV infection would have SNHL. The rates of SNHL reported by these studies ranged between 22% and 41% in

TABLE 1: Baseline characteristics of included study.

Author	Year	Country	Total	M/F	Case Gestation, weeks/ months	Birthweight/g	Total	M/F	Control Gestation, weeks/ months	Birthweight, g
Saigal	1982	Canada	47	30/17	39 ± 2.2 w	3130 ± 657	46	29/ 17	39 ± 2.5 w	3120 ± 645 g
Harris	1984	Sweden	42				51			
Kumar	1984	USA	17		7.6 (6.5-10.9) m		21		7.4 (6.5-10.9) m	
Hicks	1993	USA	34				2002			
Fowler	1997	USA	307	158/ 149			201	90/ 111		
Shan	2009	China	52				21			
Jim	2015	China	14		27.9 ± 2.6 w	1093.7 ± 251.4	41		29.2 ± 2.5	1153.7 ± 235.7 g
Uematsu	2016	Japan	54	23/31	39 (36-41) w	2634 (2497- 2771)	106	53/ 53	38 w (23-42 w)	2516-2783 g
Jin	2016	USA	186	96/90			51	35/ 16		1750-4170 g
Korndewal	2017	The Netherlands								
Kotovich	2017	Israel	90		33.1 ± 2.0 w		199		31.8 ± 2.3 w	
Lanzieri	2017	USA	92	53/39			51	37/ 14		
Pathirana	2020	South Africa	46	25/21	38 (36-40) w	2845 (2455- 3190)	84	43/ 41	38 (36-39) w	2902.5 (2595- 3195) g

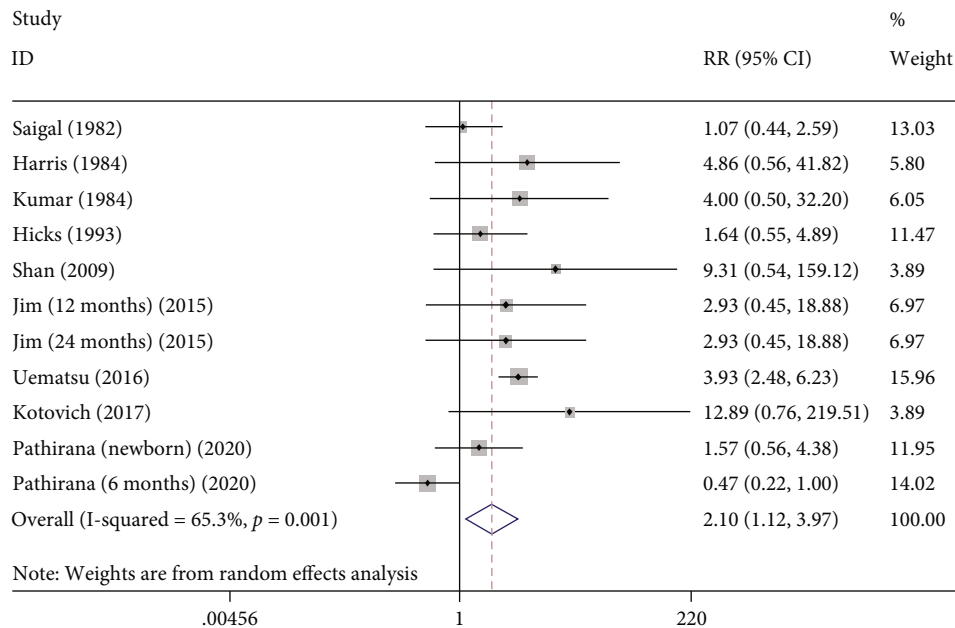


FIGURE 2: The forest plots of hearing impairment between CMV group and control group.

children with clinically apparent or symptomatic infection and between 6% and 16% in those with subclinical or asymptomatic infection. Yamamoto et al. [25] found that even in populations with near universal immunity to

CMV, congenital CMV infection is a significant cause of SNHL. This prompts that comprehensive diagnostic workup for the patient with congenital CMV infection is vital for guiding treatment and intervention options for SNHL.

TABLE 2: Overall results and sensitivity analysis.

Outcomes	RR, 95% CI	P	I ²
Hearing impairment			
Overall	2.105 (1.115, 3.971)	0.022	65.3%
Sensitivity analysis	2.105 (1.115, 3.971)		
SNHL			
Overall	17.051 (6.201, 46.886)	<0.001	0.0%
Sensitivity analysis	17.051 (6.201, 46.886)		
Microcephaly			
Overall	2.283 (1.325, 3.935)	0.003	0.0%
Sensitivity analysis	2.283 (1.325, 3.935)		
Neurodevelopmental delay			
Overall	2.910 (0.417, 20.285)	0.281	54.0%
Sensitivity analysis	2.910 (0.417, 20.285)		
MDI			
Overall	-0.940 (-3.473, 1.593)	0.467	0.0%
Sensitivity analysis	-0.940 (-3.473, 1.593)		
PDI			
Overall	2.717 (-1.068, 6.501)	0.159	0.0%
Sensitivity analysis	2.717 (-1.068, 6.501)		

SNHL: sensorineural hearing loss; MDI: mental development index; PDI: psychometric development index.

Microcephaly is generally defined as head circumference ≤ 2 standard deviations below the mean for gestational age [26]. Most microcephaly associated with congenital infections is a reflection of neurotropism for fetal central nervous system (CNS) cells, with massive destruction of neural tissue during the early development of the CNS of the fetus [27–29]. Several studies found that maternal CMV infection is associated with a 30% chance of congenital infection and as much as a 15% chance of clinically apparent manifestations at birth (symptomatic congenital CMV), with up to 50% of these infants manifesting microcephaly [30–32]. Similar results were observed in our study. This suggests that attention should be paid to microcephaly associated with congenital CMV infection in clinical practice as microcephaly is generally accompanied by mental retardation due to severe limitation of brain development.

We did not find association between congenital CMV infection and increasing risk of neurodevelopmental delay. Likewise, a cohort study, aiming to evaluate neurological and growth outcomes in South African children with congenital CMV, found that there was no significant difference in neurodevelopment between cases and controls at 12 months of age [33]. Bartlett et al. did prospective studies of asymptomatic congenital CMV infected children with follow-up of one to 6 years and reported a cumulative incidence of neurodevelopmental impairment between 0% and 9.1% [34]. In contrast, studies of symptomatic newborns reported a prevalence of 30%–50% neurological impairment

during childhood [35–37]. Although we did not find the association between congenital CMV infection and increasing risk of neurodevelopmental delay, the contradictory findings suggest us paying attention to the type of fetal infection as it showed symptomatic newborns reported higher risk of neurodevelopmental delay.

Potential confounding factors may have an impact on our result. Nevertheless, most of the articles included studies in this meta-analysis did not adjust confounding factors. Potential confounding factors may be marital status, economic situation, educational background of parents, maternal age at conception, time of maternal CMV infection, whether treated, estimated gestational age at delivery, and neonatal symptoms at birth in this study [2, 9, 38–40]. Age is a common confounding factor. Using survival analysis, a study [9] found that the proportion of SNHL in children with congenital CMV infection increased from 7% at age 3 months to 14% at age 5 years and 25% at age 18 years among case-patients and from 0% at age 5 years to 8% at age 18 years among controls. More studies will be important to confirm these findings and inform future guidance on the optimal duration of audiologic monitoring for children with congenital CMV infection. Persons of lower socioeconomic status tended to report higher risk of CMV than those in the general population [38]. This contrasts with the conclusions of Preece et al. [39], who reported once age, race, and marital status had been taken into account there was no difference in the estimated prevalence of congenital CMV between infants born to mothers from manual and nonmanual social class. Besides, the expected number of infected newborns among those in worse clinical conditions is higher than in the general population, once the deleterious effects determined by the virus begin in the fetus [40]. Notably, the birth prevalence was lower in infants born to mothers who were ascertained in the prenatal period than in infants born to mothers who were ascertained at delivery. The lower birth prevalence among women ascertained prenatally may occur because women seeking prenatal care tend to have lower risk for a variety of poor outcomes [2]. These potential confounding variables suggest that interventions might be most efficient if they are targeted toward certain groups. More original studies are needed in the future to further elucidate the association between congenital CMV infection and neonatal brain injury.

The strengths of the current study need to be mentioned. This was the first attempt based on comprehensive databases to investigate association between congenital CMV infection and brain injury in neonates. Besides, all the studies were cohort studies, making the findings more trustworthy. However, some limitations of our study must be acknowledged. First, in our study, we estimated the risk of brain injury associated with congenital CMV infection, but we did not estimate the specific maternal infection or fetal infection subtypes. In future study, we will do further study based on maternal infection or fetal infection to investigate association between congenital CMV infection and brain injury in newborn. Second, most of included studies were retrospective studies, which may lead to recall bias. Third, residual confounding

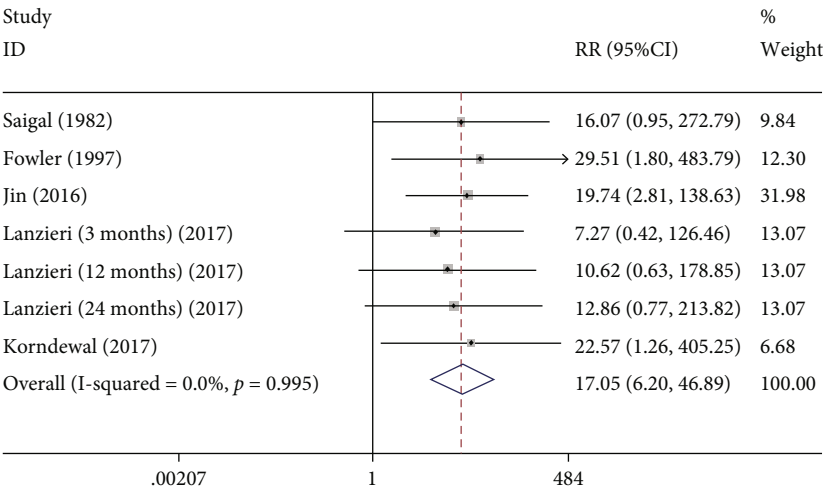


FIGURE 3: The forest plots of SNHL between CMV group and control group.

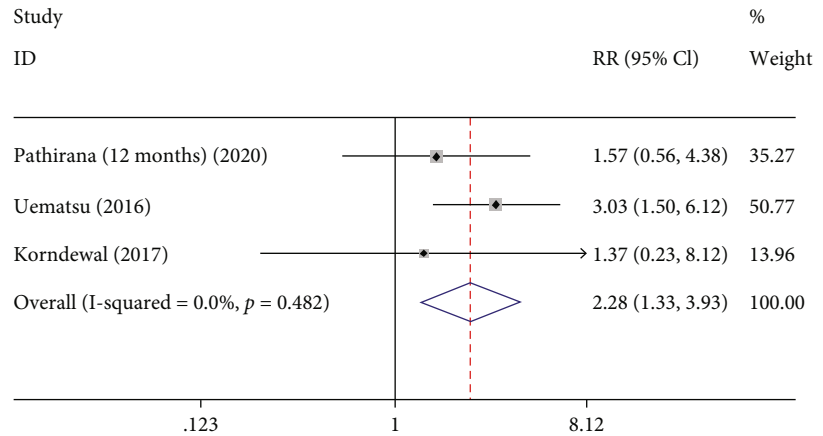


FIGURE 4: The forest plots of microcephaly between CMV group and control group.

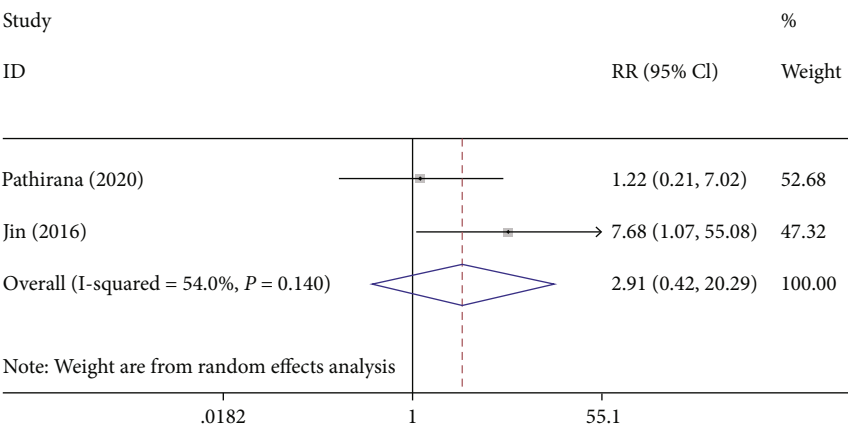


FIGURE 5: The forest plots of neurodevelopmental delay between CMV group and control group.

variables are a problem. Uncontrolled or unmeasured confounding factors have the potential for bias; the possibility that residual confounders influenced the results cannot be ruled out. Furthermore, for risk estimates of brain

injury associated with congenital CMV infection, the results mainly relied on the 13 total studies, so more studies should be included in future studies to provide further support for our results.

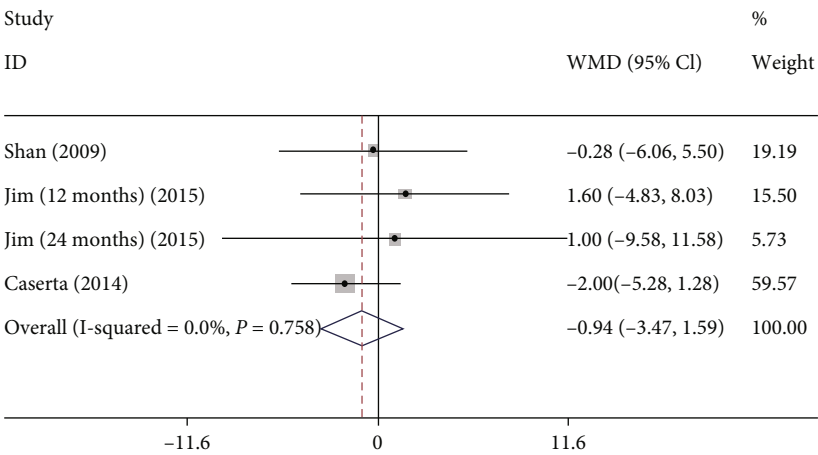


FIGURE 6: The forest plots of MDI between CMV and control groups.

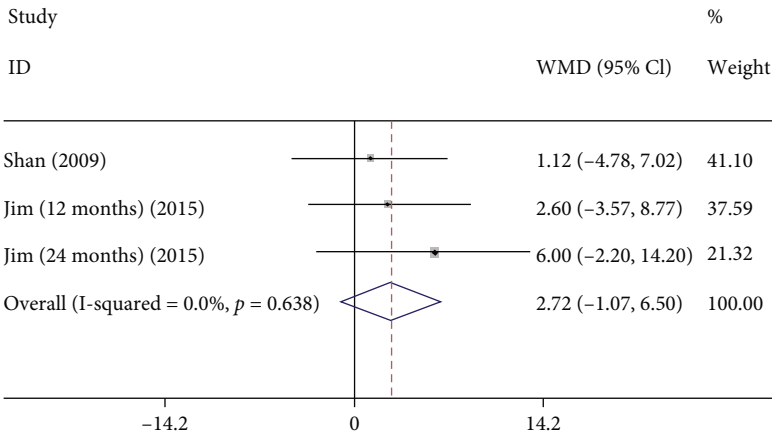


FIGURE 7: The forest plots of PDI between CMV group and control group.

5. Conclusion

This meta-analysis explored association between congenital CMV infection and brain injury in neonates based on comprehensive databases. The result suggested the risks of hearing impairment, SNHL, and microcephaly in neonates during childhood may be associated with congenital CMV infection. In clinical application, do early screening of congenital CMV infection to improve the detection rate of infected children, reducing the incidence of sequelae and improving the prognosis, finally bringing significant social benefits to improve the quality of the population.

Data Availability

The data utilized to support the findings are available from the corresponding authors upon request.

Conflicts of Interest

The authors declare that they have no conflicts of interest.

Acknowledgments

This work is supported by the Key research projects of Northwest Women’s and Children’s Hospital (No. z201301) and Scientific Research Fund Project of Health Department of Shaanxi Province (No. 2010D017).

References

[1] J. Hassan and J. Connell, “Translational mini-review series on infectious disease: congenital cytomegalovirus infection: 50 years on,” *Clinical and Experimental Immunology*, vol. 149, no. 2, pp. 205–210, 2007.

[2] A. Kenneson and M. J. Cannon, “Review and meta-analysis of the epidemiology of congenital cytomegalovirus (CMV) infection,” *Reviews in Medical Virology*, vol. 17, no. 4, pp. 253–276, 2007.

[3] Z. W. Naing, G. M. Scott, A. Shand et al., “Congenital cytomegalovirus infection in pregnancy: a review of prevalence, clinical features, diagnosis and prevention,” *The Australian & New Zealand Journal of Obstetrics & Gynaecology*, vol. 56, no. 1, pp. 9–18, 2016.

[4] A. M. Dreher, N. Arora, K. B. Fowler et al., “Spectrum of disease and outcome in children with symptomatic congenital

- cytomegalovirus infection," *The Journal of Pediatrics*, vol. 164, no. 4, pp. 855–859, 2014.
- [5] X. W. Zhang, F. Li, X. W. Yu, X. W. Shi, J. Shi, and J. P. Zhang, "Physical and intellectual development in children with asymptomatic congenital cytomegalovirus infection: a longitudinal cohort study in Qinba mountain area, China," *Journal of clinical virology : the official publication of the Pan American Society for Clinical Virology*, vol. 40, no. 3, pp. 180–185, 2007.
 - [6] M. Barbi, S. Binda, S. Caroppo, and V. Primache, "Neonatal screening for congenital cytomegalovirus infection and hearing loss," *Journal of clinical virology : the official publication of the Pan American Society for Clinical Virology*, vol. 35, no. 2, pp. 206–209, 2006.
 - [7] M. C. Cheeran, J. R. Lokensgard, and M. R. Schleiss, "Neuropathogenesis of congenital cytomegalovirus infection: disease mechanisms and prospects for intervention," *Clinical microbiology reviews*, vol. 22, no. 1, pp. 99–126, 2009.
 - [8] K. B. Fowler and S. B. Boppana, "Congenital cytomegalovirus (CMV) infection and hearing deficit," *Journal of clinical virology : the official publication of the Pan American Society for Clinical Virology*, vol. 35, no. 2, pp. 226–231, 2006.
 - [9] T. M. Lanzieri, W. Chung, M. Flores et al., "Hearing loss in children with asymptomatic congenital cytomegalovirus infection," *Pediatrics*, vol. 139, no. 3, p. e20162610, 2017.
 - [10] W. T. Jim, N. C. Chiu, C. S. Ho et al., "Outcome of preterm infants with postnatal cytomegalovirus infection via breast milk: a two-year prospective follow-up study," *Medicine*, vol. 94, no. 43, 2015.
 - [11] W. J. Ledger, "Perinatal infections and fetal/neonatal brain injury," *Current Opinion in Obstetrics & Gynecology*, vol. 20, no. 2, pp. 120–124, 2008.
 - [12] M. B. Mutnal, M. C. Cheeran, S. Hu, and J. R. Lokensgard, "Murine cytomegalovirus infection of neural stem cells alters neurogenesis in the developing brain," *PLoS One*, vol. 6, no. 1, 2011.
 - [13] V. Zupan Simunek, "Birth asphyxia in term newborns: diagnosis, prognosis, neuroprotection," *Archives de pediatrie : organe officiel de la Societe francaise de pediatrie*, vol. 17, no. 5, pp. 578–582, 2010.
 - [14] J. Goderis, E. De Leenheer, K. Smets, H. Van Hoecke, A. Keymeulen, and I. Dhooze, "Hearing loss and congenital CMV infection: a systematic review," *Pediatrics*, vol. 134, no. 5, pp. 972–982, 2014.
 - [15] A. Y. Yamamoto, A. R. T. Anastasio, E. T. Massuda et al., "Contribution of congenital cytomegalovirus infection to permanent hearing loss in a highly seropositive population: the Brazilian Cytomegalovirus Hearing and Maternal Secondary Infection Study," *Clinical Infectious Diseases : An Official Publication of the Infectious Diseases Society of America*, vol. 70, no. 7, pp. 1379–1384, 2020.
 - [16] R. D. Bradford, Y. G. Yoo, M. Golemac, E. P. Pugel, S. Jonjic, and W. J. Britt, "Murine CMV-induced hearing loss is associated with inner ear inflammation and loss of spiral ganglia neurons," *PLoS Pathogens*, vol. 11, no. 4, 2015.
 - [17] M. Carraro, A. Almishaal, E. Hillas, M. Firpo, A. Park, and R. V. Harrison, "Cytomegalovirus (CMV) infection causes degeneration of cochlear vasculature and hearing loss in a mouse model," *Journal of the Association for Research in Otolaryngology : JARO*, vol. 18, no. 2, pp. 263–273, 2017.
 - [18] S. Xiaoming, "Infant hearing screening," *Chinese Journal of Pediatrics*, vol. 40, no. 1, pp. 56–58, 2002.
 - [19] K. Fowler and B. SJ Sip, "Congenital cytomegalovirus infection," *Seminars in Perinatology*, vol. 42, no. 3, pp. 149–154, 2018.
 - [20] C. C. Morton and W. E. Nance, "Newborn hearing screening—a silent revolution," *The New England Journal of Medicine*, vol. 354, no. 20, pp. 2151–2164, 2006.
 - [21] J. J. de Vries, E. W. van Zwet, F. W. Dekker, A. C. Kroes, P. H. Verkerk, and A. C. Vossen, "The apparent paradox of maternal seropositivity as a risk factor for congenital cytomegalovirus infection: a population-based prediction model," *Reviews in Medical Virology*, vol. 23, no. 4, pp. 241–249, 2013.
 - [22] K. Ahlfors, S. A. Ivarsson, S. Harris et al., "Congenital cytomegalovirus infection and disease in Sweden and the relative importance of primary and secondary maternal infections. Preliminary findings from a prospective study," *Scandinavian Journal of Infectious Diseases*, vol. 16, no. 2, pp. 129–137, 1984.
 - [23] S. Saigal, O. Lunyk, R. P. Larke, and M. A. Chernesky, "The outcome in children with congenital cytomegalovirus infection," *American journal of diseases of children (1960)*, vol. 136, no. 10, pp. 896–901, 1982.
 - [24] A. J. Dahle, K. B. Fowler, J. D. Wright, S. B. Boppana, W. J. Britt, and R. F. Pass, "Longitudinal investigation of hearing disorders in children with congenital cytomegalovirus," *Journal of the American Academy of Audiology*, vol. 11, no. 5, pp. 283–290, 2000.
 - [25] A. Y. Yamamoto, M. M. Mussi-Pinhata, L. Isaac Mde et al., "Congenital cytomegalovirus infection as a cause of sensorineural hearing loss in a highly immune population," *The Pediatric Infectious Disease Journal*, vol. 30, no. 12, pp. 1043–1046, 2011.
 - [26] M. C. Leal, L. F. Muniz, T. S. Ferreira et al., "Hearing loss in infants with microcephaly and evidence of congenital Zika virus infection - Brazil, November 2015–May 2016," *MMWR Morbidity and mortality weekly report*, vol. 65, no. 34, pp. 917–919, 2016.
 - [27] Z. A. Klase, S. Khakhina, B. Schneider Ade, M. V. Callahan, J. Glasspool-Malone, and R. Malone, "Zika fetal neuropathogenesis: etiology of a viral syndrome," *PLoS Neglected Tropical Diseases*, vol. 10, no. 8, 2016.
 - [28] C. K. Shapiro-Mendoza, M. E. Rice, R. R. Galang et al., "Pregnancy outcomes after maternal Zika virus infection during pregnancy - U.S. territories, January 1, 2016–April 25, 2017," *MMWR Morbidity and mortality weekly report 2017*, vol. 66, no. 23, pp. 615–621, 2017.
 - [29] K. M. Adams Waldorf and R. M. McAdams, "Influence of infection during pregnancy on fetal development," *Reproduction*, vol. 146, no. 5, pp. R151–R162, 2013.
 - [30] W. J. Britt, "Congenital human cytomegalovirus infection and the enigma of maternal immunity," *Journal of Virology*, vol. 91, no. 15, 2017.
 - [31] S. B. Boppana, L. B. Rivera, K. B. Fowler, M. Mach, and W. J. Britt, "Intrauterine transmission of cytomegalovirus to infants of women with preconceptional immunity," *The New England Journal of Medicine*, vol. 344, no. 18, pp. 1366–1371, 2001.
 - [32] S. B. Boppana, K. B. Fowler, W. J. Britt, S. Stagno, and R. F. Pass, "Symptomatic congenital cytomegalovirus infection in infants born to mothers with preexisting immunity to cytomegalovirus," *Pediatrics*, vol. 104, no. 1, pp. 55–60, 1999.

- [33] J. Pathirana, L. Texeira, H. Munian et al., “Neurological and growth outcomes in South African children with congenital cytomegalovirus: a cohort study,” *PLoS One*, vol. 15, no. 9, 2020.
- [34] A. W. Bartlett, B. McMullan, W. D. Rawlinson, and P. Palasanthiran, “Hearing and neurodevelopmental outcomes for children with asymptomatic congenital cytomegalovirus infection: a systematic review,” *Reviews in Medical Virology*, vol. 27, no. 5, 2017.
- [35] S. Manicklal, V. C. Emery, T. Lazzarotto, S. B. Boppana, and R. K. Gupta, “The “silent” global burden of congenital cytomegalovirus,” *Clinical Microbiology Reviews*, vol. 26, no. 1, pp. 86–102, 2013.
- [36] S. C. Dollard, S. D. Grosse, and D. S. Ross, “New estimates of the prevalence of neurological and sensory sequelae and mortality associated with congenital cytomegalovirus infection,” *Reviews in Medical Virology*, vol. 17, no. 5, pp. 355–363, 2007.
- [37] M. Zavattoni, G. Lombardi, V. Rognoni et al., “Maternal, fetal, and neonatal parameters for prognosis and counseling of HCMV congenital infection,” *Journal of Medical Virology*, vol. 86, no. 12, pp. 2163–2170, 2014.
- [38] M. J. Cannon, D. S. Schmid, and T. B. Hyde, “Review of cytomegalovirus seroprevalence and demographic characteristics associated with infection,” *Reviews in Medical Virology*, vol. 20, no. 4, pp. 202–213, 2010.
- [39] P. M. Preece, P. Tookey, A. Ades, and C. S. Peckham, “Congenital cytomegalovirus infection: predisposing maternal factors,” *Journal of Epidemiology and Community Health*, vol. 40, no. 3, pp. 205–209, 1986.
- [40] D. V. Santos, M. M. Souza, S. H. Gonçalves et al., “Congenital cytomegalovirus infection in a neonatal intensive care unit in Brazil evaluated by PCR and association with perinatal aspects,” *Revista do Instituto de Medicina Tropical de Sao Paulo*, vol. 42, no. 3, pp. 129–132, 2000.

Research Article

The First 24h Hemodynamic Management in NICU after Revascularization Surgery in Moyamoya Disease

Jie Song , Yu Lei , Long Chen , Chao Gao , Wei Ni , Xing Wu , Gang Wu , Ying Mao , Jin Hu , and Yuxiang Gu 

Department of Neurosurgery, Huashan Hospital, Fudan University, 12 Wulumuqi Zhong Road, Shanghai 200040, China

Correspondence should be addressed to Jin Hu; hujin_dana@126.com and Yuxiang Gu; guyuxiang1972@126.com

Received 4 May 2021; Accepted 25 September 2021; Published 12 October 2021

Academic Editor: Muh-Shi Lin

Copyright © 2021 Jie Song et al. This is an open access article distributed under the Creative Commons Attribution License, which permits unrestricted use, distribution, and reproduction in any medium, provided the original work is properly cited.

Objective. To evaluate whether hemodynamic factors are risk factors for prognosis in moyamoya disease (MMD). **Materials and Methods.** The retrospective study reviewed a single-center MMD cohort in Huashan Hospital from August 2017 to January 2020. Stroke events in 30 days and follow-up modified Rankin Scale (mRS) grade were recorded. Systematic assessments with perioperative mean arterial pressure (MAP), red blood cell (RBC) parameters, and fluid management were also conducted. Logistic regressions were applied to evaluate the predictors of worse outcomes. Data was analyzed using SPSS 24.0. **Results.** Admission to neurological intensive care unit (NICU) totalled about 347 after revascularization surgery. The result showed that the higher the postoperative MAP level (favorable group 95.7 ± 11.4 mmHg vs. unfavorable group 103.6 ± 10.4 mmHg, $p < 0.001$) and the greater the MAP variability (favorable group 0.26 ± 13.2 vs. unfavorable group 7.2 ± 13.5 , $p = 0.006$) were, the higher the patient's follow-up mRS grade was. What is more, a higher early postoperative Hb level also seemed to predict a worse long-term clinical outcome (favorable group 116.9 ± 17.1 g/L vs. unfavorable group 123.7 ± 13.0 g/L, $p = 0.03$), but the difference disappeared after adjusting sex and age. Logistic regression analyses showed that a higher level of postoperative MAP ($\beta = 0.024$, 95% CI (0.004, 0.044), and $p = 0.02$) within the first 24 h in NICU might be the short-term risk factor. For long-term outcome, a higher level ($\beta = 1.058$, 95% CI (1.022, 1.096), and $p = 0.001$) and a greater variability ($\beta = 30.982$, 95% CI (2.112, 454.414), and $p = 0.01$) of postoperative MAP might be the negative predictors of mRS grade. **Conclusions.** The early postoperative hemodynamic management might be extremely critical for patients with MMD. Both high postoperative MAP levels and large MAP variability might affect the prognosis. What is more, we also found that a higher postoperative Hb level might be related with a worse outcome.

1. Introduction

Moyamoya disease (MMD) is characterized by the formation of an abnormal vascular network at the base of the brain, which could result in hemodynamic compromise significant different from normocapnia [1, 2]. Owing to the inadequacy of collateral sources of blood flow, patients with MMD often suffer from reduction of perfusion pressure, insufficiency of collateral blood supply, and ultimately decrease of blood flow in the distal territory [1–4]. Revascularization surgery is an effective surgical procedure to improve the steno-occlusive lesions, reconstruct cerebral blood supply system, and prevent the occurrence of long-term complications [4, 5]. Currently, superficial temporal artery-middle cerebral artery (STA-MCA) anastomosis with or

without indirect bypass is generally used as the standard surgical treatment for MMD [1, 2, 6–8].

Efforts have been made to modify surgical modalities for better effect and fewer complications, but revascularization surgery of MMD may instantly aggravate the chaotic state of cerebral blood flow, causing acute stroke or hyperperfusion syndrome [4, 9–12]. During the perioperative period, the type of anesthetic drug, fluid resuscitation, blood loss and hematocrit (Hct), end tidal carbon dioxide (EtCO₂), temperature regulation, urine output, and the type of surgical procedure being done may affect cerebral blood flow and cerebral perfusion pressure [8, 12–14]. Under these conditions, inadequate cerebral perfusion may augment the risk for the occurrence of cerebral infarctions in MMD with

middle cerebral artery stenosis or carotid artery occlusion [13, 15, 16]. Thus, perioperative conditions other than the surgery itself are of equal importance and are issues needed to be addressed with necessity [11, 17, 18]. A standardized protocol for the perioperative management will benefit patients with MMD and improve their short- and long-term prognosis after surgery.

Throughout the entire perioperative period, early postoperative period is particularly critical, in which intensive care is generally required [1, 5, 18, 19]. Literatures have shown that surgical complications of MMD are largely related to early postoperative management, and the hemodynamic changes in this period have the greatest impact on the prognosis [5, 18, 19]. It is speculated that there is a transient change in cerebral blood flow in the early postoperative period, and the cerebrovascular autoregulation has not fully recovered, and the ability to resist hemodynamic changes is poor [9, 10, 20]. However, it is still lacking in the researches about the hemodynamic management of MMD patients in the first 24 h in neurological intensive care unit (NICU) after revascularization surgery. In this study, we retrospectively analyzed the perioperative hemodynamic parameters of patients with MMD who received operations in our institute over last 3 years and aimed to evaluate whether perioperative hemodynamic changes are risk factors for short-term and long-term prognosis.

2. Materials and Methods

2.1. Participants. The participants enrolled in this study were a single-center cohort of patients with MMD treated at Huashan Hospital from August 2017 to January 2020. Written informed consents were obtained from all of the participants and/or their guardians at admission. The diagnosis of MMD was based on the criteria issued by the Japanese Ministry of Health, Labor, and Welfare [7]. Moyamoya syndrome was defined as a secondary moyamoya phenomenon caused by severe traumatic brain injury, head and neck irradiation, hyperthyroidism, or autoimmune disease [7]. The inclusion criteria were as follows: (1) age between 18 and 80 years; (2) MMD or moyamoya syndrome confirmed by digital subtraction angiography (DSA); (3) patients who underwent revascularization surgery; (4) after operations, patients were monitored in NICU for at least 24 hours; (5) patients who were followed up for more than six months; and (6) patients with complete information and follow-up data. We excluded patients with intracranial aneurysms or other cerebrovascular diseases. Patients with moyamoya syndrome caused by Down's syndrome, systemic vasculitis, neurofibromatosis, sickle cell disease, history of irradiation, or hyperthyroidism were also excluded [6]. The study was approved by the Huashan Hospital Research Ethics Committee.

Operations were performed by the surgeons who perform more than 200 bypass surgeries each year between August 2017 and January 2020. The surgical indications were in accordance with Japanese guidelines for diagnosis and treatment of MMD [7, 21]. The patency of bypass graft was confirmed by intraoperative indocyanine angiography routinely.

2.2. NICU Hemodynamic Management

2.2.1. Blood Pressure (BP) Management. BP control mainly depended on patients' baseline BP level and their clinical manifestations. Before revascularization surgery, the systolic BP (SBP) was maintained under 150 mmHg for all the patients, and diastolic blood pressure (DBP) was maintained under 90 mmHg. During the operation, BP was closely monitored through invasive arterial monitoring. The SBP was strictly controlled within the normal range. After patients recovered from the general anesthesia, they were transferred to the NICU and BP was measured every half an hour through noninvasive monitor. For patients with hypertension, SBP was maintained at 130~140 mmHg with the help of intravenous antihypertensive drugs. Otherwise, SBP was controlled at the baseline level.

Mean arterial pressure (MAP) and MAP variability were defined as the following formulas:

$$\begin{aligned} \text{MAP} &= \text{DBP} + \frac{1}{3} (\text{SBP} - \text{DBP}), \\ \text{MAP variance} &= \frac{\text{SBP}_{\text{post}} - \text{SBP}_{\text{pre}}}{\text{SBP}_{\text{pre}}}. \end{aligned} \quad (1)$$

2.2.2. Fluid Management. Generally, patients with MMD were in a state of fasting for at least 8 h before general anesthesia. To avoid the possible loss of extracellular fluid, each patient was given an intravenous administration of 5% glucose saline or Ringer lactate solution (1000~1500 ml) before anesthesia. During the operation, each patient would be given 1500~2000 ml intravenous fluid routinely. When transferred to NICU after surgery, sufficient fluid resuscitation was performed and all of the patients would be given another 1500~2000 ml intravenous fluids during the first 24 h. It should be noted that dehydrating agents such as mannitol were routinely used to prevent brain edema caused by surgery. Those agents were not included in the intravenous fluid we mentioned.

2.3. Neuroimaging Assessment. All of the patients included in our study underwent head computed tomography (CT), magnetic resonance imaging (MRI), DSA, and diffusion-weighted imaging (DWI) within seven days before operations. For all patients, CT scans were acquired immediately after and 24 h after revascularizations to determine whether there was any intracranial hemorrhage and/or newly developed cerebral infarction. Whenever patients had newly developed symptoms, CT or MRI scans were performed at once. During the early postoperative period, CT angiography was not performed routinely. Instead, the patency of the bypass was calculated by DSA six months after combined revascularization. Postoperative newly developed cerebral infarction was defined as a low-density lesion on CT scans, a high-signal-intensity lesion on DWI images, and a low-signal intensity lesion on the apparent dispersion coefficient images.

2.4. Follow-Up. In accordance with previous literatures, short-term phase was defined as <30 days after revascularization [1]. All of the patients with MMD were followed up

by telephone, text messaging, and/or clinical services. Clinical outcomes were recorded during follow-up, including recurrent strokes (intracranial hemorrhage or cerebral infarction after revascularization surgery), neurological status, and radiological data. If required, patients received contralateral revascularization during follow-up. For the purpose of statistical analysis, short-term outcomes were classified into 3 grades: (1) grade 1: no symptom, no stroke; (2) grade 2: symptoms onset, no stroke; and (3) grade 3: symptoms onset with stroke. A modified Rankin scale (mRS) was used to determine the neurological function outcome. Long-term outcomes were dichotomized into 2 groups accordingly: favorable group: mRS 0–2 and unfavorable group: mRS 3–5 [22].

2.5. Statistical Analysis. All statistical analyses were performed with SPSS 24.0. Demographic and baseline data and perioperative hemodynamic characteristics were compared according to the short-term and long-term prognosis groups. The Fisher exact test, the χ^2 test, and the Student *t*-test were used as appropriate. Data were presented as mean \pm standard deviation (SD), median and range, or percentage. Logistic regression models were constructed to evaluate the association between short-term and long-term outcomes (independent variables) and perioperative MAP, red blood cell (RBC) parameters, and fluid transfusion (dependent variables), adjusting age and sex. $p < 0.05$ is the cut-off point.

3. Results

Admission to NICU totalled about 347 after revascularization surgery, including 237 patients with unilateral and 55 patients with bilateral revascularization. Among them, 255 patients were diagnosed with MMD and 37 patients were diagnosed with moyamoya syndrome (36 unilateral and 1 bilateral). The baseline characteristics of patients are summarized in Table 1. Among these patients, 87 patients presented with cerebral hemorrhage and 229 patients presented with ischemic symptoms as the initial presentation. 303 underwent STA-MCA anastomosis (87.3%), and EDMS were applied in 44 patients (12.7%) under general anesthesia. The follow-up period ranged from 10 months to 31 months. Patients' average mRS score is 0.7 ± 1.10 (Table 1).

Table 2 compares the preoperative and immediate postoperative variables, respectively. After revascularization surgery, the higher the MAP level (favorable group 95.7 ± 11.4 mmHg vs. unfavorable group 103.6 ± 10.4 mmHg, $p < 0.001$) and the greater the MAP variability (favorable group 0.26 ± 13.2 vs. unfavorable group 7.2 ± 13.5 , $p = 0.006$) were in the first 24 h in NICU, the higher the patient's long-term mRS grade was. What is more, a higher early postoperative Hb level also seemed to predict a worse long-term clinical outcome (favorable group 116.9 ± 17.1 g/L vs. unfavorable group 123.7 ± 13.0 g/L, $p = 0.03$), but the difference disappeared after adjusting sex and age. However, a simple statistical comparison did not find that perioperative hemodynamic parameters had any significant effect on the stroke events in 30 days in MMD.

TABLE 1: Demographics and baseline characteristics of patients with MMD.

Variable	Value
Age, y (mean \pm SD)	43.8 \pm 11.4
Sex, male (Num. (%))	171 (49%)
Diagnosis	
Moyamoya disease (Num. (%))	307 (88%)
Moyamoya syndrome (Num. (%))	40 (12%)
Clinical type	
Ischemic (Num. (%))	229 (72%)
Hemorrhagic (Num. (%))	87 (28%)
NIHSS at onset (mean \pm SD)	2.7 \pm 3.6
NIHSS at admission (mean \pm SD)	1.5 \pm 2.2
Suzuki stage	
I (Num. (%))	0 (0%)
II (Num. (%))	11 (3.2%)
III (Num. (%))	92 (26.5%)
IV (Num. (%))	143 (41.2%)
V (Num. (%))	101 (29.1%)
VI (Num. (%))	0 (0%)
Laboratory findings	
Cholesterol (mean \pm SD)	3.8 \pm 0.9
LDL (mean \pm SD)	2.4 \pm 0.9
TG (mean \pm SD)	1.8 \pm 1.1
Glu (mean \pm SD)	5.9 \pm 1.8

Glu: glucose; LDL: low-density lipoprotein; MMD: moyamoya disease; NIHSS: National Institute of Health Stroke Scale; TG: triglyceride.

Logistic regression analyses were further executed. For short-term outcome, a higher level of postoperative MAP ($\beta = 0.024$, 95% CI (0.004, 0.044), and $p = 0.02$) within the first 24 h in NICU might be the risk factor for poor prognosis (Table 3), even after adjusting confounding factors (age and sex). For long-term outcome, the regression analysis indicated that a higher level ($\beta = 1.058$, 95% CI (1.022, 1.096), and $p = 0.001$) and a greater variability ($\beta = 30.982$, 95% CI (2.112, 454.414), and $p = 0.01$) of postoperative MAP might be the predictors of unfavorable mRS grade as shown in Table 3.

4. Discussion

This is the first study with a large sample size to obtain the intensive hemodynamic management of MMD within the 24 h in NICU after revascularization surgery. We found that both high MAP levels and large MAP variability might affect patients' short-term or long-term prognosis. Thus, it is important to strictly control postoperative MAP within normal range and keep it as the preoperative level. What is more, in the first 24 h in NICU, a higher Hb level might result in a worse mRS grade during follow-up.

Based on our results, higher MAP levels and greater variability were independently associated with unfavorable outcomes in MMD. The underlying mechanism of higher

TABLE 2: Characteristics of perioperative hemodynamic parameters grouped by short-term stroke events and long-term mRS.

Variable	Short-term stroke events			<i>p</i> value	Long-term mRS		<i>p</i> value
	1 (<i>n</i> = 179)	2 (<i>n</i> = 123)	3 (<i>n</i> = 45)		Favorable (<i>n</i> = 270)	Unfavorable (<i>n</i> = 31)	
Preoperative MAP (mmHg)	95.3 ± 10.6	97.1 ± 10.6	98.2 ± 12.1	0.18	96.1 ± 10.9	97.4 ± 10.2	0.52
Preoperative RBC parameters							
Hb (g/L)	134.8 ± 16.3	133.7 ± 18.0	135.0 ± 13.7	0.81	133.6 ± 16.7	139.7 ± 13.7	0.06
Hct (%)	40.6 ± 4.2	40.1 ± 4.8	40.5 ± 3.8	0.68	40.2 ± 4.4	41.2 ± 3.6	0.21
RBC (×10 ¹²)	4.5 ± 0.5	4.5 ± 0.5	4.5 ± 0.4	0.77	4.4 ± 0.5	4.6 ± 0.4	0.23
Postoperative MAP (mmHg)	95.7 ± 11.5	97.5 ± 12.3	99.5 ± 10.9	0.11	95.7 ± 11.4	103.6 ± 10.4	<0.001**
Postoperative RBC parameters							
Hb (g/L)	118.7 ± 16.1	116.7 ± 19.7	120.2 ± 14.5	0.43	116.9 ± 17.1	123.7 ± 13.0	0.03*
Hct (%)	35.9 ± 5.1	35.4 ± 10.4	36.4 ± 4.0	0.73	35.4 ± 7.9	37.1 ± 3.8	0.25
RBC (×10 ¹²)	4.3 ± 3.2	4.2 ± 3.5	4.0 ± 0.4	0.84	4.3 ± 3.5	4.1 ± 0.4	0.75
Variability of MAP (%)	1.0 ± 12.9	0.9 ± 13.4	2.2 ± 12.9	0.84	0.26 ± 13.2	7.2 ± 13.5	0.006*
Variability of RBC parameters							
Hb (%)	11.9 ± 10.3	12.6 ± 9.2	10.5 ± 8.1	0.46	12.3 ± 8.7	11.1 ± 8.9	0.47
Hct (%)	-11.9 ± 12.7	-13.1 ± 25.6	-11.8 ± 15.7	0.84	-12.5 ± 19.1	-9.7 ± 9.3	0.41
RBC (%)	-8.6 ± 58.8	-7.6 ± 69.3	-12.0 ± 69.3	0.91	-7.6 ± 66.3	-10.3 ± 8.9	0.82
Fluid transfusion during the first 24 h in NICU (ml)	2674 ± 777.4	2688 ± 640.9	2905 ± 743.9	0.15	2702 ± 744.2	2887 ± 726.7	0.19
Total urine volume during the first 24 h in NICU (ml)	2099 ± 678.9	2073 ± 567.7	2305 ± 694.7	0.11	2093 ± 648.5	2368 ± 748.2	0.02*
Fluid balance during the first 24 h in NICU (ml)	574 ± 564.4	614 ± 583.1	600 ± 512.7	0.84	608 ± 583.1	519 ± 494.4	0.41

p* < 0.05; *p* < 0.001. Hb: hemoglobin; Hct: hematocrit; NICU: neurological intensive care unit; mRS: modified Rankin Scale; MAP: mean artery pressure; RBC: red blood cell.

TABLE 3: Logistic regressions of perioperative factors associated with short-term stroke events and long-term mRS.

	Short-term stroke events		Long-term mRS	
	Adjusted model [†]	<i>p</i> value	Adjusted model [†]	<i>p</i> value
Preoperative MAP	0.020 (0.000, 0.041)	0.06	1.007 (0.973, 1.042)	0.69
Preoperative RBC parameters				
Hb	-0.004 (-0.022, 0.014)	0.65	1.028 (0.995, 1.064)	0.10
Hct	-0.032 (-0.097, 0.032)	0.32	1.047 (0.932, 1.175)	0.44
RBC	-0.312 (-0.891, 0.266)	0.29	1.670 (0.602, 4.631)	0.32
Postoperative MAP	0.024 (0.004, 0.044)	0.02*	1.058 (1.022, 1.096)	0.001*
Postoperative RBC parameters				
Hb	-0.006 (-0.022, 0.010)	0.50	1.025 (0.995, 1.055)	0.10
Hct	-0.010 (-0.039, 0.019)	0.49	1.008 (0.972, 1.045)	0.68
RBC	-0.025 (-0.095, 0.045)	0.48	0.952 (0.789, 1.149)	0.61
Variance of MAP	0.504 (-1.159, 2.167)	0.55	30.982 (2.112, 454.414)	0.01*
Variance of RBC parameters				
Hb	-0.552 (-3.139, 2.035)	0.68	3.996 (0.048, 329.624)	0.54
Hct	-0.319 (-1.524, 0.887)	0.60	1.090 (0.205, 5.792)	0.92
RBC	-0.074 (-0.400, 0.251)	0.66	0.787 (0.265, 2.336)	0.67
Fluid transfusion during the first 24 h in the NICU	0.000 (-2.577, 0.001)	0.07	1.000 (1.000, 1.001)	0.11
Fluid balance during the first 24 h in the NICU	0.000 (0.000, 0.001)	0.48	1.000 (0.999, 1.001)	0.62

Data are presented as β (95% CI) in multivariate regression analyses [†]adjusted for age (in continuous) and sex. **p* < 0.05; ***p* < 0.001. Hb: hemoglobin; Hct: hematocrit; NICU: neurological intensive care unit; mRS: modified Rankin Scale; MAP: mean artery pressure; RBC: red blood cell.

MAP levels might be that fragile collateral vessels cannot tolerate transient changes in cerebral blood flow after revascularization [23]. Thus, a higher level of MAP might lead to intracranial hemorrhage and resulted in devastating consequences. In 2014, Kazomata et al. have also demonstrated that the immediate postoperative intracerebral hemorrhage was associated with a high level of pre- and postoperative BP, especially about systolic BP [12]. Besides, to overcome chronic cerebral hypoperfusion and hypoxia, patients with MMD generally have compensated partially by increasing regional cerebral blood volume and regional oxygen extraction and the cerebrovascular autoregulation have impaired [4, 5, 12, 15, 18, 23]. Bypass surgery theoretically makes patients more vulnerable to an unstable BP, and patients were more likely to suffer from adverse events [5, 15, 18, 23]. Another hazard of higher MAP level is that it may lead to cerebral hyperperfusion syndrome (CHP), which is not rare in postoperative patients with moyamoya disease [11].

A great many reports have confirmed the adverse of BP variability [24–28], but rare studies have focused on the patients with MMD. It seems plausible to understand its relationship with long-term outcomes. Reasons are as follows: (1) BP variability can aggravate the severity because recurrent sudden rises/falls of BP are the contributor of hematoma expanding or ischemia areas increasing [24–26]. (2) BP fluctuations can amplify the secondary brain injury within the potentially viable perihematomal region by directly influencing CBF and CPP [26, 27]. (3) BP rise and fall can disrupt the blood-brain barrier, promote vasogenic brain edema, and cause brain cell death [26, 27]. As for BP was monitored in NICU every half an hour to ensure it is normal (as mentioned in Materials and Methods), BP fluctuations are not as significant as in patients who are not closely monitored. Smaller fluctuations of BP might have more impact on capillaries rather than larger blood vessels. Affecting large blood vessels may lead to early postoperative hematoma expanding or ischemia areas increasing, while affecting capillaries will generally decrease the patient's cognitive function, prolong the recovery period, and worsen the long-term prognosis [24–26, 28]. This maybe the main cause to explain why BP variability is only related to long-term outcomes, but not to short-term prognosis. Besides, in our study, “short-term outcome” was defined as whether patients suffered from recurrent strokes within 30 days after revascularization surgery. Mild damage caused by slight BP variability may not be detected by follow-up CT. We did not classify these invisible patients into the poor short-term prognosis group, leading to bias in the results.

Practically, the fluid management is part of the BP management. Patients with MMD can be hypotensive because preoperative fasting and intraoperative fluid loss often leave them in a state of dehydration [1, 8, 14, 23]. Furthermore, the metabolism of residual anesthetics and the use of mannitol to improve brain edema will exacerbate early postoperative patients' insufficient fluid volume. Fluid management is an easily overlooked issue, and the current articles on systematic assessment of fluid management are limited [23, 29]. Although we did not find that fluid management is related to patient's prognosis, it is reasonable to speculate a

higher Hb level leading to a worse mRS grade is caused by blood concentration and insufficient fluid volume. In other words, insufficient fluid volume in the early postoperative period might be the contributor to the worse prognosis of patients with elevated Hb level. Hemodilution is a way of improving cerebral perfusion and avoiding cerebral ischemia. Actually in our cohort, to avoid hypotension and hypovolemia, each patient was given an intravenous administration of extracellular fluid prophylactically before and after operation.

Except that higher postoperative Hb levels after surgery were suspected to cause a worse long-term prognosis of patients, other RBC-related parameters have little effect on patients during the perioperative period. The principal reason why Hb increased within the 24 h after operation in our study might be blood concentration as we mentioned before. Higher Hb level, higher hematocrit level, and blood concentration can cause increased plasma viscosity and platelet reactivity and may lead to cerebral infarction or cerebral venous thrombosis, although increasing hemoglobin can enhance the carrying capacity of brain oxygen [11, 20]. Moreover, a higher hematocrit level can also lead to intrinsic microcirculatory venous congestion at the site of the STA-MCA anastomosis [20]. Unfortunately, we did not detect the relationship between Hct and patient prognosis. In addition, the suspicious differences caused by hemoglobin disappeared after adjusting for gender and age. More researches are needed.

Our study had some limitations. First, this is a single-center and nonrandomized-controlled trial. Second, it is a retrospective study. Therefore, selection bias may have existed. Larger prospective studies are essential to further investigate how to minimize the incidence of complications for MMD patients after revascularization.

5. Conclusions

The perioperative hemodynamic factors may have a certain impact on the patients' quality of life after revascularization surgery in MMD. Both high postoperative MAP levels and large MAP variability might affect the short-term or long-term prognosis of patients with MMD. What is more, we also found that a higher postoperative Hb level might be related with a worse outcome. These findings need to be confirmed by further research with larger sample populations. Accordingly, exploring an individualized hemodynamic strategy and possibly forming a comprehensive predicting system for perioperative management could be promising to achieve a better outcome for patients with MMD.

Data Availability

The data used to support the findings of this study are available from the corresponding author upon request.

Conflicts of Interest

The authors declare no competing financial interests.

Authors' Contributions

Every author has made important contributions to our research: Jie Song is responsible for analysis of the data and draft the manuscript. Yu Lei is responsible for collection and analysis of the data. Long Chen, Chao Gao, and Wei Ni are responsible for clinical care of the patients, data collection, and organizing the data. Xing Wu and Gang Wu are responsible in taking care of the patients, designing the research, and interpreting the data. Jie Song and Yu Lei contributed equally to the work and share the first authorship.

Acknowledgments

This work was supported by the National Natural Science Foundation of China (grant numbers 81801155, 81771237, and 81761128011), the Shanghai Science and Technology Committee (grant numbers 18511102800 and 16JC1420100), the Shanghai Health and Family Planning Commission (grant number 2017BR022), the Shanghai Municipal Science and Technology 795 Major Project (grant number 2018SHZDZX01), the Program for the Professor of Special Appointment (Eastern Scholar) (grant number SHH1140004), and the Fundamental Research Funds for Central Universities (grant number lzujbky-2015-119). We thank Jin Hu, Ying Mao, and Yuxiang Gu for their efforts to the conception, manuscript revision, supervision, and final approval. And we are also especially grateful to Yuxiang Gu and Bin Xu for their contribution to the revascularization surgeries.

References

- [1] R. M. Scott and E. R. Smith, "Moyamoya disease and moyamoya syndrome," *The New England Journal of Medicine*, vol. 360, no. 12, pp. 1226–1237, 2009.
- [2] S. Kuroda and K. Houkin, "Moyamoya disease: current concepts and future perspectives," *The Lancet Neurology*, vol. 7, no. 11, pp. 1056–1066, 2008.
- [3] F. Yao, Q. Han, Z. Zhang, and Y. Huang, "Assessment of transient cerebral hemodynamic disturbance via whole-brain computed tomography perfusion after extracranial-intracranial bypass in ischemic moyamoya disease," *World Neurosurgery*, vol. 146, pp. e112–e121, 2021.
- [4] S. Miyamoto, T. Yoshimoto, N. Hashimoto et al., "Effects of extracranial-intracranial bypass for patients with hemorrhagic moyamoya Disease," *Stroke*, vol. 45, no. 5, pp. 1415–1421, 2014.
- [5] J. Li, Y. Zhao, M. Zhao et al., "High variance of intraoperative blood pressure predicts early cerebral infarction after revascularization surgery in patients with moyamoya disease," *Neurosurgical Review*, vol. 43, no. 2, pp. 759–769, 2020.
- [6] M. Zhang, J. Tang, N. Liu, Y. Xue, X. Ren, and J. Fu, "Postoperative Functional Outcomes and Prognostic Factors in Two Types of Adult Moyamoya Diseases," *J Stroke Cerebrovasc Dis*, vol. 29, no. 8, article 104846, 2020.
- [7] Research Committee on the Pathology and Treatment of Spontaneous Occlusion of the Circle of Willis and Health Labour Sciences Research Grant for Research on Measures for Intractable Diseases, "Guidelines for diagnosis and treatment of moyamoya disease (spontaneous occlusion of the circle of Willis)," *Neurologia medico-chirurgica*, vol. 52, no. 5, pp. 245–266, 2012.
- [8] L. Thines, G. Petyt, P. Aguetaz et al., "Prise en charge chirurgicale de la maladie et du syndrome de Moyamoya : concepts actuels et experience personnelle," *Revue Neurologique*, vol. 171, no. 1, pp. 31–44, 2015.
- [9] Y. J. Jung, J. S. Ahn, D. H. Kwon, and B. D. Kwun, "Ischemic complications occurring in the contralateral hemisphere after surgical treatment of adults with moyamoya disease," *Journal of Korean Neurosurgical Society*, vol. 50, no. 6, pp. 492–496, 2011.
- [10] J. K. Lee, M. Williams, M. Reyes, and E. S. Ahn, "Cerebrovascular blood pressure autoregulation monitoring and postoperative transient ischemic attack in pediatric moyamoya vasculopathy," *Pediatric Anesthesia*, vol. 28, no. 2, pp. 94–102, 2018.
- [11] J. W. Choi, S. Chong, J. H. Phi et al., "Postoperative symptomatic cerebral infarction in pediatric moyamoya disease: risk factors and clinical outcome," *World Neurosurgery*, vol. 136, pp. e158–e164, 2020.
- [12] K. Kazumata, M. Ito, K. Tokairin et al., "The frequency of postoperative stroke in moyamoya disease following combined revascularization: a single-university series and systematic review," *Journal of Neurosurgery*, vol. 121, no. 2, pp. 432–440, 2014.
- [13] N. Samagh, H. Bhagat, V. K. Grover, N. Sahni, A. Agarwal, and S. K. Gupta, "Retrospective analysis of perioperative factors on outcome of patients undergoing surgery for moyamoya disease," *Journal of Neurosciences in Rural Practice*, vol. 6, no. 2, pp. 262–265, 2015.
- [14] G. N. Williams, W. S. Jones, R. Chaudhry et al., "Intraoperative anesthesiology management and patient outcomes for surgical revascularization for moyamoya disease: a review and clinical experience," *Journal of Neurological Surgery Part A: Central European Neurosurgery*, vol. 80, no. 3, pp. 143–148, 2019.
- [15] S. J. Hyun, J. S. Kim, and S. C. Hong, "Prognostic factors associated with perioperative ischemic complications in adult-onset moyamoya disease," *Acta Neurochirurgica*, vol. 152, no. 7, pp. 1181–1188, 2010.
- [16] M. Fujimura, K. Niizuma, H. Endo et al., "Quantitative analysis of early postoperative cerebral blood flow contributes to the prediction and diagnosis of cerebral hyperperfusion syndrome after revascularization surgery for moyamoya disease," *Neurological Research*, vol. 37, no. 2, pp. 131–138, 2015.
- [17] H. Pan, W. Shi, H. Li, H. Zhang, C. Li, and Y. Wang, "Clinical prediction of surgical revascularization outcome in moyamoya disease via transcranial color sonography," *Journal of Stroke and Cerebrovascular Diseases*, vol. 29, no. 11, article 105154, 2020.
- [18] W. Park, J. S. Ahn, H. S. Lee, J. C. Park, and B. D. Kwun, "Risk factors for newly developed cerebral infarction after surgical revascularization for adults with moyamoya disease," *World Neurosurgery*, vol. 92, pp. 65–73, 2016.
- [19] S. Takahashi and T. Horiguchi, "Relationship between ischaemic symptoms during the early postoperative period in patients with moyamoya disease and changes in the cerebellar asymmetry index," *Clinical Neurology and Neurosurgery*, vol. 197, article 106090, 2020.
- [20] M. Katsuki, M. Fujimura, R. Tashiro, Y. Tomata, T. Nishizawa, and T. Tominaga, "Pre-operative higher hematocrit and lower total protein levels are independent risk factors for cerebral hyperperfusion syndrome after superficial temporal artery-

middle cerebral artery anastomosis with pial synangiosis in adult moyamoya disease patients-case-control study,” *Neurosurgical Review*, vol. 44, no. 4, pp. 2191–2200, 2021.

- [21] M. Fukui and Members of the Research Committee on Spontaneous Occlusion of the Circle of Willis (Moyamoya Disease) of the Ministry of Health and Welfare, Japan, “Guidelines for the diagnosis and treatment of spontaneous occlusion of the circle of Willis (‘Moyamoya’ disease),” *Clinical Neurology and Neurosurgery*, vol. 99, Supplement 2, pp. S238–S240, 1997.
- [22] A. Rosi, C. P. Riordan, E. R. Smith, R. M. Scott, and D. B. Orbach, “Clinical status and evolution in moyamoya: which angiographic findings correlate?,” *Brain Communications*, vol. 1, no. 1, 2019.
- [23] C. Li, N. Zhang, S. Yu et al., “Individualized perioperative blood pressure management for adult moyamoya disease: experience from 186 consecutive procedures,” *Journal of Stroke and Cerebrovascular Diseases*, vol. 30, no. 1, article 105413, 2021.
- [24] P. Castro, F. Ferreira, C. K. Nguyen et al., “Rapid assessment of blood pressure variability and outcome after successful thrombectomy,” *Stroke*, vol. 52, no. 9, pp. e531–e535, 2021.
- [25] T. J. Kim, H. K. Park, J. M. Kim et al., “Blood pressure variability and hemorrhagic transformation in patients with successful recanalization after endovascular recanalization therapy: A retrospective observational study,” *Annals of Neurology*, vol. 85, no. 4, pp. 574–581, 2019.
- [26] P. W. Chung, J. T. Kim, N. Sanossian et al., “Association between hyperacute stage blood pressure variability and outcome in patients with spontaneous intracerebral hemorrhage,” *Stroke*, vol. 49, no. 2, pp. 348–354, 2018.
- [27] K. Tziomalos, V. Giampatzis, S. D. Bouziana et al., “No association observed between blood pressure variability during the acute phase of ischemic stroke and in-hospital outcomes,” *American Journal of Hypertension*, vol. 29, no. 7, pp. 841–846, 2016.
- [28] P. Jia, H. Lee, J. Chan, K. Yiu, and K. Tsoi, “Long-term blood pressure variability increases risks of dementia and cognitive decline: a meta-analysis of longitudinal studies,” *Hypertension*, vol. 78, no. 4, pp. 996–1004, 2021.
- [29] W. Y. Jo, H. Oh, H. Kim et al., “Preoperative platelet count may predict postoperative symptomatic cerebral hyperperfusion syndrome after superficial temporal artery-middle cerebral artery anastomosis in moyamoya patients,” *Clinical Neurology and Neurosurgery*, vol. 199, article 106260, 2020.

Review Article

Effect of Acupuncture on Cognitive Function of Insomnia Patients Compared with Drugs: A Protocol for Meta-analysis and Systematic Review

Shan Qin,¹ Jing Jiang^{ID},¹ Wen-Zhong Wu,¹ Xiao-Qiu Wang,¹ Han-Qing Xi,¹ Qin-Qin Fang^{ID},¹ Bin Xu,² and Cheng-Yong Liu^{ID}¹

¹Jiangsu Province Hospital of Chinese Medicine, Affiliated Hospital of Nanjing University of Chinese Medicine, Nanjing 210029, China

²Nanjing University of Chinese Medicine, China

Correspondence should be addressed to Cheng-Yong Liu; lcy8601@163.com

Received 22 July 2021; Accepted 30 August 2021; Published 13 September 2021

Academic Editor: Muh-Shi Lin

Copyright © 2021 Shan Qin et al. This is an open access article distributed under the Creative Commons Attribution License, which permits unrestricted use, distribution, and reproduction in any medium, provided the original work is properly cited.

Insomnia, one of the most common sleep disorders, is thought to have an adverse effect on cognitive function. At the same time, people with cognitive dysfunction are more prone to insomnia. At present, pharmacotherapy is the main treatment for insomnia, but there are some shortcomings such as poor long-term efficacy and potential dependence. There is some evidence that acupuncture has some advantages in alleviating insomnia and improving cognitive function. This study is aimed at investigating the effects of acupuncture and drugs on cognitive function in patients with insomnia and evaluating the efficacy and safety of these two interventions, providing strong evidence for clinical decision-making. The study will retrieve eight major databases: China National Knowledge Infrastructure, Wanfang Database, VIP Database for Chinese Technical Periodicals, SinoMed, PubMed, Web of Science, Embase, and Cochrane Library. Dissertations, conference papers, and ongoing experiments will also be retrieved for supplement. Literature screening and data extraction will be completed by two authors independently (JJ and X-QW). If there were any disagreements, they would be discussed or referred to a third person for adjudication (W-ZW). Authors will use Cochrane risk of bias tool to assess the included studies. The Review Manager Statistical (RevMan) software is used to conduct the statistical process of meta-analysis, and funnel plot is used to evaluate reporting biases. The Grading of Recommendations Assessment Development and Evaluation (GRADE) Profiler can be used to be aware of the quality of evidence.

1. Introduction

Insomnia is one of the most common sleep disorders [1], which is mainly manifested as dissatisfaction with sleep time and quality, accompanied by daytime dysfunction, even if there is a good sleep environment and sleep opportunities [2]. One-third of the population in the United States is affected by insomnia, among which the elderly are the most common [3]. Meanwhile, compared with men, women are more prone to insomnia [4]. With the development of society, work pressure, and interpersonal conflict, the incidence of insomnia is still on the rise [5]. In addition to the health risks, insomnia also carries a substantial economic burden,

costing society up to 100 billion dollars a year [6]. Studies have shown that insomnia can lead to cognitive function decline in patients through accumulation of amyloid-beta protein and increase of inflammatory factors [7]. They have deficits in attention, memory, and executive function. Furthermore, there is an increased risk of safety accidents and complications such as dysphagia and diabetes [8–11]. Insomnia and dementia influence each other. Dementia patients are more likely than the general population to suffer from insomnia, showing reduced sleep efficiency, increased nocturnal arousal, and early wakefulness [12]. There is still no way to completely cure dementia, but there are ways to prevent it by treating insomnia. Treatments for insomnia

include psychotherapy, pharmacotherapy, and complementary and alternative therapies [13]. Among them, pharmacotherapy is the main way to treat insomnia at present [14]. The clinically commonly used sedative and hypnotic drugs are benzodiazepine receptor agonists, which are characterized by rapid absorption and quick action, but also have side effects such as “next day hangover” and potential dependence. At the same time, this drug can increase the risk of falling [15]. There are literatures which have been proved that acupuncture can effectively improve the quality of sleep and cognitive function [16–19]. It mainly improves the body’s self-regulation ability and self-recovery ability by acting on different acupoints, to achieve the therapeutic effect [20], and has the advantages of easy operation, no adverse reactions, and extensive indications [21]. There is currently no evidence to prove the difference in efficacy and safety between acupuncture and drugs in cognitive function of insomnia patients. This meta-analysis is the first quantitative study to compare acupuncture with drugs from this perspective and to analyze whether acupuncture is effective for any type of insomnia.

2. Materials and Methods

This protocol was registered at PROSPERO and written based on the guideline of Preferred Reporting Items for Systematic Reviews and Meta-analyses Protocol (PRISMA-P) [22]. Details can be viewed in the Supplementary Table S1. PROSPERO registration number is CRD42021246046.

2.1. Criteria for Included Studies

2.1.1. Types of Studies. The study will take into account all relevant randomized controlled trials. Language and publication status is not restricted. Studies that do not specify the method of randomization, but only mention randomization, also can be included. Blindness and allocation concealment are not confined. Clinical controlled trials also meet the requirements of the study and can be included.

2.1.2. Types of Participants. Patients will be enrolled as long as they meet the diagnostic criteria for insomnia. There are no restrictions on gender, age, or nationality. Diagnostic criteria for insomnia are the following: International Statistical Classification of Diseases and Related Health Problems Version 10 (ICD-10) [23], Diagnostic and Statistical Manual of Mental Disorders Version 5 (DSM-5) [24], and International Classification of Sleep Disorder Version 3 (ICSD-3) [25]. Patients meeting other internationally recognized diagnostic criteria can also be included. If the diagnostic criteria are not clearly stated, the author will be contacted for further information [26]. Whether the patient is chronic insomnia or acute insomnia, simple insomnia or comorbid insomnia can be included.

2.1.3. Types of Intervention. The experimental group received acupuncture as intervention measure, and any form of acupuncture could be included, including electroacupuncture, filiform needle therapy, body acupuncture, and auricular acupuncture. In acupuncture acupoints, the time and

frequency of treatment are not limited. The control group was treated by drugs with insomnia treatment indications, including benzodiazepine receptor agonists, melatonin receptor agonists, antihistamine H1 receptor drugs, and orexin receptor antagonists. Studies using sham acupuncture in control groups will not be included. Myocardial infarction, diabetes, Parkinson’s disease, and some other diseases are closely related to the decline of cognitive function [27–29]. The growth of age also affects people’s cognitive function, so elderly insomnia and comorbid insomnia are more prone to cognitive decline [30]. The study will allow the elderly with underlying diseases and comorbid insomnia patients to use basic drugs, but the control group and the experimental group must be used at the same time.

2.1.4. Types of Outcomes. The primary outcome indicators are the Montreal Cognitive Assessment Scale (MOCA) [31]. Secondary outcome indicators are Pittsburgh Sleep Quality Index (PSQI), Insomnia Severity Index Scale (ISI) [32, 33], and the incidence of adverse events.

2.1.5. Exclusion Criteria. Research has critical data missing, and data cannot be obtained. Research that uses wrong randomized methods will be excluded (such as generating random sequences based on parity of birth dates); combination therapy should be excluded (for example, studies using acupuncture combined with cognitive behavioral therapy). Studies with a sample size less than 30 cases should be excluded.

2.2. Search Strategy

2.2.1. Electronic Searches. Eight databases will be retrieved: China National Knowledge Infrastructure, Wanfang Database, VIP Database for Chinese Technical Periodicals, SinoMed, PubMed, Web of Science, Embase, and Cochrane Library. Retrieval time is from database inception to March 1, 2021. MeSH (Medical Subject Headings) and free text (title and abstract) will be combined to search. These MESHs will be included: acupuncture, needling, acupuncture and moxibustion, acupuncture therapy, electroacupuncture, cognition, cognitive function, insomnia, sleep initiation and maintenance disorders, randomized controlled trial, trial, randomly, randomized, and rct. The Chinese database will use the Chinese translation of the above search terms. The retrieval process of Embase can be seen in the Supplementary Table S2.

2.2.2. Other Resources. Data from unpublished randomized controlled trials is available on the International Clinical Trials Registry, ClinicalTrials.gov, and Chinese Clinical Trial Registry. In addition, we will retrieve conference papers and dissertations to ensure that all randomized controlled trials that meet the criteria are retrieved to the maximum extent possible.

2.3. Data Collection and Analysis

2.3.1. Selection of Studies. Literature retrieval and screening will be conducted independently by two authors (H-QX and Q-QF). First of all, duplicate literatures will be excluded,

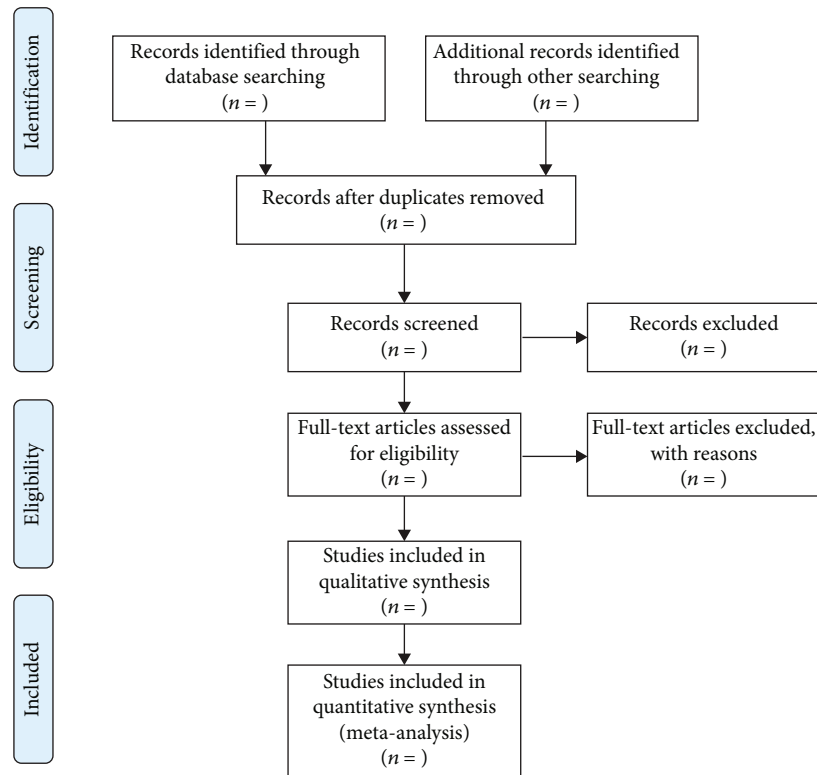


FIGURE 1

and a preliminary screening is conducted according to the title and abstract. Then, the literature that meets the standards will be screened by reading the full text. If there is a disagreement, the literature should be discussed or submitted to a third person (W-ZW) for evaluation. The EndNote software is used for literature management, and the reasons for exclusion should be recorded for excluded studies. Figure 1 shows the process of literature screening in this research.

2.3.2. Data Extraction. Two authors (JJ and X-QW) will independently produce a table to complete the data extraction work. The data extraction form includes the first author's name, publication year, follow-up situation, sample size, intervention measures, outcome, allocation concealment, randomization, selective reporting, blind method, integrity of outcome data, and the characteristics of the subjects (age, gender, course of disease, and educational level). If the results of the data extraction diverge, they are discussed or referred to a third person (W-ZW) for adjudication.

2.3.3. Assessment of Risk of Bias in the Included Studies. This study will appraise the risk of bias according to the Cochrane Handbook bias risk assessment tool [34]. The risks of bias include selection bias, performance bias, detection bias, attrition bias, and reporting bias. The study will be classified into low risk of bias, high risk of bias, and unclear risk of bias. The two authors (H-QX and Q-QF) make the assessment, and if there is a disagreement, they discuss it or refer it to a third person (W-ZW).

2.3.4. Dealing with Missing Data. If the required data is lacking, the author of the article will be contacted for relevant information, and if the data is still not available, the study with missing data will be excluded.

2.3.5. Assessment of Heterogeneity. Heterogeneity is divided into clinical heterogeneity, methodological heterogeneity, and statistical heterogeneity. The clinical and methodological heterogeneity of the included studies is first assessed, and if the clinical heterogeneity is excessive, subgroup analysis will be performed based on clinical characteristics. Q statistic and I^2 statistic are used to complete the statistical heterogeneity assessment [35]. $P \geq 0.1$ and $I^2 \leq 25\%$ indicate low heterogeneity. $P < 0.1$ and $I^2 > 50\%$ indicate high heterogeneity. The source of heterogeneity should be carefully analyzed when $I^2 \geq 75$.

2.3.6. Assessment of Reporting Biases. If more than ten articles are included [36], the existence of reporting biases could be evaluated by the symmetry of the funnel plot.

2.3.7. Data Synthesis. The RevMan software will be used for data processing. The effect index of the continuity variables is SMD (standardized mean difference) with 95% CIs (95% confidence intervals), and the categorical variable is RR (relative risk) and with 95% CIs, both of which are analyzed by inverse square examination. Considering the potential heterogeneity among acupuncture studies, this study will put to use the random effects model. If the heterogeneity is too large to identify its possible source, only descriptive analysis will be performed [37].

2.3.8. Subgroup Analysis. If the included studies show obvious clinical heterogeneity, subgroup analysis will be conducted according to clinical characteristics. In this study, we will conduct subgroup analysis according to the gender and age of patients, the types of insomnia (such as simple insomnia/comorbid insomnia), acupuncture points, treatment duration and frequency, and acupuncture methods (such as electroacupuncture/filiform needle).

2.3.9. Sensitivity Analysis. This study will carry out sensitivity analysis by changing the effect indicators, statistical model, and deleting each included study one by one [38] to verify the stability of the study results. If different conclusions are reached, the results of the meta-analysis are carefully obtained by discussion between the two authors (SQ and W-ZW) or by evaluation by a third person (X-QW).

2.4. Evidence Quality Evaluation. Cochrane Handbook bias risk assessment tool and GRADE Profiler are used to evaluate the quality of evidence by evaluating the factors that reduce the quality of evidence (risk of bias, inconsistency, indirectness, imprecision, publication bias) and the factors that increase the quality of evidence (large effect value, confounding factors that reduce efficacy, dose-effect relation) [39]. Evidence quality can be divided into four grades: high, medium, low, and very low [40].

3. Discussion

The adverse effects of insomnia and cognitive decline have caused a considerable burden on individuals, families, and society, while the incidence of insomnia and dementia continues to rise. Correct measures for patients with insomnia help to avoid the continuous deterioration of the situation. Therefore, we urgently need a relevant meta-analysis to provide reliable evidence for medical decision-making. There have been meta-analyses on acupuncture for insomnia, but they only focused on the effects of acupuncture on sleep and did not study from the perspective of acupuncture improving cognitive function in patients with insomnia [41–45]. Different from some studies only included in patients with comorbid insomnia [41–43]; this study as long as patients meet the diagnostic criteria of insomnia, whether simple insomnia or comorbid insomnia, can be included. Although it may increase the heterogeneity of the study, we can analyze whether acupuncture is effective for any type of insomnia. This study mainly includes four aspects: determining the inclusion and exclusion criteria and retrieval strategies, screening out all eligible randomized controlled trials at home and abroad, data extraction, data analysis, and processing. The study will also strive to obtain reliable conclusions through heterogeneity test, subgroup analysis, and sensitivity analysis. In addition, this study collected the relevant data of adverse events and compared the safety of acupuncture and drugs while understanding their efficacy. However, this study also has limitations: by comparing acupuncture with drugs alone, we cannot prove which is the best choice among all treatment options for improving cognitive function in insomnia

patients. If the study does not include enough high-quality randomized controlled trials, the results of meta-analysis may be affected. The electronic databases of countries such as Korea and Japan will not be searched, which may lead to the existence of selective bias [46]. Different acupuncture methods may increase the heterogeneity of the study, but we will conduct a subgroup analysis to address this issue. In addition to insomnia, cognitive decline is associated with a variety of causes, including age and neurodegenerative disease, and there is no way to determine whether the decline in cognitive function in the included patients is due to insomnia.

4. Conclusion

This is a protocol for systematic review and meta-analysis. It mainly describes the specific methods for conducting the research, aiming to make the evidence provided by meta-analysis more powerful and accurate.

Data Availability

The data analyzed and used to prepare this study are available from the corresponding author upon rational request.

Disclosure

What we write is a protocol for meta-analysis and systematic review. We will not violate the privacy and rights of any patient. The results will be published in peer-reviewed journals and at related conferences.

Conflicts of Interest

The authors declare that they have no conflicts of interest.

Authors' Contributions

Co-first authors JJ and SQ made equal contributions. JJ, SQ, and W-ZW conceived this study. JJ, SQ, and H-QX drafted this manuscript. JJ and X-QW designed the literature retrieval strategy. X-QW, Q-QF, and W-ZW revised the manuscript. C-YL is the supervisor of this review. All authors approved the final version of the manuscript.

Acknowledgments

This work was supported by the Cadre Health Research Project of Jiangsu Provincial Health Commission (Grant Number BJ19024).

Supplementary Materials

Table S1: PRISMA-P Checklist. This protocol was written based on the guideline of Preferred Reporting Items for Systematic Reviews and Meta-analyses Protocol (PRISMA-P), and Supplementary Table S1 shows the details of checklist. Table S2: search strategy: EMBASE. Details of EMBASE's Search strategy can be seen in the Supplementary Table S2. (*Supplementary Materials*)

References

- ## References
- [1] D. Burman, "Sleep disorders: insomnia," *FP Essentials*, vol. 460, pp. 22–28, 2017.
 - [2] P. Zhang and Z. Zhao, "Pay attention to the clinical practice of adult insomnia diagnosis and treatment guidelines," *Zhonghua Shen Jing Ke Za Zhi*, vol. 51, no. 8, pp. 561–564, 2018.
 - [3] P. C. Bollu and H. Kaur, "Sleep medicine: insomnia and sleep," *Missouri Medicine*, vol. 116, no. 1, pp. 68–75, 2019.
 - [4] M. A. Grandner, "Sleep, health, and society," *Sleep Medicine Clinics*, vol. 15, no. 2, pp. 319–340, 2020.
 - [5] D. Riemann, C. Baglioni, C. Bassetti et al., "European guideline for the diagnosis and treatment of insomnia," *Journal of Sleep Research*, vol. 26, no. 6, pp. 675–700, 2017.
 - [6] P. Taddei-Allen, "Economic burden and managed care considerations for the treatment of insomnia," *The American Journal of Managed Care*, vol. 26, 4 Supplement, pp. S91–S96, 2020.
 - [7] S. Sadeghmousavi, M. Eskian, F. Rahmani, and N. Rezaei, "The effect of insomnia on development of Alzheimer's disease," *Journal of Neuroinflammation*, vol. 17, no. 1, p. 289, 2020.
 - [8] K. Jash, P. Gondaliya, P. Kirave, B. Kulkarni, A. Sunkaria, and K. Kalia, "Cognitive dysfunction: a growing link between diabetes and Alzheimer's disease," *Drug Development Research*, vol. 81, no. 2, pp. 144–164, 2020.
 - [9] M. C. Espinosa-Val, A. Martín-Martínez, M. Graupera et al., "Prevalence, risk factors, and complications of oropharyngeal dysphagia in older patients with dementia," *Nutrients*, vol. 12, no. 3, p. 863, 2020.
 - [10] J. A. Brownlow, K. E. Miller, and P. R. Gehrman, "Insomnia and cognitive performance," *Sleep Medicine Clinics*, vol. 15, no. 1, pp. 71–76, 2020.
 - [11] F. Yu and Z. Zhou, "Advances in research on sleep disorders and cognitive disorders," *Chinese Journal of Stroke*, vol. 11, no. 11, pp. 966–972, 2016.
 - [12] L. Ferini-Strambi, A. Galbiati, F. Casoni, and M. Salsone, "Therapy for insomnia and circadian rhythm disorder in Alzheimer disease," *Current Treatment Options in Neurology*, vol. 22, no. 2, p. 4, 2020.
 - [13] A. Qaseem, D. Kansagara, M. A. Forciea, M. Cooke, T. D. Denberg, and for the Clinical Guidelines Committee of the American College of Physicians, "Management of chronic insomnia disorder in adults: a clinical practice guideline from the American College of Physicians," *Annals of Internal Medicine*, vol. 165, no. 2, pp. 125–133, 2016.
 - [14] Z. Wang, W. Xie, J. Que et al., "Progress in the treatment of insomnia disorder by Zaoren Anshen capsule," *Chinese Journal of Drug Dependence*, vol. 26, no. 6, pp. 407–410, 2017.
 - [15] Y. Jiang, Q. Xia, J. Wang et al., "Insomnia, benzodiazepine use, and falls among residents in long-term care facilities," *International Journal of Environmental Research and Public Health*, vol. 16, no. 23, p. 4623, 2019.
 - [16] L. Zhang, Y. Tang, R. Hui et al., "The effects of active acupuncture and placebo acupuncture on insomnia patients: a randomized controlled trial," *Psychology, Health & Medicine*, vol. 25, no. 10, pp. 1201–1215, 2020.
 - [17] Y. K. Wang, T. Li, L. J. Ha et al., "Effectiveness and cerebral responses of multi-points acupuncture for primary insomnia: a preliminary randomized clinical trial and fMRI study," *BMC Complementary Medicine and Therapies*, vol. 20, no. 1, p. 254, 2020.
 - [18] Y. Jia, X. Zhang, J. Yu et al., "Acupuncture for patients with mild to moderate Alzheimer's disease: a randomized controlled trial," *BMC Complementary and Alternative Medicine*, vol. 17, no. 1, p. 556, 2017.
 - [19] J. W. Yang, G. X. Shi, S. Zhang et al., "Effectiveness of acupuncture for vascular cognitive impairment no dementia: a randomized controlled trial," *Clinical Rehabilitation*, vol. 33, no. 4, pp. 642–652, 2019.
 - [20] H. Liu, "Mechanism of acupuncture and moxibustion treatment on the correlation between acupoints, meridians and viscera," *Liaoning Journal of Traditional Chinese Medicine*, vol. 29, no. 3, p. 170, 2002.
 - [21] B. LIU, "Acupuncture should be the pioneer of complementary advantages and coordinated development of Chinese and western medicine," *Zhongguo Zhen Jiu*, vol. 41, no. 1, p. 1, 2021.
 - [22] PRISMA-P Group, D. Moher, L. Shamseer et al., "Preferred reporting items for systematic review and meta-analysis protocols (PRISMA-P) 2015 statement," *Systematic Reviews*, vol. 4, no. 1, p. 1, 2015.
 - [23] World Health Organization, *International Classification of Diseases, ICD*, People's Medical Publishing House, Bei Jing, 2008.
 - [24] American Psychiatric Association, *Diagnostic and statistical manual of mental disorders*, Peking University Press, Bei Jing, 5th edition, 2013.
 - [25] American Academy of Sleep Medicine, *International classification of sleep disorders*, People's Medical Publishing House, Bei Jing, 3th edition, 2014.
 - [26] D. Li, L. Zhu, and D. Liu, "Acupuncture for refractory gastroesophageal reflux disease: a systematic review and meta-analysis protocol," *BMJ Open*, vol. 9, no. 8, article e030713, 2019.
 - [27] J. G. Goldman and E. Sieg, "Cognitive impairment and dementia in Parkinson disease," *Clinics in Geriatric Medicine*, vol. 36, no. 2, pp. 365–377, 2020.
 - [28] C. L. Lin, W. C. Chien, C. H. Chung, and F. L. Wu, "Risk of type 2 diabetes in patients with insomnia: a population-based historical cohort study," *Diabetes/Metabolism Research and Reviews*, vol. 34, no. 1, 2018.
 - [29] N. G. Altman, B. Izci-Balserak, E. Schopfer et al., "Sleep duration versus sleep insufficiency as predictors of cardiometabolic health outcomes," *Sleep Medicine*, vol. 13, no. 10, pp. 1261–1270, 2012.
 - [30] J. M. Dzierzewski, N. Dautovich, and S. Ravyts, "Sleep and cognition in older adults," *Sleep Medicine Clinics*, vol. 13, no. 1, pp. 93–106, 2018.
 - [31] Z. S. Nasreddine, N. A. Phillips, V. Å.©. BÅ©dirian et al., "The Montreal Cognitive Assessment, MoCA: a brief screening tool for mild cognitive impairment," *Journal of the American Geriatrics Society*, vol. 53, no. 4, pp. 695–699, 2005.
 - [32] D. J. Buysse, C. F. Reynolds III, T. H. Monk, S. R. Berman, and D. J. Kupfer, "The Pittsburgh Sleep Quality Index: a new instrument for psychiatric practice and research," *Psychiatry Research*, vol. 28, no. 2, pp. 193–213, 1989.
 - [33] C. M. Morin, G. Belleville, L. Bélanger, and H. Ivers, "The Insomnia Severity Index: psychometric indicators to detect insomnia cases and evaluate treatment response," *Sleep*, vol. 34, no. 5, pp. 601–608, 2011.
 - [34] C. Álvarez-Bueno, C. Pesce, I. Caverro-Redondo, M. Sánchez-López, M. J. Pardo-Guijarro, and V. Martínez-Vizcaino,

- “Association of physical activity with cognition, metacognition and academic performance in children and adolescents: a protocol for systematic review and meta-analysis,” *BMJ Open*, vol. 6, no. 6, article e011065, 2016.
- [35] K. T. Houghton, A. Forrest, A. Awad et al., “Biological rationale and potential clinical use of gabapentin and pregabalin in bipolar disorder, insomnia and anxiety: protocol for a systematic review and meta-analysis,” *BMJ Open*, vol. 7, no. 3, article e013433, 2017.
 - [36] R. Ren, J. Zhang, T. Zhang, Y. Peng, C. Tang, and Q. Zhang, “Auriculotherapy for sleep quality in people with primary insomnia: a protocol for a systematic review and meta-analysis,” *Medicine (Baltimore)*, vol. 98, no. 8, article e14621, 2019.
 - [37] J. Zhou, W. Peng, W. Li, and Z. Liu, “Acupuncture for patients with Alzheimer’s disease: a systematic review protocol,” *BMJ Open*, vol. 4, no. 8, article e005896, 2014.
 - [38] Z. Li, Y. Zhang, Y. Wang, X. Yan, and P. Xie, “Electroacupuncture for primary insomnia: protocol for a systematic review and meta-analysis,” *Medicine (Baltimore)*, vol. 97, no. 27, article e11063, 2018.
 - [39] H. Balshem, M. Helfand, H. J. Schünemann et al., “GRADE guidelines: 3. Rating the quality of evidence,” *Journal of Clinical Epidemiology*, vol. 64, no. 4, pp. 401–406, 2011.
 - [40] L. Shamseer, D. Moher, M. Clarke et al., “Preferred reporting items for systematic review and meta-analysis protocols (PRISMA-P) 2015: elaboration and explanation,” *BMJ*, vol. 349, p. g7647, 2015.
 - [41] T. Y. Choi, J. I. Kim, H. J. Lim, and M. S. Lee, “Acupuncture for managing cancer-related insomnia: a systematic review of randomized clinical trials,” *Integrative Cancer Therapies*, vol. 16, no. 2, pp. 135–146, 2017.
 - [42] F. Liu, J. You, Q. Li et al., “Acupuncture for Chronic Pain-Related Insomnia: A Systematic Review and Meta-Analysis,” *Evidence-based Complementary and Alternative Medicine*, vol. 2019, Article ID 5381028, 10 pages, 2019.
 - [43] B. Dong, Z. Chen, X. Yin et al., “The efficacy of acupuncture for treating depression-related insomnia compared with a control group: a systematic review and meta-analysis,” *BioMed Research International*, vol. 2017, Article ID 9614810, 11 pages, 2017.
 - [44] J. Zhang, Y. He, X. Huang, Y. Liu, and H. Yu, “The effects of acupuncture versus sham/placebo acupuncture for insomnia: a systematic review and meta-analysis of randomized controlled trials,” *Complementary Therapies in Clinical Practice*, vol. 41, p. 101253, 2020.
 - [45] F. Y. Zhao, Q. Q. Fu, G. A. Kennedy et al., “Can acupuncture improve objective sleep indices in patients with primary insomnia? A systematic review and meta-analysis,” *Sleep Medicine*, vol. 80, pp. 244–259, 2021.
 - [46] Z. Gao, C. M. Giovanardi, H. Li et al., “Acupuncture for migraine: a protocol for a meta-analysis and meta-regression of randomised controlled trials,” *BMJ Open*, vol. 8, no. 11, article e022998, 2019.

Research Article

Use of Deep-Learning Genomics to Discriminate Healthy Individuals from Those with Alzheimer's Disease or Mild Cognitive Impairment

Lanlan Li,¹ Yeying Yang,² Qi Zhang,¹ Jiao Wang,³ Jiehui Jiang^{ID},¹
and Alzheimer's Disease Neuroimaging Initiative⁴

¹Institute of Biomedical Engineering, School of Communication and Information Engineering, Shanghai University, Shanghai 200444, China

²LongHua Hospital, Shanghai University of Traditional Chinese Medicine, Shanghai 200032, China

³School of Life Science, Shanghai University, Shanghai 200444, China

⁴Indiana University School of Medicine, Indianapolis, IN 46202, USA

Correspondence should be addressed to Jiehui Jiang; jiangjiehui@shu.edu.cn

Received 14 May 2021; Accepted 11 June 2021; Published 15 July 2021

Academic Editor: Muh-Shi Lin

Copyright © 2021 Lanlan Li et al. This is an open access article distributed under the Creative Commons Attribution License, which permits unrestricted use, distribution, and reproduction in any medium, provided the original work is properly cited.

Objectives. Alzheimer's disease (AD) is the most prevalent neurodegenerative disorder and the most common form of dementia in the elderly. Certain genes have been identified as important clinical risk factors for AD, and technological advances in genomic research, such as genome-wide association studies (GWAS), allow for analysis of polymorphisms and have been widely applied to studies of AD. However, shortcomings of GWAS include sensitivity to sample size and hereditary deletions, which result in low classification and predictive accuracy. Therefore, this paper proposes a novel deep-learning genomics approach and applies it to multitasking classification of AD progression, with the goal of identifying novel genetic biomarkers overlooked by traditional GWAS analysis. **Methods.** In this study, we selected genotype data from 1461 subjects enrolled in the Alzheimer's Disease Neuroimaging Initiative, including 622 AD, 473 mild cognitive impairment (MCI), and 366 healthy control (HC) subjects. The proposed deep-learning genomics (DLG) approach consists of three steps: quality control, coding of single-nucleotide polymorphisms, and classification. The ResNet framework was used for the DLG model, and the results were compared with classifications by simple convolutional neural network structure. All data were randomly assigned to one training/validation group and one test group at a ratio of 9:1. And fivefold cross-validation was used. **Results.** We compared classification results from the DLG model to those from traditional GWAS analysis among the three groups. For the AD and HC groups, the accuracy, sensitivity, and specificity of classification were, respectively, $98.78 \pm 1.50\%$, $98.39\% \pm 2.50\%$, and $99.44\% \pm 1.11\%$ using the DLG model, while $71.38\% \pm 0.63\%$, $63.13\% \pm 2.87\%$, and $85.59\% \pm 6.66\%$ using traditional GWAS. Similar results were obtained from the other two intergroup classifications. **Conclusion.** The DLG model can achieve higher accuracy and sensitivity when applied to progression of AD. More importantly, we discovered several novel genetic biomarkers of AD progression, including rs6311 and rs6313 in HTR2A, rs1354269 in NAV2, and rs690705 in RFC3. The roles of these novel loci in AD should be explored in future research.

1. Introduction

Alzheimer's disease (AD) is the most common type of dementia and is an irreversible, progressive neurological brain disorder typically beginning with mild memory decline; in time, it can seriously impair an individual's ability to carry out daily activities and lead to loss of autonomy [1, 2]. Mild cognitive impairment (MCI) is a preclinical stage of AD, in which individuals have no obvious cognitive behavioral symptoms but can show subtle prodromal signs of dementia [3, 4]. It is widely recognized that early detection of AD and MCI is essential to slowing progression.

Among factors that influence AD progression, common genetic variants are major risk factors [5]. Currently, the development of cheap comprehensive genetic testing of peripheral blood has brought dramatic changes to studies of the mechanisms of disease development. In recent decades, several genes have been associated with AD risk based on full-genome genotyping arrays using blood samples [6, 7]. For instance, genomics analysis showed APOE to be the most strongly associated AD risk gene [8]. In addition, the CLU, PICALM, SORL1, BIN1, and TOMM40 genes have also been identified as AD risk factors in the literature [7, 9, 10].

Technological advances [11] have allowed analysis of millions of nucleotide polymorphisms from thousands of subjects, including advanced genome-wide association studies (GWAS) and whole genome sequencing [12–16] that have increased our understanding of the genetic complexity of AD susceptibility. For instance, recent GWAS from the Alzheimer's Disease Neuroimaging Initiative (ADNI) have related known AD risk genes to differences in rates of brain atrophy and biomarkers of AD in the cerebrospinal fluid [17]. Moreover, the International Genomics of Alzheimer's Project studied 74046 participants, confirming nearly all of the previous genetic risk factors and identifying 12 new susceptibility loci for AD [18]. Therefore, genomics analysis, especially GWAS analysis, has yielded important advances in AD research.

However, there are some limitations of GWAS. Firstly, traditional GWAS intergroup analysis is distorted by differences in sample sizes [19]. Secondly, traditional GWAS analysis is strongly dependent on prior knowledge and hand coding, which requires much time and energy and risks bias or errors in data entry [16] that can result in poor repeatability. Moreover, although traditional GWAS analysis can assure high specificity of disease screening, accuracy, and sensitivity are relatively low. In practice, false positives are preferred over false negatives in order to avoid omissions in disease screening. Therefore, alternative analytical tools would help to drive novel hypotheses and models.

Deep-learning algorithms implemented via deep neural networks can automatically embed computational features to yield end-to-end models that facilitate discovery of relevant highly complex features [20]. Seminal studies in 2015 demonstrated the applicability of deep neural networks to DNA sequence data [21, 22]. Deep convolutional neural networks (CNNs) have been used in recent studies to predict various molecular phenotypes on the basis of DNA sequence

alone. Applications include classifying transcription factor binding sites, predicting molecular phenotypes such as DNA methylation, microRNA targets, and gene expression [23–27]. In addition, CNNs have been utilized to call genetic variants [28] and classify genetic mutations in tumors [29]. Multitask and multimodal models and transfer learning have also been developed in genomics [30, 31]. In this work, we hypothesize that deep-learning genomics (DLG) can be applied to AD and outperform traditional GWAS analysis. We propose a DLG method to replace traditional GWAS analysis for multitasking classification of AD progression and use this approach to seek novel genetic biomarkers of AD susceptibility.

2. Materials and Methods

The experimental workflow of this study consisted of three steps as shown in Figure 1. First, we conducted quality control and SNP genotype coding for SNP genotype data. Second, we used the deep residual network ResNet for DLG. The goal of the deep residual network was to obtain a model by supervised learning for prediction and extraction of DLG features. The details of this process are described in detail in the following sections. Finally, we investigated interpretability of the DLG model by applying Gradient-weighted Class Activation Mapping (Grad-CAM).

2.1. Subjects. Data used in the preparation of this study was obtained from the ADNI database (<http://adni.loni.usc.edu/>). ADNI was launched in 2004 by the National Institute on Aging, the National Institute of Biomedical Imaging and Bioengineering, the Food and Drug Administration, private pharmaceutical companies, and nonprofit organizations, as a \$60 million, 5-year public-private partnership. In this study, 1461 individuals (622 AD, 473 MCI, and 366 healthy controls (HCs)) from the ADNI 1, ADNI 2, and ADNI GO cohorts of the ADNI database were included. Meanwhile, the following data from the 1461 ADNI participants was downloaded: Illumina SNP genotyping data, demographic information, and diagnosis information. Written informed consent was obtained from all participants, and the study was conducted with prior institutional review board approval. Clinical characteristics, including age, sex, education, and Montreal Cognitive Assessment (MoCA) results, were collected and are listed in Table 1.

The subjects were of age 55-90 (inclusive) years. The detailed ADNI eligibility criteria are available from <http://adni.loni.usc.edu/methods/documents/>. In brief, eligibility criteria for these participants were as follows: (1) normal subjects: a Clinical Dementia Rating (CDR) of 0, nondepressed, non-MCI, and nondemented; (2) MCI subjects: a memory complaint, objective memory loss measured by education adjusted scores on Wechsler Memory Scale 7/Logical Memory II, a CDR of 0.5, absence of significant levels of impairment in other cognitive domains, essentially preserved activities of daily living, and an absence of dementia; (3) AD: CDR of 0.5 or 1.0 and met the National Institute of Neurological and Communicative Disorders and Stroke and Alzheimer's disease and Related Disorders Association

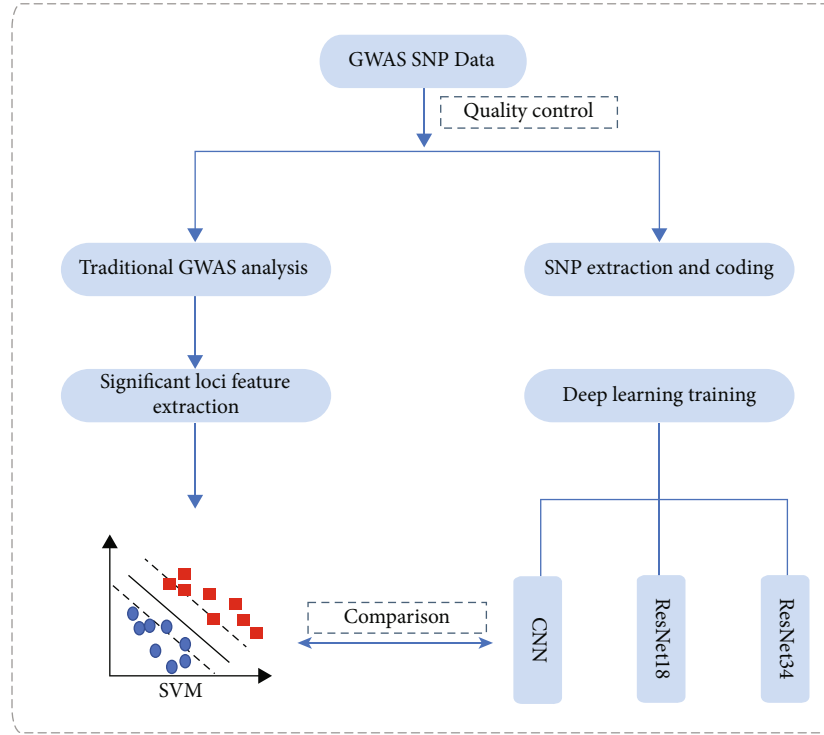


FIGURE 1: The flowchart of experimental procedures in this study.

TABLE 1: Clinical and baseline demographic characteristics of all participants.

Groups	Gender (M/F)	Age (years)	Education	MoCA
<i>Training and validation group(n = 1316)</i>				
AD (n = 560)	320/240 ^a	74.42 ± 7.26	15.54 ± 2.85 ^a	17.18 ± 5.05 ^{a,b}
MCI (n = 426)	255/171 ^c	73.27 ± 7.39	15.98 ± 2.78 ^c	23.62 ± 2.95 ^{b,c}
HC (n = 330)	163/167 ^{a,c}	73.80 ± 5.84	16.46 ± 2.54 ^{a,c}	25.88 ± 2.42 ^{a,c}
<i>Test group(n = 145)</i>				
AD (n = 62)	41/21 ^a	75.71 ± 7.99	15.55 ± 3.32	13.91 ± 6.82 ^b
MCI (n = 47)	30/17 ^c	75.56 ± 7.94	14.81 ± 3.70	22.75 ± 3.31 ^b
HC (n = 36)	14/22 ^{a,c}	75.45 ± 3.49	15.58 ± 3.59	—

Data of age and education were presented as mean ± standard deviation. MoCA: Montreal Cognitive Assessment. Group-level two-sample *t* test is conducted for age, education, and MoCA. Group-level chi-square test is conducted for gender. ^a*p* value HC vs. AD; ^b*p* value AD vs. MCI; ^c*p* value HC vs. MCI.

criteria for probable AD [32]. Specific psychoactive medications were excluded.

We investigated two groups of subjects using SNP genotype data collected from the ADNI databases. Our training and validation group contained 560 subjects with AD, 426 subjects with MCI, and 330 HC subjects. We used the SNP genotype data from this group to establish and test the validity of our predictive models. Our test group consisted of 62 AD subjects, 47 MCI subjects, and 36 HC controls, and we used the SNP genotype data to evaluate the diagnostic value of the predictive models.

2.2. DNA Isolation and SNP Genotyping. SNP genotyping for more than 620,000 target SNPs was completed on all ADNI

participants using the following protocol. First, a total of 7 mL of blood was taken from each participant and stored in EDTA-containing Vacutainer tubes, and genomic DNA was extracted using the QIAamp DNA Blood Maxi Kit following the manufacturer's protocol. Second, lymphoblastoid cell lines were established by transforming B lymphocytes with Epstein-Barr virus [33]. Fourteen genomic DNA samples were analyzed using the Human 610-Quad BeadChip according to the manufacturer's protocols. Before starting the assay, a 50 ng sample of genomic DNA from each participant was examined qualitatively on a 1% Tris-acetate-EDTA agarose gel to check for degradation. Degraded DNA samples were excluded from further analysis. Third, samples were quantitated in triplicate with PicoGreen® reagent and diluted

to 50 ng/L in TrisEDTA buffer (10 mM Tris, 1 mM EDTA, pH 8.0). A total of 200 ng of DNA was denatured, neutralized, and amplified for 22 hours at 37°C, and then fragmented with FMS reagent (Illumina) at 37°C for 1 hour, precipitated with 2-propanol, and incubated at 4°C for 30 minutes. Fourth, the resulting blue precipitate was resuspended in RA1 reagent (Illumina) at 48°C for 1 hour. Samples were then denatured (95°C for 20 minutes) and immediately hybridized onto BeadChips at 48°C for 20 hours. The BeadChips were washed and subjected to single base extension and staining. Finally, the BeadChips were coated with XC4 reagent (Illumina), desiccated, and imaged on a BeadArray Reader (Illumina). Illumina BeadStudio 3.2 software was used to generate SNP genotypes from bead intensity data.

2.3. Quality Control and APOE Genotype. The following quality control (QC) steps were performed on the 1461 samples using PLINK v1.07 software. QC processes were conducted separately between the AD and HC groups, the HC and MCI groups, and the AD and MCI groups. SNPs and participants were excluded from the analysis if they failed to meet any of the following criteria [34]: call rate per SNP $\geq 90\%$; call rate per participant $\geq 90\%$; gender check; minor allele frequency (MAF) $\geq 5\%$; Hardy-Weinberg equilibrium test of $p \leq 10^{-6}$; PI_HAT < 0.5 . After the QC procedure, the numbers of features considered for future analysis of each subject in the paired groups were as follows: 301,388 in the HC and MCI groups, 301,853 in the HC and MCI groups, and 301,138 in the MCI and AD groups. The overall genotyping rate for the remaining dataset was over 99.5%.

In addition, although the APOE gene is an important target gene in AD research, it was not available for all identified APOE SNPs on the Illumina array. Therefore, based on the reported APOE $\epsilon 2/\epsilon 3/\epsilon 4$ status, the genotypes of the unavailable APOE SNPs were added manually to ADNI genotype data before assessing sample quality.

2.4. SNP Genotype Coding. A single-nucleotide polymorphism is a DNA sequence variation which occurs when a single nucleotide (A, T, C, or G) in the genome differs among members of a biological species or across paired chromosomes. Based on the satisfactory ADNI GWAS SNP data of this study, we encoded SNPs using the following coding scheme: 1 refers to A, 2 refers to T, 3 refers to C, and 4 refers to G.

2.5. GWAS Analysis. In the multitasking classification of this study, GWAS analysis, which has emerged as a popular tool for identifying genetic variants associated with disease risk, was designed to be compared with deep-learning models. Standard analysis of a case-control GWAS involves assessing the association between each individual genotyped SNP and disease risk. Manhattan and quantile-quantile (Q-Q) plots were used to visualize the GWAS results. All association results surviving the significance threshold of $p < 1.66e^{-7}$ were saved and prepared for subsequent pattern analysis.

2.6. Deep-Learning Genomics Model Based on ResNet. The DLG model acted as a feature encoder, which had a significant impact on classification. In this study, we applied

ResNet, a deep residual network, to the classification between AD and HC groups, AD and MCI groups, and HC and MCI groups. Residual units were added to the deep residual network on the basis of CNNs.

A CNN, the most effective type deep-learning model, is generally composed of three types of layers: convolutional, pooling, and fully connected. The following describes the operation of a CNN. The first step is to convolve the input sequences with a set of filter kernels; all the features active at different positions after convolution constitute the feature map [35]. A nonlinear activation function, typically a rectified linear unit (ReLU), is applied on each layer and on the sum of the feature maps. The operation of the convolutional layer and ReLU can be expressed as follows:

$$C_n^r = \text{ReLU} \left(\sum_m v_m^{r-1} * w_n^r + b_n^r \right), \quad (1)$$

$$\begin{cases} \text{ReLU}(y_n) = \max(0, y_n), \\ y_n = \sum_m v_m^{r-1} * w_n^r + b_n^r, \end{cases}$$

where C_n^r is the n^{th} output of the r^{th} convolutional layer, n represents the number of filters in the r^{th} layer, w_n^r and b_n^r are, respectively, the weight and bias of the n^{th} filter of the r^{th} layer, v_m^{r-1} is the m^{th} output of previous layer $r-1$, and $*$ denotes the convolutional operation.

Next, the resulting feature map is processed through the pooling layer by taking either the mean or maximum activation over disjoint regions for each channel [20, 35]. By sequential combination of convolutional and pooling layers, a multilayer structure is built for feature description. Lastly, the fully connected layers are employed for classification. In total, when given a training set $\{X_j\}_j$, the learning process of a CNN with K convolutional layers, whose filter parameters are $\{W_i\}_{i=1}^K$, the bias values are $\{b_i\}_{i=1}^K$, and D refers to classification layers, can be represented as an optimization learning task:

$$\min_{\{W_i\}_{i=1}^K, \{b_i\}_{i=1}^K} \sum_j L \left(h(X_j), f \left(\{W_i\}_{i=1}^K, \{b_i\}_{i=1}^K, D \right) \right), \quad (2)$$

where L is the loss function that represents the cost difference between the true label $h(X)$ and the predictive label from the CNN model $f(X, \{W_i\}_{i=1}^K, \{b_i\}_{i=1}^K, D)$.

Based on the CNN model, the greatest advantage of the ResNet framework lies in adding identity mapping that is performed by the shortcut connections, the outputs of which are added to the outputs of the stacked layers [36]. Therefore, the ResNet addressed the degradation problem and added neither extra parameters nor computational complexity. The formula for residual learning was designed as follows: the desired underlying mapping is denoted as $H(x)$, and the stacked nonlinear layers were allowed to fit a separate mapping of $F(x, \Theta) = H(x) - x$. The original mapping was recast into $F(x, \Theta) + x$. Thus, the overall representation of the residual block was as follows:

$$H(x) = F(x, \Theta) + x. \quad (3)$$

The formulation of $F(x, \Theta) + x$ can be realized by feedforward neural networks using “shortcut connections.” A deep residual network can be established by stacking a series of residual blocks. Specifically, there were two steps in the process: forward computation and backward propagation. When K residual blocks are chosen to stack, the forward propagation of such a structure can be expressed by

$$x_K = x_0 + \sum_{r=1}^K F(x_{r-1}, \Theta_{r-1}), \quad (4)$$

where x_0 and x_1 are the input and the output of the residual network, respectively, and $\Theta_r = \{\theta_{r,l} | 1 \leq l \leq L\}$ is the weight related to the r_{th} residual block, L being the number of layers within the block.

Likewise, the back propagation of the overall loss of the neural network to x_0 can be denoted as

$$\frac{\partial L}{\partial x_0} = \frac{\partial L}{\partial x_K} \left(1 + \frac{\partial}{\partial x_0} \sum_{i=1}^K F(x_{i-1}, \Theta_{i-1}) \right), \quad (5)$$

where L is the whole loss function of the neural network.

Before modeling using the above procedures, each subject’s SNP genotype data was cropped after quality control and mapped to 776×776 pixels. The pathology type was encoded to one-hot, which was the label. Thereafter, in the training stage, SNP genotype data was fed into the network to update model parameters via backward propagation with the Adam algorithm, a first-order gradient-based optimization algorithm which has been proven to be computationally efficient and appropriate for training deep neural networks. The outputs of the network were used as the classification results, and the crossentropy of the outputs was calculated as the loss function. More specifically, the output of the network for each individual SNP could be a binary value. 1 represented the highest probability of being AD subjects, while 0 represented highest probability of being HC subjects.

We adopted ResNet18 and ResNet34 frameworks in this study. Meanwhile, we also utilized a traditional CNN model for the comparative experiments of classification. In the ResNet models, we set learning rate into $1e^{-3}$ and applied the Adam optimizer to update the model parameters with the batch size of 8. The maximum number of iterations was set into 20. Note that we used L2 regularization in this step to prevent the overfit of our model. For adjusting the CNN model parameters, we set learning rate into $1e^{-2}$ and applied the Adam optimizer to update the model parameters with the batch size of 8. The maximum number of iterations was set to 30. Above deep-learning models were processed on a GPU (graphics processing unit, GTX 1080 Ti acceleration of PyCharm 3.5).

For investigating the interpretability of the DLG model, the last convolutional layer of the last res-block was made transparent in order to extract DLG features by applying Grad-CAM and two-sample t -tests. For the first step, the last

convolutional layer of the last res-block was chosen to extract normalized DLG features. Subsequently, using a two-sample t -test with a false discovery rate [37, 38], we compared the Z -coefficients of the AD and HC groups, the HC and MCI groups, and the MCI and AD groups.

2.7. Classification. In this study, the subjects of multitasking classification were randomly divided into one training group and one independent test group at a ratio of 9:1 as shown in Table 1. The training group was then used to optimize the model parameters. We also randomly chose 25% of training group to form a validation group to guide the choice of hyperparameters.

On the one hand, we conducted training of several deep-learning models, including ResNet18, ResNet34, and a traditional CNN, and compared classification performance in order to screen for the optimum DLG. On the other hand, in order to verify the diagnostic capabilities of the DLG model compared with traditional GWAS analysis, we also designed comparative trials. Among all the gene indicators, theta proved to be the most directly related to SNP changes. APOE $\epsilon 4$ status and the normalized theta-value of the significant SNP loci found in this study were seen to be genetic predictors, and we used the support vector machine (SVM) with the linear kernel 500 times for classification of traditional GWAS.

To evaluate classification performance, we repeatedly conducted 5-fold crossvalidation in the training group. Accuracy, sensitivity, and specificity were used to evaluate the results. The mathematical expression of the three parameters was as follows:

$$\begin{aligned} \text{Accuracy} &= \frac{Tn + Tp}{Tn + Tp + Fn + Fp}, \\ \text{Sensitivity} &= \frac{Tp}{Tp + Fn}, \\ \text{Specificity} &= \frac{Tn}{Tn + Fp}, \end{aligned} \quad (6)$$

where Tn , Tp , Fn , and Fp denote, respectively, true negatives, true positives, false negatives, and false positives.

A receiver-operating characteristic (ROC) curve was produced to intuitively compare the results of the different approaches, and the area under the curve (AUC) of the ROC was computed to quantitatively evaluate classification performance.

2.8. Statistical Analysis. Demographic characteristics were compared between groups using a two-sample t -test or the chi-square test. In addition, a two-sample t -test of the extracted features was applied as a criterion to estimate the differences in DLG features between AD patients and HCs, AD patients and MCIs, and HCs and MCIs. All statistical analyses were performed using SPSS Version 22.0 software (SPSS Inc., Chicago, IL) and Matlab2016b (Mathworks Inc., Sherborn, MA, United States). All p values < 0.05 were considered significant.

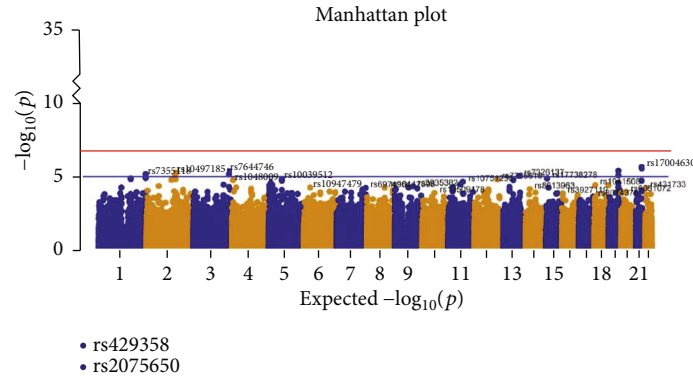


FIGURE 2: Manhattan plot of genome-wide association study (GWAS) between AD and HC groups. The y-axis shows the p value (on the $-\log_{10}$ scale) for each association test. The x-axis is the chromosomal position of each SNP. The horizontal lines in the Manhattan plot display the cutoffs for two significant levels: blue line for $p < 10^{-5}$ (generally significant level) and red line for $p < 1.66e^{-7}$.

3. Results

3.1. Outcomes of GWAS Analysis. We carried out case-control GWAS analysis between the AD and HC groups and observed two genome-wide significant loci on chromosome 19, including rs429358 (APOE, the epsilon 4 marker) and rs2075650 (TOMM40). Figures 2 and 3 show the resulting Manhattan and Q-Q plots, and Table 2 summaries the SNPs that achieved genome-wide significance. The p value used to assess significant differences was calculated as $p = 0.05/N$, where N indicates the number of satisfied SNPs.

3.2. Classification Performance. Table 3 lists the performance of the different multitasking classification methods, including classification accuracy, sensitivity, specificity, and AUC. Taking the result of classification between the AD and HC test group subjects as an example, accuracy, sensitivity, specificity, and AUC were, respectively, $71.38\% \pm 0.63\%$, $63.13\% \pm 2.87\%$, $85.59\% \pm 6.66\%$, and 0.744 , for the GWAS analysis, $92.45\% \pm 8.13\%$, 93.87 ± 12.26 , 90.00 ± 15.97 , and 0.915 for the CNN model, 97.96 ± 1.71 , 97.42 ± 3.16 , 98.89 ± 1.36 , and 0.980 for ResNet18, and $98.78\% \pm 1.50\%$, $98.39\% \pm 2.50\%$, $99.44\% \pm 1.11\%$, and 0.981 for ResNet34. We found that the deep-learning model exhibited high accuracy, sensitivity, and specificity, whereas accuracy and sensitivity were low for the GWAS analysis. Therefore, we concluded that deep-learning models were superior to traditional GWAS analysis for classification. And compared with the CNN model, the results using ResNet were more robust and stable. These results were the same using the other two group-level classifications. Based on these results, ResNet34 was chosen for the DLG model because the observed classification performance was optimal among the several deep-learning models. A more intuitive comparison is provided by the ROC curves of the multitasking classification shown in Figure 4.

3.3. Interpretability of the DLG Model. Setting a threshold of $p < 0.05$, more than ten thousand SNP loci showed differences between the groups, and even the significance of the most frequently identified loci was below 0.001 .

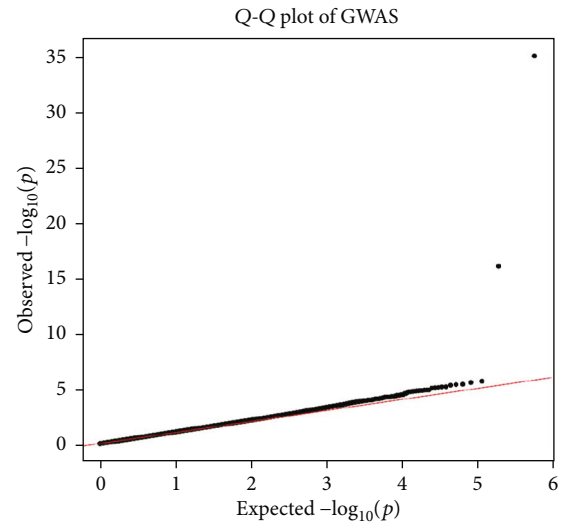


FIGURE 3: Q-Q plot of genome-wide association study (GWAS) between AD and HC groups. Genomic inflation factor is 1.084 .

Firstly, we compared the significant SNPs with those previously identified by GWAS as genetic susceptibility factors. Almost one hundred SNP loci between AD patients and HCs were consistent with findings from previous studies. Likewise, more than one hundred associated SNP loci were also found between the AD and MCI groups and between the HC and MCI groups.

Secondly, we sought significant SNP loci among three classification tasks. The gene regions of sixty-six SNP loci were shared in different stages of AD progression. Table 4 summarizes the sixty-six shared significant SNP loci among the three classifications, including, e.g., the well-known CLU, PICALM, and SORL1 gene regions. For rs11136000 (CLU) in chromosome 8, its p values were $6.63e^{-4}$ between the AD and HC groups, $8.37e^{-6}$ between the MCI and HC groups, and $1.49e^{-7}$ between MCI and AD groups. In addition, three SNP loci, rs543293, rs10501602, and rs3851179, were found in the PICALM gene region of chromosome 11, and the p values of rs3851179 for the comparisons of the three groups were $6.00e^{-3}$, $1.06e^{-6}$, and $1.51e^{-20}$, while the p

TABLE 2: SNP summaries reaching genome-wide significance after GWAS.

SNP	Position	Chr	Region or closest gene	Major/minor alleles	<i>p</i> value	OR
rs429358	44908684	19	APOE	C/T	5.407e-36	4.348
rs2075650	50087459	19	TOMM40	G/A	7.19e-17	2.737

$p < 1.66e^{-7}$ for SNPs listed above. Chr: chromosome.

TABLE 3: Performance of different classification approaches in multitasking classification.

Model	Accuracy (%)	Sensitivity (%)	Specificity (%)	AUC
<i>AD and HC groups</i>				
GWAS analysis	71.38 ± 0.63	63.13 ± 2.87	85.59 ± 6.66	0.744
CNN model	92.45 ± 8.13	93.87 ± 12.26	90.00 ± 15.97	0.915
ResNet18	97.96 ± 1.71	97.42 ± 3.16	98.89 ± 1.36	0.980
ResNet34	98.78 ± 1.50	98.39 ± 2.50	99.44 ± 1.11	0.981
<i>MCI and HC groups</i>				
GWAS analysis	56.99 ± 1.55	96.08 ± 13.92	5.94 ± 21.65	0.510
CNN model	87.47 ± 16.64	99.57 ± 0.85	71.67 ± 38.75	0.852
ResNet18	97.59 ± 3.73	100.00 ± 0.00	94.44 ± 8.61	0.966
ResNet34	99.52 ± 0.60	99.57 ± 0.85	99.44 ± 1.11	0.986
<i>AD and MCI groups</i>				
GWAS analysis	58.97 ± 0.00	72.18 ± 0.01	41.54 ± 0.01	0.569
CNN model	86.42 ± 16.02	97.42 ± 4.40	71.91 ± 39.21	0.840
ResNet18	97.80 ± 1.24	97.74 ± 2.41	97.87 ± 3.30	0.972
ResNet34	98.90 ± 1.78	100.00 ± 0.00	97.45 ± 4.13	0.981

The methods are conducted with crossvalidation, and their results are given as mean ± standard deviation.

values of rs543293 were $4.65e^{-3}$, $3.43e^{-8}$, and $2.27e^{-13}$, and the *p* values of rs3851179 were also much less than 0.001. These results are well supported by previous studies. Other significant results are detailed in Table 4, and the heatmaps of significant SNPs in chromosomes 8, 11, and 13 are shown in Figure 5. The horizontal axis represents major and minor alleles, and the vertical axis represents the *p* value of SNP loci in the chromosomes. We observed some distinct differences, for example, between rs11136000, rs3851179, and surrounding loci.

In addition, except for those in Table 4, there were also several SNP loci showing an association with AD progression in their respective classifications. Several also have been reported and confirmed in previous large-scale GWAS studies, including APOE, BIN1, CHRM1, and TOMM40 with *p* values much less than 0.001. Furthermore, it is notable that rs6311 and rs6313 in the HTR2A gene region, rs1354269 in the NAV2 gene, and rs690705 in the RFC3 gene all exhibited significant differences among the three classifications. For instance, the *p* values of rs6311 were $1.96e^{-5}$, $2.52e^{-3}$, and $1.48e^{-11}$ between the respective groups, and the *p* values of rs6313 were $3.21e^{-5}$, $4.55e^{-3}$, and $2.05e^{-12}$. An understanding of the roles of these novel loci in AD requires future study.

All of the information above was deposited in the DisGeNET database (<http://www.disgenet.org/home/>), a discovery

platform containing one of the largest publicly available collections of genes and variants associated with human disease.

4. Discussion

This study used a comparison of the performance of several different deep-learning models as a basis for proposing a deep-learning genomics method based on ResNet34. The classification results indicate that the DLG model offers a higher diagnostic value than traditional GWAS analysis.

4.1. Outcomes of GWAS Analysis. In GWAS analyses, two SNPs have been identified at the $p < 1.66e^{-7}$ significance level: APOE SNP rs429358 was determined to be the most significant genetic risk factor for AD. And the second most significant factor, TOMM40 SNP rs2075650, was found to be adjacent to the APOE SNP [10]. These results are consistent with previous studies. Although these SNP loci were identified by GWAS, traditional GWAS analysis suffers from being influenced by small sample size. Because other common genetic risk factors may have a much smaller impact on risk than the APOE gene, novel risk factors present in small samples may go undetected by GWAS analysis. Several previous studies have also demonstrated an explicit relationship between sample size and the number of significant

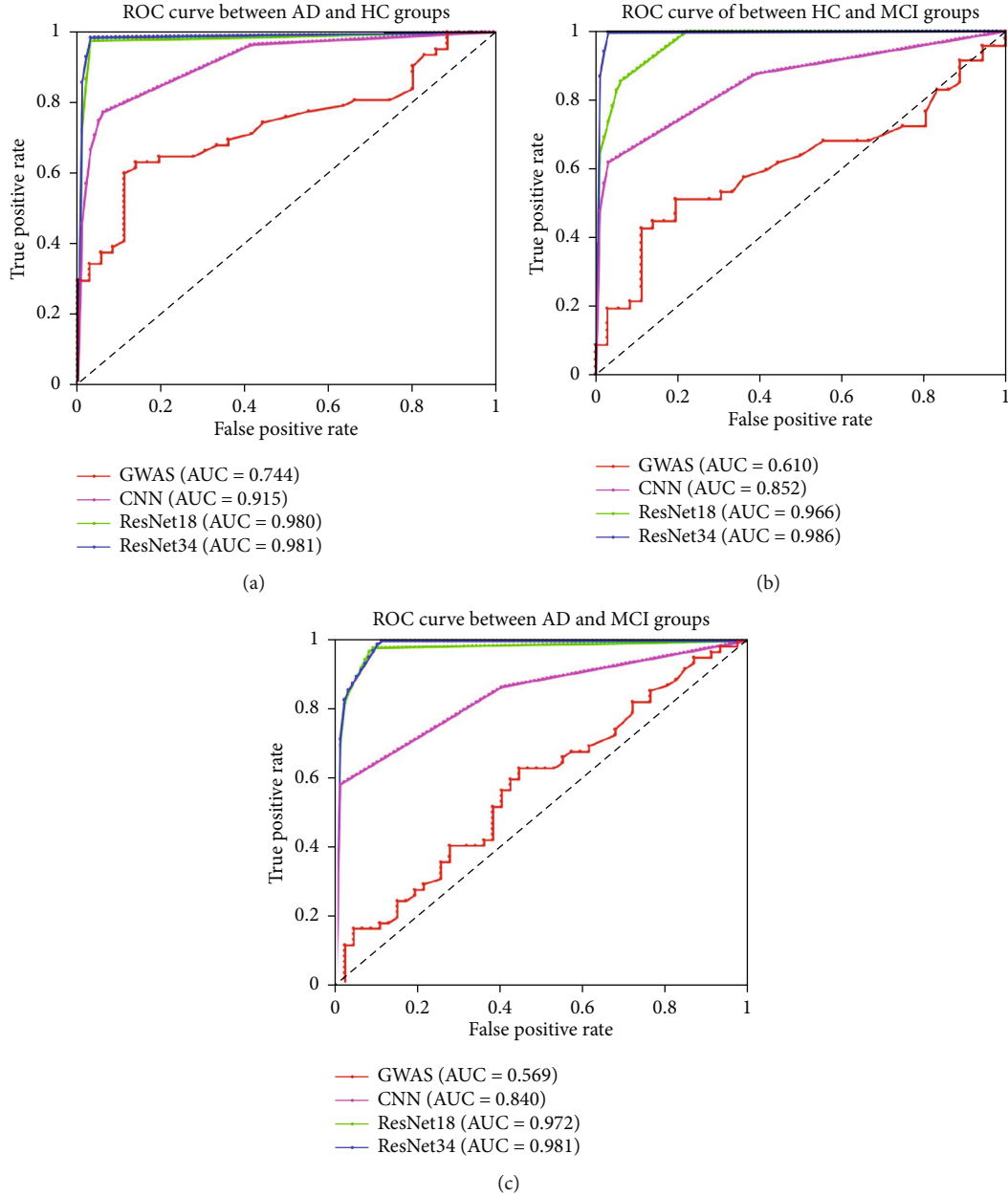


FIGURE 4: ROC curve of the performance of different classification approaches in multitasking classification. (a) ROC curve between AD and HC groups. (b) ROC curve between MCI and HC groups. (c) ROC curve between AD and MCI groups.

differences in traits identified by genome-wide association studies [18, 19].

4.2. Classification Performance. In this study, in order to construct a deep-learning genomics model, we compared the performance of several deep-learning classification methods, including a simple CNN model, ResNet18, and ResNet34. As shown in Table 3, we observed that the results of the deep residual network were superior to those of a simple CNN, and in the process of training the model, the ResNet models exhibited robustness and stability superior to those of CNNs, and furthermore, ResNet34 was superior to ResNet18. Therefore, we chose ResNet34 as the final DLG model. More importantly, we compared the performance of the DLG

model and traditional GWAS analysis under the same conditions and found the classification results of the DLG model to be superior. These results suggest that the deep-learning algorithm is effective in genome applications and that development of deep-learning genomics is worthy of further exploration.

4.3. Interpretability of the DLG Model. When we interpreted the DLG model, we found more than one thousand SNP loci with significant differences between AD patients and HCs, between the MCI and AD groups, and between the HC and MCI subjects. As is well known, rs11136000 (CLU), rs3851179 (PICALM), rs2070045 (SORL1), and rs1699102 (SORL1) have previously been identified as risk factors for

TABLE 4: Shared significant SNPs in AD multitasking classification at p threshold of 0.05.

SNP loci	Chr	Position	Region or closest gene	Major/minor alleles	p value HC vs. AD	p value HC vs. MCI	p value AD vs. MCI
rs12091371	1	238671675	FMN2	A/G	0.002227833	0.001509792	2.27881E-09
rs12129547	1	238761878	GREM2	T/C	0.002767757	0.019531535	3.93396E-11
rs1801131	1	11777063	MTHFR	C/A	0.000154746	0.007333869	6.18756E-21
rs1801133	1	11778965	MTHFR	T/C	0.000192989	0.009566143	5.35043E-21
rs17034806	2	109002337	RANBP2	G/A	0.002645921	0.028425309	3.04207E-10
rs243034	2	60456396	MIR4432HG	G/A	0.038985718	0.009492742	1.40355E-08
rs4676049	2	109001689	RANBP2	T/C	0.002215778	0.034993277	4.51555E-10
rs6714710	2	97711518	ZAP70	G/T	0.038909198	0.000768783	7.036E-09
rs1498853	3	69691797	NAN ^a	G/A	0.000708166	0.012435495	6.43721E-09
rs2289506	3	101547592	NIT2	T/C	0.000412705	0.004914541	1.07429E-18
rs288496	3	69714739	NAN ^a	T/C	0.002172998	0.009409715	4.5892E-09
rs3864101	3	188862449	NAN ^a	T/G	0.038241862	0.022506051	6.17468E-08
rs989692	3	156284059	MME	T/C	0.00243336	0.016131413	5.91293E-09
rs3796529	4	57492171	REST	A/G	0.048696066	0.004826601	7.08294E-25
rs753129	4	56363188	NAN ^a	C/T	0.004469287	1.23015E-10	0.013855564
rs1925458	6	23486930	LOC102724749; LOC105374976	T/G	0.000567167	0.000409483	3.10404E-11
rs1980493	6	32471193	BTNL2; TSBP1-AS1	G/A	0.016858811	0.000751139	3.35304E-14
rs2651206	6	43321455	TTBK1	T/C	0.034368574	2.23746E-07	1.97506E-11
rs3734254	6	35502988	PPARD	C/T	0.001667544	0.000173601	2.21574E-11
rs3747742	6	41270496	TREML2	C/T	6.7184E-06	3.50103E-05	1.19671E-08
rs6455128	6	62755705	KHDRBS2	A/C	0.008767325	0.00013524	1.45915E-14
rs11767557	7	142819261	EPHA1-AS1	C/T	0.001139233	1.20661E-07	1.96401E-07
rs11771145	7	142820884	EPHA1-AS1	A/G	0.001112928	9.62693E-08	1.8557E-07
rs2227631	7	100556258	SERPINE1	G/A	0.003024669	8.25065E-08	7.24385E-07
rs6461569	7	21502301	SP4	C/T	0.025204688	1.41338E-06	0.001322394
rs6966915	7	12232513	TMEM106B	T/C	0.031810788	0.004328052	6.57464E-09
rs11136000	8	27520436	CLU	T/C	0.000663408	8.36729E-06	1.48921E-07
rs1975804	8	109360409	EIF3E; LOC105375704	C/T	0.000833268	0.003779274	0.040135088
rs1800977	9	106730271	ABCA1; LOC105376196	T/C	0.013227434	5.61278E-05	4.22923E-14
rs2007153	9	135493640	DBH	A/G	3.88584E-05	0.000993637	4.15766E-07
rs2066715	9	106627854	ABCA1	A/G	0.004157538	0.04271672	7.79217E-05
rs2283123	9	135505118	DBH	T/C	0.000105332	0.00221966	1.99182E-07
rs2740483	9	106730356	ABCA1; LOC105376196	C/G	0.009678488	6.53287E-05	3.81638E-14
rs4149313	9	106626574	ABCA1	G/A	0.003318514	0.040059489	7.22211E-05
rs4878104	9	89382811	DAPK1	T/C	0.002309724	6.11706E-05	1.46237E-14
rs4548513	10	67710331	CTNNA3	T/C	0.004692221	0.000992064	6.62732E-08
rs7070570	10	67534610	LOC105378340; CTNNA3	G/A	0.000655491	2.34147E-05	1.63609E-06
rs10501602	11	85359037	PICALM	G/A	0.004647595	3.42511E-08	2.27238E-13
rs1133174	11	121006965	SORL1	A/G	0.010544659	0.003255318	3.13279E-05
rs12805520	11	85308059	CCDC83	T/C	0.007162755	4.02484E-08	1.90295E-11
rs1354269	11	19330820	NAV2	C/T	0.010833795	6.42781E-08	2.65216E-24
rs1695	11	67109265	GSTP1	G/A	0.006309008	6.1645E-07	2.06528E-23
rs1699102	11	120962172	SORL1	C/T	0.013141699	0.001477832	6.19383E-05
rs17571	11	1739170	CTSD	T/C	0.013910348	1.48442E-08	1.58542E-20
rs1946518	11	111540668	IL18	T/G	0.006486007	1.8075E-06	7.21291E-22
rs2070045	11	120953300	SORL1	G/T	0.014545915	0.001140944	7.97485E-05
rs3851179	11	85546288	PICALM	A/G	0.00599555	1.06305E-06	1.50773E-20
rs543293	11	85497725	PICALM	A/G	0.004782682	1.26328E-07	7.85454E-18

TABLE 4: Continued.

SNP loci	Chr	Position	Region or closest gene	Major/minor alleles	<i>p</i> value HC vs. AD	<i>p</i> value HC vs. MCI	<i>p</i> value AD vs. MCI
rs6265	11	27636492	BDNF; BDNF-AS	A/G	0.009460455	1.96067E-07	1.42052E-28
rs7120118	11	47242866	NR1H3	C/T	0.034010947	0.011720707	5.90652E-22
rs7943454	11	24478242	LUZP2	T/C	0.01777448	1.41141E-06	2.00064E-30
rs1799986	12	55821533	LRP1	T/C	0.000875404	8.1991E-06	0.000948497
rs6311	13	46369479	HTR2A	T/C	1.95644E-05	0.002519461	1.48261E-11
rs6313	13	46367941	HTR2A	T/C	3.21121E-05	0.004551786	2.05426E-12
rs690705	13	33552918	RFC3	G/A	9.15016E-07	0.000123939	0.032894005
rs7989332	13	19948575	CRYL1	A/C	0.001947338	0.038324875	0.017831896
rs10137185	14	63845529	ESR2	T/C	0.000105484	0.00099597	2.08051E-22
rs1065778	15	49307498	MIR4713HG; CYP19A1	A/G	7.88465E-05	1.51664E-05	2.28151E-18
rs2278317	15	31848032	RYR3	G/A	0.019133823	5.18518E-05	4.11594E-07
rs3751592	15	49393870	CYP19A1; MIR7973-1; MIR7973-2	G/A	0.000333452	8.25536E-05	5.77922E-13
rs11075996	16	52415525	FTO	T/C	0.021538201	9.92354E-07	0.002856803
rs11075997	16	52416413	FTO	T/C	0.023256237	1.14854E-06	0.002461173
rs6499640	16	52327178	FTO	G/A	0.016928027	4.22569E-07	0.009148135
rs1050565	17	25600202	BLMH	G/A	0.045066195	6.1136E-06	1.19122E-06
rs391300	17	2163008	SRR	A/G	0.028223591	1.90848E-06	0.000379785
rs7946	17	17350285	PEMT	C/T	0.044709718	0.000412862	2.75631E-18

SNP: single-nucleotide polymorphism. Chr: chromosome. NAN^a represents uncertain gene of the SNP loci. *p* value (HC vs. AD) represents the difference value of each SNP loci between AD and HC groups. All *p* value are calculated by a two-sample *t* test for false discovery rate correction.

AD [7, 9, 39]. Notably, they were all included among the sixty-six significant SNP loci shared in the three classification tasks in this study (as shown in Table 4 and Figure 5). For example, previous studies have shown that CLU modulates A β metabolism and is involved in A β clearance or acts as a chaperon for protein degradation [40]. PICALM, as an adaptor protein involved in clathrin-mediated endocytosis, regulates amyloid precursor protein (APP) internalization and subsequent A β generation, contributing to brain amyloid plaque load via its effect on A β metabolism [41, 42]. In addition to the analysis of the above identical SNP loci found among the three classification tasks, several differential loci were identified among one or two classification tasks, which are also consistent with previous research. Rs10194375 (BIN1), a protein that may be associated with tau-mediated pathology was identified as being significant between the AD and HC groups and the AD and MCI groups. In addition, rs2075650 (TOMM40), rs405509 (APOE), and rs429358 (APOE) were identified as significant between the HC and MCI groups and the MCI and AD groups. In summary, the DLG model is able to identify differential genomics in multitasking classification.

Most importantly, in addition to those shown to associate with AD in the past, we found several new SNP loci, including rs6311 (HTR2A), rs6313 (HTR2A), rs1354269 (NAV2), rs1946518 (IL18), rs1799986 (LRP1), rs690705 (RFC3), and rs7943454 (LUZP2), whose *p* values were highly significant (as shown in Table 4). Rs6311 and rs6313 are in the HTR2A gene region. The HTR2A gene in humans is located on chromosome 13 and consists of exons separated by only two introns and encodes one of the receptors for serotonin. According to previous publications, HTR2A has received

much attention in many psychiatric disorders such as mood disorders, attention deficit hyperactivity disorder, anxiety disorders, and schizophrenia. On the one hand, some studies have shown that medications for mood disorders and related conditions work by blocking 5-HT_{2A} and altering the function of certain brain circuits. And blocking 5-HTR2A also seems to improve the effects of some antidepressants [43]. On the other hand, the numbers of the postsynaptic receptor HTR2A are reduced in the neocortex, and it seems to be involved in memory via its role in cortical pyramidal cells. For example, in AD research, HTR2A receptor densities in the brains of AD subjects were found to be reduced compared with age-matched controls, and the researchers also found this reduction correlated with the rate of decline of cognitive scores [44]. Hence, since subjects with AD or mild cognitive impairment exhibit depression and anxiety to various degrees, it is worth exploring whether rs6311 and rs6313 of the HTR2A gene contribute to AD susceptibility. Another significant locus identified here was rs1354269 located in the NAV2 gene region. The NAV2 gene, which encodes a member of the neuron navigator gene family, is highly expressed in brain and is involved in the development of the nervous system. Hence, the role of the NAV2 gene in AD is also worthy of future investigation. In addition, rs690705 of the RFC3 gene region also exhibited a significant difference in group-level classifications, and its impact on AD should be examined in the future.

5. Limitations

It is worth noting some limitations of this study. Firstly, only gene sequences were used as inputs to the DLG classification.

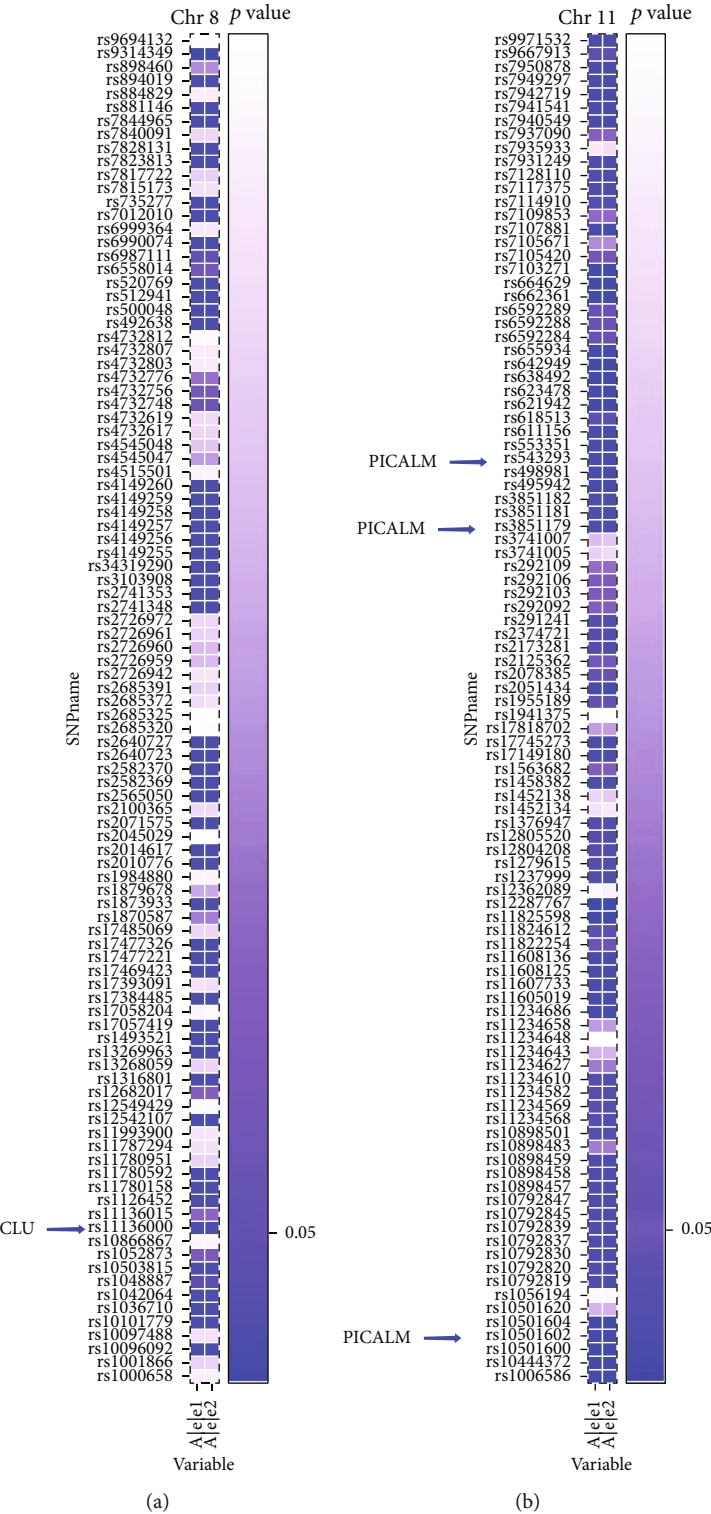


FIGURE 5: Continued.

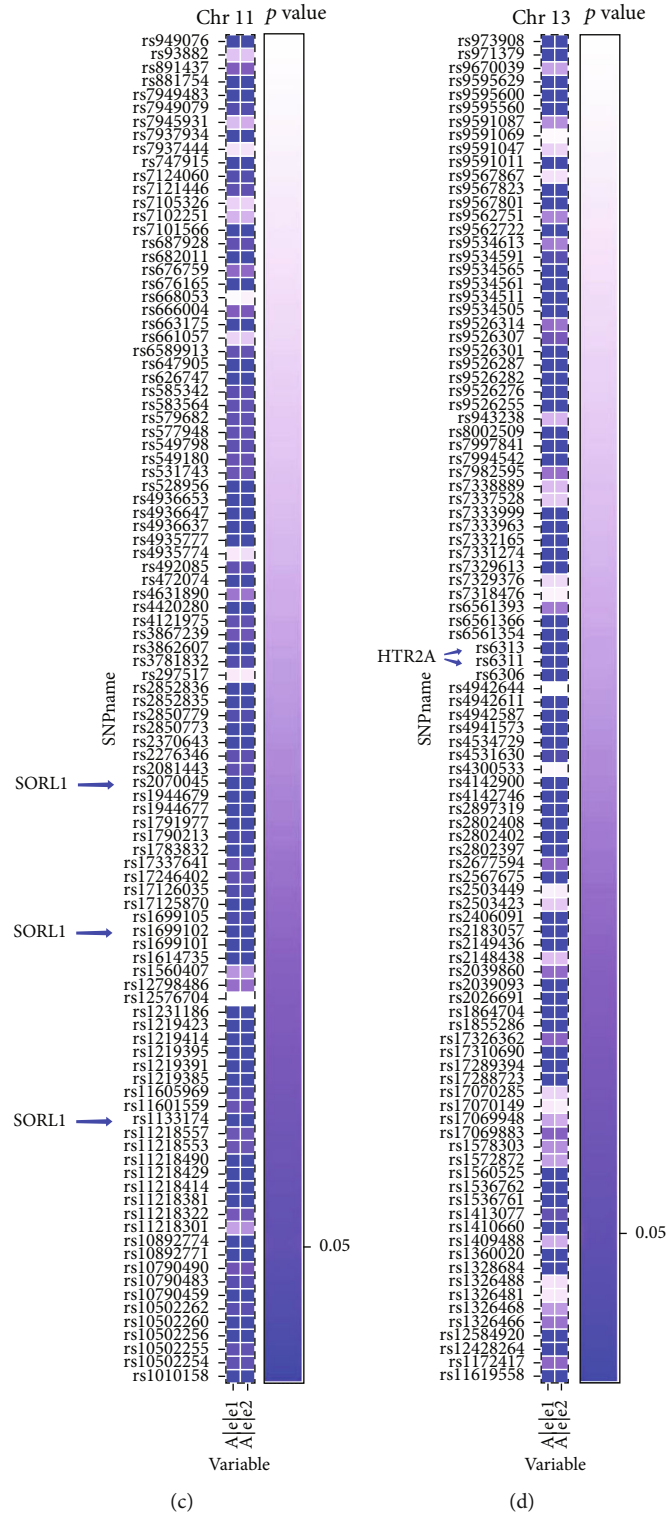


FIGURE 5: Visualization for part of shared significant SNPs in AD multitasking classification at p threshold of 0.05. Rs11136000 (CLU) on chromosome 8 (a); rs543293, rs10501602, and rs3851179 (PICALM) on chromosome 11 (b); rs2070045, rs1699102, and rs1133174 (SORL1) on chromosome 11 (c); and rs6311 and rs6313 (HTR2A) on chromosome 13 (d) are shown successively from left to right.

In the future work, we plan to combine gene sequences with clinical data and brain imaging [45] to facilitate investigation of the mechanisms of AD progression by deep-learning genomics and deep-learning radiomics approaches. Secondly, we only classified information from the ADNI dataset in this study, so the results could be strengthened by including other datasets such as the Chinese populations. Thirdly, the number of subjects represented in this study may be limiting. Lastly, although this study has demonstrated the feasibility of DLG approach, it will be important to further explore the interpretability of deep-learning genomics.

6. Conclusions

In conclusion, the current study suggests that the deep-learning genomics approach is effective for multitasking classification research on AD progression and outperforms traditional GWAS analysis. Moreover, the several novel SNP loci identified in the DLG approach including rs6311 and rs6313 in HTR2A, rs1354269 in NAV2, and rs690705 in RFC3 are worthy of further exploration to better understand the mechanisms of AD.

Data Availability

The datasets presented in this study were obtained from ADNI (<http://adni.loni.usc.edu/>).

Conflicts of Interest

The authors declare that there is no conflict of interest regarding the publication of this paper.

Authors' Contributions

Lanlan Li and Yeyang Yang contributed equally to this work.

Acknowledgments

Data collection and dissemination for this project were funded by the Alzheimer's Disease Neuroimaging Initiative (ADNI): the National Institutes of Health (grant number U01 AG024904) and the Department of Defense (award number W81XWH-12-2-0012). ADNI is funded by the National Institute of Aging and the National Institute of Biomedical Imaging and Bioengineering as well as through generous contributions from the following organizations: AbbVie, Alzheimer's Association, Alzheimer's Drug Discovery Foundation, Araclon Biotech, BioClinica Inc., Biogen, Bristol-Myers Squibb Company, CereSpir Inc., Eisai Inc., Elan Pharmaceuticals Inc., Eli Lilly and Company, EuroImmun, F. Hoffmann-La Roche Ltd. and its affiliated company Genentech Inc., Fujirebio, GE Healthcare, IXICO Ltd., Janssen Alzheimer Immunotherapy Research & Development LLC., Johnson & Johnson Pharmaceutical Research & Development LLC., Lumosity, Lundbeck, Merck & Co. Inc., Meso Scale Diagnostics LLC., NeuroRx Research, Neurotrack Technologies, Novartis Pharmaceuticals Corporation, Pfizer Inc., Piramal Imaging, Servier, Takeda Pharmaceutical Company, and Transition Therapeutics. The Canadian Institutes

of Health Research are providing funds to support ADNI clinical sites in Canada. Private sector contributions are facilitated by the Foundation for the National Institutes of Health (<http://www.fnih.org/>). The grantee organization is the Northern California Institute for Research and Education, and the study is coordinated by the Alzheimer's Disease Cooperative Study at the University of California, San Diego, CA, USA. ADNI data are disseminated by the Laboratory for Neuro Imaging at the University of Southern California, CA, USA. This study was supported by grants received from the National Natural Science Foundation of China (grant numbers 82020108013); the 111 Project (grant number D20031); the Shanghai Municipal Science and Technology Major Project (grant number 2017SHZDZX01).

References

- [1] "2019 Alzheimer's disease facts and figures," *Alzheimer's & Dementia*, vol. 15, no. 3, pp. 321–387, 2019.
- [2] "2020 Alzheimer's disease facts and figures," *Alzheimer's & Dementia*, vol. 16, no. 3, pp. 391–460, 2020.
- [3] B. Dubois, H. Hampel, H. H. Feldman et al., "Preclinical Alzheimer's disease: definition, natural history, and diagnostic criteria," *Alzheimer's & Dementia*, vol. 12, no. 3, pp. 292–323, 2016.
- [4] Q. Y. Dong, T. R. Li, X. Y. Jiang, X. N. Wang, Y. Han, and J. H. Jiang, "Glucose metabolism in the right middle temporal gyrus could be a potential biomarker for subjective cognitive decline: a study of a Han population," *Alzheimer's Research & Therapy*, vol. 13, no. 1, p. 74, 2021.
- [5] Y. Huang and L. Mucke, "Alzheimer mechanisms and therapeutic strategies," *Cell*, vol. 148, no. 6, pp. 1204–1222, 2012.
- [6] C. M. Karch, C. Cruchaga, and A. M. Goate, "Alzheimer's disease genetics: from the bench to the clinic," *Neuron*, vol. 83, no. 1, pp. 11–26, 2014.
- [7] D. Harold, R. Abraham, P. Hollingworth et al., "Erratum: Genome-wide association study identifies variants at CLU and PICALM associated with Alzheimer's disease," *Nature Genetics*, vol. 41, no. 10, p. 1156, 2009.
- [8] A. Montagne, D. A. Nation, A. P. Sagare et al., "APOE4 leads to blood -brain barrier dysfunction predicting cognitive decline," *Nature*, vol. 581, no. 7806, pp. 71–76, 2020.
- [9] B. N. Vardarajan, Y. Zhang, J. H. Lee et al., "Coding mutations in SORL1 and Alzheimer disease," *Annals of Neurology*, vol. 77, no. 2, pp. 215–227, 2015.
- [10] H. Huang, J. Zhao, B. Xu et al., "The TOMM40 gene rs2075650 polymorphism contributes to Alzheimer's disease in Caucasian, and Asian populations," *Neuroscience Letters*, vol. 628, pp. 142–146, 2016.
- [11] N. R. Wray, M. E. Goddard, and P. M. Visscher, "Prediction of individual genetic risk of complex disease," *Current Opinion in Genetics & Development*, vol. 18, no. 3, pp. 257–263, 2008.
- [12] V. Escott-Price, C. Bellenguez, L. S. Wang et al., "Gene-wide analysis detects two new susceptibility genes for Alzheimer's disease," *PLoS One*, vol. 9, no. 6, article e94661, 2014.
- [13] V. Escott-Price, R. Sims, C. Bannister et al., "Common polygenic variation enhances risk prediction for Alzheimer's disease," *Brain*, vol. 138, no. 12, pp. 3673–3684, 2015.
- [14] the Alzheimer's Disease Neuroimaging Initiative, CHARGE consortium, EADI1 consortium et al., "Common variants at

- ABCA7, MS4A6A/MS4A4E, EPHA1, CD33 and CD2AP are associated with Alzheimer's disease," *Nature Genetics*, vol. 43, no. 5, pp. 429–435, 2011.
- [15] Alzheimer's Disease Sequencing Project, J. C. Bis, X. Jian et al., "Whole exome sequencing study identifies novel rare and common Alzheimer's-associated variants involved in immune response and transcriptional regulation," *Molecular Psychiatry*, vol. 25, no. 8, pp. 1859–1875, 2020.
 - [16] Karolinska Schizophrenia Project (KaSP) consortium, T. Elväsåshagen, S. Bahrami et al., "The genetic architecture of human brainstem structures and their involvement in common brain disorders," *Nature Communications*, vol. 11, no. 1, article 4016, 2020.
 - [17] S. Kim, S. Swaminathan, L. Shen et al., "Genome-wide association study of CSF biomarkers Abeta1-42, t-tau, and p-tau181p in the ADNI cohort," *Neurology*, vol. 76, no. 1, pp. 69–79, 2011.
 - [18] European Alzheimer's Disease Initiative (EADI), Genetic and Environmental Risk in Alzheimer's Disease (GERAD), Alzheimer's Disease Genetic Consortium (ADGC) et al., "Meta-analysis of 74,046 individuals identifies 11 new susceptibility loci for Alzheimer's disease," *Nature Genetics*, vol. 45, no. 12, pp. 1452–1458, 2013.
 - [19] R. D. Ball, "Designing a GWAS: power, sample size, and data structure," *Methods in Molecular Biology*, vol. 1019, pp. 37–98, 2013.
 - [20] G. Eraslan, Ž. Avsec, J. Gagneur, and F. J. Theis, "Deep learning: new computational modelling techniques for genomics," *Nature Reviews Genetics*, vol. 20, no. 7, pp. 389–403, 2019.
 - [21] B. Alipanahi, A. Delong, M. T. Weirauch, and B. J. Frey, "Predicting the sequence specificities of DNA- and RNA-binding proteins by deep learning," *Nature Biotechnology*, vol. 33, no. 8, pp. 831–838, 2015.
 - [22] J. Zhou and O. G. Troyanskaya, "Predicting effects of noncoding variants with deep learning-based sequence model," *Nature Methods*, vol. 12, no. 10, pp. 931–934, 2015.
 - [23] M. Wang, C. Tai, W. E. and L. Wei, "DeFine: deep convolutional neural networks accurately quantify intensities of transcription factor-DNA binding and facilitate evaluation of functional non-coding variants," *Nucleic Acids Research*, vol. 46, no. 11, article e69, 2018.
 - [24] H. Zeng and D. K. Gifford, "Predicting the impact of non-coding variants on DNA methylation," *Nucleic Acids Research*, vol. 45, no. 11, article e99, 2017.
 - [25] C. Angermueller, H. J. Lee, W. Reik, and O. Stegle, "DeepCpG: accurate prediction of single-cell DNA methylation states using deep learning," *Genome Biology*, vol. 18, no. 1, article 67, 2017.
 - [26] S. Cheng, M. Guo, C. Wang, X. Liu, Y. Liu, and X. Wu, "MiRTDL: a deep learning approach for miRNA target prediction," *IEEE/ACM Transactions on Computational Biology and Bioinformatics*, vol. 13, no. 6, pp. 1161–1169, 2016.
 - [27] J. Zhou, C. L. Theesfeld, K. Yao, K. M. Chen, A. K. Wong, and O. G. Troyanskaya, "Deep learning sequence-based ab initio prediction of variant effects on expression and disease risk," *Nature Genetics*, vol. 50, no. 8, pp. 1171–1179, 2018.
 - [28] R. Luo, F. J. Sedlazeck, T. W. Lam, and M. C. Schatz, "A multi-task convolutional deep neural network for variant calling in single molecule sequencing," *Nature Communications*, vol. 10, no. 1, article 998, 2019.
 - [29] P. Chang, J. Grinband, B. D. Weinberg et al., "Deep-learning convolutional neural networks accurately classify genetic mutations in gliomas," *AJNR. American Journal of Neuroradiology*, vol. 39, no. 7, pp. 1201–1207, 2018.
 - [30] D. R. Kelley, Y. A. Reshef, M. Bileschi, D. Belanger, C. Y. McLean, and J. Snoek, "Sequential regulatory activity prediction across chromosomes with convolutional neural networks," *Genome Research*, vol. 28, no. 5, pp. 739–750, 2018.
 - [31] D. Quang and X. Xie, "FactorNet: a deep learning framework for predicting cell type specific transcription factor binding from nucleotide-resolution sequential data," *Methods*, vol. 166, pp. 40–47, 2019.
 - [32] G. M. McKhann, D. S. Knopman, H. Chertkow et al., "The diagnosis of dementia due to Alzheimer's disease: recommendations from the National Institute on Aging-Alzheimer's Association workgroups on diagnostic guidelines for Alzheimer's disease," *Alzheimer's & Dementia*, vol. 7, no. 3, pp. 263–269, 2011.
 - [33] H. Neitzel, "A routine method for the establishment of permanent growing lymphoblastoid cell lines," *Human Genetics*, vol. 73, no. 4, pp. 320–326, 1986.
 - [34] L. Shen, S. Kim, S. L. Risacher et al., "Whole genome association study of brain-wide imaging phenotypes for identifying quantitative trait loci in MCI and AD: a study of the ADNI cohort," *NeuroImage*, vol. 53, no. 3, pp. 1051–1063, 2010.
 - [35] T. Han, C. Liu, W. Yang, and D. Jiang, "Deep transfer network with joint distribution adaptation: a new intelligent fault diagnosis framework for industry application," *ISA Transactions*, vol. 97, pp. 269–281, 2020.
 - [36] K. Chen, K. Chen, Q. Wang, Z. He, J. Hu, and J. He, "Short-term load forecasting with deep residual networks," *IEEE Transactions on Smart Grid*, vol. 10, no. 4, pp. 3943–3952, 2019.
 - [37] D. Titov, J. Diehl-Schmid, K. Shi et al., "Metabolic connectivity for differential diagnosis of dementing disorders," *Journal of Cerebral Blood Flow & Metabolism*, vol. 37, no. 1, pp. 252–262, 2017.
 - [38] Alzheimer's Disease Neuroimaging Initiative, M. Wang, J. Jiang et al., "Individual brain metabolic connectome indicator based on Kullback-Leibler Divergence Similarity Estimation predicts progression from mild cognitive impairment to Alzheimer's dementia," *European Journal of Nuclear Medicine and Molecular Imaging*, vol. 47, no. 12, pp. 2753–2764, 2020.
 - [39] the European Alzheimer's Disease Initiative Investigators, J. C. Lambert, S. Heath et al., "Genome-wide association study identifies variants at CLU and CR1 associated with Alzheimer's disease," *Nature Genetics*, vol. 41, no. 10, pp. 1094–1099, 2009.
 - [40] R. Zhu, X. Liu, and Z. He, "Association between CLU gene rs11136000 polymorphism and Alzheimer's disease: an updated meta-analysis," *Neurological Sciences*, vol. 39, no. 4, pp. 679–689, 2018.
 - [41] W. Xu, L. Tan, and J. T. Yu, "The role of PICALM in Alzheimer's disease," *Molecular Neurobiology*, vol. 52, no. 1, pp. 399–413, 2015.
 - [42] Z. Wang, H. Lei, M. Zheng, Y. Li, Y. Cui, and F. Hao, "Meta-analysis of the association between Alzheimer disease and variants in GAB2, PICALM, and SORL1," *Molecular Neurobiology*, vol. 53, no. 9, pp. 6501–6510, 2016.
 - [43] I. M. Badamasi, M. S. Lye, N. Ibrahim, and J. Stanslas, "Genetic endophenotypes for insomnia of major depressive disorder and treatment-induced insomnia," *Journal of Neural Transmission*, vol. 126, no. 6, pp. 711–722, 2019.

- [44] A. Drago and D. de Ronchi, "HTR2A gene variants and psychiatric disorders: a review of current literature and selection of SNPs for future studies," *Current Medicinal Chemistry*, vol. 14, no. 19, pp. 2053–2069, 2007.
- [45] X. Q. Wang, W. J. Huang, L. Su et al., "Neuroimaging advances regarding subjective cognitive decline in preclinical Alzheimer's disease," *Molecular Neurodegeneration*, vol. 15, no. 1, p. 55, 2020.

Research Article

Dextromethorphan Dampens Neonatal Astrocyte Activation and Endoplasmic Reticulum Stress Induced by Prenatal Exposure to Buprenorphine

Chun-Hua Lin ¹, Pao-Luh Tao,² Huey-Jen Tsay,³ Yao-Chang Chiang,² Wei-Tang Chang,² Ing-Kang Ho,² and Feng-Shiun Shie ²

¹Department of Nursing, College of Nursing and Health, Kang-Ning University, Taipei, Taiwan

²Center for Neuropsychiatric Research, National Health Research Institutes, Zhunan Town, Miaoli County, Taiwan

³Institute of Neuroscience, National Yang-Ming University, Taipei, Taiwan

Correspondence should be addressed to Feng-Shiun Shie; fshie@nhri.org.tw

Received 16 April 2021; Accepted 23 June 2021; Published 12 July 2021

Academic Editor: Yu Yo Sun

Copyright © 2021 Chun-Hua Lin et al. This is an open access article distributed under the Creative Commons Attribution License, which permits unrestricted use, distribution, and reproduction in any medium, provided the original work is properly cited.

Prenatal exposure to buprenorphine renders offspring vulnerable to cerebral impairments. In this study, our data demonstrate, for the first time, that prenatal exposure to buprenorphine escalates astrocyte activation concurrent with indications of endoplasmic reticulum (ER) stress in the hippocampi of neonates, and this can be prevented by the coadministration of dextromethorphan with buprenorphine. Furthermore, dextromethorphan can inhibit the accumulation of GPR37 in the hippocampus of newborns caused by buprenorphine and is accompanied by the proapoptotic ER stress response that involves the procaspase-3/CHOP pathway. Primary astrocyte cultures derived from the neonates of the buprenorphine group also displayed aberrant ER calcium mobilization and elevated basal levels of cyclooxygenase-2 (COX-2) at 14 days *in vitro* while showing sensitivity to lipopolysaccharide-activated expression of COX-2. Similarly, these long-lasting defects in the hippocampus and astrocytes were abolished by dextromethorphan. Our findings suggest that prenatal exposure to buprenorphine might instigate long-lasting effects on hippocampal and astrocytic functions. The beneficial effects of prenatal coadministration of dextromethorphan might be, at least in part, attributed to its properties in attenuating astrocyte activation and hippocampal ER stress in neonates.

1. Introduction

Because a growing number of pregnant opioid users receive buprenorphine maintenance therapy, concerns regarding the adverse effects of this long-lasting opioid on the brain function of offspring have received increasing attention [1–4]. Indeed, visuomotor dysfunction has been reported in children prenatally exposed to opioids [5]. In neonatal animal models, offspring with prenatal exposure to buprenorphine have several brain dysfunctions, including demyelination, abnormal cholinergic/dopaminergic development, and decreased neurogenesis; such exposure may also increase the death rate in neonates [6–9]. The mechanisms underlying the adverse effects of prenatal exposure to buprenorphine on the brain function are not fully understood although μ -opioid receptor-mediated neurotoxicity in adults has been proposed [10].

Given the significant roles of astrocytic function in pathological conditions, we propose that dysfunctional astrocytes and associated oxidative and endoplasmic reticulum (ER) stress might contribute to the development of brain dysfunction triggered by the prenatal exposure to opioids. Astrocytes, which are the most abundant glia in the brain, play an important role in synaptic information processing by balancing both excitatory glutamatergic and inhibitory GABAergic neurotransmission, particularly where pre- and postsynaptic nerve endings are intricately wrapped by astrocytes [11, 12]. Astrocytic function and astrocyte-neuron intercellular communication are regulated largely by the homeostasis of intracellular calcium [13]. In many brain diseases, astrocytes are known to be critical for neuronal survival. Astrocytes become activated with morphological changes and increased expression of glial fibrillary acidic

protein (GFAP) during the pathogenesis of brain diseases [14]. Similar to microglial activation, astrogliosis is a common pathological feature shared by many brain diseases. Although astrocyte activation has been proposed to promote neuronal survival in the diseased brain, uncontrolled release of effectors derived from overactivated astrocytes triggers neuroinflammation and increases oxidative and ER stresses [15]. Indeed, proinflammatory cytokines secreted from astrogliosis in neurodegenerative diseases could compromise glutamatergic neurotransmission and synaptic activity through disrupting the interaction of postsynaptic density protein 95 with N-methyl-D-aspartate receptors (NMDARs) [16]. These consequences lead to enhanced excitotoxicity in the brain and, ultimately, loss of neuronal function.

Increased expressions of caspase-3 and C/EBP homologous protein (CHOP) are indicative of proapoptosis during ER stress [16, 17]. Other ER stress proteins and chaperones such as glucose-regulated protein (GRP) and protein-disulfide isomerase (PDI) are produced in response to ER stress in order to attenuate the accumulation of mutated gene products or misfolded proteins induced by oxidative or nitrosative stress [18]. Expression of PDI facilitates the maturation and transport of misfolded proteins, representing an adaptive response to prevent ER-associated neurotoxicity and protein misfolding [19]. Reduced PDI expression [20] or inhibition of PDI activity [18] results in aberrant ER function. G protein-coupled receptor 37 (GPR37) is an orphan G protein-coupled receptor that is expressed in the brain and is associated with neuropathology of Parkinson's disease (PD) [21, 22]. Recently, accumulation of GPR37 aggregates has been considered to result from protein misfolding, which is characteristic of ER stress [23]. GPR37 is a substrate for parkin involved in the modulation of dopaminergic signaling [24], while increasing expression and accumulation of GPR37 high-molecular-weight aggregates instigate ER stress [25]. Furthermore, the elevated expression of GPR37 has been shown to lead to protein aggregation, thus contributing to neuronal dysfunction [26, 27]. Oxidative stress refers to the production of large amounts of reactive oxygen species, such as NO derivatives, and proinflammatory cytokine/chemokines and prostanoids, which are associated with an increased activity of cyclooxygenase-2 (COX-2) and inducible nitric oxide synthase (iNOS) [28]. These effectors may directly damage neuronal function and/or lead to uncontrolled glial overactivation, amplifying a self-propelling cycle that potentiates further increase in oxidative and ER stresses [29]. The consequences include massive neuroinflammation and exacerbated neuronal dysfunction.

Dextromethorphan, a common ingredient in cough and cold remedies, has been documented to show anti-inflammatory activity and NMDAR-dependent antagonistic effects on neuroprotection in many disease models, such as lipopolysaccharide- (LPS-) induced neurodegeneration, Parkinson's disease [27, 30], seizures [31, 32], and ischemic brain injury [33]. The mechanism underlying the neuroprotective effects of dextromethorphan has been proposed to be through the reduction of NMDAR-mediated excitotoxicity, although alternative targets have also been reported [34, 35]. Dextromethorphan also modulates the behavioral

responses induced by several substance abuse drugs. For instance, dextromethorphan attenuates methamphetamine-induced rewarding as determined by conditioned place preference [36]. Therefore, as a result of its influence on the expression of neurotrophic effectors and its role in modulating glial-activation-associated neuroinflammation, we speculate that coadministration of dextromethorphan can be beneficial for offspring with prenatal exposure to buprenorphine. Our study on the therapeutic potential of dextromethorphan may provide findings that could significantly contribute to the knowledge of this important public issue in drug abuse medicine.

2. Materials and Methods

2.1. Animals. Pregnant Sprague-Dawley (SD) rats were maintained at a room temperature of $23^{\circ}\text{C} \pm 2^{\circ}\text{C}$, with a 12 h light-dark cycle and food and water *ad libitum*, throughout the experiment. Animals were handled according to the guidelines of the Institutional Animal Care and Use Committee at the National Health Research Institutes. The rats were randomly separated into the following four groups: subcutaneous injection of water (vehicle control group), buprenorphine, dextromethorphan, or buprenorphine plus dextromethorphan from embryonic day E3 to E20. Buprenorphine was delivered at 3 mg/kg once a day, while dextromethorphan was delivered at the same dose (3 mg/kg) twice a day (9 a.m. and 5 p.m.). Neonates at postnatal day 1 (P1) were used for all assessments, while offspring at postnatal day 14 were used for the hippocampal synaptic assay. Neonates in the same litter were considered identical, and the value of *n* represents the number of pregnant SD rats used in the experiments.

2.2. Primary Astrocyte Cultures. Primary astrocyte cultured cells were derived from cortices of P1 neonates with different prenatal treatments; the primary astrocyte cultures were performed as described previously [37]. Briefly, cells were dissociated using an enzyme solution containing Dulbecco's modified Eagle's medium (DMEM), ethylenediaminetetraacetic acid (0.5 mmol/L), L-cysteine (0.2 mg/mL), papain (15 U/mL), and DNase I (200 $\mu\text{g}/\text{mL}$), followed by trituration. Culture medium (DMEM with 10% fetal bovine serum, 100 U/mL penicillin, and 100 $\mu\text{g}/\text{mL}$ streptomycin) was changed after 2 h of initial seeding. After two stripping and seeding cycles during two weeks in culture, astrocytes at 14 days *in vitro* (DIV) were harvested with trypsinization and reseeded for the experiments.

2.3. Confocal Microscopy. Confocal microscopy was used for the semiquantification analysis. Brain samples from P1 neonates were subjected to paraformaldehyde (4% in PBS) fixation overnight, followed by cryoprotection with sucrose (30% in PBS). One representative 30 μm thick cryosection per neonate from the control or buprenorphine group (at least four litters) was subjected to immunohistochemical analysis using antibodies against GFAP (Millipore), GPR37 (Abnova), or PDI (Santa Cruz). Images were acquired with a 20x objective using a Leica confocal microscopy imaging

system with identical settings for the parameters, while a 63x objective was used for images of CA1 at a higher magnification. Mounting medium (Vector Lab) containing 4,6-diamidino-2-phenylindole (DAPI) was used to label the nuclei. Semiquantification of the immunoreactivity was performed using ImageJ in the fields of CA1 or hippocampal fissure, and comparisons of the mean intensity of immunoreactivity between control and buprenorphine groups in a given area were performed via *t*-test. Representative images from each group were taken for assessment.

2.4. Western Blot Analysis. Lysates from the hippocampus or primary culture were prepared using a lysis buffer (50 mM Tris, 150 mM NaCl, 0.02% NaN₃, 0.5% Nonidet P-40, 0.5% Triton X-100, and protease inhibitor mixture), and protein concentrations were determined using the Bio-Rad Protein Assay (Bio-Rad, Hercules, CA). Samples were subjected to 7.5% Tris-HCl, sodium dodecyl sulfate-polyacrylamide gel electrophoresis (SDS-PAGE), and western blot analysis, using antibodies against iNOS (BD Biosciences), COX-2 (BD Biosciences), GFAP (Millipore), GPR37 (Abnova), GRP78 (Novus), procaspase-3 (Stressgen), caspase-3 (Cell Signaling), caspase-12 (Stressgen), and CHOP (Abcam). An antibody against β -actin (Novus) was used to normalize the quantity of protein in each sample. Enhanced chemiluminescence (ECL; PerkinElmer) was used for the western blot detection. Corresponding bands were quantified with ImageJ (NIH imaging software), and one-way ANOVA was tested for significance. Data are presented as the mean \pm SEM (the standard error of the mean). At least four litters from four pregnant rats of each group were used for all assessments.

2.5. FLIPR Calcium Assay. To measure calcium transients, primary astrocytes at 14 DIV were seeded initially at 4×10^4 cells per well in 96-well plates (black with a clear flat bottom from Corning) and cultured for 48 h. The assay was performed using a FLIPR Calcium 4 assay kit (Molecular Devices) according to the manufacturer's instructions. Briefly, 1 h prior to performing the assay, the culture medium was replaced with serum-free DMEM, followed by 1 h incubation at 37°C with FLIPR calcium assay reagent dissolved in 1x assay buffer containing HBSS (5 mM KCl, 0.3 mM KH₂PO₄, 138 mM NaCl, 4 mM NaHCO₃, 0.3 mM Na₂HPO₄, 5.6 mM d-glucose, and 20 mM HEPES, pH 7.4 from Gibco) and 2.5 mM probenecid in the presence or the absence of 1.27 mM CaCl₂. After stabilization at room temperature for 1 h, the culture plates were subjected to analysis using FlexStation 3 (Molecular Devices) with robotic addition of glutamate (final concentration of 100 μ M in HBSS) into the cultures at 10 sec after the initial recording. The fluorescence was monitored at every 1.52 sec interval with an excitation wavelength of 485 nm and an emission wavelength of 525 nm for 180 sec. The intracellular calcium reached a peak at approximately 13 sec after the induction of glutamate. Data were analyzed using SoftMax Pro (Molecular Devices) and are presented as a response curve and an area under the curve normalized by the corresponding area at the basal condition. Data from duplicated experiments in two wells of each cul-

ture were averaged, and at least five litters from five pregnant rats of each group were used for quantification.

2.6. Statistical Analysis. The differences between groups were tested using one-way ANOVA followed by post hoc multiple comparisons using the Bonferroni test; assessments were done with SPSS software, while the comparisons of the immunoreactivity between control and buprenorphine groups were performed via *t*-test. Data are presented as means \pm SEM. Statistical significance was set at $p < 0.05$.

3. Results

3.1. Elevated Astrocyte Activation in the Hippocampus of Neonates with Prenatal Exposure to Buprenorphine. Previous studies have demonstrated that the GFAP protein plays a critical role and has marked upregulation in CNS injury [38, 39]. To examine whether astrocytes are activated in neonates following prenatal exposure to buprenorphine, immunofluorescent confocal microscopy was performed using an antibody against GFAP for the control and buprenorphine groups. Semiquantification of immunoreactivity demonstrated that the buprenorphine group had increased GFAP immunoreactivity, localized mainly in the hippocampal fissure ($222 \pm 32\%$ of the control group, $p < 0.01$ by *t*-test), compared to the controls ($100 \pm 11\%$) (Figure 1(a)). To quantify GFAP levels as an indication of astrocyte activation, total hippocampal lysates from all groups were analyzed by western blot. Results showed that GFAP levels in the buprenorphine group were significantly increased to $152 \pm 12\%$ of the control group ($p < 0.001$; Figure 1(b)), which is suggestive of astrocyte activation. Since dextromethorphan is known to alleviate glial activation, the effects of coadministration of dextromethorphan with buprenorphine were examined. Intriguingly, the levels of the hippocampal GFAP in the group with prenatal coadministration of dextromethorphan with buprenorphine returned to those ($127 \pm 16\%$ of the control group) similar to what is seen in the controls ($100 \pm 6\%$), while the dextromethorphan-alone group ($116 \pm 18\%$ of the control group) showed no significant effect on GFAP levels.

3.2. Prenatal Exposure to Buprenorphine Leads to Increased ER and Oxidative Stress in the Hippocampus of Neonates. Given that the accumulation of GPR37 aggregates is indicative of ER stress [22], brain tissues were then subjected to analysis under immunofluorescent confocal microscopy. The data show that the increasing GFAP immunoreactivity in the hippocampal fissure of the buprenorphine group parallels the intensity of the GPR37 punctate in the pyramidal neurons (Figure 1(a)). Results from immunohistochemistry clearly showed that GPR37 immunoreactivity was predominantly present in the pyramidal neurons of areas CA1-3 and, to a lesser extent, in the granules of the dentate gyrus (DG). As demonstrated in representative images at a higher magnification in CA1, semiquantification of immunoreactivity shows that perinuclear GPR37 punctate staining was significantly increased in the group with prenatal exposure to buprenorphine compared to the controls. Quantification of

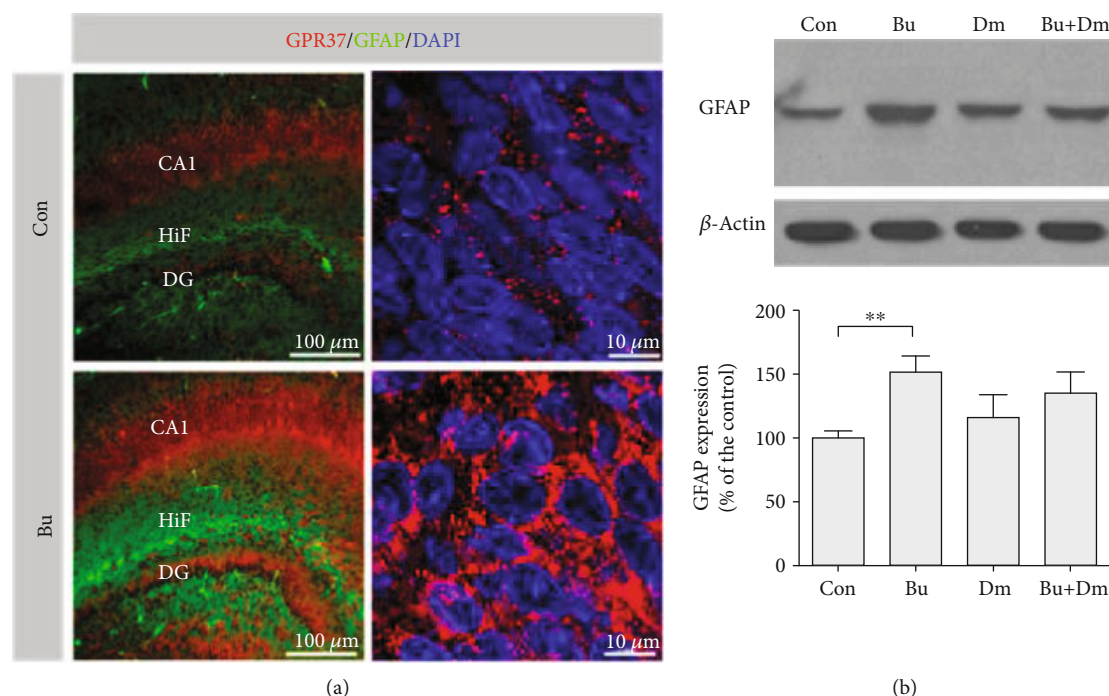


FIGURE 1: Prenatal exposure to buprenorphine escalates astrocyte activation in the hippocampus of the neonates concurrent with increased GPR37 immunoreactivity. Prenatal treatments: buprenorphine (Bu), dextromethorphan (Dm), coadministration of buprenorphine with dextromethorphan (Bu+Dm), or vehicle controls (Con). (a) Confocal images (20x objective, left panel) for GPR37 (red) and GFAP (green) immunoreactivity in the hippocampus of neonates, with images at a higher magnification (63x objective) for GPR37 punctate staining (red) in the CA1 (right panel). (b) Western blot analysis of hippocampal GFAP expression levels with quantification. DAPI (blue) staining identifies nuclei. Data are mean \pm SEM % of control, ** $p < 0.01$ vs. Con and *** $p < 0.001$ vs. Con.

GPR37 aggregates by western blot revealed that buprenorphine exposure led to an increase in GPR37 accumulation in both monomer (at 52 kDa; $131 \pm 9\%$ of the control group, $p < 0.01$) and high-molecular-weight aggregates (>170 kDa; $195 \pm 33\%$ of the control group, $p < 0.01$) compared to controls ($100 \pm 3\%$ and $100 \pm 5\%$, respectively; Figure 2(a)). The group with coadministration of dextromethorphan with buprenorphine showed reversal in the induction of GPR37 expression ($102 \pm 9\%$ of the control group) and prevention of the accumulation of GPR37 high-molecular-weight aggregates ($100\% \pm 13\%$ of the control group), while the dextromethorphan-alone group ($98 \pm 7\%$ and $109 \pm 9\%$ of the control group for monomer and high-molecular-weight aggregates, respectively) showed no changes in GPR37 levels.

Quantification of other indications of the prosurvival and proapoptotic pathways of ER stress responses from western blot analysis is presented in Figure 2(b). Data showed that the expression levels of procaspase-3 and CHOP ($135 \pm 8\%$ and $221 \pm 16\%$ of the control group, respectively) were significantly increased ($p < 0.001$ and $p < 0.01$, respectively) in the hippocampus of neonates with prenatal exposure to buprenorphine compared to that of the controls ($100 \pm 3\%$ and $100 \pm 10\%$, respectively). Intriguingly, coadministration of dextromethorphan with buprenorphine reversed the induction of procaspase-3 and CHOP expressions ($100 \pm 6\%$ and $105 \pm 11\%$ of the control group, respectively). Levels of caspase-3 appear to be higher in the buprenorphine group ($157 \pm 17\%$) than in other groups, although not significantly.

However, the expression levels of GRP78 and caspase-12 were comparable among all groups of prenatal treatments. Taken together, these data demonstrate that prenatal exposure to buprenorphine led to the accumulation of hippocampal GPR37 aggregates in the hippocampus of the neonates concurrent with proapoptotic ER stress responses involved in the procaspase-3/CHOP pathways, which is rescued by the coadministration of dextromethorphan.

For measuring oxidative stress, expression levels of iNOS and COX-2 in the hippocampus were examined. Results from the western blot analysis showed that the expression levels of iNOS were significantly increased in the buprenorphine group ($132 \pm 8\%$ of the control group, $p < 0.01$) compared to the control group ($100 \pm 5\%$). The expression levels of iNOS were not affected by dextromethorphan alone ($97 \pm 16\%$ of the control group), while the group with coadministration of dextromethorphan and buprenorphine showed no reversal in the induced iNOS expression ($146 \pm 8\%$ of the control group, $p < 0.01$). The expression levels of COX-2 were slightly increased in the buprenorphine group ($124 \pm 9\%$ of the control group), although not significantly, while those in the dextromethorphan and buprenorphine and coadministration of dextromethorphan groups were $97 \pm 16\%$ and $108 \pm 15\%$ of the control level, respectively. These were both not significantly different from the levels in the control group ($100 \pm 7\%$). Our data demonstrate that the prenatal exposure to buprenorphine induces oxidative stress as evidenced by the elevated iNOS levels in the

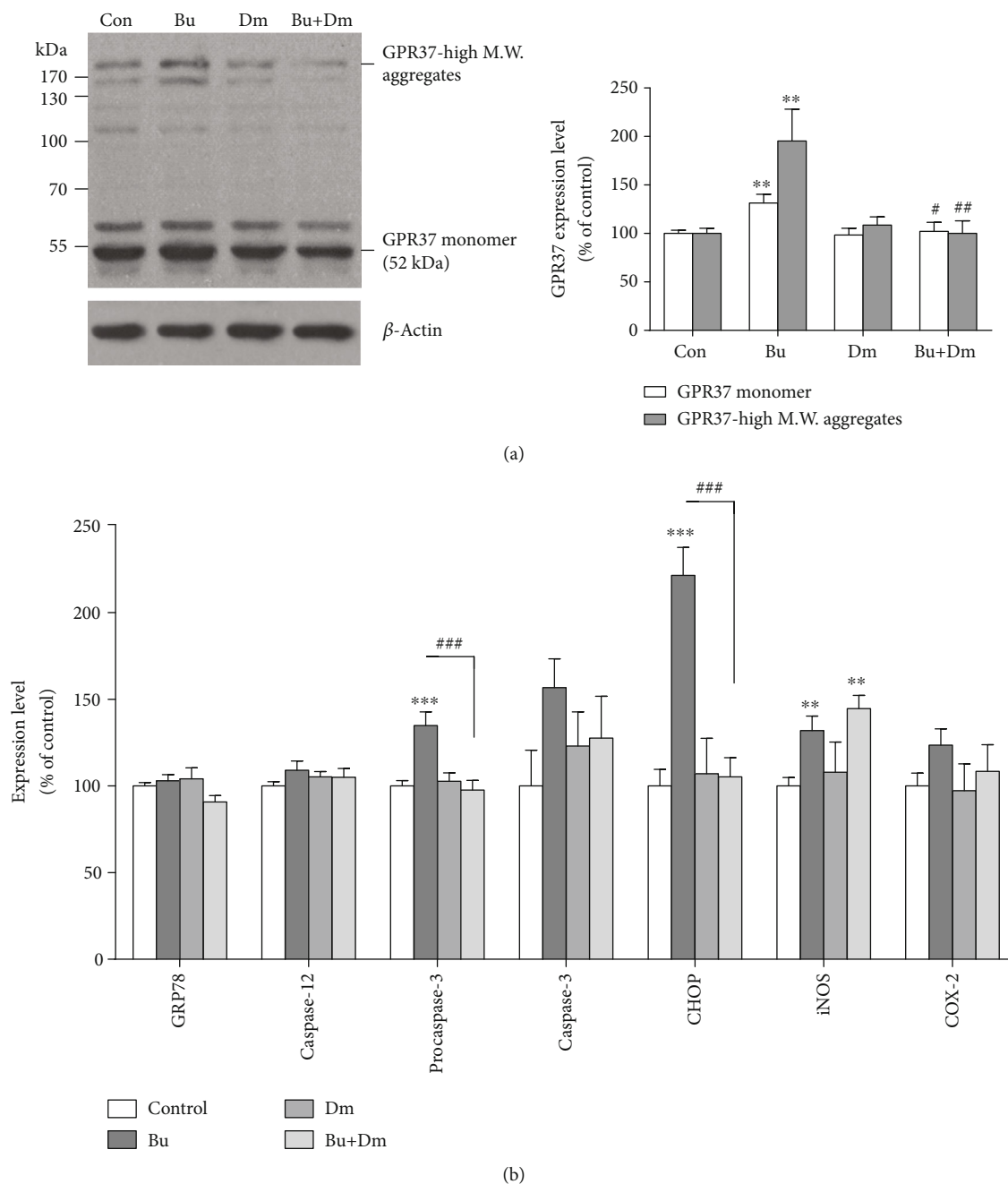


FIGURE 2: ER and oxidative stresses are induced by prenatal exposure to buprenorphine in the hippocampus of the neonates. (a) Western blot analysis of the expression levels of hippocampal GPR37 monomer and high molecular weight (M.W.) aggregates with quantification. (b) Quantification of Western blot analysis for the expression levels of GPR78, caspase-12, procaspase-3, caspase-3, CHOP, iNOS, and COX-2 in the hippocampus of the neonates with prenatal exposure to Bu, Dm, Bu+Dm, or Con. Data are mean \pm SEM % of control; ** $p < 0.01$ vs. Con and *** $p < 0.001$ vs. Con and ## $p < 0.01$ vs. Bu and ### $p < 0.001$ vs. Bu.

hippocampus. However, coadministration of dextromethorphan with buprenorphine had minimal effects on preventing induced oxidative stress.

3.3. Prenatal Exposure to Buprenorphine Increases the Levels of COX-2 Expression at Both Basal and LPS-Activated States in Primary Astrocytes. Given that astrocytes play an important role in hippocampal functioning [40], the observed long-term effects *in vivo* can be indicative of abnormal astro-

cytic functions induced by prenatal exposure to buprenorphine. Thus, we first investigated whether prenatal exposure to buprenorphine causes long-term changes in astrocytic immunity. Expressions of COX-2 and iNOS were measured in the primary astrocytes derived from neonates subjected to the various prenatal treatments. As presented in Figure 3(a), the basal levels of the COX-2 expression were higher in astrocytes in the group with prenatal exposure to buprenorphine ($388 \pm 109\%$ of the control group at basal

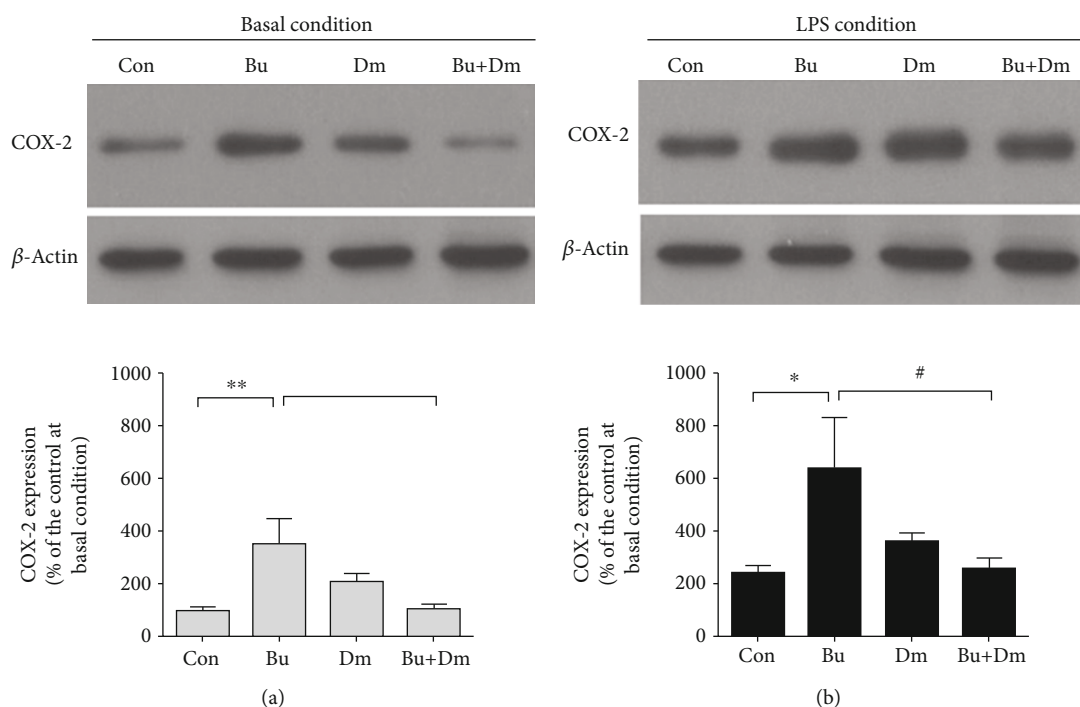


FIGURE 3: Primary astrocytes derived from the neonates of the buprenorphine group display elevated basal levels of COX-2 and sensitize to the LPS-induced expression of COX-2. Western blot analysis with quantification for COX-2 expression levels in the primary astrocytes at basal (a) or activated (LPS treatment) (b) condition. Data are mean \pm SEM % of control; * p < 0.05 vs. Con and ** p < 0.01 vs. Con and ## p < 0.001 vs. Bu.

condition, p < 0.01) compared to the control group (100 \pm 10%). Data suggest that buprenorphine-induced oxidative stress in astrocytes is sustained at 14 DIV. Surprisingly, astrocytes from the group with prenatal exposure to dextromethorphan alone also had increased basal levels of COX-2 expression (211 \pm 28% of the control group at the basal condition), although not significantly. Coadministration of dextromethorphan with buprenorphine reduced the expression of COX-2 to levels (102 \pm 20% of the control group at the basal condition) comparable to those in the controls.

We then investigated whether prenatal exposure to buprenorphine sensitizes astrocytes to a greater induction of COX-2 expression under the circumstances of an immune challenge. As presented in Figure 3(b) for the control group, expression levels of COX-2 in primary astrocytes can be significantly elevated by LPS treatments (241 \pm 29% of the control group at the basal condition). The levels of COX-2 were further enhanced in primary astrocytes derived from the buprenorphine group (640 \pm 195% of the control group at basal condition). Levels of LPS-induced COX-2 expression in groups with the administration of dextromethorphan alone and coadministration of dextromethorphan with buprenorphine were 364 \pm 26% and 259 \pm 41% of the control group at the basal condition, respectively, which were significantly higher than those of the control group at basal conditions but not higher than those of the control group that received LPS treatments. Thus, coadministration of dextromethorphan with buprenorphine appears to reverse the effects of buprenorphine on the regulation of astrocytic immunity.

Next, we examined the iNOS expression, which is another indication of immune response, in astrocytes. Since the basal levels of iNOS in the primary astrocytes were undetectable by western blot, data from LPS-activated astrocytes are presented. Our results show that the LPS-induced expressions of iNOS are comparable among all groups; the levels in the control, buprenorphine, dextromethorphan, and coadministration of dextromethorphan with buprenorphine groups were 100 \pm 18%, 82 \pm 6%, 99 \pm 18%, and 112 \pm 24% of the control group with LPS treatment, respectively. Data suggest that coadministration of dextromethorphan with buprenorphine had minimal effects on preventing the induced iNOS expression.

3.4. ER Calcium Mobilization in Response to Glutamate in Primary Astrocytes at 14 DIV Is Altered by Prenatal Exposure to Buprenorphine. Next, we investigated whether glutamate-induced ER calcium mobilization, a critical process for modulating astrocytic function in response to immune challenges in primary astrocytes, is affected by prenatal exposure to buprenorphine at 14 DIV. As shown in Figure 4, glutamate-induced transient reduction in calcium in the absence of extracellular calcium is observed in the astrocytes of the group with prenatal exposure to buprenorphine (57 \pm 7% of the control group, p < 0.05) compared to the control group (100 \pm 11%), which is suggestive of a defect in calcium mobilization from ER stores. Coadministration of dextromethorphan with buprenorphine reversed the glutamate-induced transient reduction in calcium to an extent (84 \pm 9% of the control group) that was not

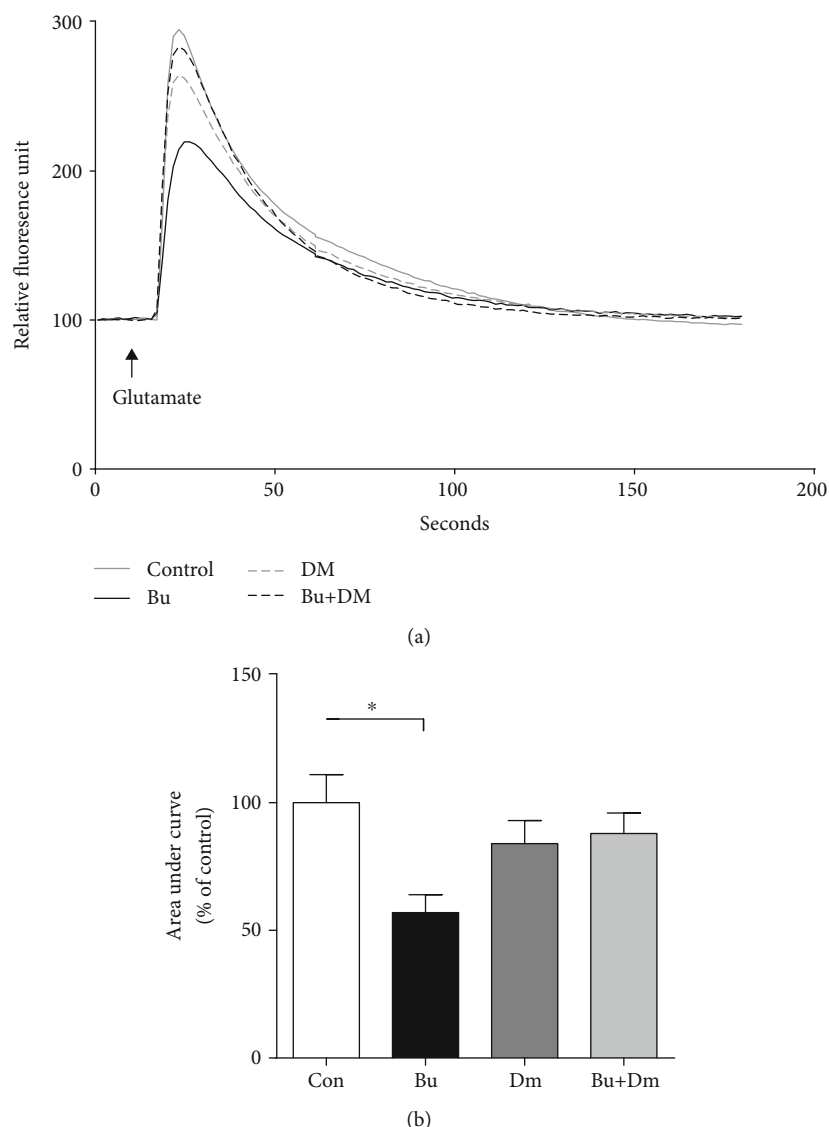


FIGURE 4: Glutamate-induced calcium transient is inhibited in the primary astrocytes from the neonates with prenatal exposure to buprenorphine. Response curve and quantification of calcium transients in the absence of extracellular calcium measured by the FLIPR calcium assay using FlexStation 3 in the primary astrocytes from neonates with prenatal exposure to Bu, Dm, Bu+Dm, or Con. Addition of glutamate (arrow) at 10 sec after the initial recording. Data are mean \pm SEM % of control; * $p < 0.05$ vs. Con.

significantly different from those in controls, while the dextromethorphan group alone had no effect on the glutamate-induced transient reduction in calcium in astrocytes ($88 \pm 8\%$ of the control group). Our data show that prenatal exposure to buprenorphine caused deficits in calcium mobilization from the ER in primary astrocytes, while coadministration of dextromethorphan completely abolished the effects. The magnitude of glutamate-induced transient reduction in total intracellular calcium as measured in the presence of extracellular calcium for all groups, including buprenorphine ($105 \pm 8\%$), dextromethorphan ($82 \pm 10\%$), and dextromethorphan-buprenorphine coadministration ($96 \pm 17\%$), was comparable to that in the controls ($100 \pm 7\%$). Thus, these data suggest that prenatal exposure to buprenorphine leads to long-term but reversible changes in astrocytic

calcium mobilization by dampening ER store release while enhancing calcium influx from an extracellular source.

4. Discussion

Although buprenorphine replacement therapy has been considered safe for pregnant women, alterations in the brain physiology of offspring in animal models have been documented. Our results reveal the first demonstration that prenatal exposure to buprenorphine could lead to an aberrant astrocyte activation and elevated oxidative and ER stresses in the hippocampus of neonates. Furthermore, our findings regarding abnormal astrocyte activation, ER dysfunction in primary cultures, and disrupted synaptic function in the hippocampus of offspring at 2 weeks of age suggest that the

impacts of prenatal exposure to buprenorphine are long lasting, both *in vivo* and *in vitro*. There is mounting evidence suggesting that astrocyte activation and the associated oxidative and ER stresses contribute to the pathogenesis of several brain diseases. Our findings provide further insights into a possible mechanistic link between astrocyte-associated oxidative and ER stresses and the development of brain dysfunction in offspring following prenatal exposure to buprenorphine. However, the possibility that other factors contribute to the underlying mechanisms, especially microglia-mediated neuroinflammation, cannot be excluded.

In our animal model, the insults to the offspring may be due to the impact of direct exposure to buprenorphine during the embryonic stages, release of proinflammatory effectors from the maternal immune system in response to the repeated exposure of buprenorphine, and stresses from self-immunity and postnatal withdrawal syndrome, all of which can either lead to further damage through uncontrolled neuroinflammation or be counteracted through neuroprotective mechanisms. Indeed, astrocyte activation is a double-edged sword that can be detrimental or beneficial to neuronal survival, which is similar to the multiple functions of microglial activation in neurodegenerative diseases. In many brain diseases, activated astrocytes provide support for damaged neuronal tissue through the release of neurotrophic factors and clearance of neurotoxic substances [37]. Thus, it is conceivable to consider astrocyte activation induced by prenatal exposure to buprenorphine as a defensive response. Alternatively, prenatal exposure to buprenorphine may render the offspring vulnerable to undergoing pathological processes with subsequent insults later in life as a result of perturbed immune machinery that was epigenetically modified during the most sensitive period of the immune system establishment. Similarly, a hypothesis has been developed that prenatal exposure to particular substances predisposes neonates to certain diseases, such as Parkinson's disease and autoimmune disease [41, 42]. This notion is also echoed by our findings that prenatal exposure to buprenorphine not only elevates basal levels of oxidative stress but also potentiates LPS-stimulated oxidative stress in primary astrocytes.

Unlike that in the animal models with neurodegenerative diseases, the extent of astrocyte activation induced by prenatal exposure to buprenorphine is mostly limited to the vicinity of the hippocampal fissure. This region-specific astrocyte activation may indicate a different vulnerability of the hippocampus. Furthermore, astrocytes in the hippocampal fissure play an important role in the regulation of local blood flow in the layers of the CA1 and dentate gyrus. Increased intracerebral blood flow in response to neuronal activity is essential to ensure blood supply to active regions, and astrocytes are critical for regulating the neurovascular response via modulation of calcium signaling [43, 44], in addition to their role in boundary demarcation and serving as scaffolds for migrating neurons. Our observations of a significant increase in astrocyte activation in the hippocampal fissure and the disruption of astrocytic calcium mobilization in primary astrocytes collectively imply that the associated oxidative and ER stress may be locally instigated. The resulting consequences may lead to abnormal astrocyte-regulated neuronal activity

in the susceptible regions, thus promoting neuroinflammation. This result may partially explain why increased GPR37 aggregates, which are an indication of ER stress, were largely located in the CA1 region.

Although the molecular mechanism responsible for the effects of dextromethorphan on counteracting the buprenorphine-induced ER stress remains unclear, one possible explanation is that the beneficial effects of dextromethorphan may be attributed to its anti-inflammatory and/or antiexcitotoxic properties. This speculation is supported by the reports that inhibition of NMDAR-mediated excitotoxicity in various models of neurodegeneration contributes to the function of dextromethorphan in protecting neurons from damage and in suppressing glial activation [45, 46]. Of note, dextromethorphan is a noncompetitive, but weak, NMDAR antagonist [47], while dextromethorphan and its metabolite dextrorphan are high-affinity agonists for the sigma-1 receptor, which is a novel nonopioid ER chaperon. Thus, the effects of dextromethorphan could possibly result from the activation of the sigma-1 receptor. Increasing evidence indicates that sigma-1 receptor agonists are anti-inflammatory and neuroprotective mainly via their chaperoning functions that counteract ER stress [48]. This notion echoes the beneficial effects of dextromethorphan in counteracting the proapoptotic ER stress observed in our study. In addition, stimulation by sigma-1 receptor ligands has been shown to modulate the glutamate-evoked calcium influx in synapses [48] and to ameliorate glutamate-/NMDA-evoked NO production [49, 50]. These findings raise the possibility that indirect suppression of NMDAR activity may contribute to the anti-inflammatory properties of dextromethorphan. However, our data show that the elevated expression of iNOS was not suppressed by the dextromethorphan treatment, suggesting that the iNOS expression induced by prenatal exposure to buprenorphine might be involved in alternative mechanisms independent of the NMDAR activity. Thus, our data imply that the beneficial effects of dextromethorphan in our animal model may not be exclusively due to its blockade of the NMDAR activity.

5. Conclusions

In conclusion, prenatal exposure of buprenorphine aroused local astrocyte activation concurrent with increases of hippocampal oxidative and ER stresses. The consequential long-term effects on astrocytic and hippocampal functions may render the offspring sensitized upon secondary challenge in their later lives. Pharmacologically inhibiting astrocyte activation and ER stress in the hippocampus by the coadministration of dextromethorphan with buprenorphine during the embryonic stages ameliorates any detrimental effects. However, it remains unknown if the effectors instigating the signaling cascades of astrocyte activation do this as a result of the insults arising from the prenatal exposure to buprenorphine and its associated oxidative and ER stresses. This merits further investigation. Further studies on the role of astrocyte activation and its reciprocal interactions with microglia and neurons in the prenatal exposure to buprenorphine may shed light on this largely unknown area in drug abuse medicine.

Data Availability

The original data used to support the findings of this study are included within the article.

Conflicts of Interest

The authors declare no competing financial interests.

Authors' Contributions

Chun-Hua Lin and Pao-Luh Tao contributed equally to this work and should be considered as co-first authors of this article.

Acknowledgments

We thank Man-Wu Sun, Tsai-Wei Hung, and Kuei-Yiing Hsu for their invaluable assistance in this study. This work was supported grants from the National Health Research Institutes (PH100PP34 to FSS and PH100PP53 to PLT) of Taiwan.

References

- [1] E. M. Lefevre, M. T. Pisansky, C. Toddes et al., "Interruption of continuous opioid exposure exacerbates drug-evoked adaptations in the mesolimbic dopamine system," *Neuropsychopharmacology*, vol. 45, no. 11, pp. 1781–1792, 2020.
- [2] E. S. Sanchez, J. W. Bigbee, W. Fobbs, S. E. Robinson, and C. Sato-Bigbee, "Opioid addiction and pregnancy: perinatal exposure to buprenorphine affects myelination in the developing brain," *Glia*, vol. 56, no. 9, pp. 1017–1027, 2008.
- [3] H. E. Jones, K. Kaltenbach, S. H. Heil et al., "Neonatal abstinence syndrome after methadone or buprenorphine exposure," *The New England Journal of Medicine*, vol. 363, no. 24, pp. 2320–2331, 2010.
- [4] J. N. Moore, M. R. Gastonguay, C. M. Ng et al., "The pharmacokinetics and pharmacodynamics of buprenorphine in neonatal abstinence syndrome," *Clinical Pharmacology and Therapeutics*, vol. 103, no. 6, pp. 1029–1037, 2018.
- [5] A. Melinder, C. Konijnenberg, and M. Sarfi, "Deviant smooth pursuit in preschool children exposed prenatally to methadone or buprenorphine and tobacco affects integrative visuomotor capabilities," *Addiction*, vol. 108, no. 12, pp. 2175–2182, 2013.
- [6] A. A. Vestal-Laborde, A. C. Eschenroeder, J. W. Bigbee, S. E. Robinson, and C. Sato-Bigbee, "The opioid system and brain development: effects of methadone on the oligodendrocyte lineage and the early stages of myelination," *Developmental Neuroscience*, vol. 36, no. 5, pp. 409–421, 2014.
- [7] H. Kuribara and S. Tadokoro, "The ambulation-increasing effect of buprenorphine in mice: comparison with the effect of morphine," *Arukoru kenkyu to yakubutsu izon= Japanese journal of alcohol studies & drug dependence*, vol. 26, no. 1, pp. 37–48, 1991.
- [8] C. C. Wu, C. J. Hung, C. H. Shen et al., "Prenatal buprenorphine exposure decreases neurogenesis in rats," *Toxicology Letters*, vol. 225, no. 1, pp. 92–101, 2014.
- [9] Y. C. Chiang, T. W. Hung, and I. K. Ho, "Development of sensitization to methamphetamine in offspring prenatally exposed to morphine, methadone and buprenorphine," *Addiction Biology*, vol. 19, no. 4, pp. 676–686, 2014.
- [10] S. Fitting, M. McRae, and K. F. Hauser, "Opioid and neuroHIV comorbidity – current and future perspectives," *Journal of Neuroimmune Pharmacology*, vol. 15, no. 4, pp. 584–627, 2020.
- [11] M. M. Halassa and P. G. Haydon, "Integrated brain circuits: astrocytic networks modulate neuronal activity and behavior," *Annual Review of Physiology*, vol. 72, no. 1, pp. 335–355, 2010.
- [12] A. Garnier, A. Vidal, and H. Benali, "A theoretical study on the role of astrocytic activity in neuronal hyperexcitability by a novel neuron-glia mass model," *The Journal of Mathematical Neuroscience*, vol. 6, no. 1, p. 10, 2016.
- [13] C. Henneberger, "Does rapid and physiological astrocyte-neuron signalling amplify epileptic activity?," *The Journal of Physiology*, vol. 595, no. 6, pp. 1917–1927, 2017.
- [14] B. Zhou, Y. X. Zuo, and R. T. Jiang, "Astrocyte morphology: diversity, plasticity, and role in neurological diseases," *CNS Neuroscience & Therapeutics*, vol. 25, no. 6, pp. 665–673, 2019.
- [15] S. Beggiato, A. C. Borelli, L. Ferraro, S. Tanganelli, T. Antonelli, and M. C. Tomasini, "Palmitoylethanolamide blunts amyloid- β 42-induced astrocyte activation and improves neuronal survival in primary mouse cortical astrocyte-neuron co-cultures," *Journal of Alzheimer's Disease*, vol. 61, no. 1, pp. 389–399, 2018.
- [16] E. S. Jung, K. An, H. Seok Hong, J. H. Kim, and I. Mook-Jung, "Astrocyte-originated ATP protects A β (1-42)-induced impairment of synaptic plasticity," *The Journal of Neuroscience*, vol. 32, no. 9, pp. 3081–3087, 2012.
- [17] Y. Li, Y. Guo, J. Tang, J. Jiang, and Z. Chen, "New insights into the roles of CHOP-induced apoptosis in ER stress," *Acta biochimica et biophysica Sinica*, vol. 46, no. 8, pp. 629–640, 2014.
- [18] T. Uehara, T. Nakamura, D. Yao et al., "S-Nitrosylated protein-disulphide isomerase links protein misfolding to neurodegeneration," *Nature*, vol. 441, no. 7092, pp. 513–517, 2006.
- [19] Š. Lehtonen, M. Jaronen, P. Vehviläinen et al., "Inhibition of excessive oxidative protein folding is protective in MPP(+)-toxicity-induced Parkinson's disease models," *Antioxidants & Redox Signaling*, vol. 25, no. 8, pp. 485–497, 2016.
- [20] S. Wang, Z. Chen, V. Lam et al., "IRE1 α -XBP1s induces PDI expression to increase MTP activity for hepatic VLDL assembly and lipid homeostasis," *Cell Metabolism*, vol. 16, no. 4, pp. 473–486, 2012.
- [21] X. Morató, R. Luján, M. López-Cano et al., "The Parkinson's disease-associated GPR37 receptor interacts with striatal adenosine A_{2A} receptor controlling its cell surface expression and function in vivo," *Scientific Reports*, vol. 7, no. 1, p. 9452, 2017.
- [22] D. Marazziti, C. di Pietro, E. Golini, S. Mandillo, R. Matteoni, and G. P. Tocchini-Valentini, "Induction of macroautophagy by overexpression of the Parkinson's disease-associated GPR37 receptor," *The FASEB Journal*, vol. 23, no. 6, pp. 1978–1987, 2009.
- [23] Y. Imai, M. Soda, S. Hatakeyama et al., "CHIP is associated with Parkin, a gene responsible for familial Parkinson's disease, and enhances its ubiquitin ligase activity," *Molecular Cell*, vol. 10, no. 1, pp. 55–67, 2002.
- [24] D. Rial, X. Morató, J. I. Real et al., "Parkinson's disease-associated GPR37 receptor regulates cocaine-mediated synaptic depression in corticostriatal synapses," *Neuroscience Letters*, vol. 638, pp. 162–166, 2017.

- [25] L. Leinartaitė and P. Svenningsson, "Folding underlies bidirectional role of GPR37/Pael-R in Parkinson disease," *Trends in Pharmacological Sciences*, vol. 38, no. 8, pp. 749–760, 2017.
- [26] M. Kaneko, "Physiological roles of ubiquitin ligases related to the endoplasmic reticulum," *Yakugaku Zasshi*, vol. 136, no. 6, pp. 805–809, 2016.
- [27] N. Hattori and Y. Mizuno, "Twenty years since the discovery of the parkin gene," *Journal of Neural Transmission*, vol. 124, no. 9, article 1742, pp. 1037–1054, 2017.
- [28] H. Y. Chung, M. Cesari, S. Anton et al., "Molecular inflammation: underpinnings of aging and age-related diseases," *Ageing Research Reviews*, vol. 8, no. 1, pp. 18–30, 2009.
- [29] A. I. Rojo, G. McBean, M. Cindric et al., "Redox control of microglial function: molecular mechanisms and functional significance," *Antioxidants & Redox Signaling*, vol. 21, no. 12, pp. 1766–1801, 2014.
- [30] C. R. A. Batista, G. F. Gomes, E. Candelario-Jalil, B. L. Fiebich, and A. C. P. de Oliveira, "Lipopolysaccharide-induced neuroinflammation as a bridge to understand neurodegeneration," *International journal of molecular sciences*, vol. 20, no. 9, p. 2293, 2019.
- [31] B. L. Eun, J. Abraham, L. Mlsna, M. J. Kim, and S. Koh, "Lipopolysaccharide potentiates hyperthermia-induced seizures," *Brain and Behavior: A Cognitive Neuroscience Perspective*, vol. 5, no. 8, article e00348, 2015.
- [32] E. J. Shin, S. Y. Nah, W. K. Kim et al., "The dextromethorphan analog dimemorfan attenuates kainate-induced seizures via sigma 1 receptor activation: comparison with the effects of dextromethorphan," *British Journal of Pharmacology*, vol. 144, no. 7, pp. 908–918, 2005.
- [33] L. X. Yang, F. Y. Chen, H. L. Yu et al., "Poncirin suppresses lipopolysaccharide (LPS)-induced microglial inflammation and ameliorates brain ischemic injury in experimental stroke in mice," *Annals of Translational Medicine*, vol. 8, no. 21, p. 1344, 2020.
- [34] S. M. Stahl, "Dextromethorphan/bupropion: a novel oral NMDA (N-methyl-D-aspartate) receptor antagonist with multimodal activity," *CNS Spectrums*, vol. 24, no. 5, pp. 461–466, 2019.
- [35] M. Keller, E. Griesmaier, M. Auer et al., "Dextromethorphan is protective against sensitized N-methyl-D-aspartate receptor-mediated excitotoxic brain damage in the developing mouse brain," *The European Journal of Neuroscience*, vol. 27, no. 4, pp. 874–883, 2008.
- [36] P. P. Yang, E. Y. K. Huang, G. C. Yeh, and P. L. Tao, "Co-administration of dextromethorphan with methamphetamine attenuates methamphetamine-induced rewarding and behavioral sensitization," *Journal of Biomedical Science*, vol. 13, no. 5, pp. 695–702, 2006.
- [37] C. C. Hung, Y. H. Lee, Y. M. Kuo et al., "Soluble epoxide hydrolase modulates immune responses in activated astrocytes involving regulation of STAT3 activity," *Journal of Neuroinflammation*, vol. 16, no. 1, p. 123, 2019.
- [38] D. Li, X. Liu, T. Liu et al., "Neurochemical regulation of the expression and function of glial fibrillary acidic protein in astrocytes," *Glia*, vol. 68, no. 5, pp. 878–897, 2020.
- [39] M. Brenner, "Role of GFAP in CNS injuries," *Neuroscience Letters*, vol. 565, pp. 7–13, 2014.
- [40] V. M. Sardinha, S. Guerra-Gomes, I. Caetano et al., "Astrocytic signaling supports hippocampal-prefrontal theta synchronization and cognitive function," *Glia*, vol. 65, no. 12, pp. 1944–1960, 2017.
- [41] D. Colle, D. B. Santos, A. A. Naime et al., "Early postnatal exposure to paraquat and maneb in mice increases nigrostriatal dopaminergic susceptibility to a re-challenge with the same pesticides at adulthood: implications for Parkinson's disease," *Neurotoxicity Research*, vol. 37, no. 1, pp. 210–226, 2020.
- [42] R. M. Gogal Jr. and S. D. Holladay, "Perinatal TCDD exposure and the adult onset of autoimmune disease," *Journal of Immunotoxicology*, vol. 5, no. 4, pp. 413–418, 2008.
- [43] T. Takano, G. F. Tian, W. Peng et al., "Astrocyte-mediated control of cerebral blood flow," *Nature Neuroscience*, vol. 9, no. 2, pp. 260–267, 2006.
- [44] S. V. Straub and M. T. Nelson, "Astrocytic calcium signaling: the information currency coupling neuronal activity to the cerebral microcirculation," *Trends in Cardiovascular Medicine*, vol. 17, no. 6, pp. 183–190, 2007.
- [45] O. V. Chechneva, F. Mayrhofer, D. J. Daugherty, D. E. Pleasure, J. S. Hong, and W. Deng, "Low dose dextromethorphan attenuates moderate experimental autoimmune encephalomyelitis by inhibiting NOX2 and reducing peripheral immune cells infiltration in the spinal cord," *Neurobiology of Disease*, vol. 44, no. 1, pp. 63–72, 2011.
- [46] W. Zhang, T. Wang, L. Qin et al., "Neuroprotective effect of dextromethorphan in the MPTP Parkinson's disease model: role of NADPH oxidase," *The FASEB Journal*, vol. 18, no. 3, pp. 589–591, 2004.
- [47] J. Church, D. Sawyer, and J. G. McLarnon, "Interactions of dextromethorphan with the N-methyl-D-aspartate receptor-channel complex: single channel recordings," *Brain Research*, vol. 666, no. 2, pp. 189–194, 1994.
- [48] N. Shioda, K. Ishikawa, H. Tagashira, T. Ishizuka, H. Yawo, and K. Fukunaga, "Expression of a truncated form of the endoplasmic reticulum chaperone protein, $\sigma 1$ receptor, promotes mitochondrial energy depletion and apoptosis," *The Journal of Biological Chemistry*, vol. 287, no. 28, pp. 23318–23331, 2012.
- [49] B. P. Lockhart, P. Souillard, C. Benicourt, A. Privat, and J. L. Junien, "Distinct neuroprotective profiles for σ ligands against N-methyl-D-aspartate (NMDA), and hypoxia-mediated neurotoxicity in neuronal culture toxicity studies," *Brain Research*, vol. 675, no. 1-2, pp. 110–120, 1995.
- [50] K. Vagnerova, P. D. Hurn, A. Bhardwaj, and J. R. Kirsch, "Sigma 1 receptor agonists act as neuroprotective drugs through inhibition of inducible nitric oxide synthase," *Anesthesia & Analgesia*, vol. 103, no. 2, pp. 430–434, 2006.

Research Article

Association between Anemia and Risk of Parkinson Disease

Yao-Chin Wang^{1,2}, Abel Po-Hao Huang³, Sheng-Po Yuan^{4,5,6}, Chu-Ya Huang⁷,
Chieh-Chen Wu⁸, Tahmina Nasrin Poly⁴, Suleman Atique⁹, and Woon-Man Kung⁸

¹Department of Emergency, Min-Sheng General Hospital, Taoyuan, Taiwan

²Graduate Institute of Injury Prevention and Control, College of Public Health, Taipei Medical University, Taipei, Taiwan

³Division of Neurosurgery, Department of Surgery, National Taiwan University Hospital, Taipei, Taiwan

⁴Graduate Institute of Biomedical Informatics, College of Medical Science and Technology, Taipei Medical University, Taipei, Taiwan

⁵Department of Otorhinolaryngology, Wan Fang Hospital, Taipei Medical University, Taipei, Taiwan

⁶Department of Otorhinolaryngology, Shuang-Ho Hospital, Taipei Medical University, New Taipei City, Taiwan

⁷Taiwan College of Healthcare Executives, Taipei, Taiwan

⁸Department of Exercise and Health Promotion, College of Kinesiology and Health, Chinese Culture University, Taipei, Taiwan

⁹Department of Health Informatics, College of Public Health and Health Informatics, University of Ha'il, Ha'il, Saudi Arabia

Correspondence should be addressed to Woon-Man Kung; nskungwm@yahoo.com.tw

Received 27 April 2021; Accepted 19 June 2021; Published 7 July 2021

Academic Editor: Hua Lin

Copyright © 2021 Yao-Chin Wang et al. This is an open access article distributed under the Creative Commons Attribution License, which permits unrestricted use, distribution, and reproduction in any medium, provided the original work is properly cited.

Background and Objective. People with anemia have higher rates of developing Parkinson disease (PD) than the general population. Previous epidemiological studies have investigated the risk of PD in patients with anemia. However, the findings are still inconclusive. Therefore, we did a systematic review with meta-analysis to clarify the association between anemia and risk of PD. **Methods.** We systematically searched articles on electronic databases such as PubMed, Embase, Scopus, and Google Scholar between January 1, 2000 and July 30, 2020. Articles were independently evaluated by two authors. We included observational studies (case-control and cohort) and calculated the risk ratios (RRs) for associated with anemia and PD. Heterogeneity among the studies was assessed using the Q and I^2 statistic. We utilized the random-effect model to calculate the overall RR with 95% CI. **Results.** A total of 342 articles were identified in the initial searches, and 7 full-text articles were evaluated for eligibility. Three articles were further excluded for prespecified reasons including insufficient data and duplications, and 4 articles were included in our systematic review and meta-analysis. A random effect model meta-analysis of all 4 studies showed no increased risk of PD in patients with anemia ($N = 4$, $RR_{adjusted} = 1.17$ (95% CI: 0.94-1.45, $p = 0.15$). However, heterogeneity among the studies was significant ($I^2 = 92.60$, $p < 0.0001$). The pooled relative risk of PD in female patients with anemia was higher ($N = 3$, $RR_{adjusted} = 1.14$ (95% CI: 0.83-1.57, $p = 0.40$) as compared to male patients with anemia ($N = 3$, $RR_{adjusted} = 1.09$ (95% CI: 0.83-1.42, $p = 0.51$). **Conclusion.** This is the first meta-analysis that shows that anemia is associated with higher risk of PD when compared with patients without anemia. However, more studies are warranted to evaluate the risk of PD among patients with anemia.

1. Introduction

1.1. Rationale. Parkinson disease (PD) is the second most common age-related neurodegenerative disorder, with more than 60,000 newly diagnosed cases yearly in the USA [1]. The incidence of PD has been increasing at an alarming rate and is estimated to be nearly 1.2 million PD cases worldwide

by 2030 and 12 million patients worldwide by about 2050 [2]. It is estimated that both direct and indirect costs regarding PD are approximately USD 52 billion only in the USA [2]. The higher amount of financial burden that places on our current health care system highlights the importance of conducting research to curb the incidence and prevalence rate of PD. Therefore, a vivid understanding of PD risk factors can

help researchers and policymaker to develop strong strategies for turning down the number of new cases and reducing costs.

The common risk factors of developing PD are exposure to pesticides, genetic variants, environment toxins, idiopathic REM sleep behavior disorder (RBD), and focal cerebrovascular damage [3–6]. However, several epidemiological studies have reported that inflammatory bowel disease (IBD) [7], head injury [8], and autoimmune rheumatic diseases (ARDs) [9] are significantly associated with increased risk of PD. An increased risk of PD was also reported in patients with anemia than those without anemia. Although the exact relationship between anemia and PD risk remains inconclusive, several possible hypotheses have been proposed. A recent study [10] reported that chronic anemia can increase brain hypoxia which is the main risk factor of Alzheimer disease (AD). Previous studies also suggested that patient with AD may experience sequela of epigenetic changes during the development stage [11, 12]. A study showed that neonatal iron deficiency is associated with modification of the AD-related gene expression [13]. Since AD is associated with PD [14], these etiology and link may lead to increased risk of PD. Furthermore, another study demonstrated that rats with iron deficiency diet reduced dopaminergic activity which might induce PD risk [15].

Anemia hampers erythropoiesis and enhances eryptosis, whereas insufficient iron is reported in the substantia nigra of PD patients [16, 17]. Increased serum iron levels are related to decreased risk of PD, and high dietary iron intake reduces PD risk [18, 19]. Moreover, dysregulation of iron metabolism is associated with oxidative stress and cell death [20–22]. Based on biological and epidemiological evidence, it is needed to conduct a study that summarizes the role of anemia on PD risk. However, to our best knowledge, no meta-analysis has been performed to assess the magnitude of association between anemia and PD.

Goal: The aim of this current systematic review and meta-analysis is to evaluate the published epidemiological studies for clarifying the association between anemia and risk of PD.

1.2. Research Questions

- (i) Study the magnitude of the risk of PD in patients with anemia and without anemia
- (ii) Calculate the magnitude difference of the risk of PD in male and female patients with anemia
- (iii) Reduce the confounding factors by evaluating the risk based on various adjustments

2. Methods

2.1. Search Strategy. We did a systematic search on electronic databases such as PubMed, Embase, Scopus, and Web of Science between January 1, 2000 and July 30, 2020. The following search terms were used to collect relevant articles: “anemia,” OR “low level hemoglobin,” “iron deficiency” And “Parkinson disease.” The initial search was conducted

by one author who is an expert in systematic review. Moreover, we searched in the reference lists of retrieved articles to ensure the comprehensiveness.

2.2. Eligibility Criteria. The eligibility criteria were restricted to observational studies (case-control and cohort) and clinical trials (randomized control trial) that evaluated the association between anemia and PD as a primary outcome. Studies were included if they were published in the form of (a) original study, (b) participants at least 200, (c) published in English, (d) provided clear definition of anemia and PD, and (e) provide proper effect size to summarized pool risk.

We excluded studies if they published in the form of review, short report, poster, editorial, case-report, and correspondence.

2.3. Selection Process. Two authors (TNP and YCW) independently reviewed all the titles and abstracts of retrieved articles. They used prespecified selection criteria to select relevant articles to be included in this meta-analysis. Any disagreement in this stage was resolved by the difference by discussing with third author.

2.4. Data Extraction. Same two authors developed data collection form for extracting the required data from the selected studies. They checked the study duplication by comparing authors' names, publication year, and location of study. Two authors collected the information about effect size (odds ratios, hazard ratios with 95% CI), adjusted factors, total number of participants, number of anemia and PD patients, inclusion and exclusion criteria of anemia and PD, age, percentage of male, duration of study period, and location.

2.5. Risk Assessment. The Newcastle-Ottawa Scale (NOS) was used to assess the quality of each study. They calculated the NOS score and divided into two groups: low and high qualities. The heterogeneity was calculated among study-specific RRs using the Q and I^2 statistic. Finally, publication bias evaluated by 3 funnel plot-based methods: the Egger's test, the Begg's test, and the trim and fill method.

2.6. Statistical Analysis. The meta-analysis was performed on selected studies that evaluated the magnitude of the association by using adjusted ORs and HRs. The pooled risk ratio (RR) was calculated from selected studies to show the effect size. The random-effect model was used in this meta-analysis. We calculated statistical heterogeneity across the various studies which were tested using the Cochran Q statistic and quantified by the I^2 value. The heterogeneity among the studies was categorized into four groups, namely, very low (<25%), low (25~50%), medium (50~75%), and high (>75%) [23–25]. When number of studies is small, the random-effect model is a perfect test to reduce bias and heterogeneity among the studies. We draw forest plot to present effect size and funnel plot to depict the publication bias. However, all the statistical analyses were performed using comprehensive meta-analysis software (V:2). The p value less than 0.5 is considered as a significant.

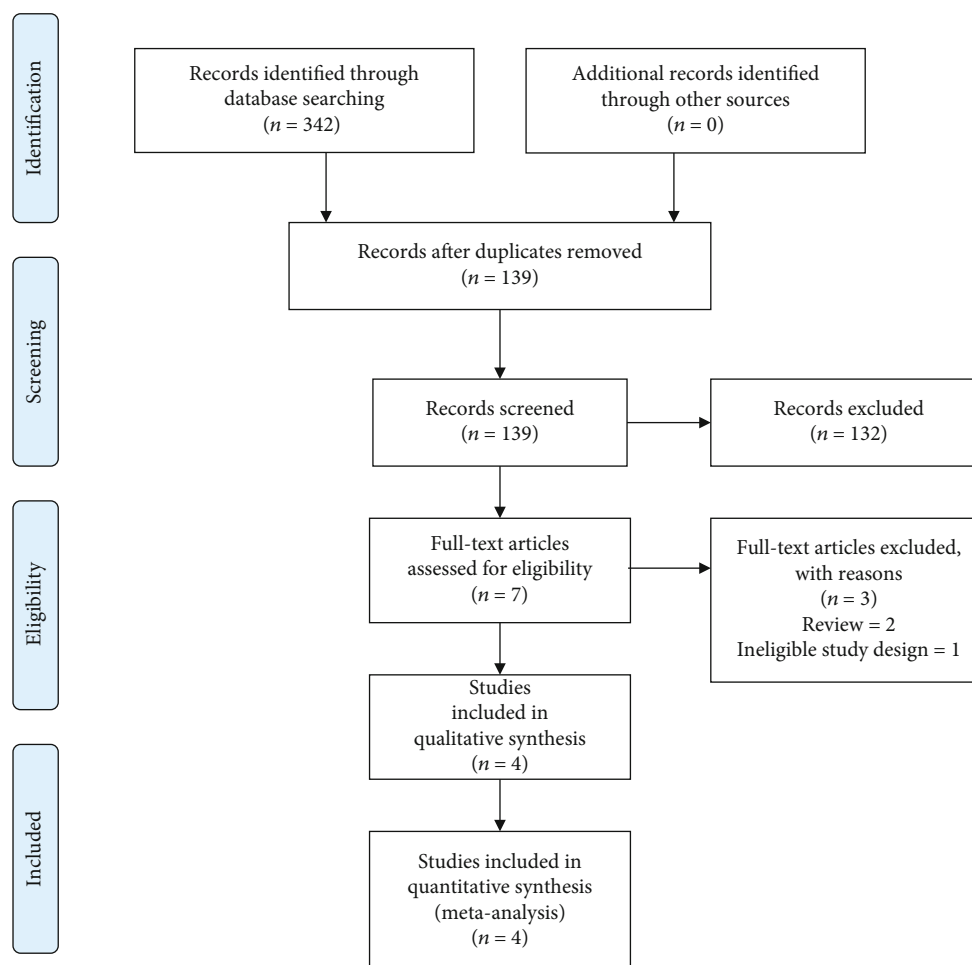


FIGURE 1: Flow diagram of the study selection process.

3. Results

3.1. Study Selection. Initial search in the electronic databases yielded 342 articles. A total of 335 articles were excluded after reviewing the titles and abstracts of retrieved articles. However, 7 articles went to full-text review, and 3 articles were further excluded due to not matching the prespecified selection criteria. Finally, 4 articles were included in the current systematic review and meta-analysis [26–29]. Figure 1 shows our study selection process.

3.2. Study Characteristics. This current systematic review and meta-analysis comprised of 4 studies including 3 cohorts and 1 case-control study (Table 1). Included studies published between 2009 and 2019; the average age of patients was from 48.7 to 71. The percentage of male patients was from 24.1 to 63%. Three studies followed World Health Organization (WHO) guidelines to be included in the anemia patients: hemoglobin level < 13 g/dL for men and < 12 g/dL for women, and one study used ICD to include anemia patients. On the other hand, three studies used ICD to include PD patients, and one study used PD registry linkage.

3.3. Anemia and Risk of PD. There were various follow-up durations for each of the 4 studies, ranging from 5 to 8.8 years. Our meta-analysis comprised a total of 92,851 PD patients. A random-effect model meta-analysis of all 4 studies showed no increased risk of PD in patients with anemia ($N = 4$, $RR_{\text{adjusted}} = 1.17$ (95% CI: 0.94–1.45, $p = 0.15$). However, heterogeneity among the studies was significant ($Q = 40.58$, $\tau^2 = 0.04$, $I^2 = 92.60$, $p < 0.0001$) (Figure 2).

3.4. Subgroup Analysis. We pooled 3 studies in order to evaluate the risk of PD based on gender. The pooled relative risk of PD in female patients with anemia was higher ($N = 3$, $R_{\text{adjusted}} = 1.14$ (95% CI: 0.83–1.57, $p = 0.40$) as compared to male patients with anemia ($N = 3$, $RR_{\text{adjusted}} = 1.09$ (95% CI: 0.83–1.42, $p = 0.51$) (Figure 3). However, a significant heterogeneity was both in male ($I^2 = 81.02$, $p = 0.005$, $Q = 10.54$, $\tau^2 = 0.03$) and female ($I^2 = 82.60$, $p = 0.003$, $Q = 11.50$, $\tau^2 = 0.05$) patients with anemia.

We also evaluated the risk of PD in patients among the studies adjusted with most common confounding factors such as diabetes and hypertension. The pooled risk ratio

TABLE 1: Baseline characteristics of included studies.

Author name	Location	Study duration	Age	Male (%)	Design	PD	Anemia criteria	PD	Mean follow-up (Yrs.)	HR/OR	Major adjustment	NOS score
Cho 2020	S. Korea	2009-2013	57.41 ± 7.51	63	Cohort	3,844	The World Health Organization (WHO): hemoglobin level < 13 g/dL for men and <12 g/dL for women	ICD-10	5	0.89 (0.80-0.98)	Smoking, alcohol, physical activity, HTN, DM, dyslipidemia, GFR	8
Rozani 2019	Israel	1999-2012	48.7	47.4	Cohort	2,427	The World Health Organization (WHO): hemoglobin level < 13 g/dL for men and <12 g/dL for women	ICD-9	8.8 ± 3.9	1.02 (0.95-1.09)	N/A	8
Hong 2016	Taiwan	N/A	56.4	24.1	Cohort	86,334	ICD-9	ICD-9	6.6	1.36 (1.22-1.52)	HTN, DM, hyperlipidemia	8
Savica 2009	USA	1976-1995	71	61.7	Case-control	196	The World Health Organization (WHO): hemoglobin level < 13 g/dL for men and <12 g/dL for women	Records linkage system	n/a	2.00 (1.31-3.06)	N/A	8

#PD: Parkinson disease; ICD: International Classification of Diseases; HR: hazard ratio; OR: odds ratio; NOS: the Newcastle-Ottawa Scale.

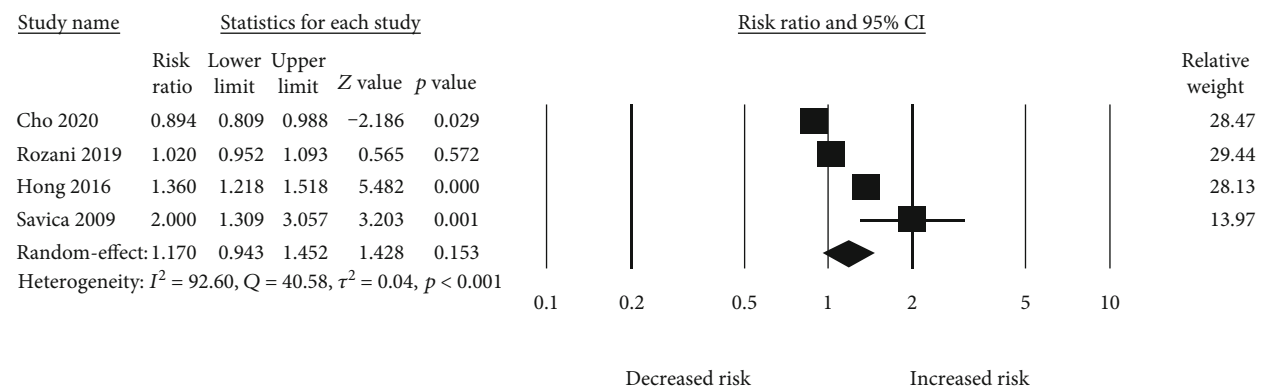
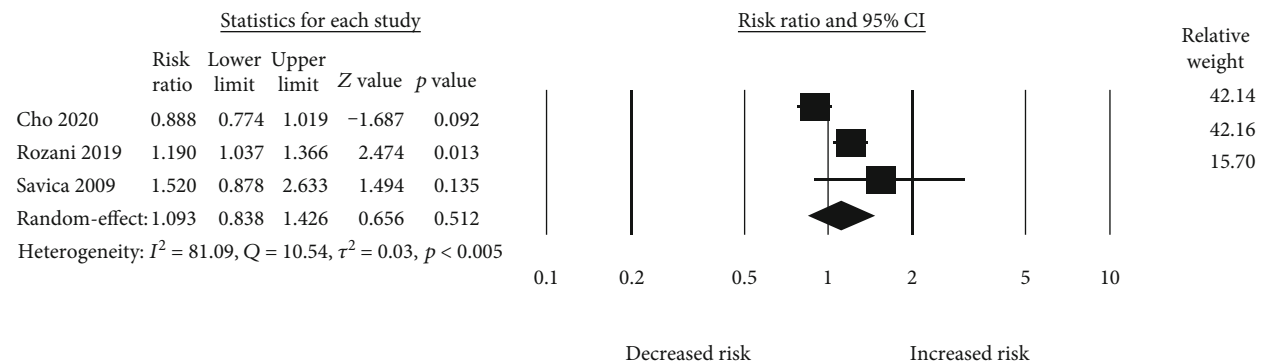
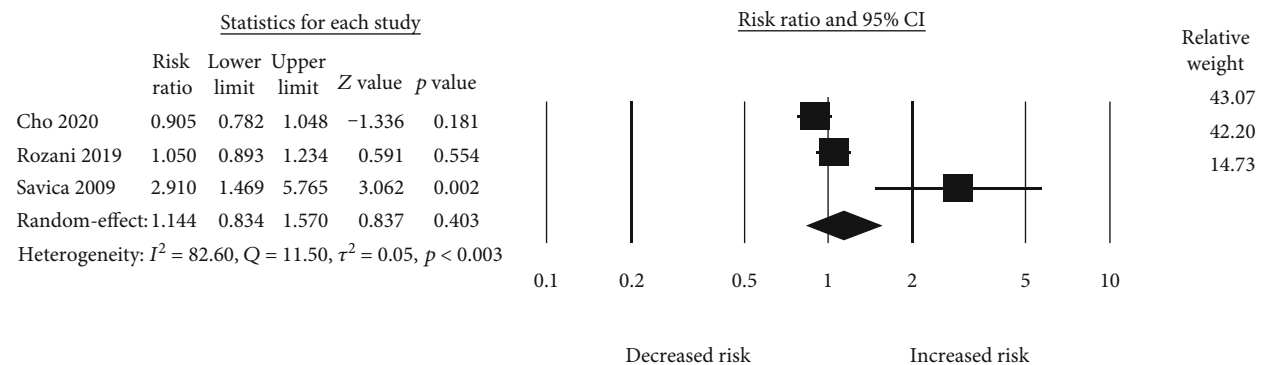


FIGURE 2: Association between anemia and risk of PD.



(a) Male patients with anemia



(b) Female patients with anemia

FIGURE 3: Risk of PD.

was ($N = 3$, $RR_{\text{adjusted with diabetes and hypertension}} = 1.10$ (95% CI: 0.73-1.66, $p = 0.64$), and heterogeneity was significant ($I^2 = 96.72$, $p = <0.001$, $Q = 30.49$, $\tau^2 = 0.08$).

3.5. Publication Bias. Figure 4 shows the funnel plot indicating possible publication bias. Egger's regression test of the funnel asymmetry presented no possible publication bias.

4. Discussion

4.1. Main Findings. To our knowledge, this is the first study to assess the risk of PD among the patients with anemia. This current meta-analysis of four observational studies showed that patients with anemia were not significantly associated

with 17% increased risk of PD as compared with nonanemia. However, male patients with anemia showed nonsignificant increased risk of PD while comparing with female patients with anemia. The strengths of this study are (a) all included studies quality were high and (b) consider adjusted effect size; therefore, risk of bias is low and (c) clear definition of anemia and PD risk.

4.2. Biological Mechanism. The biological mechanism of PD and anemia is not fully understood yet. However, there are several biological explanations that can define their association. First, the neural degeneration and disease progression among the PD patients can be induced by either apoptosis or necrosis [30]. The brain cell death is caused by DNA

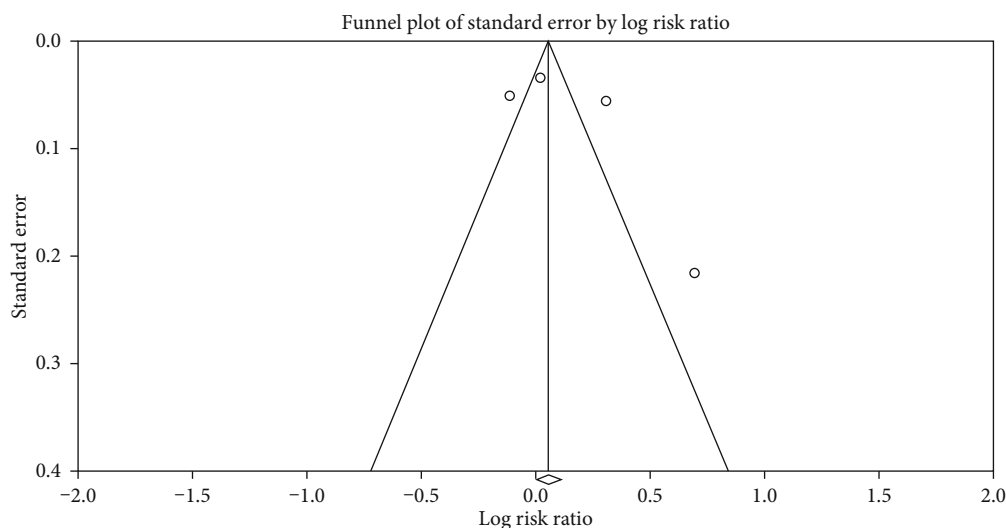


FIGURE 4: Funnel plot.

fragmentation and typical morphological changes including cell shrinkage and nuclear condensation. However, apoptosis in PD is still debatable. The animals and in vitro studies reported apoptosis as well as promoting the rate of neurodegeneration [31–33]. Second, some assumptions regarding oxidative stress and iron metabolism are likely to dopaminergic neural death in the central nervous system [34, 35]. Several studies analyzed erythrocytes of PD indicating lessened superoxide dismutase, glutathione peroxidase activity, and elevated lipid peroxidation which are responsible for the degeneration of dopaminergic neurons in the substantia nigra. All the process, however, are related to the activity of oxidative stress [36, 37]. Third, α -synuclein and etiology of PD are the main keys that can be used to explain the pathological mechanism of anemia and PD risk. Erythrocytes generate maximum portion of α -synuclein in the human blood [38]; it has shown in the previous study that the ratio of α -synuclein oligomer and total protein is higher in erythrocyte of PD patients when compared to normal patients [39]. Anxiety and depression are most common symptoms in PD that are considered as primary contributors to abnormality, low quality of life, and low survival [40, 41]. Depression in PD patient is associated with several neurotransmitter dysfunctions including serotonin, noradrenaline, and dopamine [42]. Moreover, gut brain axis (GBA) has a positive correlation with increased risk of PD. Accumulation of gut microbiota in α -synuclein in PD has received wide attention over the past years. A previous mice study showed that microbial metabolites may increase the risk of neuroinflammation by expressing proinflammatory cytokines which ultimately lead to the development of motor symptom [43]. Other study also reported a positive link of gut microbiota in neurodegeneration [44].

4.3. Clinical Implications. PD is now one of the leading causes of disability and deaths globally. A significant amount of epidemiological studies have highlighted an increased prevalence of PD which raised sheer concern and urgent need for public health strategies [45–47]. Appropriate planning would

help to reduce the number of PD patients as well as health-care cost over the coming decades [48]. The primary risk factor of PD is age, but PD also appears to be linked to anemia. However, the association between anemia and PD based on duration and severity is less well known. Since anemia and aging population are increasing globally, the prevalence of PD undoubtedly will increase. Conducting a meta-analysis can clarify the effect size in order to prevent and treat the disease both earlier and effectively.

4.4. Strengths and Limitations. Our first and rigorous meta-analysis has several strengths. First, this is the first meta-analysis that investigated the association between anemia and PD risk. Second, this study included four large observation studies from Taiwan, Israel, South Korea, and USA; healthcare data quality of these countries is world standard. They adjusted potential confounding factors to this study to reduce bias of effect size calculation. Third, this present study showed risk difference between male and female patients.

However, this study has some limitations. First, number of included studies is only four, although all are high quality study design with larger number of participants. Second, we were not able to provide risk of PD based on severity of anemia (high, moderate, and low) and BMI (overweight, obese, and underweight). Third, the pooled risk was not calculated based on location, study design, and other factors like smoking status, alcohol consumptions, and duration of anemia; it is because data were limited.

5. Conclusion

Our study shows that the risk of PD was higher among the patients with anemia as compared without anemia. The risk of PD was higher in male patients. Therefore, more protective strategies should be taken in male patients when compared to female patients. The risk of PD among patients with anemia can be explained by some biological mechanisms like oxidative stress and downregulation of iron homeostasis. More observational studies in different regions

and biological studies are warranted to clarify the mechanism underlying their association.

Data Availability

The data used to support the findings of this study are from previously reported studies and datasets, which have been cited and included within the article.

Conflicts of Interest

The author(s) declare(s) that they have no conflicts of interest.

References

- [1] W. Yang, J. L. Hamilton, C. Kopil et al., "Current and projected future economic burden of Parkinson's disease in the U.S.," *npj Parkinson's Disease*, vol. 6, no. 1, pp. 1–9, 2020.
- [2] E. R. Dorsey, A. Elbaz, E. Nichols et al., "Global, regional, and national burden of Parkinson's disease, 1990–2016: a systematic analysis for the Global Burden of Disease Study 2016," *The Lancet Neurology*, vol. 17, no. 11, pp. 939–953, 2018.
- [3] F. N. Emamzadeh and A. Surguchov, "Parkinson's disease: biomarkers, treatment, and risk factors," *Frontiers in neuroscience*, vol. 12, p. 612, 2018.
- [4] D. B. Miller and J. P. O'Callaghan, "Biomarkers of Parkinson's disease: Present and future," *Metabolism*, vol. 64, no. 3, pp. S40–S46, 2015.
- [5] R. B. Postuma, A. E. Lang, J. Massicotte-Marquez, and J. Montplaisir, "Potential early markers of Parkinson disease in idiopathic REM sleep behavior disorder," *Neurology*, vol. 66, no. 6, pp. 845–851, 2006.
- [6] R. Postuma, J.-F. Gagnon, S. Rompre, and J. Y. Montplaisir, "Severity of REM atonia loss in idiopathic REM sleep behavior disorder predicts Parkinson disease," *Neurology*, vol. 74, no. 3, pp. 239–244, 2010.
- [7] S. Park, J. Kim, J. Chun et al., "Patients with inflammatory bowel disease are at an increased risk of Parkinson's disease: a South Korean nationwide population-based study," *Journal of clinical medicine*, vol. 8, no. 8, p. 1191, 2019.
- [8] K. Rugbjerg, B. Ritz, L. Korbo, N. Martinussen, and J. H. Olsen, "Risk of Parkinson's disease after hospital contact for head injury: population based case-control study," *Bmj*, vol. 337, article a2494, 2008.
- [9] C.-C. Chang, T.-M. Lin, Y.-S. Chang et al., "Autoimmune rheumatic diseases and the risk of Parkinson disease: a nationwide population-based cohort study in Taiwan," *Annals of medicine*, vol. 50, no. 1, pp. 83–90, 2018.
- [10] A. Atti, K. Palmer, S. Volpato, G. Zuliani, B. Winblad, and L. Fratiglioni, "Anaemia increases the risk of dementia in cognitively intact elderly," *Neurobiology of aging*, vol. 27, no. 2, pp. 278–284, 2006.
- [11] J. Wu, M. R. Basha, B. Brock et al., "Alzheimer's disease (AD)-like pathology in aged monkeys after infantile exposure to environmental metal lead (Pb): evidence for a developmental origin and environmental link for AD," *Journal of Neuroscience*, vol. 28, no. 1, pp. 3–9, 2008.
- [12] J. Wu, M. R. Basha, and N. H. Zawia, "The environment, epigenetics and amyloidogenesis," *Journal of Molecular Neuroscience*, vol. 34, no. 1, pp. 1–7, 2008.
- [13] E. S. Carlson, R. Magid, A. Petryk, and M. K. Georgieff, "Iron deficiency alters expression of genes implicated in Alzheimer disease pathogenesis," *Brain research*, vol. 1237, pp. 75–83, 2008.
- [14] W. A. Rocca, J. H. Bower, J. E. Ahlskog et al., "Risk of cognitive impairment or dementia in relatives of patients with Parkinson disease," *Archives of neurology*, vol. 64, no. 10, pp. 1458–1464, 2007.
- [15] C. W. Levenson, R. G. Cutler, B. Ladenheim, J. L. Cadet, J. Hare, and M. P. Mattson, "Role of dietary iron restriction in a mouse model of Parkinson's disease," *Experimental neurology*, vol. 190, no. 2, pp. 506–514, 2004.
- [16] W. R. W. Martin, M. Wieler, and M. Gee, "Midbrain iron content in early parkinson disease: A potential biomarker of disease status," *Neurology*, vol. 70, 16, Part 2, pp. 1411–1417, 2008.
- [17] D. Dexter, F. Wells, A. Lee et al., "Increased nigral iron content and alterations in other metal ions occurring in brain in Parkinson's disease," *Journal of Neurochemistry*, vol. 52, no. 6, pp. 1830–1836, 1989.
- [18] I. Pichler, F. Greco, M. Gögele et al., "Serum iron levels and the risk of Parkinson disease: a Mendelian randomization study," *PLOS Medicine*, vol. 10, no. 6, article e1001462, p. e1001462, 2013.
- [19] Y. Miyake, K. Tanaka, W. Fukushima et al., "Dietary intake of metals and risk of Parkinson's disease: a case-control study in Japan," *Journal of the Neurological Sciences*, vol. 306, no. 1–2, pp. 98–102, 2011.
- [20] T. Grune, O. Sommerburg, and W. Siems, "Oxidative stress in anemia," *Clinical nephrology*, vol. 53, 1 Supplement, pp. S18–S22, 2000.
- [21] E. Kurtoglu, A. Ugur, A. K. Baltaci, and L. Undar, "Effect of iron supplementation on oxidative stress and antioxidant status in iron-deficiency anemia," *Biological Trace Element Research*, vol. 96, no. 1–3, pp. 117–124, 2003.
- [22] P. V. Tran, E. S. Carlson, S. J. Fretham, and M. K. Georgieff, "Early-life iron deficiency anemia alters neurotrophic factor expression and hippocampal neuron differentiation in male rats," *The Journal of nutrition*, vol. 138, no. 12, pp. 2495–2501, 2008.
- [23] M. M. Islam, U. Iqbal, B. Walther et al., "Benzodiazepine use and risk of dementia in the elderly population: a systematic review and meta-analysis," *Neuroepidemiology*, vol. 47, no. 3–4, pp. 181–191, 2016.
- [24] T. N. Poly, M. M. R. Islam, H.-C. Yang, and Y.-C. J. Li, "Non-steroidal anti-inflammatory drugs and risk of Parkinson's disease in the elderly population: a meta-analysis," *European journal of clinical pharmacology*, vol. 75, no. 1, article 2561, pp. 99–108, 2019.
- [25] M. M. Islam, H.-C. Yang, P.-A. Nguyen et al., "Exploring association between statin use and breast cancer risk: an updated meta-analysis," *Archives of gynecology and obstetrics*, vol. 296, no. 6, pp. 1043–1053, 2017.
- [26] I. Y. Cho, D. W. Shin, Y. Roh et al., "Anemia and the risk of Parkinson's disease in Korean older adults: A nationwide population-based study," *Scientific reports*, vol. 10, no. 1, article 61153, pp. 4268–4269, 2020.
- [27] C. T. Hong, Y. H. Huang, H. Y. Liu, H.-Y. Chiou, L. Chan, and L. N. Chien, "Newly Diagnosed Anemia Increases Risk of Parkinson's disease: A Population- Based Cohort Study," *Scientific reports*, vol. 6, no. 1, article 29651, 2016.

- [28] V. Rozani, N. Giladi, T. Gurevich et al., "Anemia in men and increased Parkinson's disease risk: A population-based large scale cohort study," *Parkinsonism & related disorders*, vol. 64, pp. 90–96, 2019.
- [29] R. Savica, B. Grossardt, J. Carlin et al., "Anemia or low hemoglobin levels preceding Parkinson disease: a case-control study," *Neurology*, vol. 73, no. 17, pp. 1381–1387, 2009.
- [30] J. KJont, "Cell death mechanisms in Parkinson's disease," *Journal of neural transmission*, vol. 107, no. 1, pp. 1–29, 2000.
- [31] M. Ruberg, V. France-Lanord, B. Brugg et al., "Neuronal death caused by apoptosis in Parkinson disease," *Revue neurologique*, vol. 153, no. 8-9, pp. 499–508, 1997.
- [32] W. Liu, Q. Zhang, J. Zhang, W. Pan, J. Zhao, and Y. Xu, "Long non-coding RNA MALAT1 contributes to cell apoptosis by sponging miR-124 in Parkinson disease," *Cell & bioscience*, vol. 7, no. 1, pp. 1–9, 2017.
- [33] N. Lev, E. Melamed, and D. Offen, "Apoptosis and Parkinson's disease," *Progress in Neuro-Psychopharmacology and Biological Psychiatry*, vol. 27, no. 2, pp. 245–250, 2003.
- [34] L.-H. You, F. Li, L. Wang et al., "Brain iron accumulation exacerbates the pathogenesis of MPTP-induced Parkinson's disease," *Neuroscience*, vol. 284, pp. 234–246, 2015.
- [35] J. E. Ahlskog, "Challenging conventional wisdom: the etiologic role of dopamine oxidative stress in Parkinson's disease," *Movement disorders*, vol. 20, no. 3, pp. 271–282, 2005.
- [36] A. Kilinç, A. S. Yalçin, D. Yalçin, Y. Taga, and K. Emerk, "Increased erythrocyte susceptibility to lipid peroxidation in human Parkinson's disease," *Neuroscience letters*, vol. 87, no. 3, pp. 307–310, 1988.
- [37] K. Urakami, K. Sano, E. Matsushima et al., "Decreased superoxide dismutase activity in erythrocyte in Parkinson's disease," *Psychiatry and Clinical Neurosciences*, vol. 46, no. 4, pp. 933–936, 1992.
- [38] R. Barbour, K. Kling, J. P. Anderson et al., "Red blood cells are the major source of alpha-synuclein in blood," *Neurodegenerative Diseases*, vol. 5, no. 2, pp. 55–59, 2008.
- [39] X. Wang, S. Yu, F. Li, and T. Feng, "Detection of α -synuclein oligomers in red blood cells as a potential biomarker of Parkinson's disease," *Neuroscience letters*, vol. 599, pp. 115–119, 2015.
- [40] J. H. Bower, B. R. Grossardt, D. M. Maraganore et al., "Anxious personality predicts an increased risk of Parkinson's disease," *Movement disorders*, vol. 25, no. 13, pp. 2105–2113, 2010.
- [41] A. Alonso, L. A. G. Rodriguez, G. Logroscino, and M. A. Hernan, "Use of antidepressants and the risk of Parkinson's disease: a prospective study," *Journal of Neurology, Neurosurgery & Psychiatry*, vol. 80, no. 6, pp. 671–674, 2009.
- [42] R. B. Postuma, D. Aarsland, P. Barone et al., "Identifying prodromal Parkinson's disease: pre-motor disorders in Parkinson's disease," *Movement Disorders*, vol. 27, no. 5, pp. 617–626, 2012.
- [43] T. R. Sampson, J. W. Debelius, T. Thron et al., "Gut Microbiota Regulate Motor Deficits and Neuroinflammation in a Model of Parkinson's Disease," *Cell*, vol. 167, no. 6, pp. 1469–1480.e12, 2016.
- [44] A. M. Gorecki, L. Preskey, M. C. Bakeberg et al., "Altered gut microbiome in Parkinson's disease and the influence of lipopolysaccharide in a human α -synuclein over-expressing mouse model," *Frontiers in neuroscience*, vol. 13, p. 839, 2019.
- [45] on behalf of the Parkinson's Foundation P4 Group, C. Marras, J. C. Beck et al., "Prevalence of Parkinson's disease across North America," *NPJ Parkinson's disease*, vol. 4, no. 1, pp. 1–7, 2018.
- [46] T. Pringsheim, N. Jette, A. Frolkis, and T. D. L. Steeves, "The prevalence of Parkinson's disease: A systematic review and meta-analysis," *Movement disorders*, vol. 29, no. 13, pp. 1583–1590, 2014.
- [47] J.-H. Park, D.-H. Kim, D.-Y. Kwon et al., "Trends in the incidence and prevalence of Parkinson's disease in Korea: a nationwide, population-based study," *BMC geriatrics*, vol. 19, no. 1, article 1332, p. 320, 2019.
- [48] C. Baiano, P. Barone, L. Trojano, and G. Santangelo, "Prevalence and clinical aspects of mild cognitive impairment in Parkinson's disease: a meta-analysis," *Movement Disorders*, vol. 35, no. 1, pp. 45–54, 2020.